The role of vitamin A during bio-mineral tissue development in pigs

By

Adam Clark

BSc Biochemistry with Immunology

A thesis submitted for the degree of Doctor of Philosophy (PhD)

Institute for Cellular Medicine

Newcastle University

September 2018

Abstract

Skeletal health is a critical determinant of animal health and welfare. Kyphosis is one such idiopathic skeletal disease that compromises the welfare of commercial pigs. Vitamin A regulates the expression of genes that define bone growth and development, and has been suggested to associate with kyphosis. This thesis aimed to establish the molecular basis of kyphosis, clarify vitamin A's role on the expression of genes that regulate skeletal development, and to ascertain vitamin A's role on gene expression in kyphotic pigs.

The TGF-β signalling pathway was associated with kyphotic bone and cartilage tissues. This was due to bone and cartilage tissues showing associations with small-leucine rich proteoglycans, *ASPN* and *DCN* respectively, which regulate TGF- β signalling. Potential effects as a result of differential gene expression include reduced endochondral bone growth and deterioration of articular cartilage.

The dose of vitamin A was observed to be a critical factor in the regulation of expression of skeletal genes within bone tissue. Genes related to the family of Rho-GTPases, which control cytoskeletal dynamics, were observed to be differentially regulated within the trabecular bone in response to vitamin A. In addition, vitamin A dose was observed to initially antagonise serum 25(OH) D, and upon full saturation of the liver with vitamin A, serum 25(OH) D was restored through, as of yet, unknown mechanisms.

The gene *GIT2,* which associates with Rho-GTPases, was observed to be differentially downregulated within kyphotic trabecular bone, and showed a dose-response relationship with vitamin A supplementation. Furthermore, kyphotic pigs were indicated to have reduced vitamin D status.

This research has outlined the molecular basis of kyphosis in pigs, and has indicated vitamin A and vitamin D drive the disease. The research also outlines the role of how excessive vitamin A controls the expression of genes that regulate bio-mineralisation in trabecular bone. The thesis has also offered novel insights into vitamin A's potential role in regulating gene expression during kyphotic development.

This thesis is dedicated to the memory of Karen Jean Clark, whose love, support, and passion will forever be felt, and will always set role model standards that I will strive to meet.

Acknowledgements

I would like to thank the Sage graduate school for funding this PhD and allowing me to pursue this project that I started upon graduating from Newcastle University. This journey has been both a character-forming and unforgettable life experience that would not have been possible were it not for your support.

I would also like to express sincere gratitude to Dr Anthony Oxley and Dr Christine Bosch from Leeds University, for teaching me the laboratory methods that I have used throughout my PhD, and for laying down the foundations of consistent and good lab practice. Dr Oxley has been a fantastic role model scientist whom has always allowed me to bounce ideas off him.

I must also extend my warm thanks and appreciations to Dr Neil Foster and Dr Tim Giles at the University of Nottingham for the microarray analysis of samples from the kyphosis and Gates Foundation trials. Had it not been for your invaluable collaborative support, this thesis would not have the strength and substance that has come to define it. To add to this, I would like to offer my gratitude to the Prohealth team for their funding and support, and for allowing me the opportunity to associate with the field of tackling production diseases in commercial animals.

Many thanks are also extended to Mrs Rachel Farquhar and the rest of team at XXX. The opportunity to address the kyphosis issue would not have been possible were it not for your collaborative support, and it was a genuine pleasure visiting your outdoor commercial units in person. Further thanks must also be addressed to Genus PIC, and to Dr Craig Lewis for your continued encouragement and involvement with the project. Your passion for science and desire to apply research to introduce real-changes to the world has served as a fantastic inspiration for me throughout the thesis, and I am extremely grateful for your continued support.

I must also thank everyone who helped me during tissue collection on farms that I have visited throughout my thesis. If it weren't for your help, the results of this PhD simply wouldn't have been possible. I therefore thank: Christopher Bulman, Jennifer Murray, Emma Malcolm, Sam Dove, and James Taylor for your instrumental contributions.

Over at SNES, I would like to thank Dr Panagiotis Sakkas, Ms Sheralyn Smith, and Mrs Debra Patterson for your continued encouragement over the years. I am very grateful to Dr Sakkas for allowing me to contribute to the broiler Prohealth project, to Ms Smith for her contributions towards qPCR analysis of samples, and to Mrs Patterson without whom we would all be lost and confused!

I must also express my sincere gratitude and thanks towards my supervisory team: Professor Georg Lietz, Professor Ilias Kyriazakis, and Professor Robin Henderson. You have all served as inspirations in relation to moulding my professional life, and for strengthening my core skills as a scientist and researcher. I have developed in various professional ways throughout this journey, and none of it would have been possible were it not for your outstanding support. I offer many thanks once again.

Finally, I would like to offer my most heartfelt thanks to my family and friends, who have supported me every step of the way. I would like to thank my father Neil Clark, for your consistent and firm belief in my abilities; and to my partner Charlotte Hogg, whose unparalleled love and support kept me on track during the years, and for reminding me to keep faith in myself.

Contents

List of Tables

List of Figures

List of Abbreviations

1, 25 $(OH)_2$ D	Calcitriol
25(OH) D	25-Hydroxycholecalciferol
ACTC1	Actin, Alpha, Cardiac Muscle 1
ALOX12	Arachidonate 12-lipoxygenase
ATRA	All-*trans* Retinoic Acid
ASPN	Asporin
BMPR1A	Bone Morphogenetic Protein Receptor Type 1A
BLAST	Basic Local Alignment Search Tool
BMC	Bone Mineral Content
BMD	Bone Mineral Density
BMP	Bone Morphogenetic Protein
BGLAP	Osteocalcin
Ca	Calcium
CALIB	Calibrator
CDC42	Cell Division Cycle 42
cDNA	complementary Deoxyribonucleic Acid
CILP	Cartilage Intermediate Layer Protein
cRNA	complementary Ribonucleic Acid
CYP26A1	Cytochrome P450 Family 26 Subfamily A Member 1
DCN	Decorin
DEFRA	Department For Environment and Rural Affairs
E	PCR Efficiency
ECM	Extracellular Matrix
EIF3D	Eukaryotic translation initiation factor 3 subunit D
ELISA	Enzyme linked immunosorbent assay
FLNA	Filamin A
GAG	Glycosaminoglycans
GAPDH	Glyceraldehyde-3-phosphate dehydrogenase
GEF	Guanine Exchange Factor
GIT2	G Protein-Coupled Receptor Kinase Interacting ArfGAP 2

GO	Gene Ontology
GPCR	G Protein Coupled Receptor
HPLC	High Performance Liquid Chromatography
IPA	Ingenuity Pathway Analysis
mRNA	messenger Ribonucleic Acid
MSC	Mesenchymal Stem Cell
NRC	National Research Council
NTC	Non Template Control
P	Phosphorus
PAK	p-21 Activated Kinase
PG	Proteoglycan
PPIA	Peptidyl isomerase A
POC	Primary Ossification Centre
PSMD4	26S proteasome non-ATPase regulatory subunit 4
PTK2B	Protein Tyrosine Kinase 2 Beta
qPCR	Quantitative polymerase chain reaction
RANK	Receptor Activator of Nuclear Factor kappa-B
RANKL	Receptor Activator of Nuclear Factor kappa-B ligand
RE	Retinyl Ester
RP	Retinyl Propionate
RPL37	60s ribosomal protein L37
RT	Reverse Transcription
RUNX2	Runt-related Transcription Factor 2
SLRP	Small-Leucine Rich Proteoglycan
SPARC	Osteonectin
TGF-β	Transforming Growth Factor Beta

Chapter 1: Nutrition and bio-mineral tissue development in pigs

1.1 General Introduction

Bone is a unique and diverse tissue which composes the skeleton in all vertebrates; the basic purpose of the skeleton is to provide structural integrity to the growing organism and to deliver support in relation to movement (Burr and Allen, 2014). Therefore, abnormalities in the development of bones can seriously compromise welfare, and bone development remains a critical determinant of health in animal and human medicine. Disorders such as osteoporosis in humans (Manolagas, 2000) and rickets in pigs (Madson et al., 2012) are examples which demonstrate abnormal bone development. Lameness in pigs, characterised by weakness in legs, is often associated with osteochondrosis and subsequent lack of skeletal mineralisation (Dewey et al., 1993, Etterlin et al., 2015). Other bone disorders that can contribute to lameness include osteomalacia, which is also characterised by lack of sufficient mineralisation (Sedman et al., 1987, Dewey et al., 1993). Lameness holds significant economic losses for farmers, with surveys indicating bone fractures related to lameness are a significant cause towards a drop in profitability, as well as pain in animals (Jensen et al., 2012). Therefore, bone health remains a critical factor in determining animal welfare, and maintenance of the welfare of animals within farming systems remains a focus of the industry.

One such bone disease that has been plaguing the commercial pig industry in recent decades is that of idiopathic lumbar kyphosis (Penny and Walters, 1986, Halanski et al., 2018). The disease is adequately termed due to an uncanny resemblance to Scheurmanns kyphosis in humans and is characterised by an abnormal, outward curvature of the spine at the thoraco-lumbar junction (Nielsen et al., 2005). In all vertebrates, the vertebral skeleton is ultimately derived from two tissue types: bone and cartilage (Figure 1.1), and the formation of these two tissues types initially derive from Mesenchymal stem cells (MSCs). MSCs condense into sites of differentiation to form the initial template of the skeleton and have the potential to differentiate into osteoblasts, osteoclasts, adipocytes or chondrocytes cells. These cells govern bone formation, bone resorption, fat synthesis and cartilage metabolism respectively (Karsenty et al., 2009, Gimble et al., 2006, Burr and Allen, 2014).

Endochondral ossification is a process by which MSCs differentiate into chondrocytes, which then form a cartilaginous template surrounded by a fibrous membrane that resembles the shape of bone, which is subsequently replaced by ossified tissue and mineralised matrix by invading osteoblasts (Berendsen and Olsen, 2015). The process of endochondral bone growth is tightly controlled by a variety of molecular signalling pathways, these include Bone Morphogenetic Protein (BMP), and Transforming-Growth factor – Beta (TGF- β) signalling pathways (Kronenberg, 2003, Westendorf et al., 2004). A summary of these pathways can be viewed in Figure 1.2, and the depth of their relevance to bone growth will be further explored in this review. Knockout of genes related to these processes, or use of antagonists, are associated with the development of diseases such as osteoporosis, characterised by a reduction in skeletal mineralisation and growth (Li et al., 2007, Westendorf et al., 2004). Yet it is not known how a disturbance in the delicate process of bone growth has been affected in kyphotic pigs, or which pathways associate with the disease.

Vitamin A is a fat soluble vitamin that is obtained from the diet. Excess vitamin A supplementation has been suggested to be a factor that contributes to the development of kyphosis (Belsue, 2010), and has been observed to induce fragility of bones and halt endochondral bone growth in pigs (Pryor et al., 1969, Wolke et al., 1968). The mechanisms by which vitamin A potentially contributes to kyphosis, however, remain unexplained; and the role of vitamin A in overall bone development sparks significant debate. It has also been demonstrated that excess vitamin A can regulate mRNA expression of genes related to Wnt signalling in bone marrow, but reduced Wnt signalling is observed in cortical bone (Lind et al., 2012), and this demonstrates vitamin A's apparent compartment-specific effects. However, exactly how excess vitamin A affects the molecular development of trabecular bone, which composes the main body of the vertebrae, remains unanswered. These questions need investigating not only to understand how vitamin A is contributing to vertebral trabecular bone development, but also to begin establishing a basis as to how vitamin A is associated with the development of kyphosis.

In addition, extensive work from a research group in Wisconsin have shown that vitamin D deficiency is a factor that can contribute to the development of kyphosis, and that genes which regulate osteoblast mineralisation, such as osteocalcin (*BGLAP)*, are downregulated in the bone tissue of these pigs (Amundson et al., 2016, Rortvedt and Crenshaw, 2012).

Vitamin A and vitamin D are critical factors in determining skeletal health, as demonstrated by studies associating them with bone abnormalities such as lameness, osteoporosis, and rickets (van Riet et al., 2013, Jackson and Sheehan, 2005, Ahmadieh and Arabi, 2011, Madson et al., 2012). There is also an observed interaction between vitamin A and vitamin D, with the consensus being that one vitamin has the potential to remedy toxic effects of the other. Studies in rats (Clark and Bassett, 1961), turkeys (Metz et al., 1985) and broilers (Aburto et al., 1998) have demonstrated vitamin A can counter toxic effects on bone tissue induced by vitamin D, and vice versa. The mechanisms that define these have not been fully clarified; it has been suggested that vitamin A antagonises serum vitamin D (25(OH)D) (Frankel et al., 1986) but the exact mechanisms are unclear.

The underlying molecular basis of kyphosis requires further definition so as to broaden understanding of this idiopathic disease. The group in Wisconsin have yielded interesting results in relation to association between kyphosis and vitamin D, but there remains a need to confirm this on farms in the UK. The only study investigating the association between kyphosis and vitamin A suggested that excessive feeding of vitamin A to sows drives kyphosis in resultant offspring (Belsue, 2010). But this also demonstrated the requirement for more work to investigate the association. There are still questions remaining such as: which genes and pathways are vitamin A interacting with that explains its mechanistic association with kyphosis, and is vitamin A potentially antagonising serum vitamin D in kyphotic pigs? Furthermore, there remains a need to further characterise vitamin A's roles in trabecular bone development, so as to broaden understanding of vitamin A's roles in bone growth. The aim of the thesis was to elucidate the molecular basis of kyphotic tissues, understand how excessive vitamin A affects the molecular profile of vertebral trabecular bone, and clarify the association between kyphosis and vitamin A, both in terms of the molecular level and antagonism with vitamin D. The knowledge will assist in the design of intervention strategies for kyphosis and broaden understanding of vitamin A's roles in maintaining skeletal health, all of which will contribute to the health and welfare of commercial pigs.

1.2 Skeletal Development

1.2.1 Endochondral Bone Growth

There are 4 types of bone that exist within all vertebrates: long, short, flat or irregular. A typical bone can be classed into having separate compartments: cortical, or compact, bone composes the outer, dense layer of the tissue (Thibodeau and Patton, 2010); meanwhile trabecular bone consists of a network of connections in a spongy-like structure on the endosteal, or inner, surface of cortical bone (Kenkre and Bassett, 2018). The vertebral column, otherwise known as the spine, is composed of separate, singular bones called vertebrae, which are classed as irregular bones (Thibodeau and Patton, 2010). The vertebral column is composed of a total of 5 constituents: the cervical, thoracic, lumbar, sacrum and coccyx sections (Thibodeau and Patton, 2010) (Figure 1.1). The vertebral body itself is composed of unique, defined sections, but the main body of the vertebrae consists of trabecular bone surrounded by a layer of cortical bone (Müller-Gerbl et al., 2008). Adjacent to vertebral bodies are sections of articular cartilage which make up the intervertebral disc (Thibodeau and Patton, 2010).

There are various cell types that compose bone tissues, and these can be summarised into: osteoblasts, osteoclasts, chondrocytes, and adipocytes (Burr and Allen, 2014). Osteoblasts, chondrocytes, and adipocytes are all derived from a mesenchymal stem cell (MSC) lineage (Burr and Allen, 2014), while osteoclasts are multinucleated cells of a monocyte/macrophage lineage (Hoebertz et al., 2003). Overall, skeletal development can be classed into two processes: intramembranous ossification and endochondral ossification; both of these processes initially begin with MSCs condensing into locations that define the architecture of the skeleton. In regards to intramembranous ossification, MSC condensation occurs, and these cells differentiate into osteoblasts to directly synthesise bone tissue in regions such as the skull or collarbone (Burr and Allen, 2014). Osteoblasts, termed “bone-formation cells”, produce various matrix proteins that compose bone extracellular matrix (ECM) including type 1 collagens, and non-collagenous proteins such as osteocalcin (Kim et al., 2012). Osteoblasts also play a role in bone mineralisation through contributing to hydroxyapatite crystal formation, which forms the mineral component of bone (Kenkre and Bassett, 2018). On the other hand, endochondral ossification is a more complex process

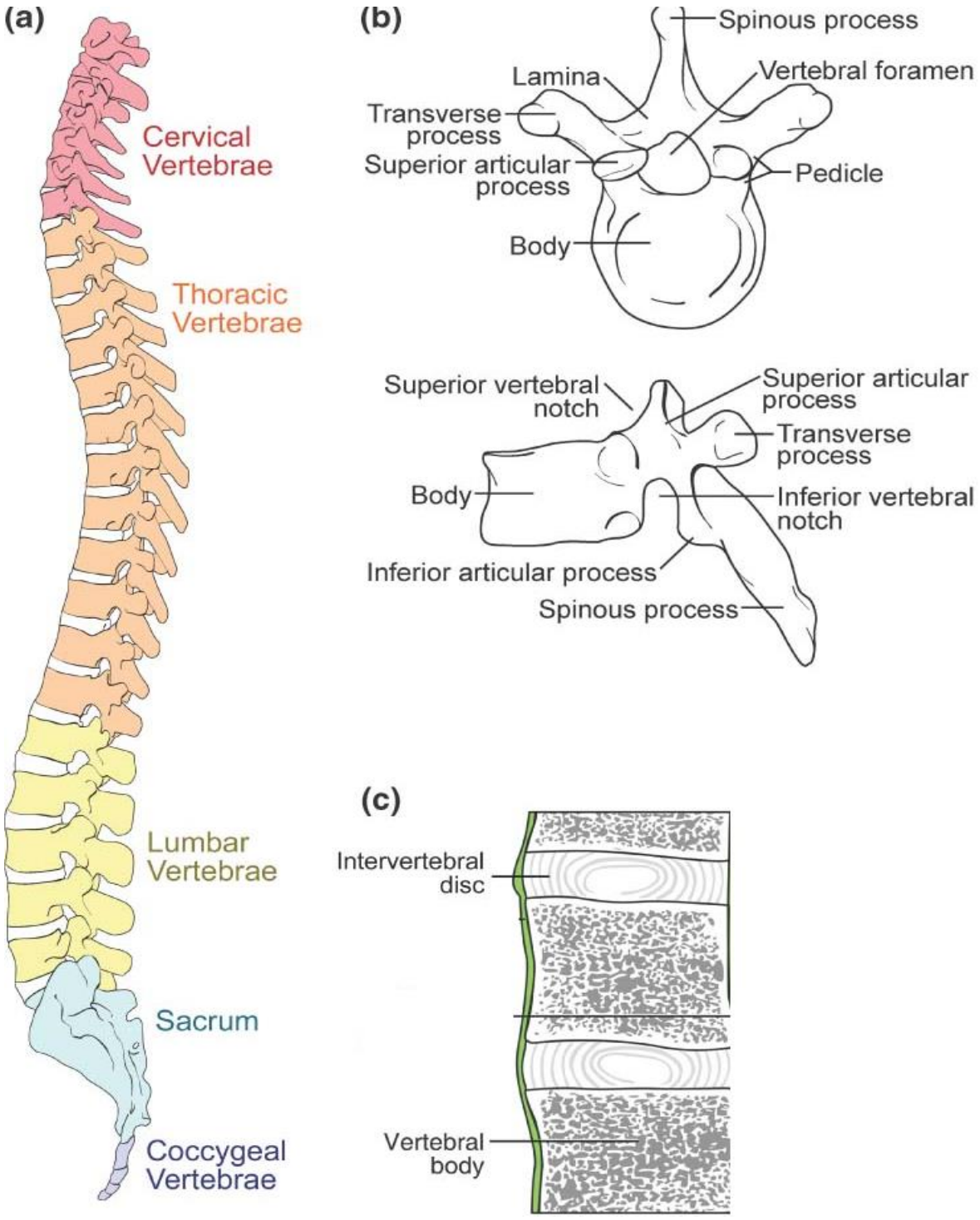

Figure 1.1: A. *The vertebral column is composed of 7 cervical, 12 thoracic, 5 lumbar, 1 sacrum, and 1 coccyx vertebrae in adult mammals.* ***B.*** *Individual vertebrae are composed of defined structures, but the main vertebral body consists of trabecular bone surrounded by a layer of cortical bone.* ***C.*** *Intervertebral discs composed of articular cartilage are layered between individual vertebrae to provide mobility to the spine. Adapted from DayDreamAnatomy (2017)*

which can be classed into two overall steps: chondrogenesis, followed by ossification. MSCs produce an ECM composed of type 1 collagens which forms the future template of the developing skeleton; these cells subsequently differentiate into proliferating chondrocytes, which produce an ECM composed of type 2 collagens (Karsenty et al., 2009). Chondrocytes continue to proliferate, and differentiate into hypertrophic chondrocytes which produce type X collagen, at this stage conditions are achieved such that the ECM surrounding hypertrophic chondrocytes is ready for mineralisation (Karsenty et al., 2009).

Vascular invasion occurs at the site of hypertrophic chondrocyte maturation and this results in the formation of a primary centre of ossification (POC), it is within this region that osteoblast precursors, osteoclasts and epithelial cells are delivered to the cartilage (Maes et al., 2010, Kenkre and Bassett, 2018). Differentiated osteoblasts at the site initially lay down an ECM rich in type 1 collagen on top of the type X ECM, and this contributes to the formation of trabecular bone, meanwhile osteoblasts delivered to the perichondrium, or outer bone surface, deposit and form cortical bone (Karsenty et al., 2009, Berendsen and Olsen, 2015). In the structure of mineralised bone tissue are osteocytes, which were formerly osteoblasts, and these compose the lacunae of compact bone (Thibodeau and Patton, 2010). Calcification of the matrix results in death of chondrocytes and vascular invasion from primary blood vessels delivers endothelial cells to the template in order to form bone marrow (Yang et al., 2014, Maes et al., 2010, Karsenty et al., 2009).

As bone continues to develop in this manner, the POC expands and secondary ossification centres form on the ends of long bones, afterwards the epiphyseal growth plate develops on the ends of long bones (Berendsen and Olsen, 2015). The epiphyseal growth plate is an essential component which determines overall longitudinal bone growth. The growth plate is composed of several zones which underpin its structure and function, however it is in its fourth region in which hypertrophic chondrocytes differentiate; as chondrocytes in the growth plate become hypertrophic, they express genes such as *RUNX2* and Matrix metalloproteinases (*MMPs*) to degrade the ECM, and allow vascular invasion and subsequent mineralisation of matrix by osteoblasts (Woods et al., 2007, Burr and Allen, 2014). The combined actions of osteoblasts, chondrocytes and osteoclasts, to remove calcified matrix before new bone is laid down by Osteoblasts, govern bone growth and modelling (Burr and Allen, 2014). The continuous mineralisation of the hypertrophic zone of

the growth plate allows for the growth of bones throughout life, eventually resulting in the thinning of the growth plate during puberty in humans (Berendsen and Olsen, 2015). Endochondral bone growth is a complex process which remains a key area of heavy research interest, and is essential for healthy growth and development of the organism.

1.2.2 Bone Remodelling

In contrast to osteoblasts and their roles in the regulation of bone formation, bone resorption is a process in which bone tissue is dissolved, and this is regulated by osteoclasts. During endochondral bone growth, osteoclasts have been observed to control skeletal shape through initiating resorption on the periosteal surface of bones to preserve the structure of the diaphysis (Kenkre and Bassett, 2018). Mature bone undergoes continuous remodelling, and the essential reasons for this are to alleviate skeletal damage, prevent the development of over-mineralised and brittle bones, and to maintain Calcium (Ca) and Phosphorus (P) homeostasis in bone and serum (Kenkre and Bassett, 2018). Osteoclasts migrate to bone surfaces and secrete proteolytic enzymes, predominantly Cathepsin K (CPK), to dissolve and remove the mineral component of bone as well as collagenous matrix (Hoebertz et al., 2003).

1.2.3 Maintenance of Articular Cartilage

The process of endochondral bone growth and bone remodelling defines the roles that cartilage and bone tissues play in the growth of the skeleton. However the articular cartilage, which composes the intervertebral disc, is also very relevant to bone biology. Articular cartilage is a unique tissue composed of collagen and proteoglycan (PG)-rich ECM, and the intervertebral disc provides the tissue with its ability to resist spinal compression and provide limited stability to the skeleton (Craddock et al., 2018, Adams and Roughley, 2006). Mature chondrocytes synthesise collagen, glycosaminoglycans (GAGs) and PGs to maintain the structure of the articular cartilage; PGs and GAGs also attract water molecules to give the disc its osmotic properties (Woods et al., 2007). Families of large and small PGs, such as Aggrecan and Decorin respectively, are dispersed among the nucleus pulposus (NP) and annulus pulposus (AP) of the intervertebral disc (Melrose et al., 2001). The combinations of type 2 collagens and PGs such as aggrecan provide the disc with its characteristic tensile and ability to resist tensile forces, indeed age-associated cartilage

degeneration is associated with loss of PGs such as aggrecan (Craddock et al., 2018). Small-leucine rich proteoglycans (SLRPs) are another class of PGs observed in articular cartilage that compose the structure of the tissue; this specialised class of PGs hold small protein cores (36 kildaltons (kda) to 42 kda) and undergo post-translational modifications that allow them to perform their functions (Nikitovic et al., 2012). These modifications present SLRPs with side chains such as chondroitin, dermatan sulfate, or keratin sulfate (Nikitovic et al., 2012). Active SLRPs are involved in the generation of type 1 collagen fibrillogenesis (Burton-Wurster et al., 2003), maintain chondrocyte differentiation, and ensure GAG production is consistent throughout the growth of the tissue (Salinas and Anseth, 2009). The intervertebral disc is another constituent of bone biology that requires maintenance in order to contribute to healthy skeletal growth.

1.3 Genetic Control of Bone Growth

1.3.1 TGF-β and RANK Canonical Signalling Pathways

As discussed above, the processes of bone and cartilage growth are extensive, unique, and diversely complex. The differentiation and function of osteoblasts and osteoclasts, from MSCs and macrophage precursors respectively, are tightly controlled by a variety of molecular signalling pathways. Should the lineage commitments of these cells become unbalanced, this is detrimental in the pathogenesis of various bone disorders; for example, enhanced adipogenesis of MSCs within bone marrow is associated with the development of osteoporosis and reduced bone mineral density (BMD) (Justesen et al., 2001, Kindblom et al., 2005). Increased bone resorption activity or a reduction in osteoblast cell numbers have also been attributed to osteoporosis (Li et al., 2011, Ruiz-Gaspa et al., 2010, Rodan and Martin, 2000). Understanding how molecular and biochemical pathways control these delicate processes is essential in order to pinpoint the mechanisms by which abnormalities in bone development can arise.

Examples of critical pathways that control endochondral bone growth, for bone and cartilage tissues, include: Indian Hedgehog (IHH), Bone Morphogenetic Protein (BMP), Transforming-Growth factor – Beta (TGF- β), and Wnt signalling pathways (Kronenberg, 2003, Westendorf et al., 2004) (Figure 1.2). Mutations in genes belonging to the TGF- β and

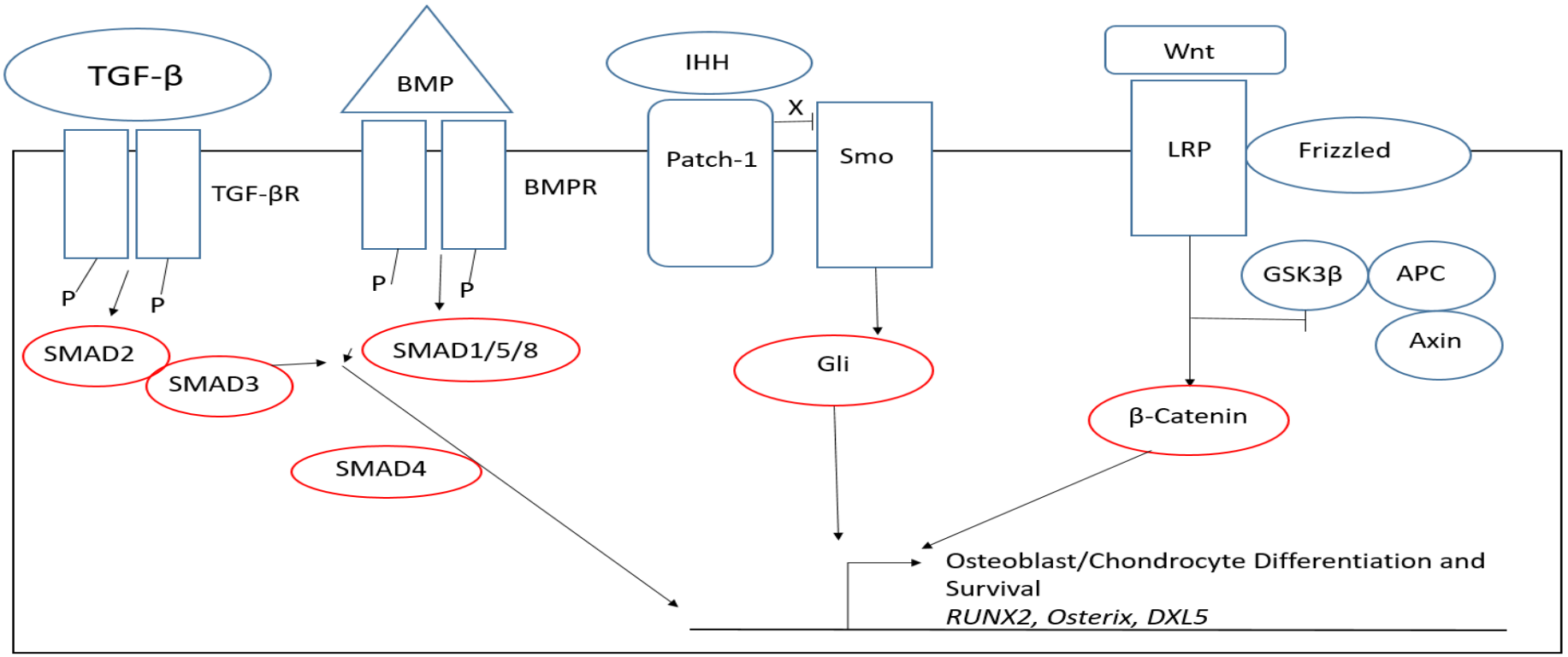

Figure 1.2: *A summary of the different molecular signalling pathways that control chondrocyte and osteoblast differentiation. TGF-β binds to its receptor, which initiates phosphorylation of Smad2 and Smad3, the complex also binds Smad4 and trans-locates to the nucleus to control gene expression. BMPs bind to their receptors and initiate phosphorylation of Smad1/5/8, of which also associates with Smad4 and trans-locates to the nucleus. Hedgehog ligands bind to receptor Patch-1, and removes its inhibitory effect on Smoothened receptor. This allows for accumulation of Gli, which trans-locates to the nucleus to control gene expression. Wnt ligands bind to Frizzled receptor, which then associates with LDL co-receptor. The resultant complex disassociates the GSK3β, APC, Axin complex, which allows for accumulation of β-Catenin in the cell, which trans-locates to the nucleus to control expression of target genes.*

BMP pathways are associated with the development of skeletal diseases (MacFarlane et al., 2017). The BMP signalling pathway, a component of the TGF- β signalling pathway, regulates skeletal development through controlling the differentiation of embryonic stem cells into osteoblasts, osteoclasts and chondrocytes. Activated BMP receptors, upon ligand binding, phosphorylate Smads 1,5, and 8; this trimeric complex then associates with smad4 and the complex translocates to the nucleus to control gene expression (Wan & Cao 2005; Kamiya et al. 2016). In addition, there is also evidence that BMPs can control MAPK or Erk signalling to control chondrocyte and osteoblast differentiation (Wan and Cao, 2005). BMPs are able to commit MSCs into osteoblasts, particularly through upregulating Runt-related transcription factor 2 (*RUNX2*) or distal homeobox-5 (*DXL5*) which in turn regulates osteoblast specific genes such as osteocalcin and osteopontin (Manolagas, 2000). While BMPs concern committing progenitor cells towards an osteoblast lineage, it is through growth factors such as TGF- β that the differentiation and replication of commited osteoblast progenitors is initiated. Upon ligating to a TGF- β I or TGF- β II receptor, phosphorylation of smad2/3 and smad4 proteins are induced and the resultant complex translocate into the nucleus to initiate the expression of osteoblastic genes, such as *RUNX2*, that commit the cell to an osteoblastic lineage (Chen et al., 2012). TGF- β has also been observed to have an effect on positively regulating chondrocyte differentiation: incubation of TGF- β with MSCs, alongside dexamethasone treatment, induces chondrogenesis, marked by increased gene expression of type II collagen. In addition to the regulation of mineralisation, TGF- β and BMP pathways also regulate genes such as *VEGF* to control angiogenesis and blood vessel formation (Goumans et al., 2009), which is required for endochondral bone growth (Maes et al., 2010).

Signalling pathways which contribute to osteoclast differentiation include: IKK, JNK, p38, ERK and Src (Boyle et al., 2003). Src and ERK signalling contribute to cytoskeletal rearrangement to allow for cell motility and adhesion, while the other pathways, including Notch signalling, control expression of osteoclast transcriptional factors such as *NFAT2* (Boyle et al., 2003, Jin et al., 2016). In physiological conditions, these pathways are controlled by the RANK signalling network, composed of Receptor Activator Of Nuclear Factor-Kappa B ligand (RANKL) binding to Receptor Activator Of Nuclear Factor-Kappa B (RANK) on the surface of macrophage precursors (Boyle et al., 2003, Boyce and Xing, 2007).

Osteoblasts have a degree of control over the RANK-RANKL axis through producing Osteoprotegerin (OPG), which acts as a decoy receptor for RANKL and prevents its bindingto RANK (Boyce and Xing, 2007). *CSF1* is another regulator of osteoclast differentiation, and initiates proliferative effects on osteoclasts through activating PI3K and Erk signalling (Ross, 2006).

1.3.2 Contributions of Cytoskeletal Dynamics to Bone Development

Another factor to consider in relation to regulation of endochondral growth and bone remodelling, aside from traditional receptor-ligand interactions and initiation of intracellular signalling, is that of the cellular cytoskeleton. The cytoskeleton is present in all eukaryotic cells and is composed of a total of 3 protein networks: actin microfilaments, microtubules and intermediate filaments (Lomri and Marie, 1996, Wangping et al., 2014). Actin filaments arise as a result of polymerisation of actin proteins, microtubules are composed of tubulin proteins, and intermediate filaments are composed of proteins such as vimentin (Langelier et al., 2000) . As a result of the organisation of these networks, the cytoskeleton provides morphology and motility to the cell. It has been demonstrated that disruption of either the microtubule or intermediate filaments of the cytoskeleton results in cellular apoptosis and inability to maintain cartilage ECM in chondrocytes (Wangping et al., 2014), and rearrangement of actin filaments has been shown to associate with osteoblast-mediated mineralisation *in vitro* (Goncharenko et al., 2016). Cells have specialised receptors on the surface termed integrin's, composed of various αβ heterodimers, which substrates such as TGF- β may interact with (Munshi et al., 2004). Additionally, integrin's on the surface of osteoblasts are able to adhere to and interact with the ECM; upon adherence, ECM proteins stimulate osteoblast differentiation through binding integrin's and initiating pathways such as Extracellular signal related kinase (ERK) and Focal adhesion kinase (FAK) to control *RUNX2* expression and alkaline phosphatase (ALKp) activity (Oh et al., 2017, Moussa et al., 2014).

The mechanical linkage between the cell and the ECM, that allows adherence between cellular integrin's and the ECM, is referred to as a focal adhesion complex, and the formation of these complexes are regulated by the actin cytoskeleton (Lomri and Marie, 1996). Reorganisation of the actin cytoskeleton is required to induce morphological changes in the cell, and these are associated with initiation of mineralisation activity in osteoblasts *in*

vitro (Goncharenko et al., 2016). Cytoskeletal reorganisation is also observed in response to integrin-mediated adhesion and subsequent differentiation of osteoblasts through ERK signalling (Hendesi et al., 2015). Furthermore, other studies have shown the composition of ECM proteins is able to influence the cytoskeletal arrangement of the osteoblast (Demais et al., 2014), and disorganisation of the cytoskeleton results in impaired morphology and differentiation of osteoblasts (Lomri and Marie, 1996). Cytoskeletal reorganisation is also very critical in controlling the differentiation of chondrocytes; this is based on evidence in which cytoskeletal reorganisation in embryonic stem cells (ESCs) was required in order to allow for the expression of differentiation factors such as SRY-Box 9 (*SOX9)* (Zhang et al., 2006). Indeed, arrangement of the actin cytoskeleton has been demonstrated to induce a rounded cellular morphology of chondrocytes and this is consistently association with differentiation of chondrocytes (Loty et al., 1995, Zhang et al., 2006). There is additional evidence indicating actin reorganisation is also required for chondrocytes to enter a hypertrophic state prior to endochondral ossification (Woods et al., 2007). Aside from cell-matrix interactions, cell-cell interactions can additionally influence the differentiation of chondrocytes, one such gene that regulates adhesiveness between cells is N-cadherin, which not only contributes to cytoskeletal function independently, but downstream targets can include the Rho-GTPases (Woods et al., 2007). Cell surface integrin's are also on the surface of osteoclasts: in particular the αVβ3 complex, upon ligand binding, induces cytoskeletal reorganisation in order to allow formation of actin rings within the ruffled border membrane, and thus regulate proteolytic enzyme release (Teitelbaum, 2011).

Regulation of actin cytoskeletal dynamics is controlled by a family of molecules termed the Rho-GTPases, these include: Cell Division Cycle 42 (CDC42), Rho, and Rac (Nobes and Hall, 1995). A summary of Rho GTPase signalling can be viewed in Figure 1.3. Further evidence which demonstrates the cytoskeleton's role in osteoclasts shows the mRNA expression of *CDC42* is required for osteoclast differentiation and bone resorption activity *in vitro* (Ito et al., 2010). The Rho-GTPases switch between GTP-bound and GDP-bound states, representing activation and inactivation respectively, and these are regulated by Rho guanine nucleotide exchange factors (Rho-GEFs) (Gao et al., 2011). Active CDC42 and Rac can induce phosphorylation of p-21 activated kinase (PAK) to control lamellipodia and fillopodia formations in the actin cytoskeleton, which ultimately contribute to

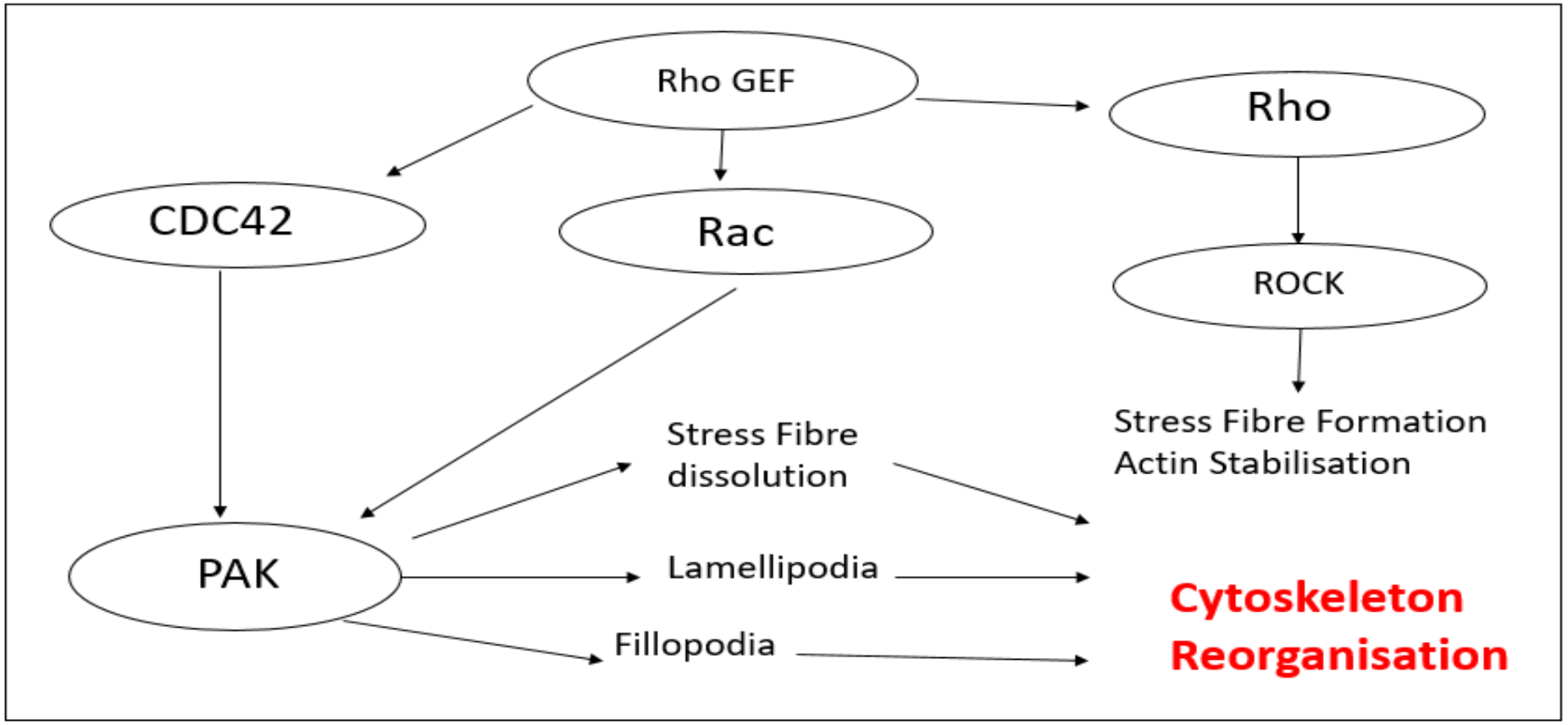

Figure 1.3: *An overview of Rho-GTPase signalling. Rho GEFs stimulate GTP binding to Rho-GTPases, allowing for their activation. Through phosphorylating and interacting with various downstream molecules, notably PAK and ROCK, the Rho-GTPases contribute to the formation and reorganisation of cytoskeletal components. The formation of stress fibres maintains adherence to the ECM.*

rearrangement and extension of the cytoskeleton which comes to define cell morphology and motility (Hoefen and Berk, 2006, Rane and Minden, 2014, Nobes and Hall, 1995). PAKSs may also phosphorylate and activate a variety of other molecules in order to stabilise polymerised actin structures, these include: myosin light chains, filamins, and LIM kinases (Rane and Minden, 2014). Rho signals through Rho-associated, coiled-coil containing protein kinase (ROCK) in order to regulate stress fibre formation, which are polymerised actin structures that maintain focal adhesions, Rho-ROCK signalling has also been demonstrated to directly influence *SOX* gene expression and the differentiation of chondrocytes to a hypertrophic state (Woods et al., 2007, Rane and Minden, 2014). In contrast, PAKs can contribute to stress fibre dissolution (Rane and Minden, 2014), although this an event required for reorganisation of the cytoskeleton (Zhang et al., 2006). Therefore the actions of Rho-GTPases and their subsequent effects on cytoskeletal reorganisation and focal adhesion maintenance, through affecting fillopodia, lamellipodia and stress fibre polymerisation, must be coordinated in order to allow for regulation of cell morphology, motility and contact with the ECM.

1.4 Idiopathic Lumbar Kyphosis

1.4.1 Aetiological and Epidemiological Findings

Kyphosis, also referred to as “humpy-back” syndrome, persists in commercial pigs (Figure 1.4) (Done and Gresham, 1988, Done et al., 1999). The mature spine does require some degree of curvature in order to provide balance, support and strength (Thibodeau and Patton, 2010), but the characteristic, abnormal curvature at the thoraco-lumbar junction in kyphosis represents an unusual case of spinal development. Although kyphosis does not cause any obvious signs of pain in affected animals, it poses various challenges, with regards to economic consequences and the compromise of welfare, to the commercial producing industry. Inflicted pigs have been reported to have growth rate severely slowed in the finisher phase, often failing to reach slaughter weight (Straw et al., 2009), and further complications arise with handling the carcass within automatic slaughterhouse systems (Holl et al., 2008). From a welfare perspective, veterinary observations have observed a compression of the spinal cord between kinked vertebrae in severely affected animals, resulting in clinical signs of weakness and partial paralysis (Done and Pearson, 2004).

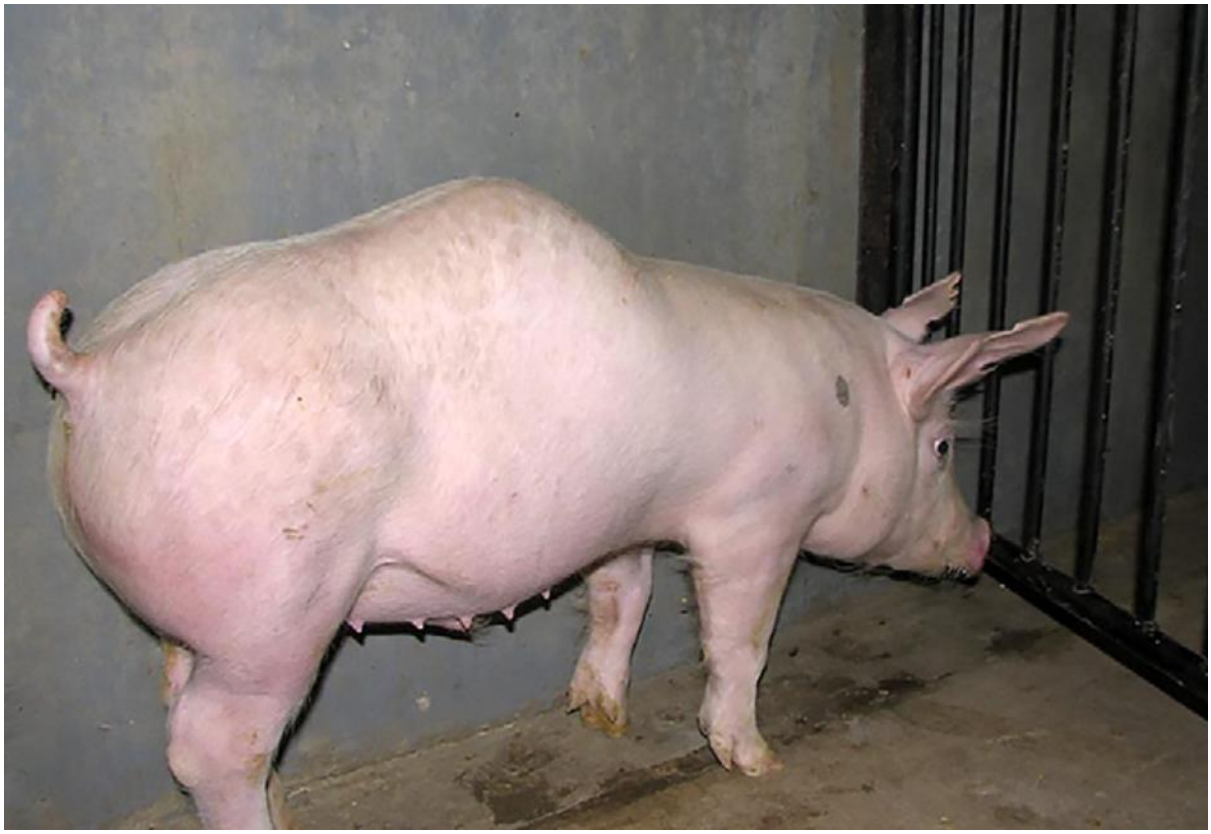

Figure 1.4: *A clinical presentation of a severe case of kyphosis, characterised by the noticeable rising of the spine at the thoraco-lumbar junction, giving a "humpy-back" appearance. Adapted from Halanski et al. (2018).*

The information available in the literature indicates that, in 1988, the average prevalence of pigs affected within herds was 4.5% (Done and Gresham, 1988) and in 2005 a prevalence up to 11.4% was observed in herds (Straw et al., 2009). The disease has been identified on a global scale with cases appearing in the USA (Rortvedt and Crenshaw, 2012), Spain (Pallarés et al., 2013), Canada (Drolet et al., 2012), Denmark and Sweden (Straw et al., 2009); and was first identified on British farms in 1979 (Penny and Walters, 1986). In addition, symptoms have ranged in new-born pigs up to pigs weighing 60kg (Done and Pearson, 2004, Done and Gresham, 1988). In several cases, the condition has been attributed to having a genetic basis (Done et al., 1999, Done and Pearson, 2004), and additional work has been done in order to verify this association (Lindholm-Perry et al., 2010, Holl et al., 2008), but this is still up for debate among the academic and commercial communities.

1.4.2 Clinical Presentation of Kyphosis

The “humpy-back” syndrome has appeared sporadically among UK pig units, presenting at least 4 different variants of the disease, each characterised by their own aetiology and post-mortem appearance. Penny and Walters (1986) first identified the disease on UK farms and observed indoor pigs, aged 3 weeks to 16 weeks of age, to develop symptoms on breeding and fattening farms. Done and Gresham (1988) observed a seasonal effect in that cases appeared after December, affected pigs had lower Ca and P values in bone, and there was occasional widening of the intervertebral disc. In a second variation of the disease, Done et al. (1999) observed the development of hemi-vertebrae within the thoracic region of affected pigs, and animals aged as early as 3-4 weeks showed symptoms. Nielsen et al. (2005) also observed hemi-vertebrae in kyphotic pigs in a separate case, and also noted insufficient vessels in these regions and incomplete mineralisation of the tissue. In a third variation, Done and Pearson (2004) observed the presentation of kyphosis was characterised by collapsing and loosening of intervertebral disc space between the 13th thoracic and 1st lumbar body of the spine. In this case, pigs showed clear signs of leg weakness and tremors, likely as a result of entrapment of the spinal cord. In Canada, another variant of kyphosis was observed in which piglets, up to 2 weeks of age, showed the characteristic symptoms with 6 out of 11 animals also showing signs of Alopecia Areata (AA), of which is an autoimmune disorder that results in hair loss (Drolet et al., 2012). Upon further examination it was also discovered that the thoracic rib-cages of humpy-back pigs bore multiple fractures one each side, along with nodular callus which appeared to be composed of demineralised cartilage (Drolet et al., 2012).

These observations highlight kyphosis as a serious skeletal disease, but the biological basis of these aetiological changes remains unknown. No studies as of yet have attempted to investigate how genes and pathways relating to endochondral bone growth or bone remodelling are affected within the tissues of kyphotic pigs, and this presents a significant gap in our understanding of the disease.

1.5 Nutritional Influence on Bone Development

1.5.1 Calcium and Phosphorus

The processes of bone metabolism are tightly controlled by present biological factors in the body such as the cell cytoskeleton, and genetically coded growth factors such as TGF-β. Yet, external factors are able to form interactions with genetic and cellular machinery in order to define bone development in the organism, and one of these key external influences is nutrition. The minerals Ca and P are vital constituents that compose 98% and 80%, respectively, of the skeleton, and these are required to be obtained from the diet (Whittemore and Kyriazakis, 2006). The hydroxyapatite crystal, which composes the mineral component of bone, predominantly consists of Ca and P [Ca_{10} ($P0_4$)$_6$(OH) $_2$], this crystal composes bone tissue alongside type 1 collagens, non-collagenous proteins and bone cells (Kenkre and Bassett, 2018). Consequently, a deficiency in the intake of Ca has significant effects on bone development. A reduction in dietary Ca intake induces bone resorption through a combined activation of Parathyroid Hormone (PTH) and 1,25$(OH)_2$D, the dissolving of Ca from bone as a result of osteoclasts allows serum Ca to be restored (Eklou-Kalonji et al., 1999, Lieben et al., 2012). In a separate study, low dietary Ca was found to reduce BMD in neonatal pigs (Mahajan et al., 2011). Aside from exerting control over bone resorption, *in vitro* evidence also indicates Ca may directly influence expression of osteoblast transcription factors such as *RUNX2* (Mahajan et al., 2011), and is required for matrix mineralisation in combination with Vitamin D (Tourkova et al., 2017).

The source of P in commercial diets is of plant origin and 2/3rds of supplementation consists of Phytate; this form of P is not readily digested in pigs therefore phytase is added in diets in order to allow for greater utilisation of P (Simons et al., 1990). P is a critical nutrient in maintaining bone development, a deficiency of P in diets clearly reduces bone mineral content (BMC) and BMD in pigs (Liesegang et al., 2002, Rortvedt and Crenshaw, 2012). P homeostasis is not as well clarified as Ca, but *FGF23* has been identified as a regulator which controls P absorption from intestines, and reabsorption from kidney and bone (Crenshaw et al., 2011, Jurutka et al., 2007). Supplementation of Ca and P to growing pigs, without unbalancing the ratios between the two minerals, increases dry weight of the femur and tibia, as well as overall ash content (Nicodemo et al., 1998). Additional research also shows

bone breaking strength to increase in growing pigs fed a diet containing 0.65% Ca in comparison to 0.4% Ca (Libal et al., 1969). The authors also observed increasing the ratio of inorganic P to dietary Ca, from 0.3% of P to 0.7% of P, resulted in increases in bone breaking strength in comparison to pigs receiving 0.3% of P (Libal et al., 1969).

This scientific evidence initially showcases the requirement of nutrition in relation to bone biology, and demonstrates how the processes of skeletal growth are influenced by nutritional input. Ca and P, however, are nutritional compounds that require homeostatic maintenance within a biological system, and one key regulator of these minerals, which also holds important roles in bone development, is vitamin D.

1.5.2 Vitamin D

1.5.2.1 Metabolism

Vitamin D is a fat-soluble nutrient that is obtained either from the diet, or is synthesised in the skin upon UV exposure (Chen et al., 2010). Upon integration into circulation, vitamin D is first delivered to the liver where it is metabolised to 25(OH) D, and this metabolite is transferred to the kidney where it is further metabolised to 1,25$(OH)_2$D (Holick, 2005). This particular metabolite is the form of vitamin D which binds vitamin D receptors (VDRs) in target tissues. Upon ligand binding, VDRs have the potential to form heterodimers with RXRs, or RARs, and the resultant complex trans-locates to the nucleus to control the expression of genes which hold vitamin D responsive elements (VDREs) (Schrader et al., 1993).

It is well-established that vitamin D, through influencing appropriate gene expression in target tissues, is responsible for mediating the absorption of Ca and P from intestines and reabsorption from kidney and bone (Haussler et al., 1997, Jurutka et al., 2007). In pigs, vitamin D supplementation has documented benefits in bone health, these include increasing cortical and total bone BMD and BMC, as well as the length of long bones (Witschi et al., 2011). Different doses of vitamin D, in the form of D3 or 25(OH)D, have also been tested experimentally, and above 800IU supplementation of D3 has been shown to improve bone strength in gilts (Lauridsen et al., 2010). In addition, vitamin D supplementation has also been reported to improve live weight of weaned pigs (Tousignant

et al., 2013), and increase the average litter weight of piglets born from sows which received 25(OH) D supplementation (Coffey et al., 2012). Vitamin D, therefore, remains an item of significant interest to the producing industry.

1.5.2.2 Relevance to Kyphosis

It is established that one of the major consequences of vitamin D deficiency is the development of rickets, characterised by a failure in endochondral ossification (Madson et al., 2012). In 2012, the adverse effects of vitamin D deficiency were further demonstrated when Rortvedt and Crenshaw (2012) established a model of kyphosis in piglets that could be induced by reducing availability of Vitamin D to the sow. They observed piglets born from Vitamin D-deficient sows, combined with nursery diets deficient in Ca and P, showed the characteristic signs of kyphosis by 13 weeks of age (Rortvedt and Crenshaw, 2012) . The implication of sow involvement suggests entire litters are at risk of developing kyphosis. Another observation by Rortvedt and Crenshaw (2012) was that all pigs that did show signs of kyphosis had been on a nursery diet deficient in Ca and P, but piglets born from vitamin D deficient sows at week 13 showed 32% prevalence, as opposed to piglets born from vitamin D adequate sows which showed 26% prevalence. In a separate study, supplementing sows with vitamin D increased serum Ca and P values in resultant offspring (Amundson et al., 2017). Complementing this, the authors also observed BMC to be lowered in pigs fed a diet deficient in Ca and P, in comparison to pigs fed a diet adequate in Ca and P, within both maternal dietary groups; and at week 9, pigs born from vitamin D deficient sows showed reduced BMD (Rortvedt and Crenshaw, 2012). Further work also demonstrated that *BGLAP* expression, a gene which regulates bone mineral deposition, in the bone of piglets was higher in response to those born from sows fed increased dietary Vitamin D, but there was no relationship established with dietary Ca and P (Amundson et al., 2016, Amundson et al., 2017). The results from these studies make it clear that availability of Ca, P and vitamin D can contribute to the development of kyphosis, but it is with vitamin D that there are links to expression of bone metabolic genes and maintenance of serum Ca and P. These would suggest that vitamin D is the critical driver in kyphosis. Furthermore, in a separate trial, the hypovitaminosis-D kyphotic pig model was characterised in further detail, and it was observed, in line with previous observations, that kyphotic pigs showed incomplete

mineralisation of growing bones, accompanied by an increase in un-ossified hypertrophic chondrocytes (Halanski et al., 2018).

However in these studies, the pigs received specified dietary treatments of Vitamin D, Ca and P in controlled conditions, and the findings may not represent spontaneous kyphosis that occurs on affected farms. There remains a need to confirm if Vitamin D is associated with the development of kyphosis on farms that suffer from outbreaks, in order to determine if the molecular, histological and bone parameter findings from these studies are relevant to spontaneous cases. In addition to vitamin D, evidence now suggests there is a relationship between kyphosis and vitamin A (Belsue, 2010).

1.5.3 Vitamin A

1.5.3.1 Absorption, Storage and Metabolism

Vitamin A is a fat-soluble micronutrient that is essential for controlling physiological processes due its ability to regulate the expression of hundreds of genes relating to stem cell differentiation and development of tissues (Kedishvili, 2013). Primary sources of Vitamin A include Retinyl esters (REs), long-chained fatty acid esters of retinol, and provitamin A carotenoids from the diet. REs are hydrolysed in the intestinal mucosa to retinol, or are re-esterified and incorporated into chylomicrons, and are absorbed into the lymphatic system (Marill et al., 2003, Harrison, 2005). Vitamin A is then stored as REs in stellate cells in the liver; REs are hydrolysed to retinol, which binds serum-retinol binding proteins, which is the form of Vitamin A which is delivered to tissues (Harrison, 2005). RE concentrations of up to 30-250 mg per kg of liver (approximately 0.09-0.827µmol/g of liver) have been observed in pig liver (Scotter et al., 1992), additionally Majchrzak et al. (2006) reported RE concentrations in commercial pigs ranged from 6.5 to 18.9mg per 100g of liver (approximately 0.215-0.625µmol/g of liver). Upon delivery to target tissues, Retinol undergoes a dehydrogenation reaction to convert into retinal, which is converted into all-trans retinoic acid (ATRA) by retinal dehydrogenases (Kedishvili, 2013). Another retinoic acid isoform that exists physiologically is 9-cis retinoic acid (Levin et al., 1992).

Retinoic acid serves as the active metabolite of Vitamin A; it exerts its effects on tissue development through binding one of three isoforms of the retinoic acid receptor (RAR), RARα, RARβ or RARG, which trans-locates to the nucleus and initiates expression of target

genes (Jacobson et al., 2004). Additionally, co-receptors associate with RARs known as Retinoid-X-receptors (RXRs), and agonist-stimulation of both of these receptors results in significantly greater transcriptional activity (de Lera et al., 2007). RXRs also exist to co-stimulate transcriptional events in response to other compounds, such as PPARs and Vitamin D (de Lera et al., 2007, Zierold and DeLuca, 1998). RAR isoforms are predominant targets of ATRA, whereas 9-cis retinoic acid has shown a higher affinity for RXRs (Levin et al., 1992). Both Osteoblasts and Osteoclasts express RAR isoforms (Conaway et al., 2011, Jacobson et al., 2004), therefore retinoic acid isoforms have the potential to control gene expression in both of these cell types and regulate bone formation and resorption processes.

1.5.3.2 Vitamin A requirements for Pigs

There is no global accepted standard for the specific nutritional requirements of pigs. Various manufacturers have contrasting claims as to the amounts of vitamins and minerals required for optimum growth and efficiency. Although it cannot be ruled out that different countries follow different husbandry practices and use different genotypes, figures from DSM reveal the UK supplies higher provisions of vitamin A to its pigs, unlike the US and Canada who follow recommendations from the National Research Council (2012) (Table 1.1). The UK recommends a much higher provision of vitamin A to its pigs, this includes a range of 1500-6000µg/kg of diet for grower diets and 3000-4500µg/kg for lactation and gestation diets (DSM, 2016). This is in contrast to recommendations from NRC in the US, that propose much lower ranges of 390-660µg/kg of vitamin A in grower diets, 1200µg/kg for gestation diets, and 600µg/kg for lactation diets (National Research Council, 2012). In the US recommendations provided by the National Research Council (2012) govern feed composition, recommending an average of 660µg of vitamin A per kg of dry diet to growing pigs. However these findings are in stark contrast to DSM guidelines which recommend almost a 10-fold increase in nutritional supply for Vitamin A to growing pigs (Table 1.1). Although legislation is not restricting Vitamin A concentrations in feeds, EU panels have recommended vitamin A concentrations should not exceed values of 1950µg/kg of feed for fattening pigs, 3600µg/kg of feed for gestating sows, and 2100µg/kg of feed for lactating sows (European Food Safety Authority, 2008).

	Growing Pigs Ranges (5kg-120kg)	*Gestating Sows*	*Lactating Sows*
Vitamin A µg/kg of feed			
NRC (2012)	**390-660**	**1200**	**600**
DSM (2016)	**1500-6000**	**3000 - 4500**	**3000 - 4500**
Vitamin D µg/kg of feed			
NRC (2012)	**3.75-5.5**	**20**	**20**
DSM (2016)	**25-50**	**37.5-50**	**37.5-50**

Table 1.1: *A list of the current recommendations for vitamin A and vitamin D in commercial sow and grower diets, as indicated in µg/kg of feed. Data are adapted from National Research Council (2012) and DSM (2016).*

Indeed feeding vitamin A to pigs approximately 25'000% above EU recommendations raises issues in relation to bone development, these include: destruction and disorganisation of epiphyseal cartilage, and a decrease in length and width of long bones (Wolke et al., 1968). The observation that feeding diets to sows containing 15000mg/kg of vitamin A contributes to kyphosis (Belsue, 2010) further highlights the potential dangers of vitamin A intake.

It is not uncommon in farming practices to supplement animals with vitamin concentrations slightly higher than official recommendations (Whittemore and Kyriazakis, 2006). A survey undertaken by Kansas State University revealed that industries across the US were feeding vitamin A to pigs up to 5 times higher than NRC recommendations in diets (Flohr et al., 2015). A greater understanding of vitamin A's effects on bone development, in which vitamin A is fed excessively above recommendations from organisational bodies, will need to be appreciated in order to provide further evidence of the potential dangers of over-supplementation.

1.5.3.3 Excessive Vitamin A intake and Bone Development

It is established that excessive vitamin A intake contributes to increased risk of fracture in humans, and induces narrowing of cortical bone compartments, which leads to thinner and fragile bones (Kneissel et al., 2005, Lind et al., 2011, Navarro-Valverde et al., 2018, Jackson and Sheehan, 2005). Studies have also demonstrated 300μg/g of Vitamin A in diets to result in focal disappearance of the growth plate with replacement by bony tissue, in rats (Soeta et al., 2000), which was also observed in pigs receiving excessive vitamin A supplementation (Wolke et al., 1968). These would suggest that excess vitamin A intake disrupts endochondral bone growth. Other observations in the hypervitaminosis-A pig model include reduced numbers of osteoblasts within trabecular bone, and decreased length of long bones (Wolke et al., 1968). Osteoporosis, characterised by a reduction in mineralisation of bone matrix, is induced in the rat upon supplementation with 70mg/kg of vitamin A in diets for 14 days (Wu et al., 1996). In addition, increasing serum retinol has been observed to share negative correlations with parameters such as BMD and ALKp activity in osteoporosis patients (Navarro-Valverde et al., 2018). Serum retinol has been analysed in studies to determine Vitamin A intake, and a general consensus is that serum retinol follows a u-curve in relation to BMD risk and osteoporosis, in that low or high concentrations of retinol can contribute to fracture risk (Promislow et al., 2002). However, it has been raised in later years that serum retinol is not the most accurate marker of Vitamin A status, and a review of studies investigating Vitamin A intake and osteoporosis have failed to identify a consistent relationship (Ahmadieh and Arabi, 2011). Nonetheless, the aforementioned studies in pigs clearly show consuming vitamin A above recommendations results in skeletal problems (Wolke et al., 1968, Belsue, 2010). Laboratory studies have given more insight into how the biology of vitamin A associates with skeletal regulation.

In vitro studies have ascertained that vitamin A is able to favour the differentiation and function of both osteoblasts and osteoclasts. Earlier laboratory studies found Retinoic acid, Retinol and β-Carotene all induce Pre-Osteoblastic cell lines towards an Osteoblast lineage (Park et al., 1997). In contrast, ATRA may promote release of *CSF1* from bone stromal cells to commit progenitor cells to an osteoclast lineage (Nakajima et al., 1994). Another study also demonstrated ATRA's ability to inhibit RANK-induced differentiation of progenitor cells

into Osteoclasts, (Hu et al., 2010); and treatment of Osteoblasts with ATRA has been observed to result in an increase in *RANKL/OPG* gene expression ratio (Jacobson et al., 2004). ATRA signalling through RARα has been shown to both upregulate *RANKL* expression (Conaway et al., 2011), and inhibit RANKL-induced osteoclastogenesis in bone marrow monocytes (Balkan et al., 2011). Conversely, other studies have observed that ATRA, acting through RARα or RARγ, downregulates osteoblast associated genes in osteoprogenitors, pre-osteoblasts and mature osteoblasts; and markers of adipogenesis were also observed to be downregulated in response to RAR-stimulation (Green et al., 2017). It is clear from these studies that vitamin A has the potential to favour osteoblast as well as osteoclast-mediated functions in cells, depending upon cell line and experimental conditions. This raises questions as to how vitamin A controls gene expression in whole bone tissue which leads to the characteristic symptoms of vitamin A toxicity.

It has now been determined that, in bone, vitamin A exerts different effects on osteoblasts and osteoclasts depending upon compartment within the tissue. Lind et al. (2011) showed that excess vitamin A intake, in rats, indeed induced narrowing of cortical bone, and that this was associated with increased osteoclast abundance on the periosteal surface of long bones. However, they observed the opposite effect when investigating endosteal and bone marrow compartments: there was increased expression of hypoxia and osteogenic genes in response to excess vitamin A (Lind et al., 2011). Further work from this group showed, via microarray analysis, the upregulation of osteogenic and hypoxia genes in marrow (Lind et al., 2012). A pathway which overlapped between marrow and cortical bone was the Wnt signalling pathway (Lind et al., 2012), and this demonstrates vitamin A's ability to interact with molecular pathways that define the growth and development of bone. Vitamin A's compartment-specific effects are further demonstrated based on observations in which osteoclast cell numbers are significantly induced in the endocranial surface, but not the periosteum or intracranial surfaces, in rats in response to Vitamin A (Lind et al., 2017). In addition, excessive ATRA treatment induces thinning of bones accompanied by increased osteoclast activity in the subperiostal compartments of cortical bone (Kneissel et al., 2005).

There is, however, relatively less information on how vitamin A affects trabecular bone development. Belsue (2010) observed lowering the concentrations of vitamin A in sow diets

removed the prevalence of kyphosis, thereby suggesting excessive vitamin A supplementation is a factor that can contribute to kyphosis. Given that the majority of vertebral bodies is composed of trabecular bone, this raises questions as to how vitamin A has affected the biology of trabecular bone development; however vitamin A's effects on trabecular bone remain relatively unclarified. Short-term exposure (8 days) to excess vitamin A reduces overall density of trabecular bone (Lind et al., 2011), but in other studies involving a longer exposure to vitamin A, there are no obvious changes in trabecular bone density (Kneissel et al., 2005, Wray et al., 2011). This is further complicated by the findings from the hypervitaminosis A pig from Wolke et al. (1968), in which pigs receiving excess vitamin A showed signs of reduced mineralisation within trabecular bone. The requirement for a greater understanding of the effects of vitamin A's effects on trabecular bone have also been raised by other authors (Henning et al., 2015). This is a gap that requires addressing not just to understand the biological mechanisms by which vitamin A is contributing to kyphosis, but also to clarify vitamin A's effects on trabecular bone and thus provide more significant understanding of vitamin A's role in overall bone development.

1.5.4 Vitamin A vs Vitamin D

In addition to regulating gene expression within bone tissue, vitamin A can exert alternative, indirect effects on bone metabolism due to its antagonistic relationship with vitamin D. This holds potential relevance to kyphosis, given that there are indications of vitamin D deficiency in kyphosis (Rortvedt and Crenshaw, 2012), and that there is still no explanation as to how kyphotic pigs on commercial farms are potentially vitamin D -deficient. Growing pigs and sows are recommended an additional thousands of units of vitamin A over vitamin D by all institutional bodies (Table 1.1), therefore antagonism of vitamin D by vitamin A could potentially occur on farms within the UK. Early studies indicated feeding rats with 60000 units of vitamin D induced narrowing of the epiphyses and increased resorption cavities in the diaphysis; however treatment groups receiving additional 30000 units of vitamin A did not show these pathological changes (Clark and Bassett, 1961). Other studies have demonstrated feeding turkeys with a diet high in vitamin A and vitamin D prevents physiological changes associated with vitamin A toxicity such as decreased BMC and tibia length (Metz et al., 1985). Furthermore, Aburto et al. (1998) observed high dietary vitamin A results in an increased requirement for 25(OH) D to maximise bone ash%, and an increased

1,25$(OH)_2$D demand to reduce rickets. Interestingly the authors also noted 1,25$(OH)_2$D decreased liver concentrations of vitamin A, and this effect was greater with birds given a high vitamin A diet (Aburto et al., 1998). It has also been demonstrated that analogues of vitamin D increase serum Ca and decrease serum P concentrations, however treatment with RA alters the ability of vitamin D to maintain these concentrations in a dose-dependent manner. This therefore suggests that RA antagonises vitamin-D mediated effects *in vivo* (Rohde and DeLuca, 2005). Overall, the results of these studies outline a clear antagonistic relationship between the two vitamins in relation to regulation of physiology, yet the exact mechanisms by which these occur have not been fully elucidated.

1.6 Objectives of the Thesis

There are unanswered questions regarding the associations between vitamin A and: trabecular bone development; relationship with vitamin D; and how vitamin A associates with the development of kyphosis. Furthermore, there have been relatively few efforts made to understand the biological basis of kyphotic bone and cartilage tissues. The gaps identified in this review have formed the objectives this thesis will experimentally address:

- Define which genes and molecular pathways are significantly associated with kyphotic tissues
- Confirm how excess vitamin A supplementation affects differential gene expression in trabecular bone, and serum 25(OH) D
- Confirm the associations of vitamin A and vitamin D with kyphotic pigs
- Determine the overlap of differential gene expression between kyphotic and vitamin A supplemented pigs

Chapter 2: Methodologies

2.1 Introduction

In order to investigate the outlined objectives of this research, the thesis utilised two separate pig trials. Samples were obtained from pigs, and appropriate controls, from both trials in order to perform molecular investigations and nutritional analysis in tissue samples representative of kyphosis and excess vitamin A intake. A microarray methodology was performed in both experiments in order to establish a molecular basis within tissues, and samples selected for analysis are indicated. The experimental setup of each trial is discussed in more detail throughout the chapter.

2.2 Kyphosis Trial - Sampling and Experimental Design

The animals used in this study consisted of a total of 97 pigs from 3 different age groups from PIC lines (Genus PIC Inc, Hendersonville, TN) on farms based in the south-east of the UK. Samples were collected from a total of 5 outdoor breeding units and 1 grower unit. Sampling on farms was performed on an ad-hoc basis in which kyphotic cases were present, between April 2015 and March 2016. Pre-weaning and weaning kyphotic cases and age matched controls were obtained from 2 breeding units in April 2015 and a further 3 units in March 2016, making a total of 5 units. Weaning and post-weaning kyphotic cases and age matched controls were obtained from a grower unit in June 2015.

Animals with clear clinical signs of kyphosis, through visual identification of the characteristic kink at the thoraco-lumbar junction, were confirmed and identified by the farmer and veterinary team on all visits. Kyphotic animals from 3 age groups (pre-weaning, weaning and post-weaning) were selected for tissue sampling alongside age-matched controls. The study applied a 3x2 design, 3 age groups and 2 phenotypes, kyphosis or control. Kyphotic pigs in each age group were paired with age and weight matched controls. A summary of the characteristics of all sampled pigs are shown (Table 2.1) For the pre-weaning group only a second control group was selected, so that a kyphotic affected pig

Age Group	*Phenotype*	*N*	*Bodyweight (Average/Kg) (SEM)*	*Litter Size (SEM)*	*Ca (mmol/L) (SEM)*	*P (mmol/L) (SEM)*
Pre-Weaning (2 weeks)	Control	17	4.7 (0.33)	11 (0.61)	2.66 (0.05)	2.77 (0.07)
	Littermate	17	4.56 (0.36)	12 (0.95)		
	Kyphosis	17	4 (0.28)	12 (0.95)	2.75 (0.062)	2.74 (0.12)
Weaning (4 weeks)	Control	16	6.51 (0.42)			
	Kyphosis	16	6.44 (0.63)			
Post-Weaning (13 weeks)	Control	7	36.71 (2.25)			
	Kyphosis	7	36.93 (2.37)			

Table 2.1: *A summary of characteristics of sampled pigs used in the study. Pre-weaning (2 weeks of age), weaning (4 weeks of age), and post-weaning (13 weeks of age) kyphotic and age-matched control pigs were sampled, and the numbers of individual pigs sampled per group are shown. Pigs were immediately weighed post-mortem and the average weight of kyphotic and control pigs per age group is shown. The average litter size of sows which gave birth to pre-weaning kyphotic and comparative control piglets is also provided, but data were not available for weaning and post-weaning groups. The average serum Calcium (Ca) and Phosphorus (P) concentrations were also calculated in pre-weaning kyphotic and non-related control pigs.*

could be compared to a littermate control which showed no clinical signs of kyphosis, and an unrelated control from a contemporary litter in which no piglets presented the characteristic signs of kyphosis. Littermate controls were not possible for the other two sample classes given the management applied on the farms. In the UK, pigs from different

litters are transferred to nursery accommodation at weaning where they are mixed. Therefore identifying littermates after weaning was not possible.

2.3 Vitamin A trial – Sampling and Experimental Design

The trial was performed at Cockle Park farm, Newcastle University, and was approved by the Animal Welfare and Ethics review board at Newcastle University (PPL 70 8262).

2.3.1 Pigs and Management

Sow management and pre-weaning husbandry was applied according to standard UK farm practices for indoor, commercial pigs. Piglets were born from Large White x Landrace sows inseminated with Hylean boar semen (Hylean MQM; Hermitage Seaborough Ltd., Devon, UK). Pigs were weaned at approximately 4 weeks of age, and a total of 64 piglets were randomly selected and moved to experimental accommodation. Pigs were randomly allocated to 8 pens consisting of 8 animals of similar weights and composed of equal ratios of males and females (4 males and 4 females). Individual pen dimensions were 337cm x 310cm, and contained space-feeders (120cm x 30cm) that allowed 4 pigs to feed simultaneously. Pens were also provided with 2 nipple drinkers which originated from a single pipeline, and had partially slatted concrete flooring. Pigs groups were kept in a total of 2 rooms throughout the experimental period, the temperature of both rooms was monitored via min-max thermometer. In room 1, the temperature was maintained between 17.8°C and 27.2°C; in room 2, the temperature was maintained between 18.8°C and 25.5°C. Upon arrival to experimental accommodation, pigs had *ad libitum* access to water and feed, and were fed a 5-stage dry-pellet based diet (Table 2.2). Flatdeck 1 diet (4950µg vitamin A/kg) (A-One feed supplements, North Yorkshire, UK) was provided to pigs at 4 weeks of age for 1 week. At 5 weeks, pigs were given a Flatdeck 150 diet (4950µg vitamin A/kg) for 1 week, and at 6 weeks of age, pigs were fed a Turbowean diet (4620µg vitamin A/kg) for 2 weeks. At 8 weeks of age, pigs were fed a mixed grower ration diet (4526.74µg vitamin A/kg) for 5 weeks. At 13 weeks of age, the feed was changed to Olympic 501 (2145µg vitamin A/kg) (ForFarmers UK limited, Bury St Edmunds, UK) and pigs remained on this diet for the rest of the experimental period.

Table 2.2 *Chemical composition of diets offered to pigs throughout the experimental period from d28. Diet values are calculated, but were analysed for Mixed Grower Ration.*

Item	*Diet*				
% Ingredient	**Flatdeck 1 (d28)***	**Flatdeck 150 (d35)***	**Turbowean (d42)***	**Mixed Grower Ration (d56)***	**Olympic 501 (d91)[A]**
Phosphorus	0.7	0.68	0.64	0.60	0.48
Sodium	0.3	0.3	0.2	0.16	0.18
Lysine	1.7	1.55	1.45	0.22	1.2
Crude Protein	22.5	21	21	n/a	16.5
Crude Fibre	2.5	3	3.5	n/a	6
Calcium	0.75	0.74	0.75	0.96	0.6
Crude Ash	6	5.5	5	2.93	4.5
Methionine	0.63	0.63	0.57	0.1	0.28
Crude Oils	8.5	6.5	6.25	n/a	5
Additives per kg					
Vitamin A (μg)	4950	4950	4620	4526.744	2145
Vitamin D3 (μg)	50	50	50	51.44	37.5
Vitamin E (μg)	167.5	167.5	107.2	91.9	n/a
Iron[1] (mg)	500	500	500	205.78	258
Iodine[2](mg)	3.33	3.33	3.33	1.37	1.6
Copper[3](mg)	640	640	640	219.4	20
Manganese[4](mg)	187.5	187.5	187.5	41.15	40
Zinc[5](mg)	169	169	169	137.19	56
Selenium[6](mg)	0.65	0.65	0.65	0.41	0.67

**Diets were provided by A-One feed supplements, Thirsk, North Yorkshire, UK. [A]Diets were provided by ForFarmers UK limited, Rougham, Bury St Edmunds, UK. Provided per kg of complete diet, [1]Ferrous Sulfate Monohydrate, [2]Calcium Iodate Anhydrous, [3]Cupric Sulphate Pentahydrate, [4]Manganous Sulfate Monohydrate, [5]Zinc Oxide, [6]Sodium Selenite*

Treatment Groups (Retinyl Propionate - µg/Kg of BW daily)	Age at sampling (weeks)	Dosing (weeks)
Control (n=8)	22	0
200µg/KG (n=8)	21	17
500µg/kg (n=8)	21	17
1250µg/KG (n=8)	*20/21	16/17
3000µg/KG (n=8)	20	16
5250µg/KG (n=8)	20	16
7500µg/KG (n=8)	19	15
10000µg/KG (n=8)	19	15

Table 2.3: *Treatment groups used in the vitamin A trial, and numbers of pigs for each group are shown. Depending upon assigned dose group, pigs were orally supplemented daily with RP in µg per kg of BW. Age of pigs at the time of sampling as well as periods of RP dosing are indicated.*

2.3.2 Experimental Procedures

Of the pigs composing the 8 pens in the current study, pigs in 7 pens received a dosage of retinyl propionate (RP) treatment, with one group receiving no dosing so as to serve as a control group (Table 2.3). Depending upon group, animals were orally supplemented, in µg per kg of bodyweight (BW), daily with RP in sunflower oil until tissue processing. Dosing began when pigs were 4 weeks old, periods of dosing and age of animals for each group upon tissue sampling are summarised in Table 2.3. The highest dose group in the current study (10000µg RP/kg BW) was prepared in order to ensure effects of excess vitamin A on biological development. For example, a 70kg pig on this diet would receive 700mg of RP daily which is over 200 times the safe upper limits set for human consumption (3mg/day) (Trumbo et al., 2001). In addition, the European Food Standards Agency (EFSA) advised vitamin A supplementation to fattening pigs should not exceed 1950µg/kg of feed (European Food Safety Authority, 2008). An 80kg pig will typically consume 3.2kg of food daily (ThePigSite, 2014), therefore on a 1950µg/kg diet this pig will accumulate 78µg/kg of BW of vitamin A daily. This would place daily consumption of vitamin A close to that of control pigs used in this trial (85.8µg/kg). This would also make vitamin A consumption, in µg/kg of BW, approximately 130 times below the accumulation pigs on the 10000µg RP/kg

BW treatment will receive. The other dose groups used in the study were prepared in order to determine dose-response relationships between vitamin A and dependent variables.

2.4 Dissection Protocol

In the kyphosis trial, all pigs were euthanized in accordance with Home Office regulations through a combined administration of midazolam for anaesthesia and lethal overdose of sodium pentothal. In the vitamin A trial, all pigs were euthanized in accordance with Home Office regulations through a combined administration of Ketamine, Midazolam and Lorazepam for anaesthesia, followed by a lethal overdose of Euthatal (Pentobarbital).

Upon euthanasia, the jugular vein was sliced and during exsanguination, blood was collected in 10ml serum blood vacutainer tubes and allowed to stand for 30 minutes to allow sufficient clotting before centrifugation (3500RPM for 15 minutes). Serum was subsequently aliquoted into duplicate 2ml Eppendorf tubes and immediately placed on dry ice. An incision was made from the shoulders to the rump, and the attached muscle and connective tissue removed in order to expose the thoracic and lumbar regions of the spine. Depending upon the size of the spine and the animal, a pair of Liston bone cutters or cordless power saw was used to extract the region of spine from the 12^{th} thoracic to 2^{nd} lumbar vertebrae. The spinal section was de-fleshed and samples of intervertebral disc cartilage between T13 and L1 was obtained. The justification of the sampling site comes from observations that abnormal disc findings at the T13-L1 junction have been identified in kyphosis cases (Done and Pearson, 2004). Upon extraction, the samples were immediately placed on dry ice. The cartilage was not sampled from vitamin A treated pigs; cartilage undergoes age-associated degeneration in mammals (Craddock et al., 2018) and due to these pigs being much older than kyphotic pre-weaners in the study (2 weeks old vs 19 weeks/22 weeks old), the comparisons between cartilage from these trials would not truly reflect the occurrences in healthy cartilage. Samples of bone from the vertebral body, containing trabecular bone, were obtained from the 13^{th} thoracic vertebrae using Liston bone cutters, after removal of muscle and connective tissue from the vertebrae This site was sampled due to it resting within the region of where the kyphotic kink occurs (Nielsen et al, 2005) and to maintain consistency with sampling sites for both trials. Upon extraction, samples were immediately placed on dry ice.

The liver was also obtained and weighed from all pigs from the kyphosis and vitamin A trials. For the kyphosis trial, samples of the lower left lobe were placed in duplicate Eppendorf tubes and immediately placed on dry ice. For the vitamin A trial, samples from all 4 lobes of the liver were placed into duplicate tubes. All liver samples were rinsed with phosphate buffered saline (PBS) before being placed into their respective tubes.

The duodenum of the small intestine was also sampled from all pigs from the kyphosis and vitamin A trials. The intestine was cut using surgical scissors to expose the inner epithelial lining, and was rinsed with PBS to remove digesta contamination. Samples of epithelium were then obtained by scraping the lining with a scalpel, and was deposited into duplicate 2ml Eppendorf tubes filed with RNAlater (Sigma-Aldrich, Irvine, UK).

2.5 Molecular Biology

2.5.1 RNA Extraction

Total RNA was extracted from tissue samples using the RNeasy lipid tissue mini-kit (Qiagen, Manchester, UK). 50mg of bone and cartilage tissues was snap-frozen in liquid nitrogen and ground to a fine powder using a steel mortar and pestle. The ground tissue was transferred to 1ml of Qiazol lysis reagent in a 1.5ml Eppendorf tube. 30mg of small intestine samples were homogenised using a plastic pestle by hand in 1ml of Qiazol reagent in a 1.5ml Eppendorf tube. After homogenisation, tubes were briefly vortexed and allowed to stand at room temperate for 5 minutes. 200µl of chloroform was added to each tube using a Hamilton syringe, vortexed for 15 seconds and allowed to stand at room temperature for 3 minutes. The tubes were then centrifuged at 12000 x g for 15 minutes at 4°C. After centrifugation, the upper layer, aqueous layer from each tube was transferred to a new 2ml Eppendorf tube, and 1 volume of 70% ethanol was added to the tube which was subsequently vortexed briefly. 700µl of the sample was added to an RNeasy mini spin-column and collection tube, the columns were then centrifuged at 8000 x g for 15 seconds and the flow-through was discarded. Using the same collection tube, the remainder of the sample in the 2ml Eppendorf tube was centrifuged and the flow-through discarded. 350µl of Buffer RW1 was added to the spin-column, and centrifuged (8000 x g for 15 seconds) to wash the membrane, before discarding the flow-through. 80µl of freshly prepared DNase I incubation mix (70ul of buffer RDD + 10µl of DNase I enzyme) was added to the membrane

in the RNeasy spin-column, and was allowed to incubate at room temperature for 15 minutes to allow for DNA digestion. 350µl of Buffer RW1 was then added to the column before centrifugation (8000 x g for 15 seconds) and discarding of the flow-through. 500µl of buffer RPE was then added to the RNeasy spin-column and centrifuged (8000 x g for 15 seconds) before discarding the flow-through; the column was washed again with 500µl of buffer RPE (8000 x g for 2 minutes) before discarding the flow-through. The membrane of the RNeasy spin-column was further dried after placing the column in a new 2ml collection tube, and centrifugation at 17'000 x g for 1 minute. The RNeasy column was then placed in a 1.5ml Eppendorf tube, and 70µl of ultrapure deionised water was added to the membrane. The column was allowed to stand at room temperature for 10 minutes, before centrifugation (8000 x g for 1 minute); the Eppendorf tubes were labelled and placed on ice before discarding the RNeasy spin-column.

The quantity (ng/µl) of RNA in each sample was quantified using the Nanodrop V2000 spectrophotometer (Thermo-Fisher, MA, USA). The Nanodrop was blanked using 2µl of ultrapure deionsed water, and 2µl of RNA sample was added to the pedestal and read at 260nm and 280nm. All samples were measured in duplicate. The ratio of the reading read at 260nm and 280nm, and 260nm and 230nm was also recorded in order to indicate the purity and quality of the RNA. RNA was then stored at -80°C until downstream applications.

2.5.2 Selection of RNA samples for Microarray Analysis from Kyphosis and Vitamin A trials

After RNA extraction, bone samples from both trials were selected for microarray analysis. In addition, RNA from cartilage samples from the kyphosis trial, and duodenum samples from the vitamin A trial were selected for microarray analysis from both trials. For the kyphosis trial, the pre-weaning age group was selected for microarray analysis. Since the sow has a major effect on the prevalence of kyphosis within litters (Rortvedt and Crenshaw, 2012), analysis of the pre-weaning group allowed to observe potential effects of gestation and lactation. A 2x2 design was implemented in selecting RNA samples for the microarray: 2 phenotypes, kyphosis and non-related control, and 2 tissue types, trabecular bone and cartilage. 4 replicates, which were randomly selected from kyphotic and control groups, were included for each group, allowing for analysis of a total of 16 samples. The RNA quality,

indicated by 260/280 ratio on a Nanodrop, was shown to be above 1.9 for all RNA samples, therefore RNA quality did not factor into sample selection for microarray analysis.

For the vitamin A trial, RNA samples from the control and 10000µg RP/kg BW groups were selected for microarray analysis. RNA from vertebral bone and duodenum tissues were selected to identify biomarkers which show differential expression in each tissue in response to excessive vitamin A intake. RNA from 4 male controls and 4 male pigs recieiving 10000µg RP/kg BW, for both tissue types, were selected for microarray analysis. The male group was selected on the basis that bone tissue in females is subject to additional hormonal regulation in comparison to males, for example estrogen deficiency can prolong osteoclast lifespan (Goldberg et al., 2015). Therefore, in order to identify differential gene expression in response to vitamin A without interference from hormonal regulation, the male groups were selected for analysis.

2.5.3 cRNA Preparation

Total RNA of 200ng from each sample was reverse-transcribed into cRNA labelled with Cy3 using the low input Quick Amp kit (one-colour) according to the manufacturers protocol (Agilent Technologies, Cheadle, UK). cRNA was purified using the RNeasy mini-kit (Qiagen, Manchester, UK) and the quality and quantity of each sample verified through spectrophotometric measurement on a Nanodrop V2000 (Fisher-Scientific, Loughborough, UK).

2.5.4 Microarray Hybridisation

Labelled cRNAs were used for hybridisation using the Quick Amp labelling with Tecan HS Pro Hybridisation kit (Agilent Technologies, Cheadle, UK). The arrays were hybridised at 65°C for 17hrs in Agilent's microarray hybridisation chambers. After hybridisation, arrays were washed according to the manufacturer's instructions. Microarrays were hybridised, washed and scanned at the School of Veterinary Medicine and Science, University of Nottingham. Arrays were scanned at 5µM resolution using the Agilent microarray scanner. Data were extracted using the Feature Extraction software (Agilent Technologies, Cheadle, UK) and saved in a TIFF format.

2.5.5 Data and Pathway Analysis

Data were normalized and analysed using the Genespring GX software version 13.0 (Agilent Technologies, Cheadle, UK). Differential expression of a gene was obtained if a fold-change greater than 2 was observed between groups in the kyphosis and vitamin A trials. Statistical analysis was performed using moderated T-Test and data were considered statistically significant if p values of $p<0.05$ were obtained.

Ingenuity pathway analysis (IPA) (Qiagen, Manchester, UK) was used to identify biological networks and regulators most affected as a result of differential gene expression. Genes from the dataset that produced a p value of <0.05, and were associated with canonical pathways and biological functions, were accepted in the analysis. IPA was additionally used to generate networks of differentially expressed genes. Gene products were represented as nodes and the biological relationships between nodes represented by edges; these were supported by at least one reference from supporting literature.

Although IPA offers powerful analysis in the interpretation of differential gene expression, the data extracted from IPA is representative of human and mouse models, and various cell lines. Therefore, the data might not be fully transferable to understanding differential regulation of gene expression within the pig. Thus, data on differentially expressed genes was also exported to Cytoscape, and biological networks were established (Kohl et al., 2011). The ClueGo app was used to visualise the Gene Ontology terms (GO terms) which had shown to be influenced in the tissue type, and to identify the associated genes in these processes (Mlecnik et al., 2013). False discovery rate, or obtainment of false-positive results, was controlled using Benjamini- Hochberg method (Javanmard and Montanari, 2017) in Cytoscape, and was used to calculate Term p-values for GO terms associated with tissues.

2.5.6 cDNA Synthesis

For the kyphosis samples, RNA was reverse-transcribed into cDNA using the Transcriptor first strand cDNA synthesis kit (Roche, Manchester, UK). 1µg of RNA was mixed with 1µl of random hexamer primers (600pmol/µl) and 2ul of oligo d (T) primers (50 pmol/µl), and diluted with ultrapure deionised water to a volume of 13µl. Samples were incubated at 65°C

for 10 minutes to ensure removal of RNA secondary structures. A mixture containing 4µl of 5X buffer, 2µl of dNTPs (10mM), 0.5µl of Protector RNase inhibitor (40U/µl), and 0.5µl of Transcriptor reverse-transcriptase (20U/µl) was added to each sample. The samples were incubated for 10 minutes at 25°C, 30 minutes at 55°C, and for 5 minutes at 85°C.

For the vitamin A samples, RNA was reverse-transcribed into cDNA using the iscript cDNA synthesis kit (Bio-Rad, CA, USA). 1µg of RNA was mixed with 4µl of 5x iscript reaction mix, containing random hexamer and oligo d (T) primers, 1µl of iscript reverse transcriptase, and diluted with ultrapure deionised water to a 20µl reaction volume. The samples were incubated for 5 minutes at 25°C, 20 minutes at 46°C, and 1 minute at 95°C.

cDNA was diluted 1 in 10 in ultrapure deionised water, and aliquoted into 4x50µl aliquots which were stored at -20°C. An aliquot was taken from each sample, per tissue, and was pooled to form a calibrator for which to normalize samples during qPCR. The calibrator was then aliquoted into single-use aliquots for qPCR plate preparation.

2.5.7 Primer Verification

2.5.7.1 Primer Design

The genomic and FASTA sequences for the gene of interest were obtained from the NCBI database, and aligned using the program Splign in order to identify exon-intron junctions within RNA sequences. Primers were designed to flank exon-intron junctions in RNA sequences; or if not possible, to bind in separate exons. Primers were designed using Primer3 (Untergasser et al., 2012). Obtained primer sequences were then entered into Nucleotide BLAST (Ladunga, 2009) in order to indicate primer target specificity. Upon BLAST, primers were ordered from Eurofins (Eurofins Genomics, Ebersberg, Germany).

2.5.7.2 Primer Standard Curve

Primers were reconstituted in ultrapure deionised water, and a 4µM working stock solution was prepared and aliquoted for each primer. A SYBR green master mix (FastStart Essential DNA Green Master, Roche, Manchester, UK) was prepared (Table 2.4), and a 1 in 3 dilution

Reagent	Volume per 15µl reaction
SYBR Green Mastermix	7.5µl
Forward Primer (4µM)	0.75µl
Reverse Primer (4µM)	0.75µl
Ultrapure deionised water	2.25µl
cDNA	3.75µl

Table 2.4: *Constituents of PCR mastermix, adding to a total reaction volume of 15µl*

series was prepared from cDNA, and each dilution point was prepared in triplicate. Reverse transcriptase minues (RT-) and non-template controls (NTC) were also prepared on plates, in order to indicate genomic DNA contamination and assay contamination respectively (Figure 2.1).

2.5.7.3 Standard Curve Efficiency Calculation

The efficiency of all primer pairs was calculated automatically on the Roche lightcycler 96 software. The average Cq of triplicates for each dilution series was obtained, and plotted against log RNA concentrations in order to obtain the slope of the standard curve. The following calculation was used to determine primer efficiency:

$$E\% = ((10^{(-1/slope)})-1)*100$$

Current standards recommend primer pairs to achieve an efficiency between 1.9 and 2.1, equalling 90% and 110% efficiency respectively (Agilent, 2012). This was taken into consideration for selection of the best primer pairs. Also considered was the primers error, Cq in which amplification was detected, and R value of the standard curve.

2.5.7.4 Gel Electrophoresis

PCR products of primers were subsequently run on 8% agarose gels in order to confirm product size and therefore primer specificity. 0.8g of agarose was prepared in 45ml of 1X TAE buffer in a conical flask, and placed in a microwave for approximately 45 – 60 seconds. The gel was allowed to cool before pipetting 4.5µl of SYBR safe DNA gel stain(Invitrogen, MA, USA) into the gel, and swirled.

	1	2	3	4	5	6	7	8	9	10	11	12
A	1	1	1	1IN3	1IN3	1IN3	1IN9	1IN9	1IN9	1IN27	1IN27	1IN27
B	RT	NTC										

Gene Name	RARG.
Slope	-3.5882
Efficiency	1.90
Error	0.50
R^2	0.95
Y-Intercept	30.87

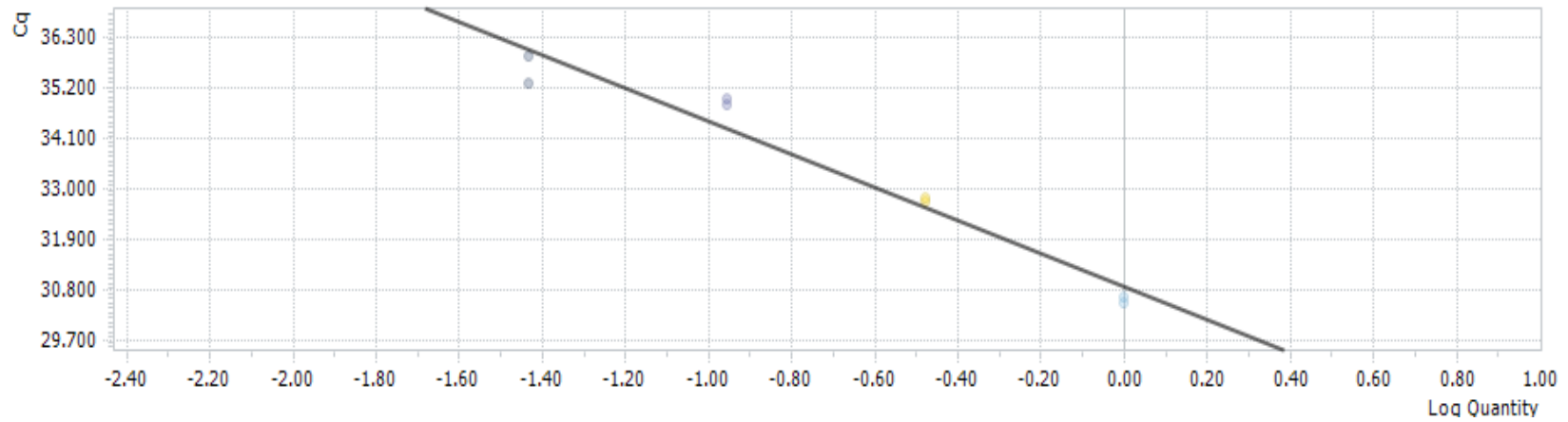

Figure 2.1: *A standard curve calculated and prepared on the Roche lightcycler 96 software. Row A shows how dilution series were prepared on the 96-well plate, row B shows the reverse transcriptase minus (RT-), and non-template controls (NTC). Indicated are the calculated efficiency, error and R values, as well as the first Cq in which amplification is detected (Y-intercept).*

The gel was then poured into a casting tray with a comb insert and allowed to stand. For PCR products and subsequent RT- and NTC products for each primer pair, 8µl of sample was pipetted from the 96 well plate into a 0.2ml PCR tube, and then 2µl of GelPilot loading dye 5x (Qiagen, Manchester, UK) was pipetted into each tube.

The gel and casting tray were placed in a gel tank and submerged in 1x TAE buffer. 5µl of DNA ladder IV (Invitrogen, MA, USA) was pipetted into the first well, and 10µl of samples were pipetted into subsequent wells. The gel was allowed to run at 90v to achieve migration of PCR products.

2.5.7.5 Gel Image Viewing

When gel dye bands were roughly 2/3 down the well, the gel was retrieved from the tank and placed in a LI-COR Odyssey gel viewing system (LI-COR, Cambridge, UK), and viewed at a wavelength of 600nm. Gels representing primers used in the thesis are in Figures 2.2 and 2.3. Sequences for primers of genes analysed per chapter are shown in each chapter.

2.5.8 Quantitative real-time PCR

2.5.8.1 Housekeeper Gene Selection

A total of 5 housekeeping (HK) genes were identified from literature (Kouadjo et al., 2007), and primers were designed for: Ribosomal Protein L37 (*RPL37)*, Glyceraldehyde-3-Phosphate Dehydrogenase (*GAPDH)*, Eukaryotic translation Initiation factor 3 sub-unit D (*EIF3D)*, Peptidylprolyl Isomerase A *(PPIA)* and Proteasome 26S Subunit, Non-ATPase 4 (*PSMD4)*. In the kyphosis trial, all 5 genes were analysed in bone and cartilage cDNA from all age groups in order to indicate the degree of deviation and error of primers between kyphotic and control groups (Table 2.5). In the vitamin A trial, all 5 genes were analysed in the control group and highest supplementation group (10000µg RP/kg BW) in order to indicate the deviation and error of primer pairs across these groups (Table 2.6). In regards to the standard curves, *RPL37* and *PPIA* produced the best curves in regards to reproducibility, with *RPL37* showing higher efficiency (Table 2.7). For cartilage tissues obtained from kyphotic and control pigs, *RPL37* showed the lowest standard deviation, as well as the earliest Ct cycle to be detected. For bone tissues obtained from kyphotic and control pigs,

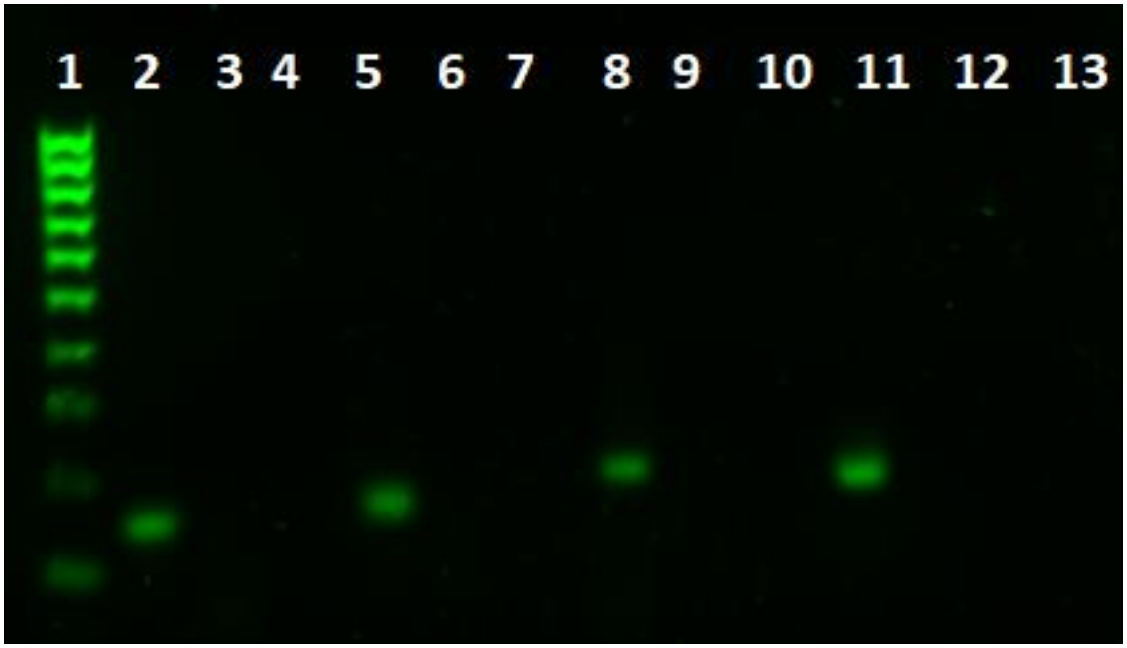

Figure 2.2: *An 8% agarose gel electrophoresis image of primers used in the thesis. Lane 1: DNA ladder IV 100-1000bp Lane 2: TGF-β (151 bp) LANE 3: TGF- β RT- Lane 4: TGF- β NTC Lane 5: BMPR1A (162 bp) Lane 6: BMPR1A RT- Lane 7: BMPR1A NTC Lane 8: PTK2B (199 bp) Lane 9: PTK2B RT- Lane 10: PTK2B NTC Lane 11: ASPN (200 bp) Lane 12: ASPN RT- Lane 13: ASPN NTC*

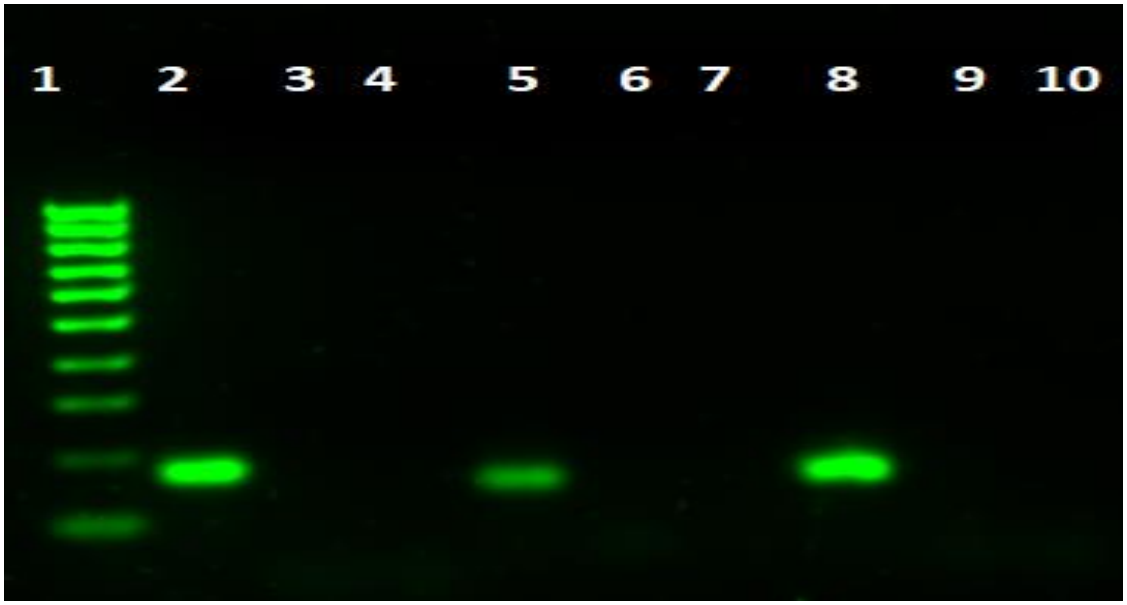

Figure 2.3: *An 8% agarose gel electrophoresis image of primers used in the thesis. Lane 1: DNA ladder IV 100-1000bp Lane 2: BGLAP (176 bp) Lane 3: BGLAP RT- Lane 4: BGLAP NTC Lane 5: DCN (159 bp) Lane 6: DCN RT- Lane 7: DCN NTC Lane 8: RPL37 (166 bp) Lane 9: RPL37 RT- Lane 10: RPL37 NTC*

	Cartilage		Bone	
Gene Name	Average Cq	STDEV	Average Cq	STDEV
RPL37	21.42	1.24	21.41	1.49
GAPDH	24.50	1.79	24.70	1.50
PSMD4	29.19	1.50	28.47	1.47
PPIA	23.40	1.73	22.82	1.64
EIF3D	26.60	1.53	25.88	1.50

Table 2.5*: The average Cq, and standard deviation (STDEV) for each of the 5 housekeeper genes (HKs) for each tissue for the kyphosis trial. HKs were ran in duplicate for all kyphotic and control samples.*

Gene Name	***Average Cq***	***STDEV***
RPL37	23.07	1.01
GAPDH	29.54	1.42
PSMD4	35.27	1.1
PPIA	26.45	1.55
EIF3D	30	1.82

Table 2.6: *The average Cq, and standard deviation (STDEV) for each of the 5 housekeeper genes (HKs) for bone tissue for the vitamin A trial. HKs were ran in duplicate for all 10000*µg *RP/kg BW and control samples.*

	GAPDH	*PSMD4*	*EIF3D*	*PPIA*	*RPL37*
Slope	-3.2772	-3.0626	-3.4279	-3.6549	-3.6268
Efficiency	2.02	2.12	1.96	1.88	1.89
Error	0.21	0.47	0.31	0.11	0.12
R-value	0.99	0.97	0.99	1.0	1.0

Table 2.7: *The slope, efficiency, error and R-values for each primer pair calculated by generation of a standard curve using the Roche lightcycler 96 software. Dilutions were prepared in triplicate, and the standard curve was generated from 4 dilution points diluted 1 in 5.*

all 5 genes showed similar standard deviations, with *PSMD4* showing the lowest deviation, yet it was detected very late in the PCR cycle. *RPL37* showed the lowest average Ct cycle to be detected. For bone tissues obtained from pigs in the vitamin A trial, *RPL37* showed the lowest standard deviation, as well as the earliest Ct cycle to be detected. Due to its early detection, relatively low standard deviation across all 3 tissues, and its reproducibility, *RPL37* was selected as the HK gene of choice for experiments in this thesis.

2.5.8.2 qPCR Plate Setup

Real-time PCR was performed using SYBR green assays in a 15µl reaction composing 3.75µl of diluted cDNA, 4µM primers, 2.25µl PCR-grade water and 7.5µl FastStart Essential DNA green master mix (Roche, Manchester, UK) (Table 2.4). All samples were run on 96 well plates, and performed in triplicate in order to control the variation. All reactions were performed in a light cycler 96 system (Roche, Manchester, UK) with the following cycling conditions: a pre-incubation step of 95° for 10 minutes followed by 40 cycles of 95° for 15 seconds, annealing at 60° for 15 seconds, and elongation at 72° for 20 seconds. A melting curve step was incorporated at the end of the cycles to determine the inclusion of non-specific PCR products. (Table 2.8). A calibrator was also ran in triplicate for each gene on all 96 well plates in order to normalise results between plates (Figure 2.4).

Step	Temperature	Time	Cycles
Preincubation	95°C	10 mins	1
3-step amplification	95°C	15 sec	40
	60°C	15 sec	40
	72°C	20 sec	40
Melting curve analysis	95°C	10 sec	
	65°C	60 sec	
	97°C	1 sec continuous	

Table 2.8: *Cycling conditions for all genes analysed by qPCR on a Roche lightcycler 96 system.*

	1	2	3	4	5	6	7	8	9	10	11	12
A	**S1**	**S1**	**S1**	**S2**	**S2**	**S2**	**S3**	**S3**	**S3**	**S4**	**S4**	**S4**
B	**S5**	**S5**	**S5**	**S6**	**S6**	**S6**	**S7**	**S7**	**S7**	**S8**	**S8**	**S8**
C	**S9**	**S9**	**S9**	**S10**	**S10**	**S10**	**S11**	**S11**	**S11**	**S12**	**S12**	**S12**
D	**S13**	**S13**	**S13**	**S14**	**S14**	**S14**	**S15**	**S15**	**S15**	**CALIB**	**CALIB**	**CALIB**
E	**S1**	**S1**	**S1**	**S2**	**S2**	**S2**	**S3**	**S3**	**S3**	**S4**	**S4**	**S4**
F	**S5**	**S5**	**S5**	**S6**	**S6**	**S6**	**S7**	**S7**	**S7**	**S8**	**S8**	**S8**
G	**S9**	**S9**	**S9**	**S10**	**S10**	**S10**	**S11**	**S11**	**S11**	**S12**	**S12**	**S12**
H	**S13**	**S13**	**S13**	**S14**	**S14**	**S14**	**S15**	**S15**	**S15**	**CALIB**	**CALIB**	**CALIB**

Figure 2.4: *A typical well map of analysis for 1 gene of interest in samples. Samples (S) were run in triplicate horizontally across the plate, with the calibrator (CALIB) placed at the end of each row for the gene. Samples for the gene of interest are highlighted in blue, whereas samples for the housekeeper gene are highlighted in green.*

2.5.8.3 Calculation of Normalized Expression

Samples from the kyphosis and vitamin A trials were normalized using the housekeeper gene *RPL37,* and fold-changes in gene expression were calculated relative to the calibrator on each plate. The calibrator was used to remove inter-plate variability, and normalized expression of target genes in all samples was automatically calculated using the Pfaffl comparative method:

$$\text{Normalized Ratio} = (E_{target})^{Ct\ target\ gene\ (calibrator\text{-}sample)} / (E_{reference})^{Ct\ reference\ gene\ (calibrator\text{-}sample)}$$

E is the calculated efficiency of primer pairs obtained from the standard curve. The calibrator was the calibrator sample prepared in triplicate on each plate. In the kyphosis trial, data were presented relative to the pre-weaner control; and in the vitamin A trial, data were presented as relative to the control group

2.6 Analytical Chemistry

2.6.1 Retinoid Extractions from Liver

Liver samples from all pigs were extracted in duplicate. 150-200mg of liver were homogenised in 2ml of PBS in a glass PTFE 3ml tapered tissue grinder (Wheaton Science Products, NJ, USA). The homogenate was transferred to a 12ml glass tube using a glass Pasteur pipette, and the tissue grinder was washed with 2ml of Ethanol (0.01%BHT) before the homogenate was added to the same 12ml glass tube. 20µl of the internal standard (0.5mM Retinyl Acetate) was added directly to the ethanol phase, and the tube was vortexed for 10 seconds. 4ml of hexane (0.01% BHT) was added to each tube, and tubes were mixed for 1 hour at 1800rpm on an orbital shaker. The tubes were centrifuged at 3000rpm for 5 minutes, and the supernatant was transferred to a new 12ml glass tube using a glass pasteur pipette. The samples were extracted a further 2 times with 4ml of hexane, however tubes were vortexed for 10 seconds, as opposed to 1 hour, in between steps. The combined hexane phases (12ml) in the new 12ml glass tubes were dried down under a gentle steam of nitrogen gas in a heat block set at 35°C. Residues were re-dissolved in 1ml of ethyl acetate and transferred to an amber vial before storage at -80°C until HPLC analysis. On every day of sample extraction, 20µl of the internal standard was added to 980µl of ethyl

acetate and was used to calculate % recovery of REs for samples extracted on that same day. The internal standard was stored at -80°C in an amber vial until HPLC analysis.

2.6.2 HPLC

The HPLC mobile phase consisted of Acetonitrile/1,4-Dioxane/Alcohol mixture/Triethylamine (79:14.8:6:0.2, v/v). The alcohol mixture consisted of 1:1 methanol:isopropanol and 1.16g of Ammonium Acetate. The gradient flow was 1ml/min, all esters were resolved within 32 minutes and injection volume was 10µl. The column was a Sphereclone C18 5µm 250x4.6mm with a security guard column C18 4x3.00mm. All samples were analysed on a HPLC system with a Shimadzu SPD-M20A photodiode array detector set to 325nm. Intra and inter day variation of each batch run was calculated by extractions from the same source of liver, and these samples were placed at the beginning, middle and end of each analysis. Between these 3 samples at these points, intra-variation did not exceed 0.75%, and inter-day variation was 6.25%. The retention times for each ester are listed in Table 2.9. All samples were run in duplicate.

Compound	Retention Time/mins
Retinol	3.98
Retinyl Acetate (Internal Standard)	4.30
Retinyl Linoleate	14.64
Retinyl Oleate	20.15
Retinyl Palmitate	21.68
Retinyl Stearate	30.14

Table 2.9: *Typical HPLC retention times (mins) for individual REs after a 10µl injection through a Sphereclone C18 5µm 250x46mm column with a Security guard column C18 4x3.00mm.*

2.7 ELISA Analysis for Serum 25(OH) D

2.7.1 Plate Setup

Serum samples were extracted from -80°C storage and kept for an hour at room temperature to allow thawing. 25(OH) D concentrations in serum were quantified using a 25-Hydroxy vitamin D ELISA kit (Immunodiagnostic systems Inc, Boldon, UK). Samples of serum from each pig sample was pooled and aliquoted, and one aliquot prepared per plate to serve as a calibrator and measure coefficient variation.

25µl of standards and samples were added to a borosilicate glass tube, before addition of 1ml of 1X 25-D Biotin- buffer. The tube was vortexed for 10 seconds, and 200µl of sample was added to each well. Calibrators were placed at the beginning, middle and end of the plates (Figure 2.5). The plate was left to stand for 2 hours at room temperature, then the contents of the wells were discarded. 300µl of 1X wash buffer was added to all wells using a multi-channel pipette, the contents were discarded, and the plate was firmly tapped against blotting paper in order to fully discard the contents of the wells. The plates were manually washed 3 times, before addition of 200µl of enzyme-conjugate to all wells using a multi-channel pipette. The plate was allowed to stand at room temperature for 30 minutes, before discarding the contents. The plate was washed with 1x wash buffer a further 3 times, before addition of 200µl of enzyme substrate to all wells using a multi-channel pipette. The plate was allowed to stand at room temperature for 30 minutes, then 100µl of stop solution was added to all wells using a multi-channel pipette. The concentrations of pre-prepared standards for each kit are provided (Table 2.10). The intra-variation of the kits did not exceed 10% on any plate and inter-variation was 7.7%. Each plate also contained a positive and negative control which represented elevated and reduced serum 25(OH) respectively. All samples, standards and controls were ran in duplicate.

	1	2	3	4	5	6	7	8	9	10	11	12
A	STD 0	STD4	Ctrl 2	WC6	WC10	WC14	PK2	PK5	PK9	PK13	PC1	PC5
B	STD 0	STD4	Ctrl 2	WC6	WC10	WC14	PK2	PK5	PK9	PK13	PC1	PC5
C	STD1	STD5	CALIB1	WC7	WC11	WC15	PK3	PK6	PK10	PK14	PC2	PC6
D	STD1	STD5	CALIB1	WC7	WC11	WC15	PK3	PK6	PK10	PK14	PC2	PC6
E	STD2	STD6	WC4	WC8	WC12	WC16	PK4	PK7	PK11	PK15	PC3	PC7
F	STD2	STD6	WC4	WC8	WC12	WC16	PK4	PK7	PK11	PK15	PC3	PC7
G	STD3	Ctrl 1	WC5	WC9	WC13	PK1	CALIB2	PK8	PK12	PK16	PC4	CALIB3
H	STD3	Ctrl 1	WC5	WC9	WC13	PK1	CALIB2	PK8	PK12	PK16	PC4	CALIB3

Figure 2.5: *A typical well map used for each ELISA plate. STD 0-6: Standards used to generate curve. Ctrl 1: Positive control Ctrl 2: Negative control CALIB1-3: Calibrators to measure CV%*

***Table 2.10**: The concentrations (ng/ml) of each standard prepared on each 96 well ELISA plate.*

STD	ng/ml
0	0
1	6.5
2	11.5
3	18.5
4	32
5	44
6	94.4

2.7.2 Data Analysis

Upon addition of the stop solution, the plate was read at 450nm and 650nm on a Multiskan Go Spectrophotometer (Thermo-Fisher Scientific, MA, USA). 450nm represented the abundance of 25(OH) D in each well, while 650nm represented potential protein retained in the well. The OD of 650nm was subtracted from the OD of 450nm in order to obtain the final OD reading for each sample. Data were then exported to GraphPad prism (GraphPad Software, CA, USA) and the standard curve was automatically generated using non-linear regression. Standard concentrations can be viewed in table 2.10. The OD values for each sample were then calculated automatically in GraphPad, based on the standard curve.

2.8 General Data Analysis

All approaches for statistical analysis of data for all experiments in this thesis are indicated in each experimental chapter. Methods unique to each experimental chapter are also provided in each chapter. Outliers were determined in all data using the rule: $\mu \pm 2\sigma$. Values that fell outside of this range were excluded from the data.

Chapter 3: Molecular characterisation of idiopathic lumbar kyphosis in pigs

3.1 Introduction

The underlying cause of kyphosis in pigs remains elusive and unclear. Literature on the topic is relatively limited, however an estimated 11% of pigs born alive will show symptoms (Straw et al., 2009). The disease has doubled in incidence since 1980, when 5% of pigs had been diagnosed with the condition (Straw et al., 2009). The disease is a problem on-farm: affected pigs have shown signs of paralysis (Done and Pearson, 2004), are suspected of having a reduced growth rate (Straw et al., 2009) and automatic machinery within the slaughterhouse is not accustomed to accept a carcass with an abnormality of this nature (Holl et al., 2008). There remains a need for a more in-depth characterisation of the basis of the disease so intervention strategies can become implemented in practice.

Upon anatomical examinations, kyphotic pigs have shown signs of mineralisation defects within bone tissue. There have been cases in which bone tissue content of Ca is clearly reduced (Done and Gresham, 1988) and severe cases have shown development of hemi-vertebrae within the final thoracic sections of the spine (Nielsen et al., 2005, Done et al., 1999). Following vascular invasion of the cartilage template, osteoblasts contribute to the formation of POCs, from which cartilage is eroded and replaced by mineralised bone matrix, allowing for endochondral bone growth (Karsenty et al., 2009, Maes et al., 2010). The development of hemi-vertebrae within kyphotic tissue reveals a loss of a POC, and indicates a reduction in endochondral bone growth or angiogenesis, which allows for osteoblasts to be delivered to the growing tissue (Nielsen et al., 2005, Maes et al., 2010). Subsequent failure of ossification results in incomplete mineralisation of the tissue, and provides a "kinked" morphology to the vertebrae that contributes to the characteristic kink of kyphosis. The differentiation and function of chondrocytes and osteoblasts, which regulate endochondral bone growth, are controlled by a variety of molecular signalling pathways, including: TGF- β, BMP, Wnt, or IHH pathways (Karsenty et al., 2009, Kronenberg, 2003, Chen et al., 2012). In addition, these pathways have also been demonstrated to regulate angiogenesis (Goumans et al., 2009, Olsen et al., 2017, David et al., 2009). Due to their roles in mediating osteoblast differentiation, targeting BMP, IHH or Wnt pathways have been

recommended in the treatment of bone diseases such as osteoporosis (Zhao et al., 2017, Li et al., 2016). However, studies have observed that mutations in genes belonging to TGF- β or BMP pathways not only associate with osteoporosis, but a variety of other skeletal disorders such as osteoarthritis and osteogenesis imperfecta (MacFarlane et al., 2017). It is therefore possible that downregulation of the TGF- β signalling pathway, which includes the BMPs, may be associated with kyphosis bone tissue, but there is currently no evidence to support this.

Additionally, Done and Pearson (2004) observed increased disc space, and occasional collapsing of the disc, between the final thoracic and first lumbar vertebrae in kyphotic pigs. The intervertebral disc is composed of layers of chondrocytes, collagen fibres and PGs, which hold organisational roles in the coordination of fibrillogenesis to retaining the tissues structure (Melrose et al., 2001, Bock et al., 2001, Burton-Wurster et al., 2003). Evidence has indicated that during Osteoarthritis, a condition characterised by cartilage deterioration, a disruption in cytoskeletal organisation within chondrocytes, which subsequently impairs chondrocyte differentiation, contributes to articular cartilage degeneration (Loty et al., 1995, Capin-Gutierrez et al., 2004). Actins are vital components of the cytoskeleton, and are required for cytoskeletal reorganisation in order to allow for cell migration, motility and interaction with the ECM (Liu et al., 2017). How genes which represent cytoskeletal components, such as actins, have been influenced in kyphotic articular cartilage has not been explored. In addition, PGs within the cartilage such as SLRPs may induce chondrocyte differentiation through upregulation of genes such as *ACAN,* and promote glyosaminoglycan (GAG) production (Salinas and Anseth, 2009). Yet in models of osteoarthritis, there is an observed upregulation of SLRPs within affected cartilage (Bock et al., 2001). The SLRPs have been demonstrated to facilitate TGF- β, BMP and Wnt pathways (Nikitovic et al., 2012), yet evidence shows that they also have the potential to inhibit TGF- β signalling in particular (Yao et al., 2016). TGF- β signalling is critical in allowing the differentiation of chondrocytes (Ying et al., 2018), yet there is no evidence in current literature that could explain its potential association within kyphotic cartilage. The TGF- β pathway has very clear roles in promoting the differentiation of MSCs into chondrocytes and osteoblasts, therefore it could be hypothesised that this pathway is potentially responsible for abnormal bone and cartilage development during kyphosis, but there is currently no evidence to support this.

The molecular events that occur during kyphosis require clarity and definition in order to further our understanding of this idiopathic disease. Thus, the objectives of this study were to determine if the TGF- β signalling pathway is associated with kyphotic bone and cartilage tissue. The hypotheses for the study are as follows:

- TGF- β signalling pathway will be downregulated in kyphotic trabecular bone, due to endochondral mineralisation and angiogenesis being potentially disrupted during kyphosis (Nielsen et al., 2005, Done et al., 1999), and because of the TGF- β pathways associations with skeletal disorders (MacFarlane et al., 2017).
- Actin genes will be downregulated within kyphotic cartilage, due to their regulatory roles in chondrogenesis (Liu et al., 2017); and SLRPs, due to their associations with osteoarthritis, will show upregulation within kyphotic cartilage, and this will associate with the TGF- β signalling pathway.
- The TGF- β pathway will overlap in kyphotic bone and cartilage tissues.

3.2 Materials and Methods

3.2.1 General Methods

The experimental design and seletion of kyphotic pigs, as well as methods related to this chapter, can be found in Chapter 2. This includes methods for: Tissue extraction, RNA extraction, cDNA synthesis, Microarray Analysis, Microarray Data and Pathway Analysis, qPCR analysis, and calculation and presentation of qPCR data.

Gene biomarkers were selected for qPCR verification based on their consistency among GO terms in Cytoscape, overlap between GO terms and canonical pathway analysis in IPA, and the biological role and relevance of affected genes to the context of bone metabolism was also considered. If initial analysis of gene expression between kyphosis and non-related control pre-weaners showed only marginal fold-changes, these genes were not investigated in the older age groups.

3.2.2 Statistical Analysis

Before statistical analysis, data were tested for normal distribution using Shapiro-Wilk test and observing skewness and kurtosis (SPSS Software). Data were ln transformed to achieve

normal distribution, however normal distribution could not be achieved for all variables. Therefore, the non-parametric Kruskal-Wallis test was used to observe the effects of age and phenotype on dependent variables, and Mann-Whitney test was used to observe effects between kyphotic and control pigs in individual age groups. A p value <0.05 was considered as statistically significant.

3.3 Results

3.3.1 Microarray Profiling of Kyphotic Trabecular Bone

In the trabecular bone of kyphotic pre-weaners, a total of 1196 transcripts were found to be differentially expressed with a fold change greater than 2. Of these, 477 were upregulated (39.9%) and 719 were downregulated (60.1%) in comparison to age-matched non-related control piglets. The top 5 upregulated and downregulated genes which showed the greatest fold-changes in kyphotic trabecular bone are shown in Table 3.1.

IPA identified the top canonical signalling pathways affected in the bone of kyphosis pre-weaners (Table 3.2). “TGF- β signalling” and “BMP signalling” were the pathways most significantly associated with kyphotic trabecular bone ($p<0.05$), and IPA identified TGF- β as the most significantly affected regulatory gene to associated with this tissue (Table 3.2). The TGF- β signalling pathway was significantly downregulated within kyphotic trabecular bone ($p<0.01$). Furthermore, many of the genes that showed differential expression were found to share associations with TGF- β, including mineralization genes such as *BGLAP*, Bone Morphogenetic protein Receptor 1A (*BMPR1A)*, and Asporin (*ASPN).* These relationships are presented in Figure 3.1.

Cytoscape identified a total of 59 GO terms affected by differential gene expression in the trabecular bone of kyphosis pre-weaners with a total of 19 associated genes. The most significantly affected GO terms, ranked by Term p-value corrected with Benjamini-Hochberg, related to “BMP signalling”, “Regulation of Biomineral Tissue Development,” and “Biomineral Tissue Development” (Table 3.3). Genes such as *BMPR1A*, *ASPN*, Protein Tyrosine kinase 2 Beta (*PTK2B)*, and *BGLAP* showed consistency among IPA and Cytoscape, and “BMP signalling” was identified in both of types of analysis.

Gene Symbol	Gene Title	Molecular Function	Fold-change	p-value
SNCG	synuclein, gamma (breast cancer-specific protein 1)	beta-tubulin binding	11.92↑	0.0143
RH	Rh protein	ammonium transmembrane	8.16↑	0.0308
CD5L	CD5 molecule-like	scavenger receptor activity	7.32↑	0.0229
ALOX12	Arachidonate 12-lipoxygenase	Adipocyte Differentiation	7.25↑	0.0042
HP	Haptoglobin	Osteoclast activation	5.23↑	0.0097
POSTN	periostin, osteoblast specific factor, transcript	Differentiation of Osteoblasts	59.13↓	7.79E-04
ACAN	Aggrecan	extracellular matrix structural constituent	14.83↓	0.00107
C1QTNF3	C1q and tumor necrosis factor related protein 3	Osteoclast activation	14.07↓	4.46E-05
IGF2	Insulin-like growth factor 2	Differentiation of Osteoblasts	13.72↓	7.82E-04
BGLAP	Bone gamma-carboxyglutamate (gla)	Differentiation of Osteoblasts	13.32↓	9.68E-04

Table 3.1*: The top 5 up and downregulated genes, with regards to fold-change, in the trabecular bone of kyphotic pre-weaners, as determined by Genespring. Indicated is the gene name, the process the gene regulates, fold-change and p-value calculated by moderated T-Test.*

The genes that showed consistency among IPA and Cytoscape, and had relevant biological roles in the context of bone metabolism, were selected for qPCR verification in order to validate the findings. The genes: *TGF*-β, *BMPR1A*, *ASPN*, *BGLAP*, and *PTK2B* were analysed. *PTK2B* was analysed in the pre-weaning group, but was not analysed in the older age groups due to showing marginal fold-changes and no indications of significance in expression.

Kyphotic Bone			Kyphotic Cartilage		
Top Upstream Regulator	**p-value**		**Top Upstream Regulator**	**p-value**	
TGF-β - Inhibited	4.69E-27		TGF-β - Activated	3.16E-15	
Pathway	**p-value**	**Genes**	**Pathway**	**p-value**	**Genes**
Role of Osteoblasts, Osteoclasts and Chondrocytes in Rheumatoid Arthritis	7.4131E-05	BGLAP↓, TGFB1↓, TNFSRF1A↓, MAPK12↓, BMPR1A↓, PT2KB↑, SMAD7↑	**Gap Junction Signalling**	1.47911 E-06	GNAS↑, ACTB↑, ACTC1↑, ACTA2↑, ACTA1↑
BMP signalling	0.00039	BMPR1A↓, SMAD7↑, BMP1↓, MAPK12↓	**Remodelling of Epithelial Adherens Junctions**	2.39883 E-06	ACTB↑, ACTC1↑, ACTA2↑, ACTA1↑
Integrin Signalling	0.00055	ARPC2↓, ASAP1↓, FYN↓, ACTA2↓, ACTA1↓	**EIF2 signalling**	4.16869 E-06	ACTB↑, ACTC1↑, ACTA2↑, EIF4A2↑, ACTA1↑
TGF- β Signalling	0.00088	BMPR1A↓, TGFB3↓, SMAD7↑, TGFB1↓, MAPK12↓	**Integrin signalling**	0.00145	ACTB↑, ACTC1↑, ACTA2↑, ACTA1↑
FAK signalling	0.0019	ASAP1↓, FYN↓, GIT2↓, ACTA2↓, ACTA1↓	**Osteoarthritis Pathway**	0.0066	ACAN↑, DCN↑, ATF4↑, RARRES2↑

Table 3.2: *The top upstream regulators, and Canonical pathways affected in the bone and cartilage of pre-weaning kyphotic pigs in comparison to non-related controls, as indicated by IPA. The direction of differential expression for each gene is shown, as well as p-values calculated by Fishers-Exact test.*

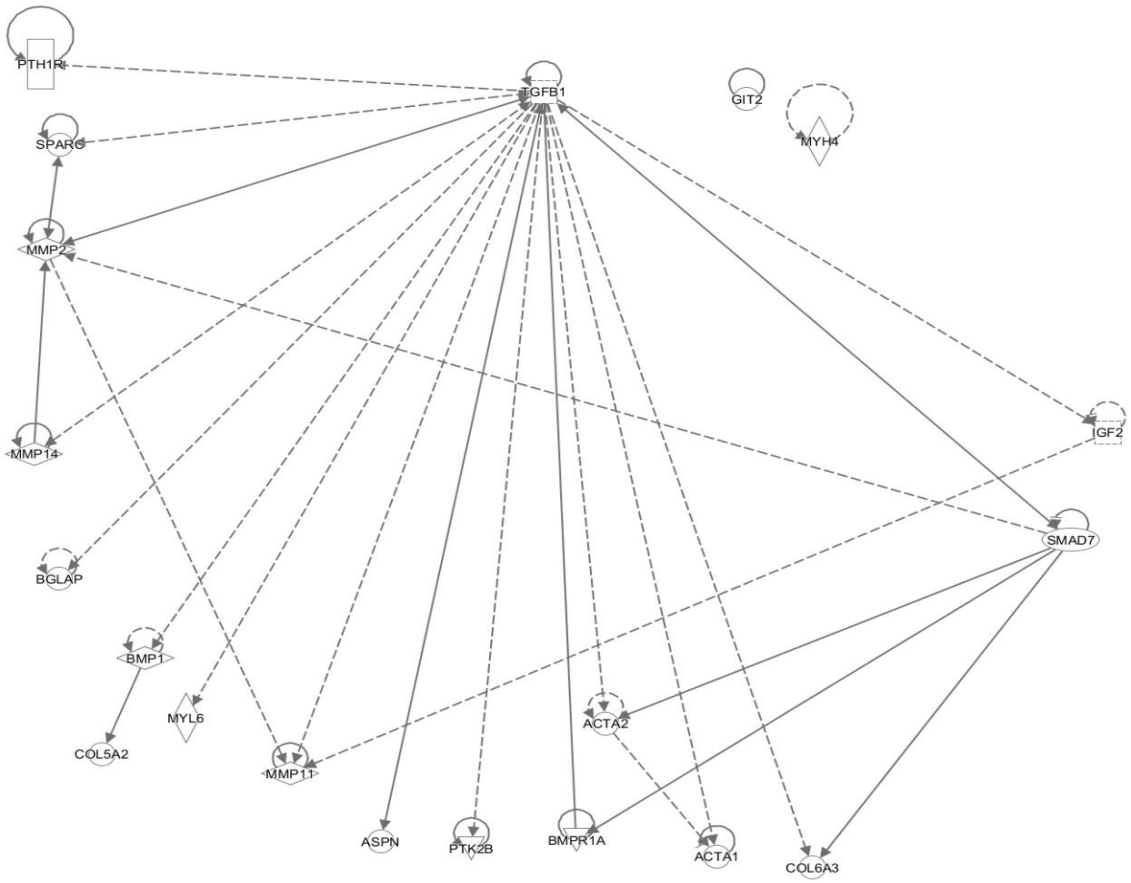

Figure 3.1: *Graphic representation of the most relevant genes differentially expressed in pre-wenaing kyphotic bone, identified by IPA. Genes are represented by nodes, and relationships by edges*

3.3.2 Microarray Profiling of Kyphotic Intervertebral Cartilage

In the intervertebral cartilage of kyphotic pre-weaners, a total of 348 transcripts were found to be differentially expressed >2-fold. Of these transcripts, 310 were upregulated (89.1%) whereas only 38 were downregulated (10.9%) in comparison to age-matched non-related control piglets. The top 5 upregulated and downregulated genes with the greatest fold-changes are shown in Table 3.4. IPA identified the top canonical signalling pathways affected in the cartilage of kyphotic pre-weaners (Table 3.2).

GO TERM	Kyphosis Differential Gene Expression - Bone			
BMP signalling*	BMPR1A↓	ID1↓	SMAD7↓	
Reg. of Biomineral Tissue	BMPR1A↓	ASPN↓	BGLAP↓	PTK2B↑
Biomineral Tissue Development*	BMPR1A↓	ASPN↓	BGLAP↓	PTK2B↑
Regulation of ossification*	BGLAP↓	BMPR1A↓	ID1↓	PTK2B↑
Ossification*	BMPR1A↓	ASPN↓	BGLAP↓	ID1↓
	Kyphosis Differential Gene Expression - Cartilage			
Peptide Crosslinking*	DCN↑			
Neg. reg. of insulin-like growth factor receptor signalling*	CILP↑			

Table 3.3: *Gene ontology pathways affected by differential gene expression in bone and cartilage tissues of kyphotic piglets in comparison to age-matched non related controls. Term Pvalue corrected with Benjamini-Hochberg *P<0.01*

Actin-associated genes showed consistency among top canonical pathways, which is in agreement with the original hypotheses in that there would be a differential regulation of these genes. However, unlike the original hypotheses stating these genes would be downregulated, the analysis has indicated these genes were upregulated. The "Osteoarthritis pathway" also showed in canonical pathways ($p<0.05$) and this showed an upregulation of the SLRP Decorin (*DCN).* Cytoscape identified a total of 20 GO terms affected by differential gene expression in the intervertebral cartilage of kyphotic pre-weaners with a total of 7 associated genes. The most relevant and significantly affected GO terms, ranked by Term P-value corrected with Benjamini-Hochberg, related to "negative regulation of insulin-like growth factor receptor signalling" and "peptide cross-linking via chondroitin 4-sulfate glycosaminoglycan", which associated genes in these pathways, were Cartilage intermediate later protein (*CILP)* and *DCN* respectively (Table 3.3).

Gene Symbol	Gene Title	Molecular Function	Fold-change	p-value
COMP	cartilage oligomeric matrix protein	calcium ion binding	25.07↑	0.0101
ACAN	Aggrecan	extracellular matrix structural constituent	23.91↑	0.0404
MGP	matrix Gla protein	calcium ion binding	21.79↑	0.0493
COL14A1	collagen, type XIV, alpha 1	extracellular matrix structural constituent	19.70↑	0.0018
THBS3	thrombospondin 3	calcium ion binding	16.20↑	0.0157
LCN2	lipocalin 2	protein homodimerization	13.02↓	0.0233
RPS6KC1	ribosomal protein S6 kinase, 52kDa,	transferase activity	4.32↓	0.0393
SLC16A12	solute carrier family 16, member 12	symporter activity	4.17↓	0.0472
SPRYD7	SPRY Domain Containing 7	protein binding	4.07↓	0.0314
INHBB	inhibin beta(b)-subunit	growth factor activity	3.54↓	0.0497

Table 3.4: *The top 5 up and downregulated genes, in regards to fold-change, in the intervertebral cartilage of kyphotic pre-weaners, as indicated by Genespring. Indicated is the gene name, the process this gene regulates, fold-change and p-value calculated by moderated T-Test.*

The relationships among genes identified in IPA and Cytoscape are presented in Figure 3.2. *DCN* therefore showed consistency among IPA and Cytsocape and so was selected for qPCR verification. Actin, Alpha, Cardiac Muscle 1 (*ACTC1)* was analysed in the pre-weaning group, but was not analysed in the older age groups due to showing marginal fold-changes and no indications of significance in expression.

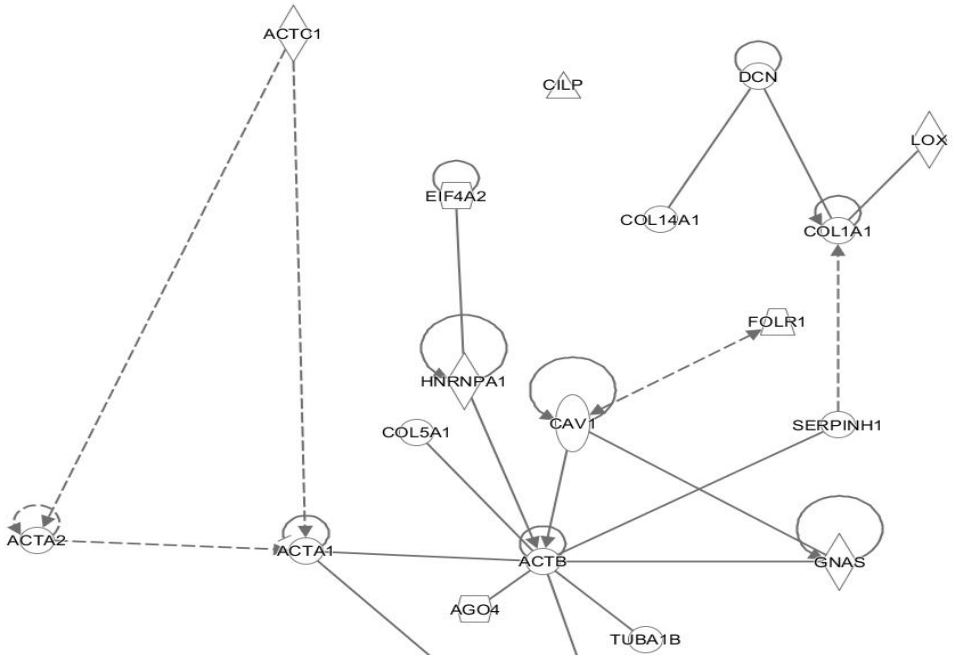

Figure 3.2: *Graphic representation of the most relevant genes differentially expressed in pre-weaning kyphotic cartilage, identified by IPA. Genes are represented by nodes, and relationships by edges.*

3.3.3 Verification of Gene Expression in Kyphotic Tissues using qPCR

A list of primer sequences for all genes of interest can be seen in Table 3.5.

3.3.3.1 Expression of *TGF*- β in Kyphotic Bone

There were no significant differences in expression between kyphotic pre-weaners and non-related controls (Fold-change (FC) -1.31, p=0.235), or with littermates (FC -1.02, p=0.442), but a tendency was observed between littermates and non-related controls (FC -1.27, p=0.084) (Figure 3.3). No significant differences in expression were observed in kyphotic weaners (FC-1.03, p=0.631) or kyphotic post-weaners (FC -1.18, p=0.180). There was no significant effect of phenotype (p=0.803) or age (p=0.175) on gene expression. The results indicate that, *TGF*- β was not differentially expressed in kyphosis bone tissue.

3.3.3.2 Expression of *BMPR1A* in Kyphotic Bone

There was a tendency for *BMPR1A* expression to be downregulated in kyphotic pre-weaners in comparison to non-related controls (FC -1.86, p=0.097), but not with littermates (FC-1.01, p=0.693), or between littermates and non-related controls (FC-1.84, p= 0.136) (Figure 3.4).

Table 3.5: *List of primer sequences for genes of interest for quantification of gene expression by real-time quantitative polymerase chain-reaction (q.PCR)*

PRIMER ID	***SEQUENCE 5'-3'***
RPL37 (HK)	F: GCCTACCATCTCCAGAAGTC R: CTTCACGGAATCCATGCCTG
TGF- B1	F:GGAGCTATACCAGAAATACAGCA R:GCGAAAACCCTCTATAGCCTC
BMPR1A	F:GCCCTACATAATGGCTGATATCT R:TTGACACACACAACCTCACG
BGLAP	F:TGAAGAGACTCAGGCGCTAC R:CTGCGAGGTCTAGGCTATGC
ASPN	F:ACCCCTTCTTCCCATTCGAT R:AGCATAAAGTGAGGTGAGTCC
PTK2B	F: GTGGAAGCTGAGTGGAGGTA R: CTTTGAAGAACCGCCTGAGC
ACTC1	F: ACTGCTGAGCGTGAAATTGT R: TACCAATGAAGGAGGGCTGG
DCN	F:AAAATCAGCCCTGGAGCATT R:GTGCCAAGTTCTACGACGAT

RPL37, Ribosomal protein sub-unit L37, TGF-β, Transforming Growth Factor Beta, BMPR1A, Bone Morphogenetic Protein Receptor Type 1A, BGLAP, Osteocalcin, ASPN, Asporin, PTK2B, Protein Tyrosine Kinase 2 Beta, ACTC1, Actin, Alpha, Cardiac Muscle 1, DCN, Decorin.

There were no significant differences observed in kyphotic weaners (FC+1.10, p=0.740) or in kyphotic post-weaners (FC-1.11, p=1.0). A clear effect of age was observed on gene expression ($p<0.01$) in that biomarker expression decreased after the pre-weaning stage, but not with phenotype (p=0.486).

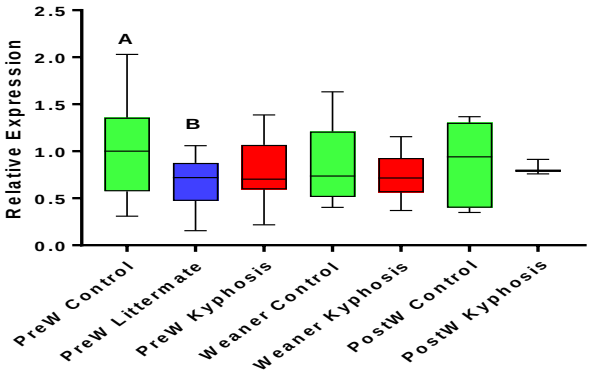

Figure 3.3: *Relative real-time PCR expression of TGF-β in the trabecular bone of pre-weaning (PreW) (n=17 per group), weaning (n=16 per group), and post-weaning (PostW) (n=7 per group) kyphotic and control pigs, calculated by qPCR. Data are presented as relative to the pre-weaner control, and in boxplots with median, 25th and 75th quartile ranges, and upper and lower limits. Mann-whitney AB p=0.084.*

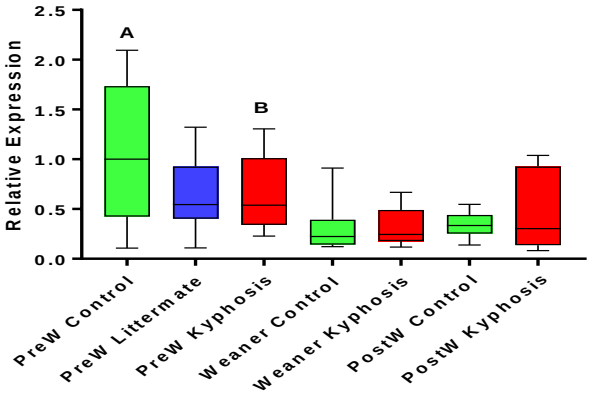

Figure 3.4: *Relative real-time PCR expression of BMPR1A in the trabecular bone of pre-weaning (PreW) (n=17 per group), weaning (n=16 per group), and post-weaning (PostW) (n=7 per group) kyphotic and control pigs, calculated by qPCR. Data are presented as relative to the pre-weaner control, and in boxplots with median, 25th and 75th quartile ranges, and upper and lower limits. Kruskal-Wallis Age p<0.01, Mann-Whitney AB p=0.097*

3.3.3.3 Expression of *BGLAP* in Kyphotic Bone

There were no significant differences in expression in kyphotic pre-weaners in comparison to non-related controls (FC+1.01, p=0.603), or with littermates (FC+1.73, p=0.129), or between littermates and non-related controls (FC+1.75, p=0.250) (Figure 3.5). No significant differences were observed in kyphotic weaners (FC-1.05, p= 0.931) or kyphotic post-

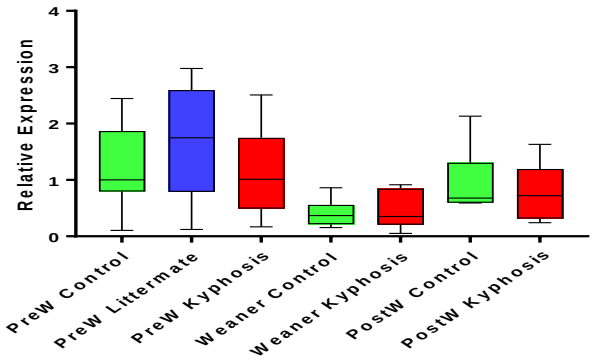

Figure 3.5: *Relative real-time PCR expression of BGLAP in the trabecular bone of pre-weaning (PreW) (n=17 per group), weaning (n=16 per group), and post-weaning (PostW) (n=7 per group) kyphotic and control pigs, calculated by qPCR. Data are presented as relative to the pre-weaner control, and in boxplots with median, 25th and 75th quartile range, and upper and lower limits. Kruskal-Wallis Age p<0.01*

weaners (FC+1.06, p= 0.519). A clear effect of age (p<0.01) was observed on *BGLAP* expression in that biomarker expression decreases after the pre-weaning stage, but no effects were observed for phenotype to have an effect on gene expression (p=0.713).

3.3.3.4 Expression of *ASPN* in Kyphotic Bone

There were no significant differences in *ASPN* expression in kyphotic pre-weaners in comparison to non-related controls (FC-1.30, p=0.155), or between kyphotic pre-weaners and littermate piglets (FC -1.28, p=0.210), or between littermate piglets and non-related controls (FC-1.01, p=0.973) (Figure 3.6). There were no significant differences in expression observed in kyphotic weaners (FC-1.28, p=0.901), but a significant difference was observed in kyphotic post-weaners (FC -1.40, p=0.025). There was no overall effect of phenotype (p=0.209), but there was an effect of age (p<0.01) due to biomarker expression decreasing over time. The current data suggests *ASPN* is downregulated in kyphotic bone at the post-weaning stage.

3.3.3.5 Expression of *PTK2B* in Kyphotic Bone

The differences in *PTK2B* expression in the bone of kyphotic pre-weaners did not indicate significance (FC-1.05, p=0.395) (Figure 3.7). Due to these marginal changes, *PTK2B* was not

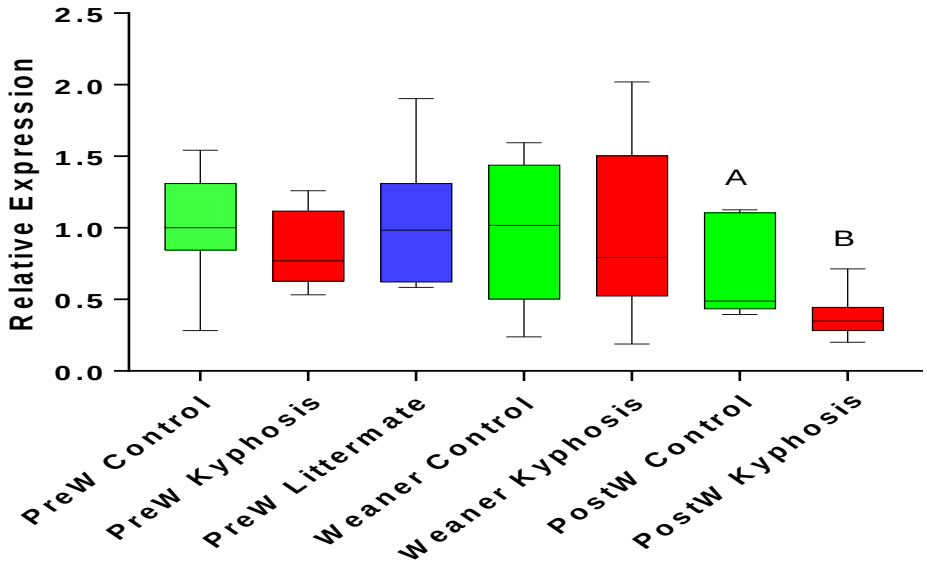

Figure 3.6: *Relative real-time PCR expression of ASPN in the trabecular bone of pre-weaning (PreW) (n=17 per group), weaning (n=16 per group), and post-weaning (PostW) (n=7 per group) kyphotic and control pigs, calculated by qPCR. Data are presented as boxplots showing medians, 25th and 75th quartiles and upper and lower limits. Kruskal-Wallis Age p<0.01, Mann-Whitney AB p=0.025).*

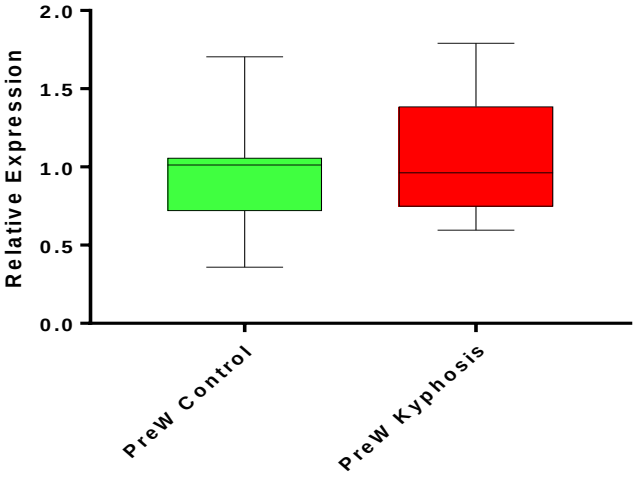

Figure 3.7: *Relative real-time PCR expression of PTK2B in the bone of pre-weaning (PreW) kyphotic (n=17) and control (n=17) pigs, calculated by qPCR. Data are presented as boxplots showing medians, 25th and 75th quartiles and upper and lower limits.*

Due to these marginal changes, *PTK2B* was not analysed in the older age groups.

3.3.3.6 Expression of *ACTC1* in Kyphotic Cartilage

The differences in *ACTC1* expression in the cartilage of kyphotic pre-weaners was notable, but not significant (FC-1.51, p=0.308) (Figure 3.8). *ACTC1* did not show changes that were as significant as the changes in gene expression for *DCN* and was not analysed in the older age groups.

3.3.3.7 Expression of *DCN* in Kyphotic Cartilage

DCN was observed to be upregulated in kyphotic pre-weaners in comparison to non-related controls (FC+1.30, p=0.04), but not in comparison to littermates (FC-1.43, p=0.664), and *DCN* was significantly upregulated in littermates in comparison to non-related controls (FC+1.87, p=0.011) (Figure 3.9). There were no significant differences in expression observed in kyphotic weaners (FC+1.15, p=0.462) or in kyphotic post-weaners (FC+2.09, p=0.568). There were no overall effects of phenotype (p=0.133) or age (p=0.166) on expression. The results indicate that *DCN* is upregulated within kyphotic cartilage at the pre-weaning stage, and that this effect is confined to the litter.

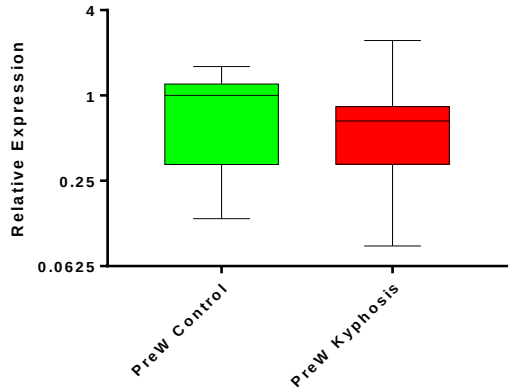

Figure 3.8: *Relative real-time PCR expression of ACTC1 in the cartilage of pre-weaning (PreW) kyphotic (n=17) and control (n=17) pigs, calculated by qPCR. Data are presented as boxplots showing medians, 25th and 75th quartiles and upper and lower limits*

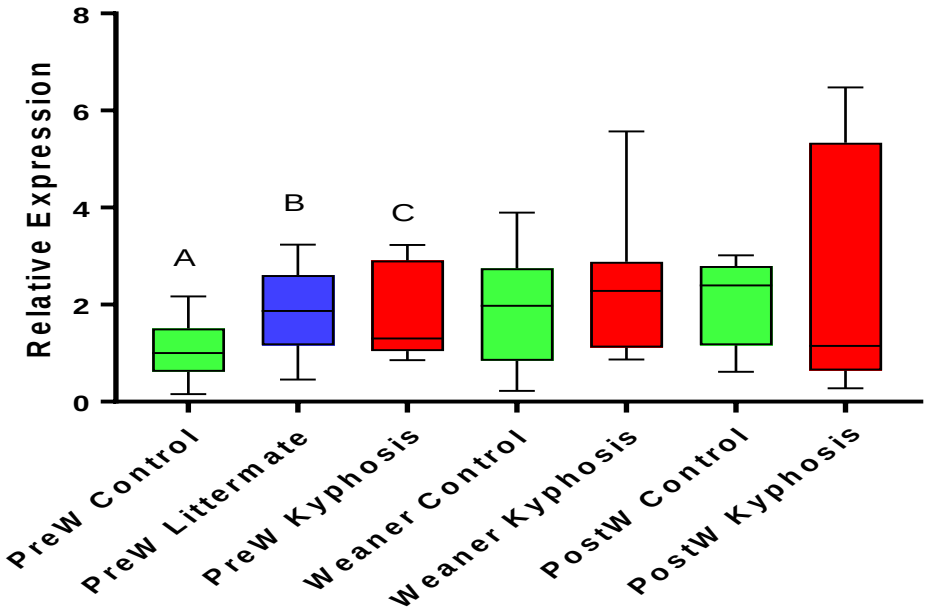

Figure 3.9: *Relative real-time PCR expression of DCN in the cartilage of pre-weaning (PreW) (n=17 per group), weaning (n=16 per group), and post-weaning (PostW) (n=7 per group) kyphotic and control pigs, calculated by qPCR. Data are presented as boxplots showing medians, 25th and 75th quartiles and upper and lower limits. Mann-Whitney AB p=0.011 AC p=0.04.*

3.4 Discussion

The original hypotheses stated that the TGF- β signalling pathway will be downregulated in kyphotic bone, SLRPs and actin genes will show upregulation in kyphotic cartilage tissues, and the TGF- β pathway will associate with both tissue types. However qPCR analysis indicated the TGF- β pathway is not downregulated in kyphotic trabecular bone. Nor were actin genes associated with kyphotic cartilage. However, the results agree with the original hypotheses in that SLRPs are upregulated in kyphotic cartilage, in particular *DCN*. The analysis also showed the SLRPs *ASPN* and *DCN* to associate with kyphotic bone and cartilage tissues respectively, and both of these genes influence TGF- β signalling (Yao et al., 2016, Nakajima et al., 2007). This finding therefore overlaps the TGF- β signalling pathway in kyphotic bone and cartilage tissues, and agrees with the original hypotheses. With biomarkers such as *BMPR1A*, *BGLAP* and *ASPN*, there were effects of age observed in that biomarker expression decreased over time, however only *ASPN* was indicated to be

differentially regulated in the post-weaning stage. Otherwise, in all cases, the greatest effects in regards to fold-changes and p-values were observed within the pre-weaning group.

3.4.1. TGF-β Pathways and Bone Mineralisation in Kyphotic Bone

In the present study, TGF-β was identified as the molecular regulator most significantly associated with kyphotic bone and cartilage tissues, as opposed to other pathways that regulate bone growth such as IHH or Wnt signalling. However, qPCR analysis showed that although TGF- β followed the trend in the microarray in that this gene was downregulated in the bone of kyphotic pre-weaners in comparison to controls, this was not observed to be significant (Figure 3.3). However, TGF- β showed a tendency to be downregulated in littermates in comparison to non-related controls (Figure 3.3), which might suggest the effect is confined to the litter. TGF- β belongs to the TGF- β superfamily composed of over 40 molecules, also including BMPs, and functions by transmitting signals across the plasma membrane through ligating with TGF- β receptors and inducing signalling cascades through phosphorylation of smad 2/3 proteins to control gene expression of bone formation genes (Chen et al., 2012). However, in low physiological doses, TGF- β has been observed to induce osteoclast differentiation, and this outlines the pathways dual roles in regulating bone homeostasis (MacFarlane et al., 2017). Yet, TGF- β has been observed in separate experiments to regulate genes related to osteoblast differentiation that showed in the current study*: TGF-* β positively regulates expression of genes such as Actins (Xu et al., 2001), *IGF2* (Goel et al., 2013), and *BMP1* (Lee et al., 1997). The relevance of actins to bone mineralisation is that reorganisation of the cell cytoskeleton, which is composed of actin filaments, is associated with mineralisation of *in vitro* cell cultures (Goncharenko et al., 2016). However the lack of differential expression of TGF- β by qPCR indicates this pathway, and the aforementioned genes induced by TGF- β that regulate mineralisation, is not associated with the development of kyphotic bone.

The expression of other genes in the study that associate with TGF- β, and regulate mineralisation, were also investigated. GO term “BMP signalling” was identified by both IPA and Cytoscape analysis, and *BMPR1A* showed consistency among these. qPCR analysis showed *BMPR1A* had a tendency to be downregulated within trabecular bone of kyphotic

pre-weaners, thus following the trend indicated by the microarray (Figure 3.4). The BMP signalling pathway serves as a component of the TGF- β pathway; though TGF- β promotes the cellular differentiation of committed progenitor cells towards an osteoblast lineage, BMPs are required to commit uncommitted MSCs towards an osteoblast lineage and thus initiate the initial stages of organ morphogenesis (Manolagas, 2000). *BMPR1A* codes for the BMP type I receptor, which interacts with BMP ligands and therefore associates with the TGF- β signalling pathway (Chen et al., 2012). Specific knockout of *BMPR1A in vivo* results in a failure of mesenchymal condensation preceding endochondral ossification (Lim et al., 2015), an increase in immature osteocyte abundance in bone (Kamiya et al., 2016); yet other experiments have indicated the expression of this gene is required to promote adipogenesis differentiation (Chen et al., 1998). A downregulation of *BMPR1A* could therefore indicate either: a reduction in endochondral bone growth, or adipocyte differentiation, or potentially both processes.

A prominent marker of bone formation observed in the current study was *BGLAP*, which regulates hydroxyapatite crystal deposition that forms the mineral component of bone (Tsao et al., 2017). Although *BGLAP* was identified as a differentially expressed gene in a vitamin-D induced model of kyphosis (Amundson et al., 2016), qPCR analysis did not return significant, differential expression of *BGLAP* between kyphotic or control pigs in the present study (Figure 3.5). This finding suggests *BGLAP* expression, unlike the hypovitaminosis D model of kyphosis, is not affected in the bone of spontaneous kyphotic cases.

Yet, qPCR analysis showed that *ASPN*, a regulator of TGF- β, was significantly downregulated in the bone of kyphotic post-weaners in comparison to age-matched controls (Figure 3.6). *ASPN* has been observed to inhibit TGF- β binding to TGF- β receptor II and therefore silence expression of TGF- β target genes; likewise, TGF- β also induces *ASPN* expression, indicating a regulatory feedback mechanism between the two genes (Nakajima et al., 2007). Separate studies confirm positive regulation of *ASPN* by *TGF*- β, but also observe an induction of *TGF*- β by *ASPN* (Kou et al., 2007), therefore highlighting the regulatory role *ASPN* has on TGF- β signalling. In regards to regulation of mineralisation, *ASPN* has been demonstrated to upregulate *RUNX2* and *OSTERIX* at the developing cartilage template and induce osteoblast differentiation and mineralization to form ossified bone (Kalamajski et al., 2009). Yet in periodontal tissue, *ASPN* has been demonstrated to negatively regulate mineralisation (Tomoeda et al., 2008), in contrast to the findings of Kalamajski et al. (2009). This could

indicate a difference in function between tissue types, but *ASPN's* role as a regulator of bone mineralisation is clear. Therefore a downregulation of this gene at the post-weaning stage could either: be a factor that contributes to reduced bone mineralisation in kyphotic pigs (Nielsen et al., 2005, Done et al., 1999, Done and Gresham, 1988) ; or potentially is a compensatory mechanism induced by the tissue to upregulate the TGF- β pathway and restore osteoblast differentiation. Overall, these indicate osteoblast differentiation and subsequent activity is reduced in post-weaning kyphotic trabecular bone.

In summary, the TGF- β signalling pathway, as a result of *ASPN* differential expression, is associated with the trabecular bone of kyphotic post-weaners, but there were no clear indications that the pathway is downregulated in kyphotic trabecular bone. Downregulation of *ASPN* in post-weaning kyphotic trabecular bone could indicate reduced endochondral bone growth. The BMP signalling pathway could also be downregulated in the bone of kyphotic pre-weaners as a result of *BMPR1A* showing a trend to be downregulated.

3.4.2. Angiogenesis in Kyphotic Bone

From the list of differentially expressed genes, genes that associate with TGF- β and BMPs appear to associate with regulation of angiogenesis. *BMPR1A* and *PTK2B* are associated with regulation of angiogenesis (Xiao et al., 2015, Weis et al., 2008), and were analysed by qPCR in the current study. As discussed above, microarray and qPCR analysis indicated *BMPR1A* to be potentially downregulated within the bone of kyphotic pre-weaners (Figure 3.4). Selective inhibition of *BMPR1A*, with subsequent silencing of smad/ID signalling, disrupts angiogenesis *in vitro* (Xiao et al., 2015). qPCR analysis showed *PTK2B* followed the trend in the microarray in that this gene was upregulated in kyphotic trabecular bone (Figure 3.7), but this change was not significant. The current data supports the hypotheses that the process of angiogenesis has been disrupted in kyphotic trabecular bone tissue, due to *BMPR1A* showing a tendency to be downregulated in kyphotic pre-weaners. Other genes in the microarray such as *SMAD7,* indicated to be upregulated, is associated with angiogenesis, particularly in that it inhibits the TGF- β signalling pathway so as to prevent induction of *VEGF* (Peng et al. 2013). *ID1*, a downstream molecule of *BMPR1A,* was indicated to be downregulated by Cytoscape and IPA; through activation of NF-kB pathway, *ID1* induces angiogenesis *in vitro* (Su et al. 2013).

Nielsen et al. (2005) observed that a lack of blood supply to the bone was also contributing to the development of kyphosis. During endochondral ossification, the extending cartilage template requires vascular invasion in order to deliver osteoblasts that will replace the cartilage template with ossified tissue and thus allow the growth of the tissue (Burr and Allen, 2014, Karsenty et al., 2009, Maes et al., 2010) . This has not been observed in any other reported case of kyphosis, yet the current study provides evidence that regulation of angiogenesis could potentially be disrupted as a result of fluctuations in genes such as *BMPR1A*. These findings once again demonstrate the critical role of the TGF-β and BMP pathways in regulating organ morphogenesis, and that there are other biological processes, as opposed to osteoblast differentiation, affected by these pathways that could be contributing to kyphosis.

3.4.3 Actin Regulation in Kyphotic Cartilage

In IPA canonical pathways, the genes *ACTC1*, *ACTA1* and *ACTA2* showed frequent consistency (Table 3.2). *ACTC1* was selected for qPCR verification, based on evidence that the expression of this gene can influence the expression of the other skeletal actins (Kumar et al., 1997). However, qPCR indicated the expression of *ACTC1* to be downregulated 1.56-fold in the cartilage of pre-weaning kyphotic pig in comparison to non-related controls, but this was not significant (Figure 3.8). Therefore, the original hypotheses which stated that genes relating to actin regulation will be affected within kyphotic pigs is rejected.

3.4.4 TGF-β Pathway and Cartilage Metabolism in Kyphotic Cartilage

In kyphotic cartilage, IPA identified TGF- β as the top upstream regulator, yet TGF- β was not identified as a differentially expressed gene. *DCN* was observed in “osteoarthritis pathway” canonical pathway (Table 3.2). However, Cytoscape analysis indicated two genes differentially expressed within the cartilage, *CILP* and *DCN,* to be upregulated in kyphotic cartilage (Table 3.3). Both of these genes have been identified to influence TGF- β signalling (Yao et al., 2016, Mori et al., 2006). Upon qPCR verification, *DCN* was shown be upregulated in the cartilage of pre-weaning kyphotic piglets and littermate pre-weaners in comparison to non-related controls (Figure 3.9), thereby suggesting the effect is confined to the litter. This result agrees with the original hypotheses in that SLRPs will show upregulation in kyphotic cartilage, and that the TGF- β pathway will associate with kyphotic cartilage.

DCN belongs to the family of SLRPs which compose cartilage ECM, and holds an established role in regulating collagen fibrillogenesis by aiding fibril growth, inducing expression of collagens, and maintaining cartilage ECM (Gubbiotti et al., 2016, Salinas and Anseth, 2009). Elevated expression of *DCN* is also associated with the development of osteoarthritis (Bock et al., 2001) , as well as experimental models of disc decay (Melrose et al., 1997). Whether this is a cause or effect remains up to debate; Bock et al. (2001) suggested increased synthesis of Decorin was to restore PG losses that have occurred during osteoarthritis. Nonetheless, the observed upregulation of *DCN* within the cartilage of kyphotic and littermate pre-weaners suggests these pigs are experiencing the early stages of disc degeneration.

DCN interacts with TGF- β, in that it binds TGF- β and prevents subsequent signalling (Yao et al., 2016), although other studies also showcase *DCNs* ability to facilitate binding of TGF- β to its receptors (Takeuchi et al., 1994). Therefore, based on these observations, the upregulation of *DCN* could indicate either: a compensatory mechanism induced by the cartilage to re-upregulate TGF- β signalling, or that *DCN* is binding TGF- β and preventing subsequent Smad signalling. TGF-Smad signalling has been demonstrated to be critical in cartilage growth and repair (Ying et al., 2018), and upregulation of type II collagen expression, a marker of differentiating chondrocytes has been observed in response to TGF-β treatment *in vitro* (Johnstone et al., 1998). However, Smad molecules were not indicated to be differentially expressed in kyphotic cartilage, therefore suggesting that TGF-Smad signalling has possibly not been compromised by *DCN*. Rather, it is likely that *DCN* may be attempting to facilitate TGF- β binding to its receptors (Takeuchi et al., 1994) in an attempt to repair the cartilage.

The anatomical examinations of the intervertebral cartilage from previous cases (Done and Pearson, 2004) were performed on older, finishing pigs; therefore it would be useful to confirm if similar changes in cartilage morphology are occurring at pre-weaning in order to confirm or deny the possibilities suggested by differential expressions of these genes. Though Done and Pearson (2004) identified a collapsing of the thoraco-lumbar junction, this has not been observed in other cases of kyphosis; therefore the collapsing of the junction might indeed be contributed to by increased muscle mass in older, kyphotic pigs. However the data obtained in the current study also suggests biological changes are occurring in the

cartilage of very young kyphotic pigs that could potentially lead to a collapse of the thoraco-lumbar junction.

3.4.5 Overlap between Kyphotic Bone and Cartilage Tissues

ASPN belongs to the SLRP family alongside *DCN*, *DCN* mirrors *ASPN*s functions in sharing a regulatory relationship with TGF- β (Kalamajski et al., 2009). Furthermore, *DCN* and *ASPN* compete for collagen binding during cartilage bio mineralisation (Kalamajski et al., 2009); therefore an upregulation of *DCN* within the cartilage at pre-weaning may prevent Asporin-collagen interactions and inhibit subsequent endochondral ossification. This could be another mechanism that contributes to reduced mineralisation and growth of vertebrae in kyphosis.

These findings therefore associates the family of SLRPs with the pathogenesis of kyphosis. Due to their roles in regulation of TGF- β activity, the differential expression of *ASPN* and *DCN* in bone and cartilage tissues suggests the TGF- β pathway has been affected in both tissues.

3.5 Conclusions

Upregulation of SLRPs in kyphotic cartilage, and overlap of the TGF-β pathway in kyphotic bone and cartilage tissues agrees with the original hypotheses. The study suggests the TGF-β pathway does not directly contribute to kyphosis, but differential regulation of *ASPN* and *DCN* in bone and cartilage tissues could indicate this pathway is rather being utilised in an attempt to repair kyphotic tissue. Due to its associations with cartilage deterioration and potential reduction of endochondral bone growth, the current study highlights a critical role for *DCN* in bone pathogenesis. *DCN* should be considered as a diagnostic marker for kyphosis in pigs.

Chapter 4: The effect of vitamin A supplementation on vitamin D status and differential gene expression in the trabecular bone of growing pigs

4.1 Introduction

Vitamin A and vitamin D are fat-soluble nutrients obtained from the diet (Harrison, 2005, Holick, 2005). These vitamins share an interaction, but the basis of this relationship is subject to debate. Early studies in rats and turkeys indicated vitamin A antagonises physiological effects brought about by vitamin D toxicity on bone tissue, and vice versa (Clark and Bassett, 1961, Metz et al., 1985). Furthermore, Aburto et al. (1998) observed high dietary vitamin A to increase requirements for 25(OH) D and 1,25$(OH)_2$D to maximise bone ash %, and to reduce rickets severity respectively in broilers. In rats, vitamin D increases serum Ca and decreases serum P concentrations, however vitamin A reduces the ability of Vitamin D to maintain these concentrations in a dose-dependent manner (Rohde and DeLuca, 2005). Overall, the results of these studies suggest an antagonistic relationship between the two vitamins in regulation of skeletal physiology, yet the basis of this antagonism has not been fully elucidated.

Studies in salmon have shown vitamin A decreases plasma 1,25$(OH)_2$D after 5 days (Ornsrud et al., 2009), and exposure to vitamin A decreased serum 25(OH) D in rats in a time-dependent manner (Frankel et al., 1986). These studies therefore suggest vitamin A antagonises serum 25(OH) D and thus lowers vitamin D availability to tissues. Vitamin A and vitamin D have been proposed to have their intestinal absorption regulated by cholesterol transporters (Harrison, 2005, Reboul, 2015), therefore excess vitamin A could potentially outcompete vitamin D for absorption. Vitamin D holds significant, commercial relevance to pigs due to its positive regulatory effects on skeletal health and growth (Holick, 2005, Witschi et al., 2011, Crenshaw et al., 2011). Therefore there is a requirement to further characterise the vitamin A-vitamin D relationship in pigs. While vitamin D has been demonstrated to antagonise liver RE storage dose-dependently in broilers (Aburto et al., 1998), it is not known whether vitamin A will also affect serum 25(OH) D in a dose-dependent manner.

Excessive vitamin A supplementation has been observed to induce narrowing and fragility of bones in pigs and rats (Pryor et al., 1969, Broulik et al., 2013, Kneissel et al., 2005), as well as disrupt endochondral bone growth in pigs (Anderson et al., 1966). Over-supplementation with vitamin A has also been suggested to contribute to lameness (van Riet et al., 2013) and the development of kyphosis in pigs (Belsue, 2010). There is a requirement to further characterise the mechanisms of excess vitamin A's effects on skeletal development in pigs. Kneissel et al. (2005) observed excess vitamin A to induce thinning of the cortical compartment of long bones, yet trabecular BMC remained unchanged. However Lind et al. (2011) observed trabecular BMD to decrease in response to excessive vitamin A. This is further complicated by findings which also show feeding rats vitamin A over a period of up to 20 months did not induce changes in trabecular bone mass (Wray et al., 2011). Lind et al. (2012) demonstrated excess vitamin A upregulates expression of osteoblast-associated genes within the marrow compartments of long bones, but these changes do not persist in cortical bone. These findings demonstrate the compartment-specific effects of excess vitamin A supplementation on bone development, but it is not clear as to whether excess vitamin A will affect differential gene expression in trabecular bone similar to what was observed within endosteal and marrow compartments (Lind et al., 2011, Lind et al., 2012). The effect of vitamin A supplementation on trabecular bone development requires further investigation, if we are to understand the full scope of excess vitamin A's effects on skeletal development.

The present study set out to investigate how high doses of vitamin A supplementation will affect serum 25(OH) D and differential gene expression in the trabecular bone of growing pigs. The hypotheses for the study are as follows:

- Based on Frankel et al. (1986) findings that suggest an antagonistic relationship between vitamin A and serum 25(OH) D, the hypotheses is that vitamin A will antagonise serum 25(OH) D in a dose-dependent manner, and this will likely relate to intestinal absorption.
- Based on Lind et al. (2012) findings that excessive vitamin A induces expression of mineralisation genes in interior bone compartments, and that trabecular bone mass remains unchanged over time in response to vitamin A (Wray et al., 2011, Kneissel

et al., 2005), the hypotheses is that genes which regulate osteoblast differentiation will show upregulation in trabecular bone in response to excess vitamin A.

4.2 Materials and Methods

The trial was performed at Cockle Park farm, Newcastle University, and was approved by the Animal Welfare and Ethics review board at Newcastle University (PPL 70 8262).

4.2.1 Pigs and Experimental Procedures

The experimental setup of the trial, as well as laboratory procedures relating to RNA extraction, cDNA synthesis, Microarray analysis, Microarray Pathway Analysis, qPCR analysis, qPCR data analysis, HPLC, and ELISA are summarised in Chapter 2. Other methods specific to this experiment are indicated below.

4.2.2 Feed Intake

Individual feed intake was not monitored throughout the trial period, but it is estimated that a pig will consume approximately 4% of its BW per day. These data were then used to calculate the total average intake of vitamin A from diets, and dose, both in total µg over time and µg per kg of BW over time, for all pigs throughout the experimental period.

4.2.3 Serum Biochemistry

Serum Ca, P and ALKp were determined in control and treated pigs; samples were analysed at the Laboratory of Blood Sciences in the Royal Victoria Infirmary. ALKp is routinely measured in serum in order to indicate early pre-osteoblast differentiation, and thus act as a serum marker of bone formation activity (Skillington et al., 2002). The assays were performed on a Roche Cobas 8000 analytical line with kits for each assay, SOPs can be viewed in the appendix (B-D).

4.2.4 Confocal Microscopy

Samples from all 4 lobes of the liver were taken (roughly 0.1cm dimensions) and submerged in 1% glutaraldehyde solution before storage at 4°C. Confocal microscopy was performed on liver samples in order to allow for visualisation of the abundance and distribution of REs in response to vitamin A dose. Optimal focal plane within the tissue was determined through

excitation at 488nm and observing autofluorescence (emission between 495-562nm). Single plane confocal images were then acquired - using minimal noise reduction to avoid photobleaching - through excitation at 360nm (long pass) with emission between 415-548nm (blue) followed by collection of autofluorescence through excitation at 488nm and emission between 495-562nm at the same plane. All sections were scanned under identical conditions and any manipulation of images was applied to all equally. Image J software was used to visualise fluorescent changes in tissues.

4.2.5 Statistical Analysis

Before statistical analysis, data were tested for normal distribution using Shapiro-Wilk test and observing skewness and kurtosis (SPSS Software). Data were ln transformed to normalise the distribution for all data sets, however this was not possible to achieve normal distribution for all data. Therefore, the non-parametric Kruskal-Wallis test was used to determine the effects of vitamin A dose on dependent variables, and the Mann-Whitney test was used to determine significant differences between individual groups. A p value <0.05 was considered statistically significant.

4.3 Results

In the 5250µg RP/kg BW group, 1 pig had to be sampled 2 weeks earlier due to signs of compromised welfare. In the 10000µg RP/kg BW group, 2 pigs had to be sampled 2 weeks earlier due to signs of compromised welfare. In both cases, the animals showed signs of severe tremors and difficulties with movement.

4.3.1 Vitamin A consumption and Bodyweight

The average vitamin A intake, in terms of total intake and intake in µg/kg of BW, was calculated for each treatment group based on diet and assigned RP dosage (Figure 4.1). The average BW was also measured for all pigs on a weekly basis (Figure 4.1). At the time of tissue sampling, the average total vitamin A consumed in µg per week ranged from 7849µg for controls, to 778310µg for pigs receiving 10000µg RP/kg BW.

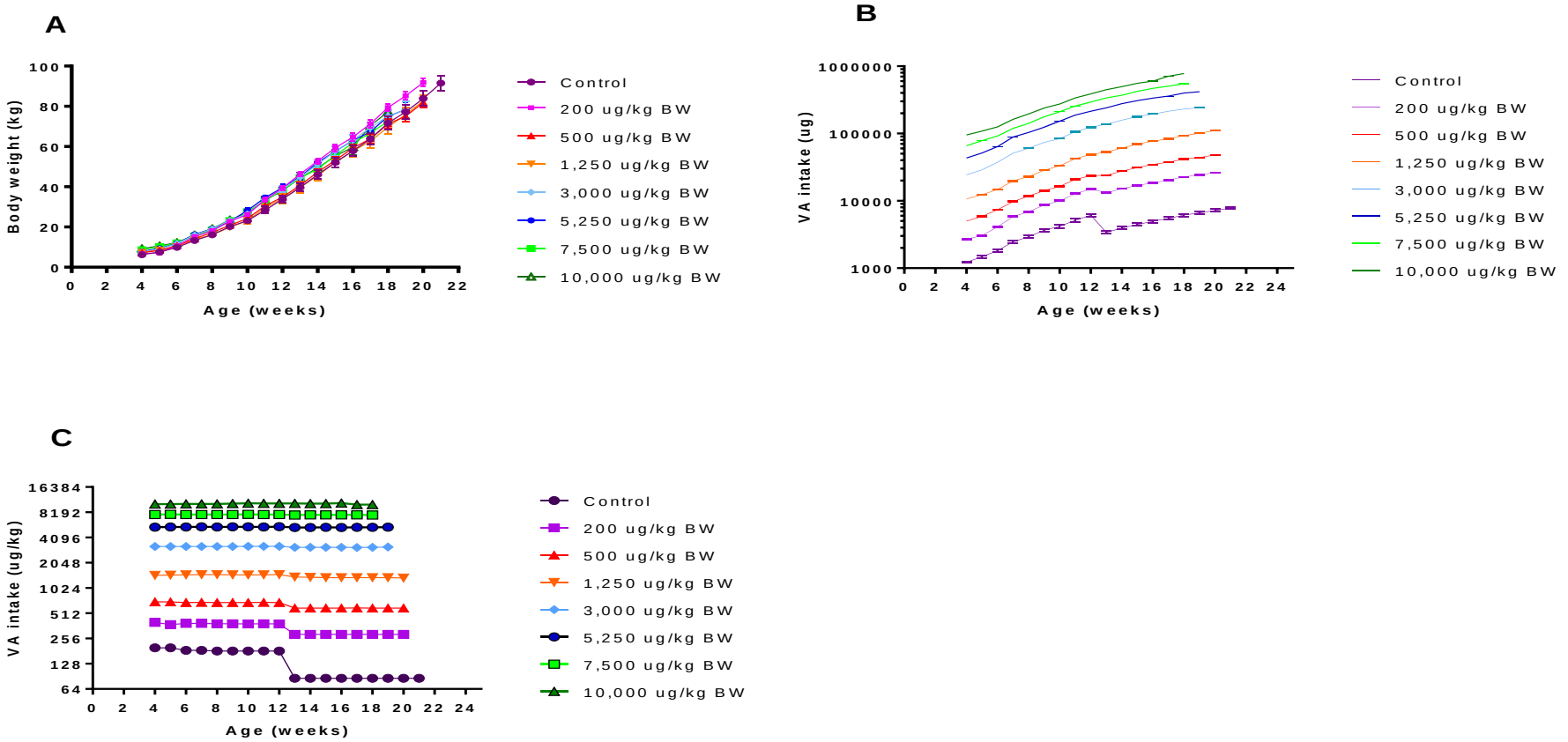

Figure 4.1: *Bodyweight (BW) and estimated vitamin A intake from diet and dose per pig group (n=8 per group) calculated over the experimental period from 4 weeks to 22 weeks of age**.** The assumptions of the calculations were that each pig will eat approximately 4% of its BW daily, and that pigs were fully supplemented with their assigned RP dosage.* ***A****. The average BW of pigs per group* ***B.*** *The average total intake of vitamin A, in µg, over time per pig group. Y-axis is in a log10 scale to allow for presentation of data.* ***C*** *The average intake of vitamin A, in µg per kg of BW, per pig group. Y-axis is in a log2 scale to allow for presentation of data. All data are presented as Mean ± SEM.*

At the time of tissue sampling, the average vitamin A consumed in µg/kg BW ranged from 85.8µg/kg BW for controls, to 10106µg/kg BW for pigs receiving 10000µg RP/kg BW. The data indicates that the assigned doses for the study were successful in mediating vitamin A accumulation according to dose group, taking into consideration the differences in time of which pigs were sampled. No significant differences in BW were observed between control pigs or treated pigs at any time points. At the time of sampling, average BWs for all pigs ranged from 91.48kg for controls, to 77.33kg for pigs receiving 10000µg RP/kg BW.

4.3.2 Retinol and Retinyl Ester Concentrations in Liver

Retinol and RE concentrations (µmol/g of liver) were calculated in the livers of control and treated pigs (Figure 4.2). From control to 3000µg RP/kg BW, there was a clear dose-response relationship in the saturation of the liver with total REs, these concentrations increased from 0.43µmol/g of liver to 12.46µmol/g of liver ($p<0.01$). Between 3000µg RP/kg BW and 5250µg RP/kg BW, there was a tendency for total REs to drop from 12.46µmol/g of liver to 7.16µmol/g of liver ($p=0.078$), and no significant differences were observed between treatment groups between the 3000µg RP/kg BW and 10000µg RP/kg BW groups. The results indicate that the liver is saturated around the intake of 3000µg RP/kg BW, and that no further increase in liver RE concentrations can be achieved. Confocal microscopy also showed that pigs receiving 3000µg RP/kg BW showed extreme saturation of REs in liver stellate cells in comparison to control pigs (Appendix A). This analysis offers a visual confirmation of RE storage in the livers of pigs receiving 3000µg RP/kg BW.

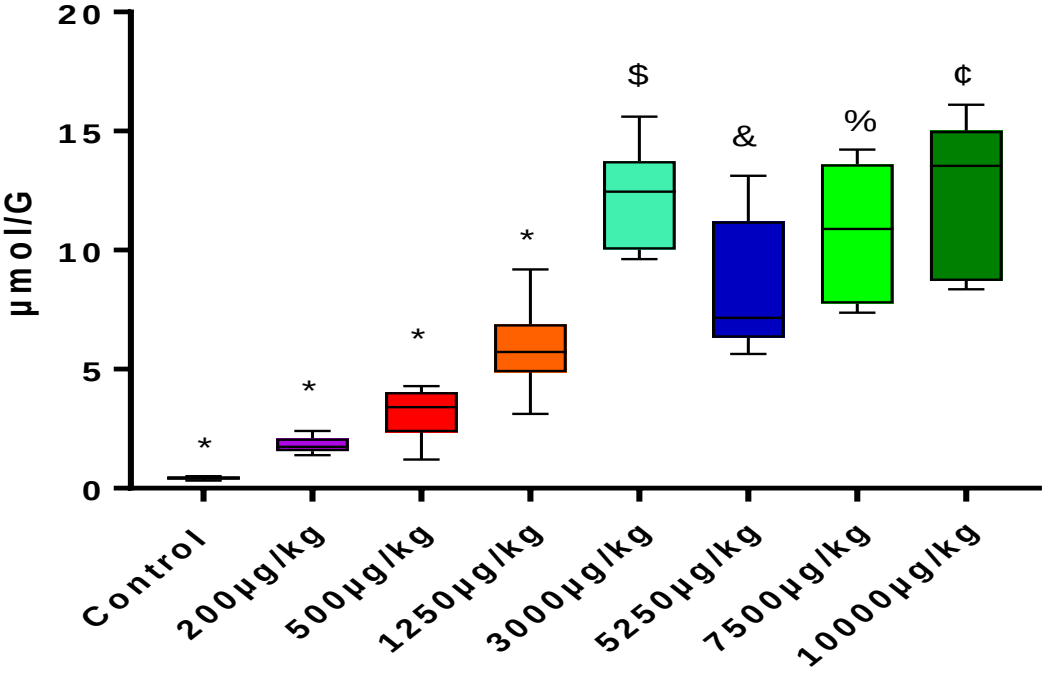

Figure 4.2: *The concentrations (µmol/g of liver) of total retinyl esters in the livers of pigs receiving different doses of Retinyl Propionate (RP) (n=8 per group) post-mortem. Data are presented in boxplots showing the median, 25th and 75th quartile ranges, and upper and lower limits.*

Mann-Whitney:

**p<0.05 from all*

$ p<0.05 from all except 7500µg/kg and 10000µg/kg

& p<0.05 from all except 7500µg/kg

% P<0.05 from all except 3000µg/kg, 5250µg/kg and 10000µg/kg

¢ p<0.05 from all except 3000µg/kg and 7500µg/kg

4.3.3 25(OH) Vitamin D Serum Concentrations

The average serum concentrations of 25(OH) D were calculated in control and treated pigs (Figure 4.3). Overall, there was an effect of supplemented vitamin A to affect 25(OH) D serum concentrations ($p<0.05$). Between controls and pigs receiving 500µg RP/kg BW, serum 25(OH) D decreased from 21.48ng/ml to 18.73ng/ml ($p<0.05$). Between controls and pigs receiving 1250µg RP/kg BW, serum 25(OH) D had a tendency to be reduced from

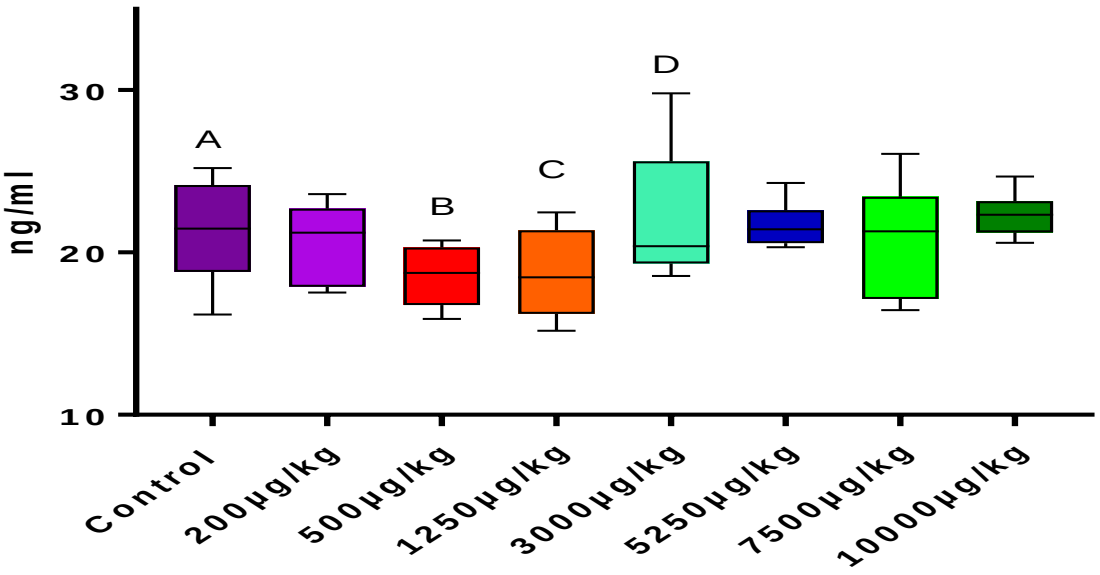

Figure 4.3: *The concentrations of 25(OH) D (ng/ml) in the serum of pigs receiving different doses of RP treatment (n=8 per group) post-mortem. Data are presented in boxplots showing the median, 25th and 75th quartile ranges, and upper and lower limits. Mann-Whitney Test AB p<0.05, AC p=0.074, BD p=0.059, CD p<0.05*

21.48ng/ml to 18.48ng/ml (p=0.074). From 1250µg RP/kg BW to 3000µg RP/kg BW, serum 25(OH) D increased from 18.48ng/ml to 20.38ng/ml (p<0.05).

4.3.4 Serum Biochemistry

There were no effects of treatment observed on the serum concentrations of Ca or P in control or treated pigs during the experimental period. There were also no effects of treatment on serum ALKp during the experimental period (Table 4.1).

Treatment Groups (Retinyl Propionate - µg/Kg of BW daily)	ALKp (U/L) (SEM)	Ca (mmol/L) (SEM)	PO_4 (mmol/L) (SEM)
Control (n=8)	129.38(7.67)	2.60 (0.04)	2.82 (0.10)
200µg/KG (n=8)	134.50 (12.74)	2.57 (0.03)	2.82 (0.03)
500µg/kg (n=8)	137 (11.30)	2.65 (0.04)	2.79 (0.12)
1250µg/KG (n=8)	125.38 (8.85)	2.59 (0.03)	2.82 (0.11)
3000µg/KG (n=8)	112.25 (12.13)	2.60 (0.03)	2.71 (0.07)
5250µg/KG (n=8)	104.00 (4.26)	2.64 (0.03)	2.62 (0.05)
7500µg/KG (n=8)	116.86 (7.78)	2.63 (0.03)	2.57 (0.06)
10000µg/KG (n=8)	121.14 (14.88)	2.60 (0.02)	2.63 (0.08)

Table 4.1: *The average serum concentrations of Alkaline Phosphatase (ALKp), a serum marker of bone formation, Calcium (Ca) and Phosphorus (P) in control and treated pigs (n=8 per group) post-mortem are shown.*

4.3.5 Microarray Profiling of Duodenum of Vitamin A treated Pigs

In the duodenum of pigs receiving 10000µg RP/kg BW, a total of 5953 transcripts were found to be differentially expressed > 2-fold. Of these transcripts, 4813 were found to be upregulated (80.85%) and 1140 were downregulated (19.25%) in comparison to control pigs receiving no vitamin A supplementation.

Genes which hold roles in the apical and basolateral absorption of vitamin D were investigated in the data. From the list of differentially expressed genes, the results showed the genes Cluster Determinant-36 (*CD36)*, Scavenger Receptor Class B member 1 (*SR-BI)* and ATP Binding Cassette Subfamily A member 1 (*ABC1)* are differentially expressed in response to 10000µg RP/kg BW (Table 4.2). These genes regulate intestinal absorption of vitamin D (Reboul, 2015, Harrison, 2005, Silva and Furlanetto, 2018). The gene Transient Receptor Potential Cation Channel Subfamily V Member 6 (*TRPV6)*, which regulates Ca absorption, was also regulated in the intestines of pigs receiving 10000µg RP/kg BW (Table 4.2). Furthermore, Cytochrome p450, family 27, sub-unit B1, (*CYP27B1)*, a gene which synthesises the active metabolite of vitamin D: 1,25 $(OH)_2$ D (Holick, 2005), was upregulated in response to 10000µg RP/kg BW (Table 4.2).

Gene Name	*Regulated Process*	*Fold-Change*	*p-value*
Cluster Determinant 36/ *CD36*	Vitamin D absorption – Apical	2.52↑	0.02
Scavenger Receptor Class B member 1 /*SR-B1*	Vitamin D absorption – Apical	4.45↓	0.0067
ATP Binding Cassette Subfamily A member 1 /*ABC1*	Vitamin D absorption – Basolateral	3.45↑	0.01
Cytochrome p450, family 27, sub-unit B1, /*CYP27B1*	1,25(OH)2D synthesis from 25(OH)D	3.32↑	0.008
Transient Receptor Potential Cation Channel Subfamily V Member 6/*TRPV6*	Ca absorption – Apical	4.64↓	0.0015

Table 4.2: *Differential expression of transporters related to vitamin D absorption in the small intestines of pigs receiving 10000µg RP/kg BW. The direction and fold-changes in gene expression in comparison to control pigs are shown, as well as the p-value calculated by moderated T-Test in Genespring.*

4.3.6 Microarray Profiling of Trabecular bone of Vitamin A-treated Pigs

In the trabecular bone of pigs receiving 10000µg RP/kg BW, a total of 318 transcripts were found to be differentially expressed >2-fold. Of these transcripts, 199 were found to be upregulated (62.58%) and 119 were downregulated (37.42%) in comparison to control pigs receiving no vitamin A supplementation. The most affected genes, in regards to fold-changes, are shown in Table 4.3. Cytoscape identified a total of 5 genes to be differentially expressed in the trabecular bone of pigs treated with 10000µg RP/kg BW. Various GO terms were associated with each gene, but no GO terms overlapped between any genes.

Gene Symbol	Gene Title	Molecular Function	Fold-change	p-value
CLSTN1	Calsyntenin-1	*calcium ion binding*	18.68↑	0.0193
MAP3K2	mitogen-activated protein kinase kinase kinase 2	*MAPK signalling*	15.49↑	0.0140
CDC5L	cell division cycle 5-like	*Cell Cycle*	14.38↑	0.0324
PI4KB	phosphatidylinositol 4-kinase, catalytic, beta	*transferase activity*	13.47↑	0.0363
ZFP36L1	ZFP36 ring finger protein-like 1	*Adipocyte Differentiation*	12.49↑	0.0366
NDUFS2	NADH dehydrogenase (ubiquinone) Fe-S	*NADH dehydrogenase (ubiquinone)*	12.99↓	0.0152
ARHGAP31	Rho GTPase Activating Protein 31	*GTPase activator activity*	6.07↓	0.0282
KIFAP3	kinesin-associated protein 3	*kinesin binding*	4.36↓	8.92E-04
FAM175B	family with sequence similarity 175, member B	deubiquitination	3.36↓	2.50E-04
CSN1S2	alpha(s2)-casein	*transporter activity*	3.08↓	6.08E-04

Table 4.3: *The top 5 up and downregulated genes in the trabecular bone of pigs receiving 10000µg RP/kg BW, as indicated by Genespring. The gene name, the process this gene regulates, fold-change and p-value are indicated. P-value was calculated by moderated T-Test.*

Biomarkers	GO Terms				
MESP1*↓	Negative Regulation of Gastrulation	endodermal cell fate specification	negative regulation of mesodermal	positive regulation of cell fate	mesodermal cell migration
ARID4A*↓	Peptidyl-lysine trimethylation	histone H3-K4 trimethylation	histone H3-K9 trimethylation	histone H4-K20 methylation	histone H4-K20 trimethylation
NR1H4*↓	negative regulation of bile acid biosynthetic process	positive regulation of ammonia assimilation cycle	positive regulation of cellular amino acid metabolic process	regulation of glutamate metabolic process	
PRNP*↓	negative regulation of calcineurin-NFAT signalling cascade	negative regulation of calcium-mediated signalling			
ZFP36L1*↑	proepicardium development	septum transversum development			

Table 4.4: *Gene ontology pathways affected by differential gene expression in the trabecular bone of pigs receiving 10000µg RP/kg BW, as indicated by Cytoscape. Term pvalue corrected with Benjamini-Hochberg *p<0.01*

The most relevant and significantly affected GO terms, ranked by Term P-value corrected with Benjamini-Hochberg, related to “negative regulation of gastrulation” , “positive regulation of cell fate commitment” , “histone h3-k4 trimethylation” and “regulation of gamma delta T cell activation” (Table 4.4). The genes AT-Rich Interacting Domain 4A (*ARID4A)*, ZFP36 ring finger protein-like 1 (*ZFP36L1)*, and Nuclear Receptor Subfamily 1 Group H Member 4 (*NR1H4)* were found to share associations with osteoblast differentiation (Tseng et al., 2017, Monroe et al., 2010). IPA observed canonical pathways relating to “ILK signalling”, “Actin Nucleation by ARP-WASP Complex”, and “Actin Cytoskeletal signalling” to be significantly associated in the trabecular bone of pigs receiving 10000µg RP/kg BW (Table 4.5). The genes that consisted most among these pathways were *CDC42*, followed by Filamin A (*FLNA)*.

Vitamin A supplementation – Bone		
Pathway	**p-value**	**Genes**
ILK signalling	0.00630957	CDC42↑, FLNA↓, MYH4↑, RHOF↓
Caveolar-mediated Endocytosis signalling	0.00851138	MAP3K2↑, FLNA↓
Actin Nucleation by ARP-WASP Complex	0.04365158	CDC42↑,RHOF↓
Actin Cytoskeleton signalling	0.04570882	CDC42↑,MYH4↑,FLNA↓,TMSB10/TMSB4X↓

Table 4.5*: Canonical pathways affected in the trabecular bone of pigs receiving 10000µg RP/kg BW, as indicated by IPA. The p-value, as determined by Fishers-Exact test in IPA, and genes belonging to each pathway are also shown.*

Both of these genes relate to actin cytoskeletal dynamics and integrin related signalling. A gene network representing some of the relationships between identified genes and vitamin A is presented in Figure 4.4.

4.3.7 Candidate Gene Expression Verification

No genes were observed to overlap between IPA and Cytoscape in the current study. Cytoscape indicated *ZFP36L1* to be differentially expressed (Table 4.4), and the microarray indicated *ZFP36L1* to be in the top 5 differentially expressed genes in regards to fold-change (Table 4.3). *ZFP36L1* has also been demonstrated to influence osteoblast differentiation (Tseng et al., 2017), and was thus selected for qPCR analysis. *CDC42* and *FLNA* consisted among canonical pathways in IPA (Table 4.5), and both of these genes interact with one another to regulate cytoskeletal dynamics (Hu et al., 2017). Cytoskeletal dynamics have been illustrated to influence osteoblast differentiation and osteoclast activity (Lomri and Marie, 1996). Therefore, *CDC42* and *FLNA* were also selected for qPCR verification. Primer sequences for all genes of interest analysed in the current study can be seen in Table 4.6.

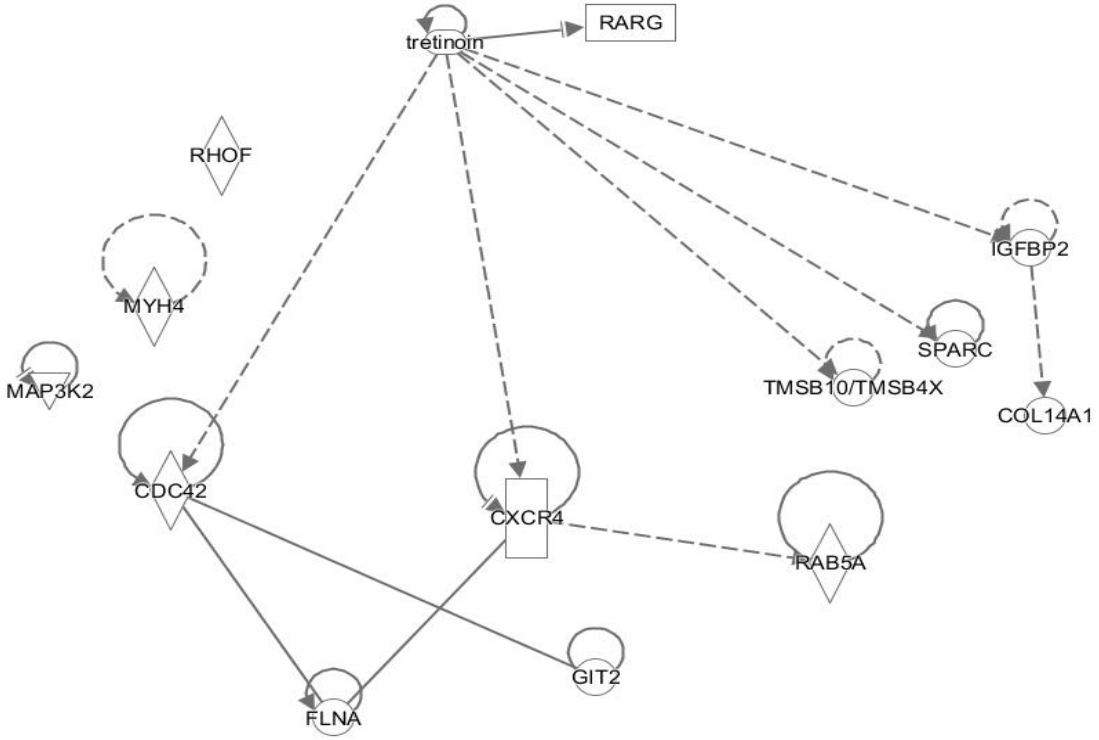

Figure 4.4: *Graphic representation of differential gene expression in the trabecular bone of pigs receiving 10000µg RP/kg BW, synthesised in IPA. Genes are represented by nodes, and relationships by edges.*

Table 4.6: *List of primer sequences for genes of interest for quantification of gene expression by real-time quantitative polymerase chain-reaction (q.PCR)*

PRIMER ID	***SEQUENCE 5'-3'***
RPL37 (HK)	F: GCCTACCATCTCCAGAAGTC R: CTTCACGGAATCCATGCCTG
CDC42	F: AGAAAAGTGGGTGCCTGAGA R: ACTCCACATACTTGACAGCCT
FLNA	F: GTCTTCAGGAGTCAGGGCTAA R: TCAATCAGGTAGACGCCGTT
ZFP36L1	F: GCGAAGTTTTATGCAAGGGTAAC R: CTGAGGAGCTGGTTCTGGTG

RPL37, Ribosomal protein sub-unit L37, CDC42, cell division cycle 42, FLNA, Filamin A, ZFP36L1, Zinc-finger protein C3H Type-Like 1

The following groups were selected for qPCR analysis in the current study: Controls, 200µg RP/kg BW, 1250µg RP/kg BW, 3000µg RP/kg BW, 5250µg RP/kg BW, and 10000µg RP/kg BW. This was due to these particular groups showing the most notable changes in RE liver storage when livers were analysed for REs post-mortem (Figure 4.2).

4.3.7.1 Expression of *ZFP36L1* in Trabecular Bone

There was a tendency for treatment (p=0.085) to have an effect on *ZFP36L1* expression in trabecular bone. Between controls pigs and pigs receiving 3000µg RP/kg BW, gene expression increased (Fold Change (FC) +1.47, p=0.037) (Figure 4.5). No significant differences were observed between controls or other treated groups.

4.3.7.2 Expression of *CDC42* in Trabecular Bone

There was not an effect of treatment (p=0.147) observed on *CDC42* expression in trabecular bone (Figure 4.6). This suggests no dose-response relationship exists between *CDC42* expression in trabecular bone and with vitamin A. Between control pigs and pigs receiving 3000µg RP/kg BW as well as 10000µg RP/kg BW, differences were observed (FC +1.32, p=0.036; FC + 1.70 fold, p=0.032, respectively), however these were not significant to the extent to conclude an overall effect of treatment.

4.3.7.3 Expression of *FLNA* in Trabecular Bone

There was a clear effect of treatment (p<0.01) on *FLNA* expression in trabecular bone (Figure 4.7), which verifies a relationship between *FLNA* expression in trabecular bone and vitamin A dose. Between control pigs and pigs receiving 3000µg RP/kg BW, *FLNA* expression increased (FC +8.17-fold, p<0.01), but no significant differences were observed in the earlier treatment groups in comparison to control pigs. Between pigs receiving 3000µg RP/kg BW and 5250µg RP/kg BW, *FLNA* expression decreased such that gene expression was increased 3.16-fold relative to control pigs (p=0.024). Pigs receiving 10000µg RP/kg BW showed an increase in *FLNA* expression relative to control pigs, but this was not observed to be significant (FC +1.30-fold, p=0.269). The results indicate that *FLNA* expression in trabecular bone is most significantly upregulated in response to 3000µg RP/kg BW, but is not as significantly upregulated in expression in response to higher doses of RP.

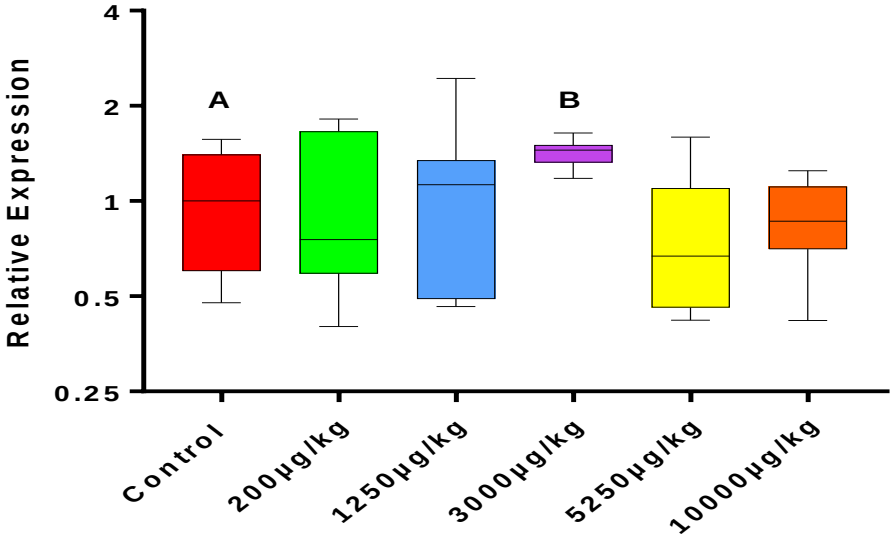

Figure 4.5: *Relative real-time PCR expression of Zinc-finger protein C3H Type-Like 1 (ZFP36L1) in the trabecular bone of pigs receiving different doses of RP treatment (n=8 per group) post-mortem. Data are presented in boxplots showing the median, 25th and 75th quartile ranges, and upper and lower limits. Mann-Whitney Test AB p=0.021*

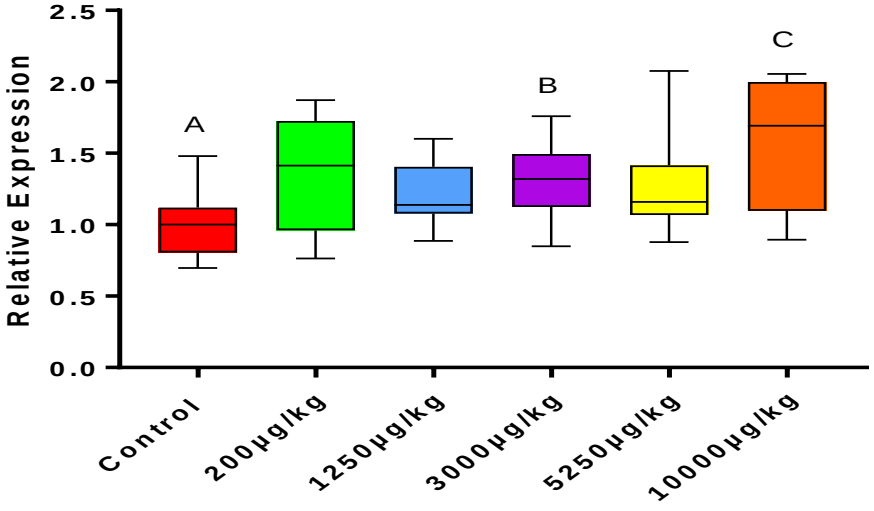

Figure 4.6: *Relative real-time PCR expression of Cell Division Cycle 42 (CDC42) in the trabecular bone of pigs receiving different doses of RP treatment (n=8 per group) post-mortem. Data are presented in boxplots showing the median, 25th and 75th quartile ranges, and upper and lower limits. Mann-Whitney Test AB p=0.036 AC p=0.032*

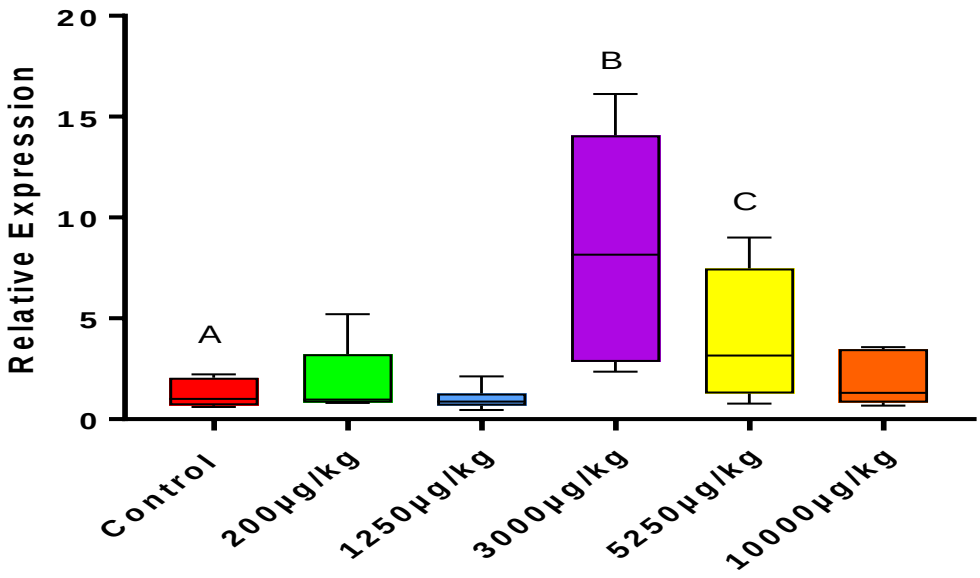

Figure 4.7: *Relative real-time PCR expression of Filamin A (FLNA) in the trabecular bone of pigs receiving different doses of RP treatment (n=8 per group). Data are presented in boxplots showing the median, 25th and 75th quartile ranges, and upper and lower limits. Mann-Whitney Test AB p<0.01 AC p=0.024*

4.4 Discussion

The objectives of this study were to characterise how doses of Vitamin A supplementation affect serum 25(OH) D, and to identify genes and gene pathways affected by vitamin A supplementation in trabecular bone tissue. Based on previous results showcasing chronic treatment of Vitamin A to antagonise serum 25(OH) D in rats (Frankel et al., 1986), the hypotheses was that vitamin A dosing would reduce serum 25(OH) D. Between control pigs and pigs receiving 500µg RP/kg BW, serum 25(OH) D was reduced by 2.75ng/ml. Serum 25(OH) D was then restored to concentrations similar to controls at 3000µg RP/kg BW. The results agree with the hypotheses in that vitamin A will antagonise serum 25(OH) D, but the data also suggests that this is not done in a consistent dose-dependent manner. Transporters related to vitamin D and Ca intestinal absorption were differentially regulated in response to 10000µg RP/kg BW, and this could imply that vitamin A is affecting absorption of these minerals. No differences in serum ALKp or Ca or P were observed in response to treatment. The hypotheses also stated that genes related to osteoblast mineralisation will be upregulated in trabecular bone in response to excess vitamin A doses.

This was due to Lind et al. (2012) identifying upregulation of mineralisation genes in interior bone compartments in response to excessive vitamin A, and due to findings that trabecular bone mass remains unchanged over a period of exposure to vitamin A supplementation (Wray et al., 2011, Kneissel et al., 2005). Microarray and qPCR analysis indicated the Rho-GTPase associated gene *FLNA* to be most significantly affected in trabecular bone in response to 3000µg RP/kg BW. *FLNA* has been indicated to regulate bone formation *in vitro* and *in vivo* (Lian et al., 2017, Hong et al., 2010). Evidence also shows *FLNA* can regulate osteoclast activity (Goldberg et al., 2015, Leung et al., 2010). The original hypotheses predicted vitamin A supplementation will favour bone formation processes in trabecular bone. An upregulation of *FLNA* now suggests bone resorption has also been upregulated in trabecular bone as a result of vitamin A. This now suggests vitamin A supplementation promotes overall bone metabolism in trabecular bone.

4.4.1 Vitamin A and Vitamin D Relationship

Serum 25(OH) D was reduced in pigs receiving 500µg RP/kg BW in comparison to controls, however serum 25(OH) D was restored to the same levels as controls at 3000µg RP/kg BW (Figure 4.3). The results in the current study suggest that prolonged exposure to excess vitamin A will initially antagonise serum 25(OH) D dose-dependently, but not at doses above 500µg RP/kg BW. Serum 25(OH) D has been observed to be decreased in rats in response to chronic Vitamin A treatment over 9 weeks, and $1,25(OH)_2D$ has been observed to be decreased in plasma in response to 100µg/g of BW of Vitamin A treatment after 5 days (Frankel et al., 1986, Ornsrud et al., 2009). Aburto et al. (1998) observed increasing dietary concentrations of 1, $25(OH)_2$ D reduced RE concentrations in the liver in a dose-dependent manner over a period of 16 days. Rohde and DeLuca (2005) reported, over a period of 33 days, feeding rats 400µg of RA and 5ng of Vitamin D inhibited Vitamin D-mediated effects on Ca and P, but rats fed 10ng of Vitamin D maintained serum Ca and P despite being fed 400µg of Vitamin A. The finding that 500µg RP/kg BW reduced serum 25(OH) D is in agreement with these studies in that vitamin A antagonises vitamin D. It is possible this is due to increased competition between vitamin A and vitamin D for transporter binding in the small intestines. However, the lack of a consistent dose-response decrease indicates a more complex relationship than previously thought between serum 25(OH) D and excess vitamin A. A critical difference between other experiments investigating the vitamin A-

vitamin D relationship and the current study is that the current experiment was performed over a much longer period (at least 15 weeks of dosing). It is possible in response to doses above 3000µg RP/kg BW over a prolonged period of time, compensatory mechanisms have been induced in an attempt to restore serum 25(OH) D.

Systematic studies have determined that Vitamin D potentially competes with free fatty acids for intestinal absorption, particularly for the transporters *CD36* and *SR-BI* (Silva and Furlanetto, 2018, Harrison, 2005). *CD36* and *SR-BI* have been identified in other reviews as regulators of vitamin D intestinal absorption, particularly absorption through the apical membrane (Reboul, 2015, Borel et al., 2015). This therefore raises the question of whether vitamin A could affect the expression of transporters that could control vitamin D absorption through the basolateral membrane. Vitamin D, in association with chylomicrons, is secreted into the lymph from the basolateral membrane, yet evidence suggests it may also be secreted into lymph via the transporter *ABCA1* (Reboul, 2015). In line with all of these findings, microarray analysis of intestinal samples from pigs receiving 10000µg RP/kg BW indicated *CD36* and *ABCA1* to be upregulated, and *SR-BI* to be downregulated (Table 4.2). These biomarkers should be assessed by qPCR in future studies, and ascertain how intestinal absorption of vitamin D has been influenced according to vitamin A dose. One hypotheses could be that these transporters become differentially upregulated at doses 3000µg RP/kg BW and above. This is based on evidence in the current study which shows vitamin A doses above 3000µg RP/kg BW do not affect serum 25(OH) D in comparison to controls, and that serum 25(OH) D increases between 1250µg RP/kg BW and 3000µg RP/kg BW. It is possible the restoration in serum 25(OH) D between these groups could be due to the expression of identified transporters in small intestine.

There were no differences observed in serum Ca in the groups in which serum 25(OH) D showed differences (Table 4.1). Rohde and DeLuca (2005) observed Vitamin A to antagonise the intake of Ca into serum in response to Vitamin D, and Johansson and Melhus (2001) observed vitamin A to abolish absorption of Ca in response to vitamin D after 8 hours. These studies suggest vitamin A antagonises the absorption of Ca alongside vitamin D. However, other studies show treatment with vitamin A antagonises plasma 1, 25 $(OH)_2$ D, but not serum Ca, over a period of 7 days (Ornsrud et al., 2009). The current study was performed over a longer time period than these previous studies, and this raised the question as to

whether, similar to serum 25(OH) D, prolonged exposure to excess vitamin A has also maintained serum Ca. Microarray analysis of intestinal tissue samples revealed the genes *CYP27B1*, which synthesises 1,25 $(OH)_2$D from 25(OH) D was upregulated in pigs receiving 10000µg RP/kg BW (Table 4.2). Yet *TRPV6*, a Ca transporter, was observed to be downregulated in the intestines of pigs receiving 10000µg RP/kg BW (Table 4.2). 1,25$(OH)_2$D is the hormonally active metabolite of vitamin D which directly regulates *TRPV6* expression to absorb Ca in the intestines (Jurutka et al., 2007); its differential expression in small intestines could be an attempt to re-upregulate *TRPV6*. A downregulation of *TRPV6* could suggest, in response to excess vitamin A, Ca absorption is compromised, which would agree with previous studies that vitamin A antagonises Ca (Rohde and DeLuca, 2005, Johansson and Melhus, 2001). However, it is also known from previous studies that excess vitamin A induces bone resorption in the cortical compartment of bone, which would release dissolved Ca into circulation (Lind et al., 2011, Lind et al., 2012). Cortical bone was not sampled for gene expression in the current study to confirm if there is an upregulation of osteoclast activity. Yet elevated Ca deposition into serum as a result of bone resorption could likely contribute to downregulation of *TRPV6* to prevent hypercalcemia. *TPRV6* should be verified in future qPCR experiments in order to confirm how different vitamin A doses affect genes that govern Ca absorption. Overall, the data obtained for vitamin D and Ca suggest that excess vitamin A, over a period of time, induces differential gene expression in the small intestines, and these could be responsible for maintaining serum concentrations of these nutrients.

In addition, serum P was not affected by vitamin A dose (Table 4.1). This is consistent with other studies (Ornsrud et al., 2009, Broulik et al., 2013), apart from findings reported by Rohde and DeLuca (2005) who observed vitamin A to increase serum P, however no potential mechanism was explained or provided. Furthermore, microarray analysis observed no transporters of P to be differentially regulated in small intestine or kidney tissues. The study, therefore, suggests there is no effect on P homeostasis.

Overall, these results and findings suggest that vitamin A has the potential to antagonise vitamin D absorption, but compensatory effects in the small intestine likely maintain vitamin D, and Ca, in response to very high doses of vitamin A. These identified biomarkers should

be assessed in future qPCR studies in order to illustrate the molecular mechanisms by which excess vitamin A affects vitamin D and Ca intestinal absorption.

4.4.2 Excess Vitamin A and Differential Gene Expression in Trabecular Bone

IPA and Cytoscape identified different sets of genes to be affected in the trabecular bone of pigs receiving 10000µg RP/kg BW. Cytoscape identified genes such as *ZFP36L1* and *ARID4A* to be differentially regulated in response to vitamin A: both of these genes have been demonstrated to control osteoblast differentiation (Tseng et al., 2017, Monroe et al., 2010). *ZFP36L1* was selected for qPCR verification, however qPCR analysis did not determine there was a significant effect of treatment on gene expression (Figure 4.5).

IPA observed the differential regulation of genes such as *CDC42* and *FLNA* to be associated with vitamin A supplementation, both of these genes are associated with the Rho-GTPase family of signalling molecules (Nobes and Hall, 1995, Hu et al., 2017). But upon qPCR analysis, there was no clear overall effect of vitamin A dose on *CDC42* differential expression (Figure 4.6). Yet there was a more clear effect of vitamin A dose to affect *FLNA*: *FLNA* was observed to be upregulated 8.17-fold in response to 3000µg RP/kg BW, and then decreased in expression in later treatment groups (Figure 4.7). Interestingly, 3000µg RP/kg BW also induced the first significant fold-change in expression of *CDC42* (FC, +1.32). As *FLNA* expression decreased in groups beyond 3000µg RP/kg BW, *CDC42* expression increased at 10000µg RP/kg BW. *FLNA* binds *CDC42* and directs actin stress fibre formation (Hu et al., 2017). Through upregulating *FLNA*, vitamin A could be indirectly influencing *CDC42* activity. This could also explain as to why no clear responses to vitamin A dose were observed with *CDC42*.

The family of Rho-GTPases control cytoskeletal reorganisation, and regulate the formation of lamellipodia, fillopodia, through activation of p-21 activated kinase (PAK), and assembly of actin stress fibres (Nobes and Hall, 1995, Rane and Minden, 2014, Hoefen and Berk, 2006). *CDC42,* which codes for cell division cycle 2, is one of the three Rho-GTPases that directly control PAK phosphorylation and subsequent cytoskeletal dynamics (Hoefen and Berk, 2006, Nobes and Hall, 1995). *FLNA* codes for Filamin A, which is an actin-binding protein which has been demonstrated to bind and stabilise Rho-GTPases, including *CDC42* (Hu et al., 2017). Furthermore, *FLNA* contributes to the stabilisation of the actin

cytoskeleton, as well as inducing F-actin stress fibre formation and cell spreading (Hu et al., 2017).

Given the role of the cytoskeleton in mediating osteoblast differentiation through integrin-mediated adhesion to the ECM (Lomri and Marie, 1996, Hendesi et al., 2015) and Rho-GTPases in controlling cytoskeletal dynamics, it could be hypothesised that silencing of *FLNA* expression or activation would result in decreased bone formation. Indeed, *FLNA*-null mice show indications of reduced bone formation, evidenced by underdeveloped vertebrae (Lian et al., 2017). In addition, *FLNA* has been observed to be upregulated in differentiating osteoblasts *in vitro* (Hong et al., 2010). *FLNA's* combined actions on stress fibre formation, which are required to maintain focal adhesions (Rane and Minden, 2014), and actin polymerisation (Hu et al., 2017) could be responsible for these effects on bone formation. However, the cytoskeleton also holds a role in mediating osteoclastic cell function, as well as mediating osteoblast differentiation. In osteoclasts, reorganisation of the actin cytoskeleton plays a role in cell migration, adhesion to bone surfaces, and vesicle trafficking of proteolytic enzymes which dissolve bone matrix (Lomri and Marie, 1996, Teitelbaum, 2011). Leung et al. (2010) observed *FLNA* to control monocyte migration prior to osteoclast differentiation, and that this was accomplished in association with *CDC42*. Surprisingly, the authors also noted knock out of *FLNA* induced bone mineralisation losses reminiscent of osteoporosis, and credited the changes to low turnover osteoporosis of which is characterised by reduced BMD, osteoblast and osteoclast cell numbers (Leung et al., 2010). Additionally, knock-out of *FLNA* in ovariectomized mice do not show changes in trabecular bone mechanical properties in comparison to control mice, despite estrogen deficiency promoting bone resorption (Goldberg et al., 2015). This result therefore suggests that *FLNA* regulates osteoclast resorption of bone matrix. Due to an upregulation of *FLNA* in trabecular bone at 3000µg RP/kg BW, the results therefore indicate that both bone formation and resorption processes have been upregulated. *FLNA* upregulation in trabecular bone in response to 3000µg RP/kg BW also provides evidence that the physiological changes occurring in the tissue occur as a result of actin cytoskeletal dynamics.

FLNA is a critical regulator of both osteoblasts and osteoclasts. The results obtained in the current study suggest, at the molecular level, excess vitamin A favours bone formation and resorption, which is not observed in either cortical or marrow compartments in response to

excess vitamin A (Lind et al., 2012). This finding suggests overall bone metabolism is promoted in the trabecular bone of pigs receiving vitamin A supplementation.

4.5 Conclusions

This study has shown that prolonged exposure to vitamin A can antagonise serum 25(OH) D, but very high doses of vitamin A, above 3000µg RP/kg BW, maintain serum 25(OH) D through, as of yet, unverified mechanisms. However, the study has identified potential biomarkers in small intestines which could regulate vitamin D absorption in response to excess vitamin A intake, and these should be investigated in future work. The study has also demonstrated excess vitamin A intake upregulates *FLNA* in trabecular bone, which possibly leads to increased bone metabolism in trabecular bone. The study has further highlighted the compartment-specific roles excess vitamin A has on overall bone development, and has also elaborated on vitamin A's association with Rho-GTPases.

Chapter 5: The associations of vitamin A and vitamin D with kyphosis in growing pigs

5.1 Introduction

In recent years, nutrition has been identified as a potential driver in the development of kyphosis in growing pigs. Reducing the concentrations of Vitamin A in sow diets, from 15,000mg/kg of diet to 8,500mg/kg of diet, has been observed to remove the prevalence of kyphosis from the herd, which suggests excessive vitamin A may be involved in the syndrome (Belsue, 2010). Yet, Belsue (2010) did not verify individual vitamin A concentrations in the livers of kyphotic and healthy pigs so as to assess vitamin A status. An association between kyphosis and vitamin A is possible as vitamin A has a clear influence on the expression of genes which regulate bone growth and mineralisation (Lind et al., 2011, Lind et al., 2012). Furthermore, vitamin D deficiency has been demonstrated to be a factor that drives kyphosis (Halanski et al., 2018, Amundson et al., 2016, Rortvedt and Crenshaw, 2012). Frankel et al. (1986) showed that exposure to vitamin A supplementation over a period of 9 weeks reduces serum 25(OH) D, thus demonstrating vitamin A has the potential to antagonise serum vitamin D availability. Thus, the association between kyphosis and vitamin A warrants further investigation.

Reduction of vitamin D in sow diets resulted in 30% of pigs within a litter showing symptoms by 13 weeks of age (Rortvedt and Crenshaw, 2012, Amundson et al., 2016). Indeed, some kyphotic cases, in outdoor farms, have been reported to occur in the winter periods (Done et al., 1999). During these periods, there is less available sunlight and therefore less natural vitamin D synthesis. This body of evidence supports the hypothesis in that vitamin D deficiency drives kyphosis, but there remains a need to confirm if pigs on units which suffer from spontaneous outbreaks show reduced vitamin D status. The question of how kyphotic pigs become potentially vitamin D-deficient requires investigation. It could be argued that vitamin A-associated antagonism of vitamin D (Frankel et al., 1986) occurs in kyphotic pigs, but there is no evidence that suggests this particular interaction is occurring in kyphotic pigs. This is a question that requires answering if the scope of vitamin A's effects during kyphosis are to be clarified.

Vitamin A deficiency has been observed to drive scoliosis, which bears significant resemblance to kyphosis in that the spine suffers from curvature (Li et al., 2012). Skeletal growth and development is controlled by the processes of endochondral bone growth and remodelling (Karsenty et al., 2009, Kronenberg, 2003). The end-result of various signalling pathways that control endochondral bone growth is to regulate genes, which allow for osteoblast differentiation and the production of non-collagenous proteins to regulate bone metabolism (Kronenberg, 2003, Al-Qtaitat and Aldalaen, 2014). The loss of a POC in the vertebral trabecular bone of kyphotic pigs (Nielsen et al., 2005, Done et al., 1999) could suggest that either pathways which regulate osteoblast differentiation, or expression of non-collagenous proteins which regulate bone metabolism, are downregulated in kyphotic trabecular bone. There is currently no published data which indicates how vitamin A regulates gene expression within vertebral trabecular bone, but studies have demonstrated that excess vitamin A can induce the expression of genes, such as BMPs or Wnt genes, which stimulate osteoblast differentiation within the marrow compartments of long bones (Lind et al., 2012). Various *in vitro* experiments also show vitamin A contributes to regulation of non-collagenous proteins that control mineralisation, such as Osteonectin (*SPARC)* (Ng et al., 1989). Given that vitamin A deficiency can drive skeletal diseases characterised by spine curvature (Li et al., 2012) and that vitamin A supplementation can drive the expression of mineralisation genes (Lind et al., 2012, Ng et al., 1989), it could be hypothesised that a reduced vitamin A status will associate with kyphosis. A reduction in vitamin A could also contribute to the downregulation of mineralisation genes in vertebral trabecular bone preceding the characteristic POC formation in kyphosis, but it is not known how, or if, vitamin A-regulated biomarkers that control bone formation are affected in kyphosis.

The objectives of this study were to investigate overlap of differential gene expression in trabecular bone between the kyphosis and vitamin A trials in order to identify vitamin A-regulated biomarkers in kyphosis. Additionally, the study aimed to verify the associations of vitamin A and vitamin D with kyphosis. The hypotheses are as follows:

- Kyphotic pigs will show reduced vitamin D status due to the diseases prevalence in winter months, and due to previous trials showing that vitamin D deficiency drives kyphosis.

- Kyphotic pigs will show reduced concentrations of liver REs, and therefore reduced vitamin A status.
- Vitamin A-regulated genes representing bone mineralisation will be downregulated within kyphotic trabecular bone, but will be upregulated in response to vitamin A supplementation for the vitamin A trial.

5.2 Materials and Methods

5.2.1 Kyphosis Trial

Details of the experimental design for the kyphosis trial can be viewed in Chapter 2.

5.2.2 Vitamin A Trial

Details of the experimental design for the vitamin A trial can be viewed in Chapter 2.

5.2.3 General Methods

All methods relating to this chapter can be seen in Chapter 2. This includes: Tissue Extraction, RNA extraction, cDNA synthesis, Microarray Analysis, Microarray Data and Pathway Analysis, qPCR analysis, and qPCR data analysis and presentation, HPLC and ELISA.

5.2.4 Statistical Analysis

Before statistical analysis, data were tested for normal distribution using Shapiro-Wilk test and observing skewness and kurtosis (SPSS Software). Data were ln transformed to normalise data distribution, however it was not possible to achieve normal distribution for all data sets. Therefore, the non-parametric Kruskal-Wallis test was used to determine the effects of treatments (vitamin A dose or phenotype in kyphosis trial) on dependent variables, and the Mann-Whitney test was used to determine significant differences between individual groups. A p value <0.05 was considered statistically significant.

In addition, Spearman's test was used to determine correlations between serum 25(OH) D and liver REs in kyphotic pigs.

5.3 Results

5.3.1 Vitamin A and Vitamin D in Kyphotic Pigs

5.3.1.1 Serum 25(OH) D

There was a significant effect of phenotype on 25(OH) D concentrations (p=0.012), but not age (p=0.783) (Figure 5.1). 25(OH) D serum concentrations were decreased in kyphotic pre-weaners and their littermates in comparison to non-related controls (Kyphosis: -5.42ng/ml, p=0.028; Littermates: -5.17ng/ml, p=0.011). There were no significant differences observed between pre-weaning kyphotic and littermate piglets (-0.25ng/ml, p= 0.763). There were no significant differences observed in kyphotic weaners (-2.74ng/ml, p=0.190) or kyphotic post weaners (-1.11ng/ml, p=0.475) in comparison to age-matched controls. Serum Ca and P was also measured in the serum of pre-weaning kyphotic and non-related controls, but no differences were observed (Appendix A).

5.3.1.2 Liver Retinol and Retinyl Esters

Individual and total retinol ester concentrations, µmol per g of liver, were determined in the livers of kyphotic and control pigs (Figure 5.2). There was an effect of age (p<0.01) and phenotype (p=0.012) on µmol/g of total REs, with an average decrease of 0.033µmol/G in kyphotic pigs when compared to control pigs. There was a tendency for REs to be decreased in kyphotic pre-weaners in comparison to non-related control pre-weaners (-0.0173µmol/G, p=0.09), but there were no significant differences observed between pre-weaning kyphotic and littermate piglets (-0.0035µmol/G, p=0.474), or between littermates and non-related controls (-0.0137µmol/G, p=0.296). There were no significant differences observed in kyphotic weaners (-0.0176µmol/G, p=0.664), however kyphotic post-weaners showed a significant reduction of REs (-0.07µmol/G, p<0.01). The results indicate that overall REs stored in liver (µmol/G of liver) are decreased within kyphotic as opposed to control pigs, particularly at the post-weaning stage.

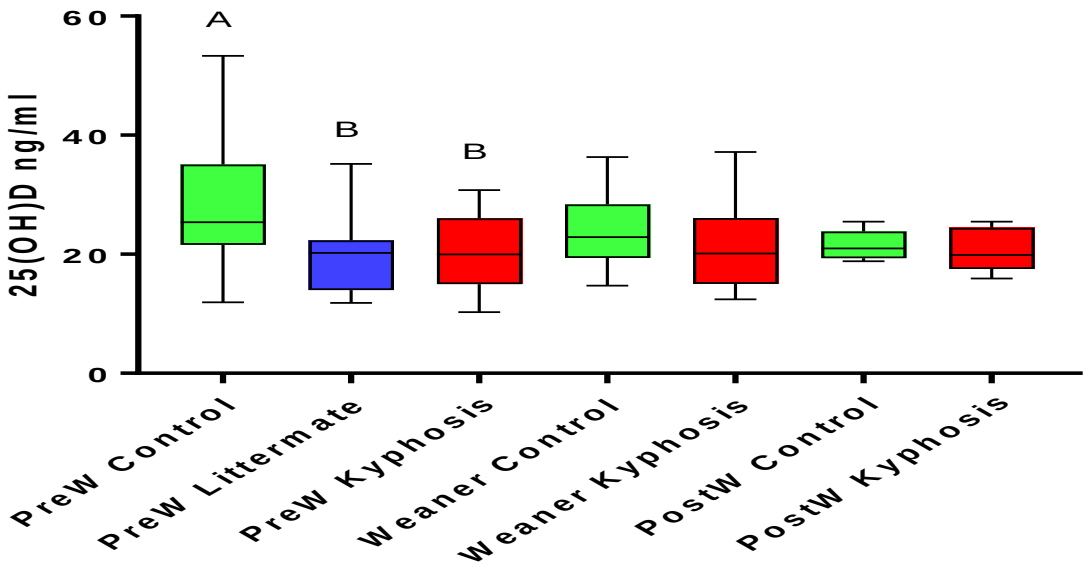

Figure 5.1: *25(OH) D concentrations (ng/ml) in the serum of Pre-weaning (PreW) (n=17 per group), Weaning (n=16 per group), and Post-weaning (PostW) (n=7 per group) kyphotic and control pigs post-mortem. Data are presented as boxplots showing the median, 25th and 75th quartile ranges, and upper and lower limits. Mann-Whitney AB p<0.05*

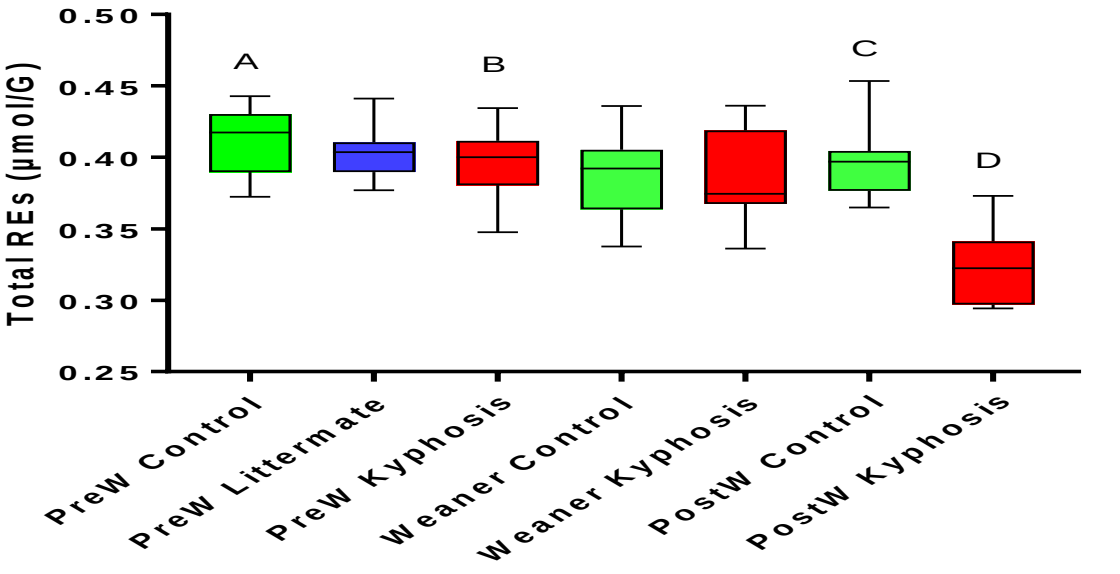

Figure 5.2: *Total retinol and retinyl esters (µmol/g of liver) stored in the livers of Pre-weaning (PreW) (n=17 per group), Weaning (n=16 per group), and Post-weaning (PostW) (n=7 per group) kyphotic and control pigs post-mortem. Data are presented as boxplots showing the median, 25th and 75th quartile ranges, and upper and lower limits. Kruskal-Wallis Age p<0.01 Phenotype p=0.021, Mann-Whitney AB p=0.09 CD p<0.01*

5.3.1.3 Vitamin A and Vitamin D Interaction

The data obtained for vitamin A and vitamin D indicates both of these vitamins are reduced in kyphotic pigs. In order to investigate this further, REs in liver and serum 25(OH) D were analysed to indicate if a correlation exists between these data. The results indicate that there is no antagonistic relationship between vitamin A and vitamin D during kyphosis ($r=0.089$, $p=0.590$).

5.3.2 Overlap of Differential Gene Expression between Kyphotic and Vitamin A-Pigs

A total of 11 genes were found to share overlap in the trabecular bone of pre-weaning kyphotic pigs and pigs receiving 10000µg RP/kg BW. Of these genes, 45% were shown to be regulated in opposite directions by kyphotic pre-weaners and pigs receiving 10000µg RP/kg BW, whereas 55% of genes were regulated in the same direction in both pig groups. Genes regulated by kyphotic pre-weaners and pigs receiving 10000µg RP/kg BW can be viewed in Table 5.1.

Two genes were observed from this list that have direct influence on bone metabolism: *SPARC* and G Protein-Coupled Receptor Kinase Interacting ArfGAP 2 (*GIT2). SPARC* codes for osteonectin, which is secreted by osteoblasts and regulates both osteoblast and osteoclast activity, thus identifying this gene as a critical regulator of bone remodelling (Rosset and Bradshaw, 2016). *GIT2* codes for G Protein-Coupled Receptor Kinase Interacting ArfGAP 2. GIT proteins act as scaffolding molecules for: Rho-GTPases, kinases such as MEK1 and PAK, and also regulate G-protein coupled receptor internalisation and sequestration through their ARF-GAP domains (Hoefen and Berk, 2006). This gene holds relevance to bone metabolism, due to a knock-out of this gene resulting in reduced bone mineralisation in rats (Wang et al., 2012).

In addition, retinoic acid receptor gamma *(RARG)* was observed to share overlap between the two trials. *RARG* is one of 3 retinoic acid receptor isoforms; evidence demonstrates it has a role in inhibiting gene expression of osteoblast-mineralisation genes *in vitro* (Green et al., 2017), while knockout of *RARG* in a mouse results in increased bone resorption activity (Green et al., 2015). Due to its roles in modulating retinoic acid signalling and in bone metabolism, this gene holds significant relevance to the study.

Gene Symbol	Gene Name	Kyphosis		Vitamin A	
		Fold-change	p-value	Fold-change	p-value
CLSTN1	Calsyntenin 1	2.93↓	0.0393	18.68↑	0.0193
FHL3	Four And A Half LIM Domains 3	4.05↓	0.0114	2.45↓	0.0453
MICAL3	Microtubule Associated Monooxygenase	3.29↓	0.0223	2.06↑	0.0255
CHCHD10	Coiled-Coil-Helix-Coiled-Coil-Helix Domain Containing	3.23↓	0.0175	2.28↓	0.019
MESP1	Mesoderm Posterior BHLH Transcription Factor 1	3.33↓	0.0255	2.91↓	0.0376
RARG	Retinoic Acid Receptor Gamma	6.23↓	0.00364	2.63↑	7.88E-04
MYH4	Myosin Heavy Chain 4	2.90↑	0.0449	2.21↑	0.0129
SPARC	Osteonectin	3.87↓	0.0212	2.06↓	0.0255
GIT2	GIT ArfGAP 2	3.11↓	0.0395	13.08↑	0.0377
PRNP	Prion Protein	3.59↓	0.0254	2.06↓	0.0255
BIN1	Bridging Integrator 1	4.39↓	0.0112	2.21↑	0.0314

Table 5.1**:** *Classification of genes that were differentially expressed in the trabecular bone of pre-weaning kyphotic pigs, and pigs receiving 10000*μg *RP/kg BW of vitamin A supplementation. The results were generated from Genespring. The fold change and p-value, calculated by moderated T-Test, are shown.*

5.3.3 Candidate Gene Expression Verification using qPCR

Due to their associations with bone metabolism and retinoid signalling: *SPARC*, *GIT2*, and *RARG* were selected for qPCR analysis. A table showing the sequences of primers used to analyse genes of interest is in Table 5.2.

5.3.3.1 Expression of *RARG* in Trabecular Bone of Kyphotic and Vitamin A Pigs

In the kyphosis trial, *RARG* showed a tendency to be downregulated in the trabecular bone of kyphotic pre-weaners in comparison to non-related controls (Fold-change, (FC) -1.40, p=0.087) (Figure 5.3). There were no significant differences in *RARG* expression observed between pre-weaning kyphotic and littermate piglets (FC-1.11, p=0.585), or in pre-weaning littermates in comparison to non-related controls (FC-1.26, p=0.249).

In the vitamin A trial, there was an effect of vitamin A dose on *RARG* gene expression (p=0.036) (Figure 5.3). From controls to 1250µg RP/kg BW, *RARG* expression decreased in the trabecular bone (FC-3.92, p=0.027), yet from 1250µg RP/kg BW to 3000µg RP/kg BW, *RARG* expression increased (FC +2.50, p<0.01). No significant differences were observed in the later treatment groups in comparison to controls.

Table 5.2: *List of primer sequences for genes of interest for quantification of gene expression by real-time quantitative polymerase chain-reaction (q.PCR)*

GENE NAME	PRIMER SEQUENCE 5' -3'
GIT2	F: CTCCAACATTGCTTCAGATGGT R: GCGGTGGACAAATGCTAACA
SPARC	F: GGACCTTGCAAATACATCCCC R: CGTGGATCTTCTTCACTCGC
RARG	F: GATGACACAGAGACAGGGCT R: CCTTTCTGCTCCCTTGGTG
RPL37 (HK)	F: GCCTACCATCTCCAGAAGTC R: CTTCACGGAATCCATGCCTG

RPL37, Ribosomal Protein L37, RARG, Retinoic Acid Receptor Gamma, SPARC, Osteonectin, GIT2, G Protein-Coupled Receptor Kinase Interacting ArfGAP 2

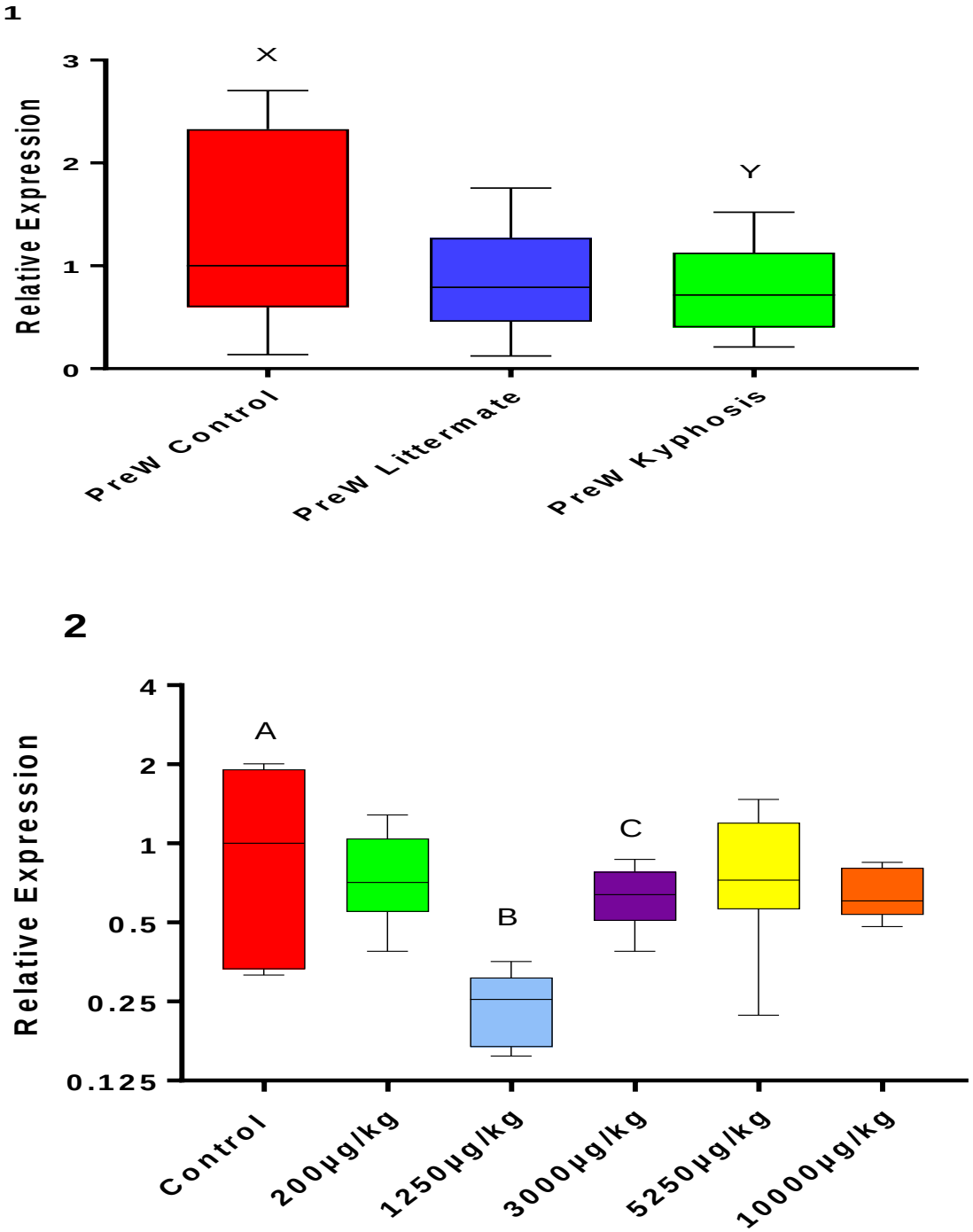

***Figure 5.3**: Relative real-time PCR expression of Retinoic Acid Receptor Gamma (RARG) in the trabecular bone of **1**. Pre-weaning (PreW) kyphotic (n=17), littermate (n=17) control pigs (n=17) post-mortem, and **2.** Pigs receiving vitamin A supplementation (n=8 per group) post-mortem, y-axis is in a log2 scale. are presented boxplots showing the median, 25th and 75th quartile ranges, and upper and lower limits. Mann-Whitney XY p= 0.087, AB p=0.027, BC p<0.01*

5.3.3.2 Expression of *SPARC* in Trabecular Bone of Kyphotic and Vitamin A Pigs

In the kyphosis trial, *SPARC* was not observed to be differentially expressed between kyphotic or littermate (FC -1.31, p=0.692) or control piglets (FC+1.56, p=0.264) (Figure 5.4). Due to the non-significant results in gene expression, *SPARC* was not analysed in the remaining age groups.

In the vitamin A trial, there was an effect of vitamin A dose on *SPARC* expression (p=0.039) (Figure 5.4). *SPARC* significantly increased in expression in response to 3000µg RP/kg BW (FC +4.66, p<0.01). No significant fold-changes were observed in later treatment groups in comparison to controls.

5.3.3.3 Expression of *GIT2* in Trabecular Bone of Kyphotic and Vitamin A Pigs

In the kyphosis trial, *GIT2* was observed to be downregulated in the trabecular bone of kyphotic pre-weaners in comparison to controls (FC -1.88 p<0.01), and in the trabecular bone of littermate pre-weaners in comparison to non-related controls (FC-1.68, p=0.013) (Figure 5.5). There were no significant differences between pre-weaning kyphotic and littermate piglets (FC-1.12, p=0.418). Due to the significant and notable differences in gene expression, *GIT2* was analysed in the older kyphotic age groups. There was a tendency for an effect from age in that *GIT2* expression was reduced in the weaning and post-weaning groups (p=0.097), but no significant differences were observed between kyphotic and control pigs in either of these age groups.

In the vitamin A trial, there was a significant effect of vitamin A dose on gene expression of *GIT2* (p<0.01) (Figure 5.5). The expression of *GIT2* was significantly different in all dose groups in comparison to controls, and *GIT2* followed a dose-response relationship with vitamin A up until 3000µg RP/kg BW, where gene expression peaked in expression (FC +8.34, p<0.01).

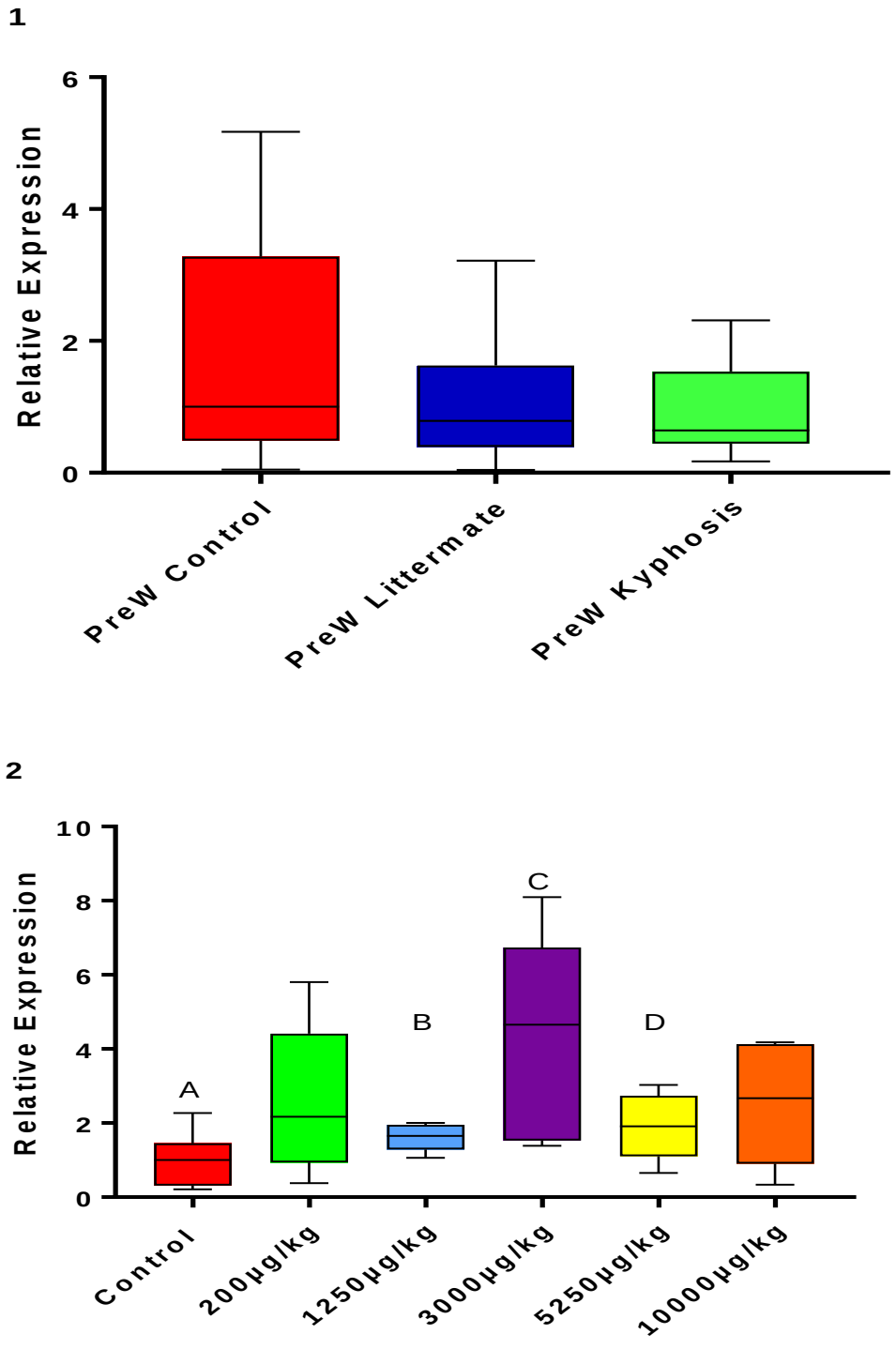

Figure 5.4: *Relative real-time PCR expression of Osteonectin (SPARC) in the trabecular bone of **1**. Pre-weaning (PreW) kyphotic (n=17), littermate (n=17) and control pigs (n=17) post-mortem, and **2**. pigs receiving vitamin A supplementation (n=8 per group) post-mortem. Data are presented in boxplots showing the median, 25th and 75th quartile ranges, and upper and lower limits. Mann-Whitney AB p=0.081 AC p<0.01 AD p=0.07*

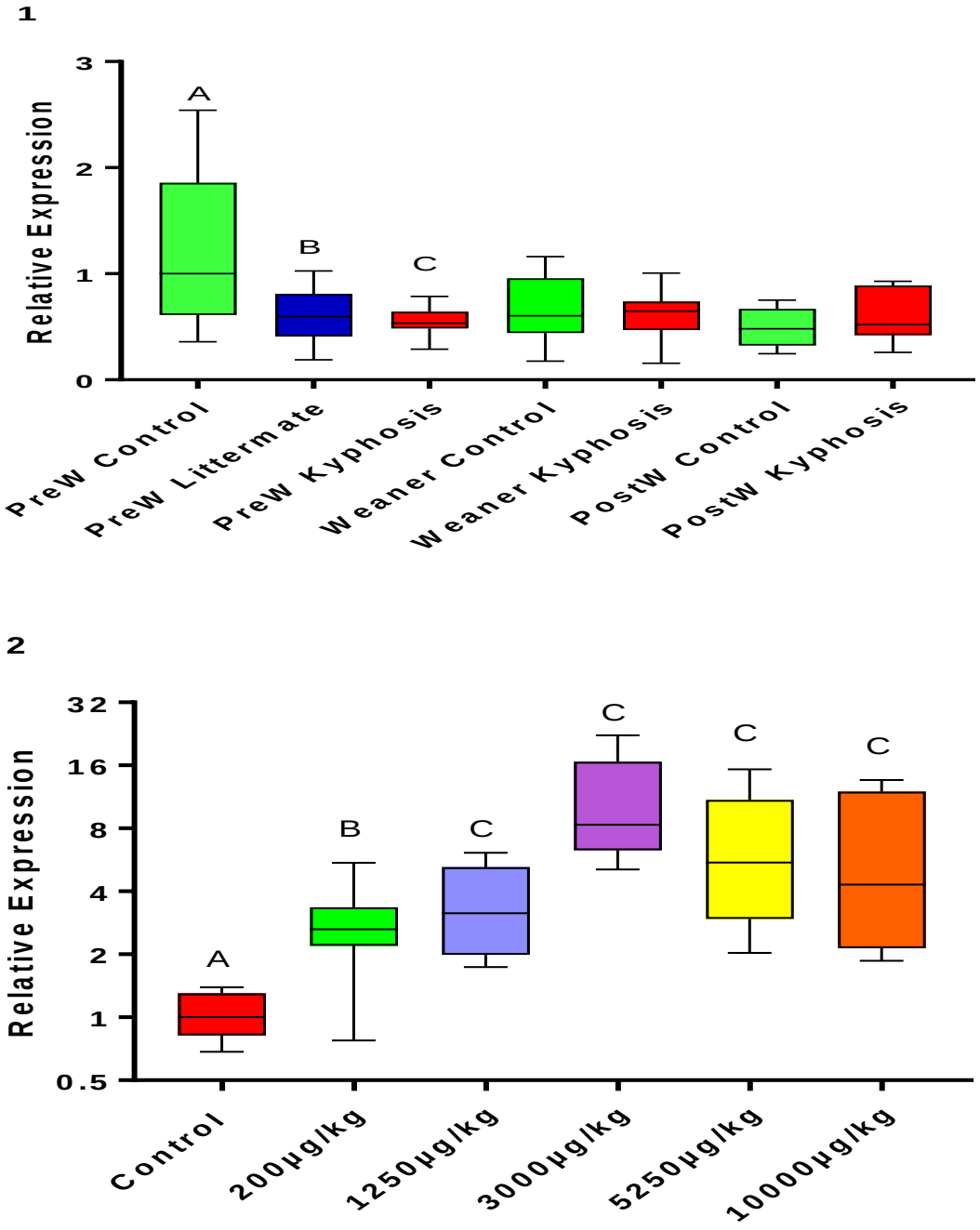

Figure 5.5: *Relative real-time PCR expression of G Protein-Coupled Receptor Kinase Interacting ArfGAP 2 (GIT2) in the trabecular bone of* ***1.*** *Pre-Weaning (PreW) (n=17 per group), Weaning (n=16 per group), and Post-weaning (PostW) (n=7 per group) kyphotic and Control pigs post-mortem, and* ***2.*** *Pigs receiving vitamin A supplementation (n=8 per group) post-mortem, data are presented in a log2 scale. Data are presented in boxplots showing the median, 25th and 75th quartile ranges, and upper and lower limits. Mann-Whitney AB $p<0.05$, AC $p<0.01$*

5.4 Discussion

In this study, the overlap of differential gene expression was investigated in pigs from the kyphosis and vitamin A trials, as was the vitamin A-vitamin D relationship in kyphotic pigs. The hypotheses stated that kyphotic pigs would show reduced vitamin A and vitamin D status in comparison to control pigs. Liver REs were reduced in kyphotic post-weaners, and serum 25(OH) D was reduced in pre-weaning kyphotic and littermate piglets in comparison to non-related controls. Therefore, these results support the original hypotheses. No negative correlations between vitamin A and vitamin D were observed in kyphotic pigs, therefore it is likely vitamin A does not antagonise vitamin D in growing kyphotic pigs.

Additionally, the hypotheses also stated that genes which control bone mineralisation will overlap between the kyphosis and vitamin A trials. These genes were predicted to show downregulation within kyphotic bone, and upregulation in response to vitamin A. In particular, *GIT2* showed a dose-response relationship to vitamin A supplementation in the vitamin A trial, and was downregulated in the trabecular bone of kyphotic and littermate pre-weaners in comparison to age-matched non-related controls. *GIT2* promotes bone formation and mineralisation, but also regulates osteoclast function (Wang et al., 2012). Therefore, the original hypotheses can be accepted in that vitamin A regulates bone formation genes that are associated with kyphosis. But the findings from the current study now suggest bone resorption is also affected by vitamin A in kyphotic pigs as a result of *GIT2* differential regulation.

5.4.1 Vitamin A and Vitamin D in Kyphosis

Serum 25(OH) D was observed to be reduced in pre-weaning kyphotic pigs and littermate piglets in comparison to non-related controls (Figure 5.1). Due to the observation being confined to the litter, this suggests the sow has had an effect on the vitamin D status of these piglets. Supplementing gilts with vitamin D has been demonstrated to improve the vitamin D status of the developing foetus (Coffey et al., 2012). In addition, piglets, from 0 to 7 weeks of age, had serum 25(OH) D concentrations that increased depending upon the level of vitamin D supplementation offered to the sow (Amundson et al., 2017). Piglets born from vitamin D deficient sows also showed a higher prevalence of kyphosis development (Amundson et al., 2017). The results from these studies clearly demonstrate the effect of

the sow in relation to the piglet's vitamin D status, and support the findings in the current study which suggests a link between vitamin D status, the sow, and kyphosis. Nonetheless, these findings are in agreement with previous studies which have shown Vitamin D supply to the sow to be a critical factor that contributes to the development of kyphosis (Rortvedt and Crenshaw, 2012, Halanski et al., 2018, Amundson et al., 2016). Due to findings that demonstrated BMD is reduced in the hypovitaminosis-D kyphosis model (Rortvedt and Crenshaw, 2012) and given vitamin D's role in regulating skeletal growth in pigs (Witschi et al., 2011), the results support a role of vitamin D deficiency contributing to reduced bone mineralisation. The results obtained in the current study support an association of vitamin D supply with kyphotic pigs on UK outdoor farms.

The current study also showed RE stores in liver to be reduced particularly in post-weaning kyphotic pigs (Figure 5.2). Pre-weaning kyphotic piglets did show a tendency to have reduced liver RE stores in comparison to non-related controls, but there were no clear indications that there was an effect confined to the litter. The reduction of liver RE stores, in kyphotic post-weaners and potentially kyphotic pre-weaners, could indicate farm management factors are responsible for this effect. Epidemiological studies should be pursued in future work in order to identify if there is an effect of management. The results in the current study are in contrast to the findings of Belsue (2010), which suggested vitamin A supplementation drives kyphosis. Studies which support the findings in the current study are results which show vitamin A deficiency drives curvature of the spine, in the form of scoliosis in rats (Li et al., 2012). Yet meta-analysis studies also demonstrate that high and low serum retinol can contribute to osteoporotic fractures (Navarro-Valverde et al., 2018, Wu et al., 2014), the results of which support both the current study and Belsue (2010) study. While the current study does not conclude a maternal effect in relation to vitamin A and kyphosis, the Belsue (2010) study showed there is a maternal effect when the sow is supplemented with vitamin A. It is possible the vitamin A-vitamin D antagonistic relationship (Aburto et al., 1998, Clark and Bassett, 1961, Frankel et al., 1986) is attributable to the abnormal skeletal development in the Belsue (2010) study, however serum 25(OH) D was not measured so there is no evidence to support this. Furthermore, a vitamin A-vitamin D antagonistic relationship was not identified to be associated with kyphotic pigs in the current study. Overall, it is likely that both excess and deficient vitamin A intake has the

potential to contribute to kyphosis, depending upon maternal exposure to vitamin A. Supporting this, the pigs in the vitamin A trial for the current study did not develop kyphosis, but the pigs received no effect from the sow due to entering the experimental period at 4 weeks of age.

In summary, the results of the current study indicate kyphotic pigs have reduced status of both vitamin A and vitamin D. The results support a justification to incorporate these vitamins into intervention trials in order to confirm their associations with kyphosis.

5.4.2 Differential Gene Expression in Trabecular Bone

The kyphosis and vitamin A trials in the current study represent two different scenarios, but both have an impact on bone development. This is highlighted by kyphotic pigs showing decreased bone mineralisation (Nielsen et al., 2005, Done et al., 1999), and excess vitamin A inducing narrowing and fragility of bones in rats and pigs (Pryor et al., 1969, Lind et al., 2011). Due to post-weaning, and potentially pre-weaning, kyphotic pigs showing reduced liver REs, biological effects observed in kyphotic pigs could be representative of reduced vitamin A status. Meanwhile, liver REs markedly increased for pigs in the vitamin A trial, as shown in Chapter 4; therefore this trial represents the effects of excess intake of vitamin A.

In the kyphosis and vitamin A trials, microarray analysis indicated *RARG* to be downregulated within the trabecular bone of kyphotic pre-weaners in comparison to non-related controls, and upregulated in pigs receiving vitamin A supplementation. qPCR analysis showed that the difference in *RARG* expression between kyphotic pre-weaners and non-related controls was not significant, but did show a tendency to be downregulated in kyphotic pre-weaners (Figure 5.3). There were no significant upregulations of *RARG* observed in any dose groups in comparison to controls for the vitamin A trial (Figure 5.3). This could suggest that *RARG* is not the most accurate predictor of excess vitamin A intake, and raises questions as to how this gene has been regulated in trabecular bone. *RARG* codes for retinoic acid receptor gamma, which is one of the three isoforms of the retinoic acid receptor. Knock-out of *RARG* in mice abrogates the effects of excess vitamin A, although it must be noted that bone tissue was not included in the investigations (Ross et al., 2000, Look et al., 1995). However, given that vitamin A, in combination with RAR and RXR isoforms, has the potential to regulate over 500 proposed genes (Balmer and Blomhoff,

2002), this can make it difficult to ascertain which exact pathways and genes have been affected as a result of *RARG* differential regulation in trabecular bone tissue.

Due to *RARG* not showing any clear dose response relationships to vitamin A in the vitamin A trial, this suggests that the ligands for *RARG*, *all-trans* retinoic acid (ATRA) or *9-cis* retinoic acid, might not be responsible for the observed interaction. Studies have demonstrated RAR and RXRs have the potential to form heterodimers with vitamin D receptors (VDRs), and a combination of ATRA and vitamin D facilitated binding of a RARα-VDR complex to responsive elements to mediate gene expression (Schrader et al., 1993). More recent evidence has demonstrated vitamin D responsive elements (VDREs) do bind *RARG* as well as VDRs (Koszewski et al., 2010). These studies imply that vitamin D holds a role in regulating the actions of *RARG* on target gene expression. In addition, kyphotic pigs showed reduced serum 25(OH) D (Figure 5.1), and showed a tendency to have reduced *RARG* expression in comparison to controls. However, data from Chapter 4 indicated there is no difference in serum 25(OH) D between control pigs and pigs receiving 1250µg RP/kg BW, between which a difference in *RARG* expression was observed. However, in neither of the trials was 1, $25(OH)_2D$ assessed in serum, which serves as the metabolite of vitamin D which binds the VDR. Analysing $1,25(OH)_2D$ in the serum of kyphotic and vitamin A treated pigs in future studies could offer more insight into the relationship between *RARG* expression and vitamin D metabolism. In summary, analysis of both trials shows that *RARG* does not serve as a biomarker of vitamin A supplementation, but highlights the requirement to assess *RARG's* association with vitamin D metabolism.

Microarray and qPCR analysis showed *SPARC* and *GIT2* to associate with kyphotic and vitamin A-supplemented pigs; however qPCR confirmed *SPARC* to not be a differentially regulated gene in kyphotic trabecular bone (Figure 5.4). *GIT2* was downregulated in pre-weaning kyphotic pigs (Figure 5.5), and these pigs showed a tendency to have reduced vitamin A status. Yet *GIT2* was upregulated in response to vitamin A supplementation in the vitamin A trial (Figure 5.5). These findings offer evidence that the regulation of *GIT2* in trabecular bone is controlled by vitamin A. Furthermore, pre-weaning littermates also showed a reduced expression of *GIT2* in comparison to non-related controls, therefore suggesting the effect is confined to the litter. *GIT2* codes for G Protein-Coupled Receptor Kinase Interacting ArfGAP 2. Knock out of *GIT2* has a detrimental effect on bone

development, this includes: loss of function for osteoclasts, decreased bone mass, and MSCs are favoured towards an adipocyte, over an osteoblast, lineage (Wang et al., 2012). *SPARC* codes for osteonectin, of which is a secreted non-collagenous protein that has been demonstrated to regulate osteoblast differentiation, as well as osteoclast activity (Delany and Hankenson, 2009, Delany et al., 2003, Delany et al., 2000). A critical difference between these two genes is that while *SPARC* is a non-collagenous protein, *GIT2* is an intracellular scaffolding molecule that controls cell differentiation. The results could suggest that vitamin A has not affected expression of non-collagenous protein synthesis in pre-weaning kyphotic pigs; indeed the vitamin A trial demonstrated doses up to 3000µg RP/kg BW of vitamin A are required to induce differential expression of *SPARC*.

GIT2 is a scaffolding protein that exists in oligomeric complexes with PAK-interacting exchange factor (PIX), and can interact with Rho-GTPases to control cytoskeletal regulation, and also controls G-protein coupled receptor (GPCR) internalisation (Hoefen and Berk, 2006). Cytoskeletal dynamics in osteoblasts and osteoclasts contribute to cell growth, migration, assemble focal complexes with and adhere to the ECM (Lomri and Marie, 1996, Goncharenko et al., 2016). Integrin-adhesion to the ECM on MSCs is required for ECM proteins to initiate osteoblast differentiation (Oh et al., 2017, Hendesi et al., 2015, Zouani et al., 2013). Cytoskeletal reorganisation is also required for migration and adhesion of osteoclasts to bone surfaces, adhesion to bone surfaces, and proteolytic enzyme release (Lomri and Marie, 1996, Teitelbaum, 2011). *GIT2* also regulates the desensitisation of GPCRs. Through initiating GTP hydrolysis through their ARF-GAP domains, GIT proteins are able to interact with and activate ADP ribosylation factors (ARF) proteins, which regulate membrane trafficking to and from the Golgi apparatus (Hoefen and Berk, 2006, Premont et al., 2000). Overexpressing *GIT1* or *GIT2 in vitro* results in decreased sequestration and increased desensitisation of the β2-adrenergic receptor, (Premont et al., 1998, Premont et al., 2000). Therefore, it could be hypothesised that a reduced expression of GIT proteins would increase sequestration of GPCRs and therefore limit the effects of certain ligands and agonists across osteoblasts and osteoclasts. Examples of GPCRs conserved across these cells include: calcium-sensing receptor or P2Y receptor (Bowler et al., 1998). However, for the moment, there is no clear evidence that showcases *GIT2's* effects on GPCR-associated bone metabolism. Nonetheless, regardless of the mechanism, a reduction of *GIT2* in trabecular

bone could contribute to the reduced endochondral bone growth in kyphotic pigs (Nielsen et al., 2005). However, it must be stressed that *GIT2*-mechanisms alone cannot be responsible for kyphosis, as littermate piglets also showed a reduced expression of this biomarker and did not show any signs of kyphosis.

The downregulation of *GIT2* in pre-weaning kyphotic trabecular bone, which showed a clear dose-response to vitamin A in the vitamin A trial, supports that kyphotic pigs have reduced vitamin A activity in the bone. However, kyphotic post-weaners did not show differential regulation of *GIT2* in trabecular bone, despite showing reduced liver REs. While *GIT2* was confined to the pre-weaning litter, this effect was not observed with liver REs. Therefore, while the results in the current study agree with the hypotheses in that kyphotic pigs will have reduced vitamin A status, it is likely that liver REs are not directly linked to differential gene expression in trabecular bone. It is possible other factors such as retinoic acid concentrations in trabecular bone are contributing to differential gene expression. This could be confined to pre-weaning kyphotic and littermate piglets, explaining how *GIT2* is confined to the litter. Retinoic acid concentrations in trabecular bone, for both trials, should be assessed in future studies in order to confirm the contributions. These answers will be required in order to understand the full scope of the link between vitamin A metabolism and the regulation of vitamin A-biomarkers in kyphotic vertebral trabecular bone.

In summary, the study has identified *GIT2* to be a vitamin A–regulated biomarker that is downregulated in pre-weaning kyphotic and littermate piglets. The exact biological mechanism of *GIT2's* effect on bone metabolism in kyphosis, as well as the full scope of its association with vitamin A metabolism, will require clarification in future studies.

5.5 Conclusions

The current study has added an additional layer of evidence in the association between kyphosis and vitamin D deficiency, and adds further justification for the application of vitamin D in kyphosis intervention trials. The study has also highlighted that reduced vitamin A status is associated with growing kyphotic pigs, and demonstrates the need to investigate how this is occurring on UK farms.

The current study has also identified that vitamin A potentially contributes to kyphosis through regulating *GIT2*, which has a subsequent effect on bone metabolism. The study has highlighted the larger role of *GIT2* in bone pathogenesis, and also offers more insight as to how vitamin A regulates trabecular bone development. *GIT2* should be considered as a diagnostic biomarker in assessing pigs at risk from developing kyphosis.

Chapter 6: General Discussion

6.1 Introduction

This thesis addressed several key questions concerning bio-mineral tissue development in commercial growing pigs. These ranged from understanding the molecular basis of events in kyphotic tissues, to clarifying vitamin A's association with the development of kyphosis and its role in trabecular bone metabolism. The relationship between vitamin A and vitamin D was also further characterised, as well as how these vitamins associate with kyphosis.

The kyphosis trial was unique to this thesis, as it included kyphotic and control pigs from farms which suffer from spontaneous outbreaks. Thus, biological results obtained from this trial would provide the most accurate picture of the biological basis of kyphosis on UK farms. By pursuing molecular investigations in kyphotic bone and cartilage tissues, the thesis has identified genes and molecular pathways that are likely contributing to the physiological changes of kyphosis (Chapter 3, Chapter 5).

The novel design of the vitamin A trial allowed for very high doses of vitamin A consumption over a prolonged period of time. Unanswered questions in relation to vitamin A and bone health include how various high doses of vitamin A affect differential gene expression particularly within trabecular bone, and how it influences serum 25(OH) D. The two trials used in this thesis allowed for characterisation of how various doses of vitamin A associate with serum 25(OH) D, and how the relationships between these vitamins relate back to skeletal diseases. Both trials also allowed for identification of vitamin A regulated biomarkers in trabecular bone that regulate tissue metabolism and further characterise how vitamin A contributes to the development of the tissue (Chapter 4, Chapter 5).

In addition, assessing both the kyphosis and vitamin A trials in this thesis has allowed for identification of vitamin A-regulated genes in kyphotic trabecular bone (Chapter 5). This has illustrated the requirement for vitamin A's association with kyphosis to be confirmed via an intervention trial.

The current chapter will integrate findings from preceding experimental chapters in order to critically discuss the overall relevance of the findings. Recommendations for future work are also provided at the end of the chapter.

6.2 The Molecular Basis of Kyphosis in Pigs

One of the objectives of this thesis was to confirm the genes and molecular pathways associated with kyphotic tissues. Kyphosis in pigs is not characterised by consistent aetiological observations, but some of these have included: a loss of a POC in thoracic and lumbar vertebrae (Nielsen et al., 2005, Done et al., 1999), reduced mineral content of bone (Done and Gresham, 1988), and collapsing of the thoraco-lumbar junction (Done and Pearson, 2004). Through clarifying genes and molecular pathways associated with kyphotic bone and cartilage tissues, the thesis aimed to establish an underlying biological basis for the physiological changes. This was accomplished through performing a pathway analysis of tissues to identify differentially expressed genes and pathways (Chapter 3), and by comparing which genes overlapped with genes induced by vitamin A (Chapter 5).

The microarray and pathway analysis of kyphotic tissues in Chapter 3 led to the observation of the SLRP *DCN* upregulation in intervertebral cartilage of kyphotic pre-weaners. This approach also showed the SLRP *ASPN* to be downregulated in the trabecular bone of kyphotic post-weaners. The analysis also suggested that the TGF-β pathway does not directly contribute to kyphosis, as was suggested in the original hypotheses. *DCN* is associated with experimental models of disc degeneration (Melrose et al., 1997) as well as osteoarthritis, and it has been proposed that its function in osteoarthritis is to restore PG losses (Bock et al., 2001). Therefore, the upregulation of *DCN* in the cartilage of kyphotic pre-weaners implies the cartilage is comparable to that of osteoarthritis. This critical finding suggests the initial basis of the collapsing of the thoraco-lumbar junction begins at pre-weaning, and is not just attributed to heavy musculature in older kyphotic pigs as has been previously suggested (Done and Pearson, 2004). Another interesting implication is that though *ASPN* regulates mineralisation of cartilage into ossified tissue, *DCN* can compete for collagen binding and inhibit the mineralisation process (Kalamajski et al., 2009). Therefore, an upregulation of *DCN* in intervertebral cartilage at pre-weaning could offer implications that *DCN* is out-competing *ASPN* at these stages for collagen binding, and thus contributing to reduced endochondral bone growth. In addition, *DCN* binds TGF- β (Hildebrand et al., 1994); this interaction has been proposed to prevent TGF- β binding to its cellular receptors and initiate signalling (Gubbiotti et al., 2016). Conversely, *DCN* has also been suggested to facilitate binding of TGF- β to its receptors (Takeuchi et al., 1994). An overview of *DCN's*

interaction with TGF- β is provided (Figure 6.1). TGF-β was not identified to be differentially expressed in kyphotic cartilage, but an upregulation of *DCN* could be an attempt to facilitate binding of TGF- β to its receptors in order to ameliorate damage in the tissue. This effect is more likely because if *DCN* was directly contributing to downregulation of TGF- β signalling, then genes such as *SMAD4*, which carries the intracellular signal from TGF- β, would have also likely shown differential expression. Regardless, the mRNA expression of *DCN* in human tumour tissues positively correlates with concentrations of Decorin in serum (Appunni et al., 2017); therefore Decorin could be considered as a potential diagnostic blood marker for kyphosis. Pathway analysis of kyphotic trabecular bone also showed that *ASPN* was downregulated at the post-weaning stage. *ASPN* has been demonstrated to induce mineralisation of the extending collagen template and thus regulate the process of endochondral bone growth (Kalamajski et al., 2009), therefore this finding would indicate this process is halted in kyphotic pigs at 13 weeks of age. Similar to *DCN*, *ASPN* also has the potential to bind TGF- β, and *in vitro* analysis shows that *ASPN* may block TGF- β binding to its receptor; likewise, silencing of *ASPN* also induces expression of TGF- β (Nakajima et al., 2007, Kou et al., 2007) (Figure 6.1). It is likely that the downregulation of ASPN could be a biological attempt to allow available TGF- β to bind to its receptors and repair the damage to the kyphotic tissue.

Through identifying differentially expressed genes from the kyphosis trial which overlapped with those from the vitamin A trial, the gene *GIT2* was confirmed by qPCR to be downregulated in kyphotic trabecular bone at the pre-weaning stage (Chapter 5). Knockout of *GIT2* in a mouse results in decreased BMD and bone volume in trabecular compartments (Wang et al., 2012); this phenotype strikes similarities to kyphosis due to the loss of a POC in kyphotic pigs (Nielsen et al., 2005). *GIT2* performs two major functions: to regulate ARF proteins which control trafficking of GPCRs to and from the plasma membrane, and to bind CDC42-PAK complexes such that high local concentrations of PAK induce auto-phosphorylation (Hoefen and Berk, 2006) (Figure 6.2). PAK phosphorylation and its subsequent effects in cytoskeletal rearrangement are detrimental in regulating osteoblast differentiation and osteoclast resorption activity (Hoefen and Berk, 2006, Rane and Minden, 2014, Lomri and Marie, 1996). The finding that *GIT2* was downregulated in kyphotic trabecular bone at the pre-weaning stage is a novel finding for numerous reasons. Due to

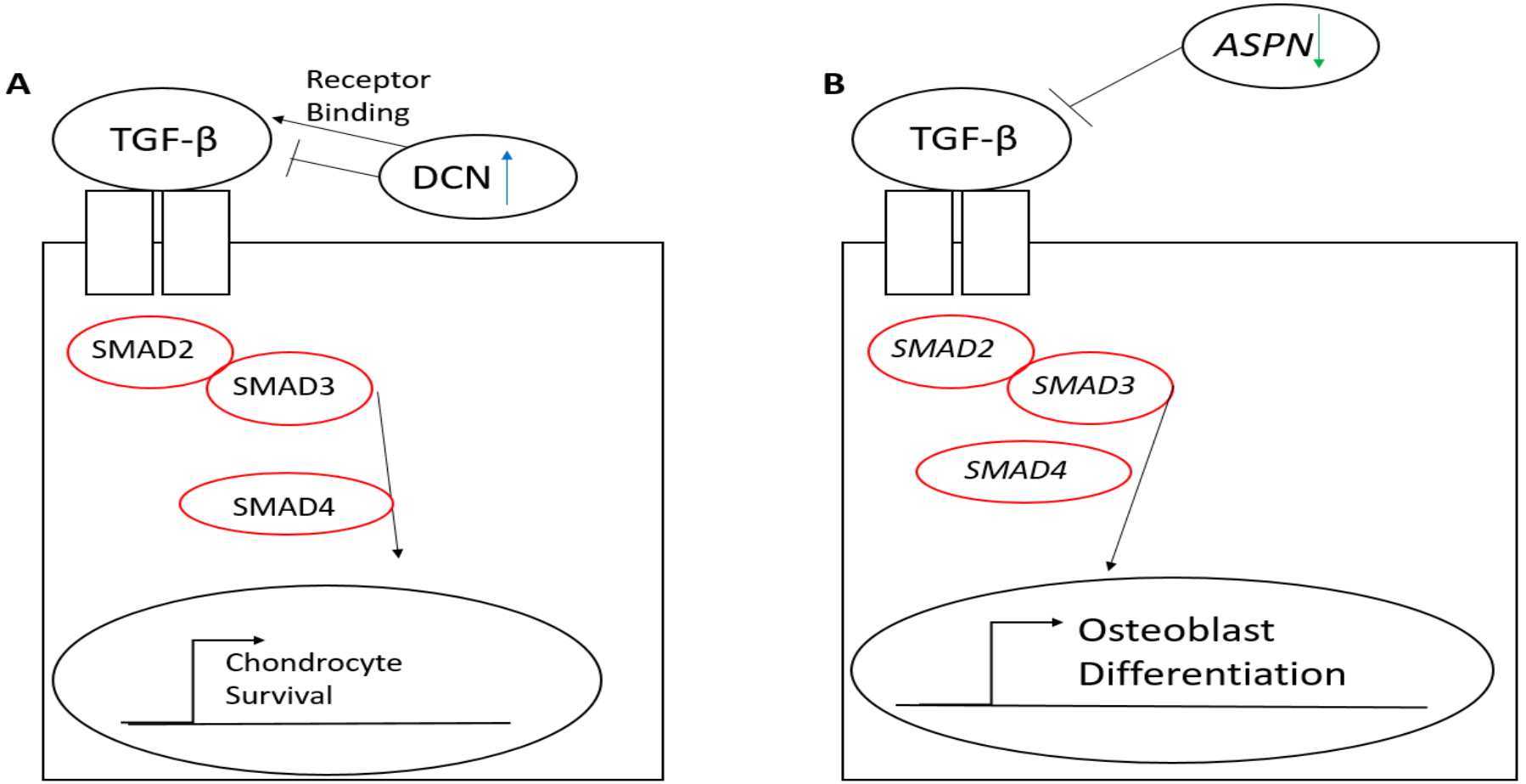

Figure 6.1: A*. An upregulation of DCN in the intervertebral cartilage of kyphotic pre-weaners could be an attempt to either downregulate TGF-β, or to re-upregulate the TGF-Smad signalling in order to alleviate abnormal tissue development.* ***B****. A downregulation of ASPN in the trabecular bone of kyphosis post-weaners could be an attempt to remove any inhibitory effects on TGF-β signalling in order to ameliorate the abnormal tissue development.*

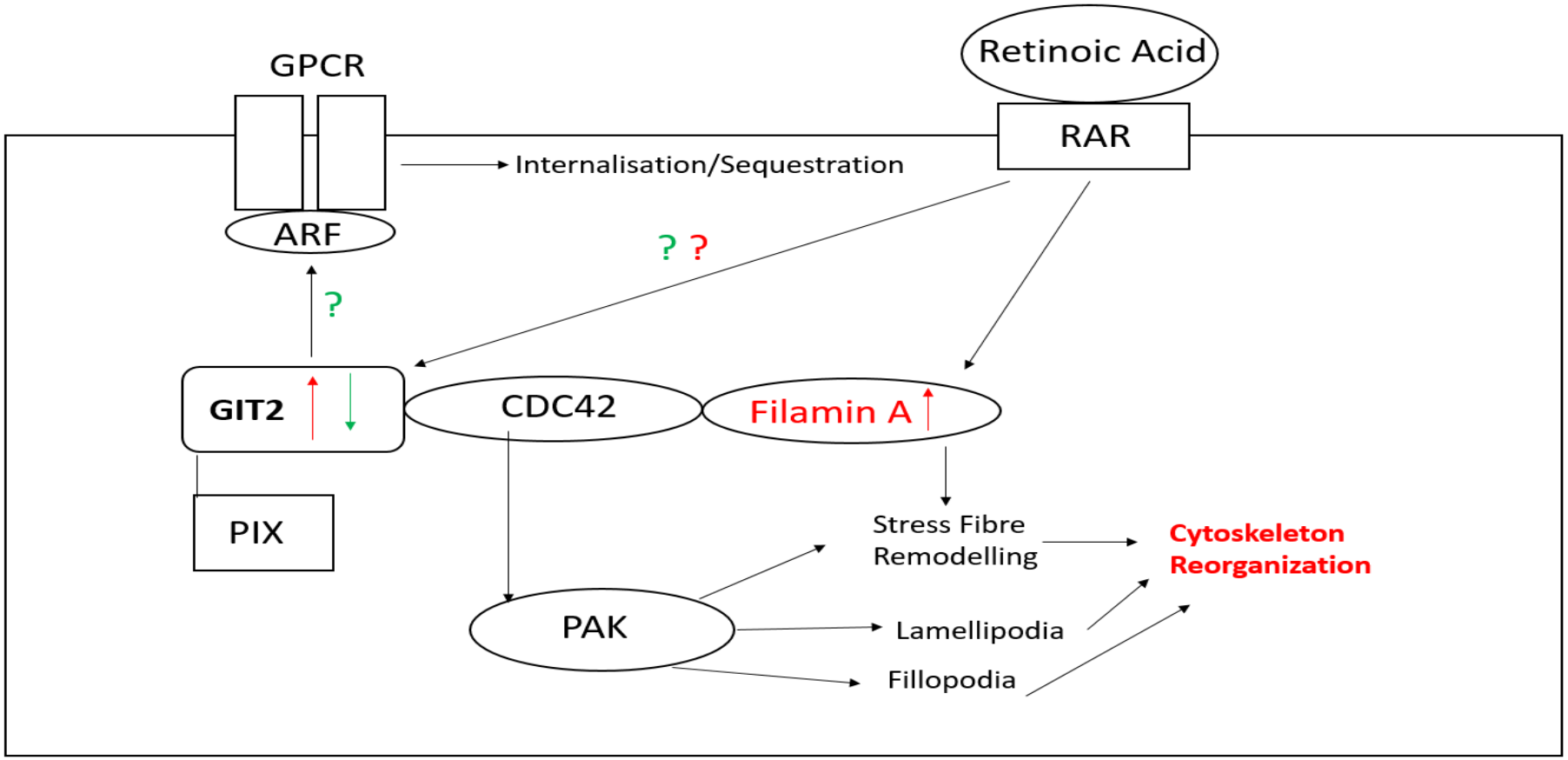

Figure 6.2: *A summary of the overlap of gene expression between kyphosis (↓↑) and vitamin A supplementation (↓↑). GIT2 was differentially regulated in the trabecular bone of kyphotic pre-weaners, and pigs receiving vitamin A supplementation. Vitamin A upregulated GIT2 and FLNA, of which are associated with the Rho-GTPase CDC42. This set of molecules share a common association in that they induce cytoskeletal rearrangement, of which has a subsequent effect on osteoblast differentiation and osteoclast activity. Rho-GTPases were not differentially regulated in kyphotic trabecular bone; it is possible GIT2-associated GPCR sequestration is linked to kyphosis.*

the vitamin A trial ascertaining *GIT2* as a vitamin A regulated gene (Chapter 5), this demonstrates how vitamin A is biologically contributing to kyphosis. The finding also implies that, due to *GIT2's* role in mediating osteoblast and osteoclast activity (Wang et al., 2012), the processes of endochondral bone growth and bone remodelling are downregulated in kyphotic pre-weaners. Recent reviews have also identified *GIT2* as a potential contributory cause to osteoporosis due to its roles in bone metabolism (van Gastel et al., 2018), and the results of this thesis further demonstrate *GIT2's* critical role in bone development. *GIT2's* differential regulation particularly at the pre-weaning stage also illustrates that this a critical period of kyphotic development, and should be focussed upon in intervention, which is discussed in more detail below. There are no established blood markers representative of *GIT2* activity, but if bone biopsies of pigs are to be obtained *GIT2* could serve as a diagnostic or prognostic marker of kyphotic development.

Due to *GIT2* and *DCN* differential expression being associated with kyphotic pigs at the pre-weaning stage, this suggests that outbreaks of kyphosis will initially occur on breeding farms. The gene expression changes at this age likely initiate the template of the kyphotic kink before normal growth and development through weaning. *ASPN's* differential expression in trabecular bone at post-weaning possibly indicates an effect to initiate TGF-β, as discussed, but the data obtained by extrapolating the kyphosis and vitamin A trials suggests the dominant changes are occurring at pre-weaning. Another critical implication was that *DCN* and *GIT2* were observed to associate with littermate pre-weaners as well as kyphotic pre-weaners. This implies that the sow, and therefore exposure of the piglet to factors during gestation and lactation, has had an effect on these changes. One such factor is vitamin A supply to the sow, which subsequently affects litter prevalence of kyphosis (Belsue, 2010). Since *GIT2* was identified as a vitamin A regulated biomarker in kyphotic pigs (Chapter 5), this serves as evidence that vitamin A supply from the sow to piglet is contributing to kyphosis as well as the entirety of the litter. These previous studies did not assess, anthropometrically or biochemically, how littermate piglets have been affected by treatments provided to the sow. Due to the data in this thesis showing that differential gene expression changes are confined to the litter, this emphasises that the whole litter is potentially at risk from developing kyphosis. Ultimately, this suggests that the sow will require priority focus in intervention trials.

Although *GIT2* was identified as a vitamin A regulated biomarker in kyphosis (Chapter 5), this was not the case with *ASPN* and *DCN*. The expression of these genes are possibly an effect of kyphosis, as discussed, but no firm conclusions can be drawn. Another approach that should be considered in future studies should be epigenetic analyses. The degree of DNA methylation on identified biomarkers could be responsible for gene expression changes. *In vitro,* methylation of CpG islands in the 5'UTR of *DCN* results in reduced mRNA expression (Qian et al., 2014). The aforementioned results were produced from a human cancerous cell line, which holds a different genetic make-up to a pig, but clearly demonstrate the requirement for investigating the role of epigenetic regulation in future studies. In addition to microarray analysis of kyphotic pre-weaners, it would also be beneficial to see which genes, or pathways, are conserved over time in kyphotic pigs, or if other pathways are affected. To this effect, tissues from weaning and post-weaning kyphotic pigs should be assessed via microarray. This would be critical in determining whether there are more effects, outside the influence of the sow, contributing to kyphosis.

In cartilage, Aggregan (*ACAN*) is established as a major ECM protein required for healthy cartilage growth (Zhang et al., 2012). In line with *DCN* upregulation, *ACAN* was identified by the microarray to be upregulated in kyphotic intervertebral cartilage (Chapter 3) and *DCN* has been observed to directly link aggrecan and collagens, thus contributing to the development of the tissue (Gubbiotti et al., 2016). It is likely that the functions of these glycoproteins are attempting to repair and stabilise the intervertebral cartilage of kyphotic pigs. Chapter 3 also indicated that angiogenesis could be affected in trabecular bone if there is a differential regulation of *BMPR1A*. However, vascular endothelial growth factor (*VEGF*), which is the master regulator of angiogenesis, nor *RUNX2*, the master regulator of osteoblast differentiation, were identified to be differentially expressed by the microarray. The relevance of *RUNX2* is discussed in more detail below, but the lack of *VEGF* differential expression ultimately shows that angiogenesis is not affected in the bone of kyphotic pigs.

It will be desirable to have whole vertebral samples from kyphotic and control pig assessed for bone volume or mineral density. Due to technical issues associated with sample storage, this experiment was not possible for the thesis. This must be taken into consideration for future studies, as it will be critical to confirm if a downregulation of *GIT2* is associated with changes in bone structure in kyphotic pigs. While major cases of kyphosis have shown

significantly compromised bone integrity as a result of a loss of a POC (Nielsen et al., 2005), this is often not consistent among all cases (Penny and Walters, 1986, Done and Gresham, 1988). To summarise, the thesis has identified novel genes in kyphosis that are indicative of reduced bone metabolism and proteoglycan losses in bone and cartilage tissues respectively. The thesis has therefore provided a molecular basis to the physiological changes that occur in kyphotic tissues. The thesis has also indicated that there is likely a maternal effect due to gene expression being confined within the litter. This implies that the pre-weaning period is a critical stage for the development of kyphosis.

6.3 The Vitamin A – Vitamin D Relationship and Vitamin A's role in Trabecular Bone Development

Another objective this thesis was to confirm how vitamin A supplementation affects differential gene expression in trabecular bone and serum 25(OH) D. Through assessing differential gene expression by pathway analysis (Chapter 4) and by identifying vitamin A regulated biomarkers that overlapped with kyphotic pigs (Chapter 5), the thesis identified Rho-GTPase molecules *FLNA*, *GIT2* and *SPARC* to be regulated by vitamin A in trabecular bone. In a rat model, osteoporosis is induced in response to 2 weeks of treatment with a diet containing 70mg/kg of vitamin A (Wu et al., 1996). This included decreased thickness of trabecular bone and number (Wu et al., 1996). Other observations show excess vitamin A to result in: decreased trabecular BMD (Lind et al., 2011), and decreased osteoblast cell numbers in trabecular bone (Wolke et al., 1968). Altogether, these observations implied that vitamin A induces bone resorption in trabecular bone, but the genes *GIT2*, *FLNA*, and *SPARC* function to regulate overall bone metabolism in relation to both osteoblasts and osteoclasts (Leung et al., 2010, Hong et al., 2010, Wang et al., 2012, Delany et al., 2003, Delany and Hankenson, 2009). Considering that the vitamin A trial was performed over a period of 15-22 weeks, these results demonstrate that long term exposure to high doses of vitamin A will favour expression of bone metabolic genes. Previous studies demonstrating that vitamin A compromises the structural integrity of trabecular bone (Lind et al., 2011, Wu et al., 1996, Wolke et al., 1968) were performed over a much shorter period than the vitamin A trial in the current study; therefore this demonstrates the differences acute and chronic exposure to vitamin A exert on trabecular bone. *FLNA* and *SPARC*, but not *GIT2*, were not differentially expressed in kyphotic pigs, whom received no specified vitamin A

treatments. In addition, *SPARC* and *FLNA* only showed differential expression in response to 3000µg RP/kg BW, the same treatment which resulted in full saturation of REs in liver, whereas *GIT2* was expressed in response to 200µg RP/kg BW, as well as in kyphosis pre-weaners. This suggests that *GIT2* is a more sensitive marker to vitamin A. Genes such as *FLNA* or *GIT2* contribute to osteoblast differentiation, but it is the synthesis of non-collagenous proteins that directly interact with and regulate bone matrix. Given that *SPARC*, an abundant non-collagenous protein in bone matrix, was only expressed in response to very high doses of vitamin A, this demonstrates that very high concentrations of vitamin A are required in order to directly exhibit effects on trabecular bone. Existing knowledge established that excess vitamin A affects Wnt signalling in cortical bone, and bone marrow (Lind et al., 2011, Lind et al., 2012); yet these studies were also performed over a much shorter period than the vitamin A trial. The thesis now suggests that long term exposure to excess vitamin A allows for interaction with Rho-GTPases to regulate bone metabolism; altogether these findings illustrate how excess vitamin A controls influences bone development.

In relation to the vitamin A-vitamin D relationship, the thesis aimed to further characterise the antagonistic relationship between the two vitamins, as well as whether this relationship can be associated with the development of skeletal diseases. This was accomplished through assessing how doses of vitamin A affect serum 25(OH) D (Chapter 4), as well as how vitamin A and vitamin D associate with a skeletal abnormality, in this case represented by kyphosis (Chapter 5). In the UK, recommendations from DSM (2016) suggest supplementing pigs additional thousands of µgs of vitamin A over vitamin D, but it has not been clarified as to whether this could potentially induce antagonism of vitamin D by vitamin A. The pigs used in the kyphosis trial, representative of outdoor pig farms, did not show any indications of antagonism of vitamin D by vitamin A. In fact, the vitamin A trial showed that doses up to 500µg RP/kg BW were required in order to observe a reduction in serum 25(OH) D. The pigs assigned to the 500µg RP/kg BW diet consumed, on average, 643µg/kg of BW of vitamin A daily (Chapter 4). If pigs consumed a diet with the highest concentrations of vitamin A recommended by DSM (2016) (6000µg/kg) this would result in an approximate 240µg/kg of BW daily intake of vitamin A, which is roughly 2.5 times below the daily intake of vitamin A observed to antagonise serum 25(OH)D in the vitamin A trial. Therefore, the thesis suggests

that the vitamin A-vitamin D antagonistic relationship does not contribute to kyphosis, nor is an issue that is contributing to abnormal skeletal health on UK pork farms. The thesis supports the recommendations from DSM in relation to vitamin A supplementation.

The thesis has identified several biomarkers in the small intestine which could explain how vitamin D is absorbed in response to excess vitamin A (Chapter 4). These biomarkers will need to be assessed by qPCR in future analysis in order to confirm their dose-responses to vitamin A and discuss their roles in nutrient absorption. Analysing serum 1,25 $(OH)_2$D should also be done in order to establish the end effects of 1-αhydroxylase expression in small intestines. Determining serum 1, 25 $(OH)_2$ D could also shed further light on the *RARG* expression profile in trabecular bone (Chapter 5), given that this chapter suggested that *RARG* gene expression is possibly regulated by vitamin D. Chapter 4 also argued that serum 25(OH) D and Ca levels are restored and maintained at the time of tissue sampling. Ideally, blood samples should have been obtained at time intervals during the experimental period to verify how acute and chronic exposure to vitamin A will affect maintenance of 25(OH) D and Ca over time. These data can then support or disprove the suggestion that these nutrients are initially antagonised in response to excess vitamin A, before being restored via intestinal mechanisms suggested in Chapter 4. Altogether, the data would provide a more complete picture of feedback mechanisms characterizing the relationship between vitamin A, and circulating vitamin D and Ca.

*CYP26A1 (*Cytochrome P450 Family 26 Subfamily A Member 1) is a protein responsible for hydroxylating and removing ATRA present in the cell, so as to control ATRA's effects on gene expression (Kedishvili, 2013). Despite being fed excess vitamin A, *CYP26A1* was not observed to be differentially expressed in the trabecular bone of treated pigs, nor was *CYP26A1* associated with kyphotic pigs. This finding draws comparisons back to the effects of excess vitamin A on bone marrow, in which *CYP26A1* was not significantly expressed, but was so in cortical bone (Lind et al., 2011). Furthermore, Abu-Abed et al. (2002) observed that, in the embryo, CYP26A1 was not detected in developing vertebrae. These findings could imply that *CYP26A1* is not naturally nor highly expressed within bone tissue, and therefore detecting differences in expression will require the application of more sensitive technologies. A relatively new qPCR protocol, termed "nested real time-PCR", has been demonstrated to improve assay sensitivity, and detect target transcripts at lower Ct thresholds (Tran et al.,

2014). This method relies on two sets of primer pairs acting on the template per round of PCR, essentially allowing for amplification of two PCR products. This method should be considered in order to confirm *CYP26A1* expression in vitamin A-treated, as well as kyphotic, pigs.

The gene expression results obtained for the trabecular bone represent novel findings, and have filled a knowledge gap into how excess vitamin A affects trabecular bone development at the molecular level, but how the structural integrity of the trabecular bone has been affected by differential gene expression will require confirmation in follow-up studies. A limitation of the vitamin A trial was that trabecular bone samples were not obtained to be assessed for BMD or volume. However, cortical bone from the femur was obtained from control and treated pigs. Some cortical bone samples were initially assessed via MicroCt, and the preliminary results showed that the cortical bone from the femurs of pigs receiving 5250µg RP/kg BW and 10000µg RP/kg BW had decreased bone volume in comparison to controls (Table 6.1). This finding is in agreement with previous studies showing excessive vitamin A induces narrowing of the cortical compartment of bone, in rat and pig studies (Pryor et al., 1969, Lind et al., 2011, Lind et al., 2012, Wray et al., 2011). Nonetheless, the next step to take will be to verify how the trabecular bone volume is affected. The finding that cortical thickness was reduced in the vitamin A trial could serve as a positive control for

	Groups					
	Control (n=2)	500µg/kg (n=3)	3000µg/kg (n=3)	5250µg/kg (n=3)	10000µg/kg (n=3)	Treatment p-value
Object Volume/ mm3	4852.69	5670.50	4600.97	3807.87*	3893.33*	<0.01
SEM	619.54	5.45	413.32	274.52	136.34	
% Object Volume	19.36	22.62	17.72	15.19*	15.53*	<0.01
SEM	2.47	0.022	2.28	1.10	0.54	

Table 6.1: *The object volume and % object volumes of cortical bone from the femur of the right, rear leg of control and treated pigs. One-way ANOVA found a significant effect of treatment on bone volume of cortical bone. *when compared to A group p<0.05.*

the trial setup, in that the method of the trial will accurately showcase excess vitamin A's effects on bone volume. The upregulation of bone metabolic genes in trabecular bone could suggest that these are effects in order to maintain trabecular bone mass over time. Lind et al. (2011) showed excess vitamin A to reduce trabecular bone density by 1 week. Furthermore, Wolke et al. (1968) observed decreased osteoblast cell numbers in the trabecular bone of pigs fed increasing levels of vitamin A over 5 weeks, which could suggest a loss of mineral density. On the other hand, Wray et al. (2011) showed, in comparison to control rats, rats fed supplementary vitamin A did not show changes in trabecular density or thickness from 2 to 10 months of age. Therefore, after a certain period of time, there could be a point in which excess vitamin A no longer reduces trabecular density, but rather restores bone mass. Whole vertebral samples, or defined regions of the diaphysis and epiphysis from the femur, should be assessed for trabecular bone volume, such as using a microCt approach, in future studies in order to determine excess vitamin A's end effects on the tissue.

To summarise, the thesis has determined that doses of vitamin A higher than current recommendations are required in order to antagonise vitamin D, and that vitamin A controls bone metabolism in trabecular bone through interacting with genes that control Rho-GTPase-mediated cytoskeletal dynamics. Further work should assess trabecular bone volume or mineral density in order to clarify the effects of upregulated genes within the tissue, and identified biomarkers in small intestines should be assessed by qPCR.

6.4 Kyphosis and its association with Vitamin A and Vitamin D

The final objectives of this thesis were to confirm how vitamin A and vitamin D associate with kyphotic pigs, and to determine if vitamin A contributes to differential gene expression in kyphotic pigs. Kyphotic and littermate pre-weaners, raised outdoors, showed reduced serum 25(OH) D in comparison to controls, but older pigs did not show differences (Chapter 5). Likewise control pigs from the vitamin A trial, representing standard grower pigs raised according to UK husbandry, did not show differences in serum 25(OH) D in comparison to the lower vitamin A dose groups (Chapter 4). These could imply that vitamin D limitation is an issue in relation to outdoor piglets. It has been acknowledged that differences in vitamin D consumption by the sow will influence vitamin D status and skeletal health in offspring

(Witschi et al., 2011). A study conducted in the USA showed that outdoor pigs during winter periods have serum 25(OH) D below reference values (Arnold et al., 2015). Given that pigs in the kyphosis trial were raised outdoors, whereas those in the vitamin A trial were not, the data in this thesis indicates that vitamin D should be supplemented to outdoor sows in order to assist in the eradication of kyphosis. The finding that pre-weaning kyphotic pigs showed reduced serum 25(OH) D is in agreement with previous trials which have shown vitamin D supply to the sow will affect the prevalence of kyphosis (Rortvedt and Crenshaw, 2012). In order to avoid complications associated with vitamin D deficiency, the thesis suggests that additional vitamin D supplementation should be considered for outdoor sows on UK farms, especially during winter periods.

Liver REs were not observed to be reduced in kyphotic pre-weaners. Yet the thesis clearly demonstrated an effect of vitamin A during kyphosis, given the dose-response relationship of *GIT2* with vitamin A (Chapter 4) and *GIT2's* downregulation in trabecular bone of kyphotic pre-weaners (Chapter 5). Given that *GIT2* was confined to the pre-weaning litter, this implies that vitamin A supply from the sow, through either gestation or lactation, is having an effect on *GIT2* expression in trabecular bone. Although previous studies have demonstrated an effect with vitamin D (Rortvedt and Crenshaw, 2012) and have suggested vitamin A supply from the sow is critical in relation to kyphosis (Belsue, 2010), this is the first study to characterise how vitamin A is biologically contributing to kyphosis. A summary of *GIT2* signalling and how it relates to kyphosis is provided (Figure 6.2). There does remain the question as to which component of *GIT2* mechanics, cytoskeletal rearrangement or GPCR sequestration, are affected in kyphosis. No Rho-GTPases, or associated molecules, were observed to be differentially expressed in the trabecular bone of kyphotic pigs. This could suggest that *GIT2*-associated GPCR sequestration, rather than *GIT2*-regulated cytoskeletal dynamics, could be contributing to the physiological consequences of kyphosis. If there is a difference in *GIT2* mechanisms between the two trials, this could indicate that differences in vitamin A intake induce different mechanisms through *GIT2* on bone metabolism. More work in the fields of *GIT2* and GPCR-associated regulation of bone metabolism will need to be performed until more solid answers can be provided. Due to the clear link between *GIT2* and vitamin A metabolism, the major question remains as to whether vitamin A supplementation will eradicate a prevalence of kyphosis.

It cannot be ruled out that the pigs from the two different trials in this thesis were of different genotypes, were raised in separate commercial environments, and exhibited a large difference in age during the experimental period. However, results obtained from a cell line or separate model organism would not have been as comparable to kyphotic pigs as the pigs used in the vitamin A trial. Moreover, although liver REs were reduced in kyphotic post-weaners, the thesis cannot confirm what the effect of this due to the lack of differential gene expression in kyphotic post-weaners. It is also likely that vitamin A metabolism, rather than intake, has been affected in kyphotic pre-weaners, but the thesis has not been able to address this. Molecular analysis from small intestine, kidney and liver tissues could have provided more answers in relation to vitamin A and vitamin D metabolism. Analysis of the α-hydroxylase enzyme in the kidney could offer insight as to how 1, 25$(OH)_2$D synthesis has been affected in kyphotic pigs. Also, analysis of differential gene expression in liver could provide more answers as to how vitamin A metabolism is affected in kyphotic pigs which results in *GIT2* downregulation in trabecular bone. One hypotheses could be that the expression of retinol-binding protein (RBP), which delivers retinol to extrahepatic tissues (Kedishvili, 2013), is downregulated in kyphotic livers. However, there is no evidence to support this, and this shows the requirement to analyse other tissues in kyphotic pigs.

Overall, the thesis has argued that decreased vitamin A activity in the vertebral trabecular bone of kyphotic pre-weaners contributes to reduced bone metabolism through *GIT2*. Kyphotic pre-weaners did not show reduced RE storage in liver (Chapter 5), but the only method that will conclude whether vitamin A intake will associate with kyphosis is to perform an intervention trial. Although Belsue (2010) showed excess vitamin A has the potential to induce kyphosis, they did not confirm if reduced vitamin A intake will also contribute to kyphosis, as suggested by the data synthesised in this thesis. Human studies have shown that approximately 60 times more vitamin A is transferred to offspring during the first 6 months of lactation in comparison to 9 months of gestation (Stoltzfus and Underwood, 1995). In addition DSM (2016) do not recommend additional feeding of vitamin A for lactating sows over gestating sows. Considering the significant demand for vitamin A during lactation, this raises the question as to whether lactating sows are receiving adequate vitamin A that satisfy nutritional demand in piglets. Therefore the proposed trial

should incorporate feeding reduced, adequate, or supplementary vitamin A to outdoor sows during gestation and lactation periods. Upon weaning, piglets should be split into two groups: diets with adequate or marginal concentrations of Ca and P, while containing similar levels of vitamin A. This setup will be crucial in determining if vitamin A supply during gestation and lactation will contribute to kyphosis, as suggested by the laboratory data. Given vitamin A's hormonal control over skeletal development, it will be critical to observe if vitamin A supply during gestation and lactation will induce kyphosis in pigs fed a diet adequate in Ca and P. It will also be important to observe if a reduction in Ca and P will exaggerate kyphosis prevalence in response to vitamin A supply. Desired data that should be collected from the trial should include: kyphosis prevalence, and average weekly weight gain according to treatment. In addition, pigs should be tissue sampled at 2 weeks, 4 weeks, and 13 weeks of age, similar to the experimental design used in this thesis. Desired data from tissue should include: qPCR verification of *GIT2* expression in trabecular bone, MicroCt analysis of individual vertebrae, liver RE concentrations, and serum Ca and P. The expression of *GIT2* can be compared back to results obtained in this thesis in order to confirm if the proposed mechanisms indeed occur in response to vitamin A intake. If vitamin A is found to affect the prevalence of kyphotic pigs in this proposed intervention trial, a separate trial can be set up which can test if supplementation with vitamin A and vitamin D will eradicate prevalence of the disease.

To summarise, the thesis has shown vitamin A potentially contributes to kyphosis through regulating *GIT2* in vertebral trabecular bone, and this establishes vitamin A as a factor that can contribute to the disease. However vitamin A will need to be directly tested in an intervention trial to confirm if vitamin A intake is associated with kyphosis.

6.5 Alternative Approaches for Future Work

6.5.1 Zinc and Copper

The underlying constituents of bone tissue are the minerals Ca and P (Whittemore and Kyriazakis, 2006). In order to progress from this research, it will be necessary to identify input from other nutritional factors that will be affecting Ca and P availability. A similar approach for how this thesis assessed the association of kyphosis with vitamin A should be considered in future work investigating vitamin D and kyphosis. This will allow for

identification of vitamin D regulated biomarkers in kyphosis that will contribute to Ca and P utilisation in bone. Another avenue to consider is how other minerals in the diet could be interfering with the activity of the enzyme phytase, which is required in pigs to digest P from phytate. Phytate binds ions such as Ca, or Zinc (Zn) and forms a divalent complex, digestion of these complexes by phytase allows for release and digestibility of these minerals (Bikker et al., 2013). However, supplementation of zinc to phytase-supplemented diets have demonstrated this lowers availability and digestibility of P (Poulsen et al., 2016, Lizardo et al., 2004). This could imply that, through limiting availably of P and therefore potentially bone mineralisation, zinc supplementation could contribute to kyphosis. To investigate this, zinc was preliminarily analysed in the serum of kyphotic and non-related control pre-weaners via ICP-MS. The method allowed for analysis of copper, zinc, iron, and manganese in serum. While the results did not observe a difference in serum Zn, serum Cu was significantly reduced in kyphotic pre-weaners (Figure 6.3). However it must be noted that these data were not normalised according to parameters in blood such as protein content, nor were metal-ion free vacutainer tubes used to collect blood samples. Nonetheless, these initial results can direct the research in new directions.

Low serum Cu concentrations have been associated with reduced BMD (Qu et al., 2018). In addition, supplementing Cu to broilers increased bone volume, trabecular thickness, as well as thickness of articular and epiphyseal cartilage (Muszyński et al., 2018). There is, however, no clear interaction between Cu and phytase (Bikker et al., 2013). Cu could have an effect on cartilage, and thereafter, bone metabolism due its role in the activation of the lysyl oxidase enzyme, which regulates collagen cross-linking (Medeiros, 2016). It is highly recommended that this work be continued in future studies, and verify if serum and tissue concentrations of these metal ions can be associated with kyphosis across the 3 age groups analysed in this thesis. To summarise, Cu and Zn should be investigated as the next dietary culprits in relation to the development of kyphosis. The data acquired from this analysis would add further insight into the role of nutrition in skeletal development.

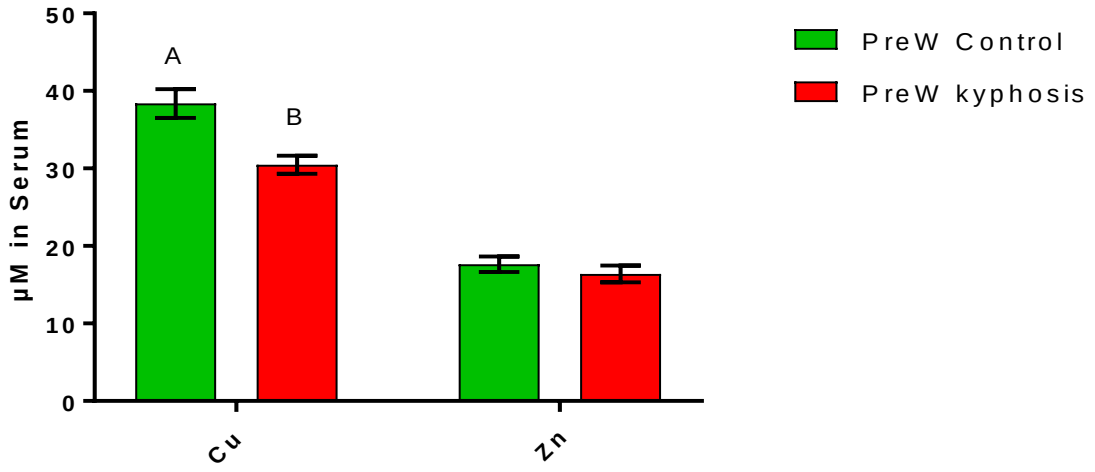

Figure 6.3: *The concentrations (µM) of Copper (Cu) and Zinc (Zn) in the serum of pre-weaning (PreW) kyphotic and non-related control pigs. Data are presented as Arith means ±SEM One way ANOVA AB p<0.05*

6.5.2 Recommended Experiments for Future Work

One of the primary aims of this thesis was to characterise molecular associations within trabecular bone tissue in vertebrae. Although trabecular bone is the primary tissue type that composes the vertebral body, other constituents such as bone marrow persist within vertebrae. Due to logistical reasons, it would have been impractical to sample pure trabecular bone from vertebral samples in the field. Therefore, the findings in this thesis more accurately represent changes occurring within the vertebral body, which includes trabecular bone and bone marrow. The strength of this approach is that it emphasises the overall changes occurring within the vertebrae, but the main drawback is that it is not possible to pinpoint exact tissue or cellular type in which these changes are occurring. It would be useful to incorporate a histology approach in future efforts so as to identify changes in tissue architecture, as well as immunohistochemistry to visualise cellular localisation of translated proteins. Though the thesis has added significant knowledge in relation to the molecular basis of vertebral bone development, no precise biological mechanisms can be defined or proposed until it is possible to directly visualise and observe the changes occurring within the tissue.

One potential weakness of the approaches used in this thesis is that a microarray methodology was applied. This methodology can now be considered outdated in regards to emerging technologies which analyse differential gene expression. In recent years, RNA-sequencing (RNA-seq) has been shown to have particular advantages over traditional microarrays (Wang et al., 2009). RNA-seq is not limited by detecting transcripts which correspond to a known genomic sequence, background noise is markedly reduced, and can detect a higher range of genes expressed at very low or high levels (Wang et al., 2009). An RNA-seq approach may therefore identify differentially expressed transcripts of which a microarray may not detect, but ultimately it would be beneficial to observe if transcripts overlap between the two technologies. Another item to take into consideration is interpretation from qPCR results which showed late Ct's. A late cycle number in qPCR correlates with low copy numbers of the target transcript, and this can be problematic in relation to assay sensitivity. This is because, in the presence of low copies of the target transcript, primers can end up interacting with themselves to form primer-dimers, or with leftover RNA, resulting in the formation of non-specific PCR products. As a result, samples which show late Ct's may therefore not be generating a signal truly representative of target transcript expression, which would lead to inaccuracy of results. Throughout this thesis, melting curve analysis was used to indicate the presence of non-specific PCR products, and therefore help identify samples producing a signal representative of the target transcript. This approach therefore added reliability to the obtained data from qPCR, and justifies the interpretation of the results in the thesis.

The thesis has been unable to identify genes that are specifically confined to kyphotic pigs. However molecular investigations are not going to provide a complete picture of the biology of the disease. In addition, non-collagenous proteins which directly regulate bone matrix metabolism, such *SPARC* or *BGLAP,* were not indicated to be differentially expressed in kyphotic pigs. The answer, however, may not lie at the mRNA level. Post-translational modifications (PTMs) can occur on translated proteins to modulate or induce functional diversity; this field of research is termed "Proteomics" (Jensen, 2004). In the case of *BGLAP*, studies have shown the osteocalcin protein is glycated on its N-terminus, resulting in addition of a sugar to a free amine group (Thomas et al., 2017). The glycation of osteocalcin has been proposed to affect its ability to bind collagens and other non-collagenous proteins

during matrix mineralisation (Thomas et al., 2017). Furthermore, addition of mannose-type sugars to bone osteonectin have been identified that allow it to interact with various collagens, unlike platelet osteonectin which does not share similar PTMs (Kelm and Mann, 1991). With TGF- β and BMP signalling, phosphorylation of TGF- β receptors, as well as downstream Smad molecules, is required in order to activate these molecules and thus regulate transmission of the pathway (Chen et al., 2012). In addition to this, PAK is phosphorylated upon interaction with Rho-GTPases in order to regulate cytoskeletal dynamics (Rane and Minden, 2014).

However, proteomics should also be utilised to verify one critical question: the activity of *RUNX2* in kyphotic and vitamin A treated pigs. This thesis has argued that osteoblast differentiation has been affected in both of these groups of pigs. Yet *RUNX2* was not observed to be differentially expressed in either trials. However, studies in human BMSCs *in vitro* have shown that, unlike in rodent studies, the mRNA level of *RUNX2* does not correspond to osteoblast differentiation (Shui et al., 2003). Rather, the authors observed the degree of phosphorylation of *RUNX2* was more related to its ability to regulate osteoblast differentiation, despite no differences in mRNA or protein levels (Shui et al., 2003). *RUNX2* has been observed to be phosphorylated by the MAPK pathway (Xiao et al., 2000).
The purpose of GIT2-regulated cytoskeletal dynamics are to initiate integrin-adhesion to the ECM, which is required to activate MAPK and ERK pathways (Hoefen and Berk, 2006, Hamidouche et al., 2009). In accordance with this, microarray analysis of trabecular bone showed *MAPK12* and *MAPK6* to be downregulated and upregulated in kyphotic and vitamin A pigs, respectively (Table 6.2). Therefore, *GIT2* differential expression could be contributing to the degree of MAPK-dependent phosphorylation of *RUNX2*, which subsequently affects osteoblast differentiation in kyphotic and vitamin A pigs. Proteomics should be seriously considered as a follow-up to this thesis, in order to gain insight into how translated proteins and their functions have been affected in kyphotic pigs and pigs receiving vitamin A supplementation.

Pig Trial	Gene Name	Regulation	p-value
Kyphosis	Mitogen activated kinase 12/MAPK12	4.28↓	0.007
Vitamin A	Mitogen activated kinase 6/MAPK6	2↑	0.041

Table 6.2: *Differential expression of Mitogen activated protein kinases in the trabecular bone of pre-weaning kyphotic pigs, and pigs receiving 10000μg RP/kg BW. The results were generated in Genespring, and the fold-change and p-value, determined by moderated T-Test in Genespring, is provided.*

Approaches beyond the laboratory also need to be considered if the causes of kyphosis are to be identified. While laboratory methods will help establish the biological basis of kyphosis, they will not confirm what factors, environmental or at the farm management level, cause kyphosis. To this end, an epidemiology survey must be performed in follow-up work. This approach will allow answers for critical questions such as: whether there is truly a seasonal effect in relation to kyphosis, in what age group are cases frequently observed, and whether particular feeding strategies on different farms can be attributed to kyphosis. This data, in combination with insights from laboratory analysis and intervention trials, will be able to provide the most detailed understanding of what causes kyphosis in pigs.

6.6 Final Conclusions

The research synthesised in this thesis has provided the first direct evidence of the underlying molecular mechanisms associated with the development of kyphosis in pigs. The thesis has illustrated the critical implications of *DCN* and *GIT2* with bone development.

Investigations have also revealed vitamin A's association with Rho-GTPase pathways in trabecular bone, which has not been previously observed. The thesis has demonstrated how high doses of vitamin A regulates bone metabolism in trabecular bone. The thesis has also revealed that very high doses of vitamin A do not antagonise serum 25(OH) D, and that the relationship between the two vitamins is not simply antagonistic as previously assumed.

The thesis has also ascertained vitamin A's association with the molecular basis of kyphosis, particularly with *GIT2* regulation in trabecular bone. The thesis adds justification to

determine if vitamin A supplementation will assist in the eradication of the disease. In addition, the thesis has illustrated that vitamin D deficiency is also associated with kyphotic pigs on UK farms, and supports a role for its use in intervention trials.

Multiple approaches, beyond molecular investigations, are recommended for future endeavours in order to provide a complete picture of vitamin A's roles in bone biology and to elucidate the cause of idiopathic lumbar kyphosis.

Bibliography

ABU-ABED, S., MACLEAN, G., FRAULOB, V., CHAMBON, P., PETKOVICH, M. & DOLLE, P. 2002. Differential expression of the retinoic acid-metabolizing enzymes CYP26A1 and CYP26B1 during murine organogenesis. *Mechanisms of Development* 110**,** 173-7.

ABURTO, A., EDWARDS, H. M. J. & BRITTON, W. M. 1998. The Influence of Vitamin A on the Utilization and Amelioration of Toxicity of Cholecalciferol, 25-Hydroxycholecalciferol, and 1,25 Dihydroxycholecalciferol in Young Broiler Chickens. *Poultry Science,* 77**,** 585-93.

ADAMS, M. A. & ROUGHLEY, P. J. 2006. What is Intervertebral Disc Degeneration, and What Causes It. *Spine* 31**,** 2151-61.

AGILENT, T. 2012. Introduction to Quantitative PCR. Agilent Technologies

AHMADIEH, H. & ARABI, A. 2011. Vitamins and bone health: beyond calcium and vitamin D. *Nutrition Reviews,* 69**,** 584-98.

AL-QTAITAT, A. I. & ALDALAEN, S. M. 2014. A Review of Non-Collagenous Proteins; their Role in Bone. *American Journal of Life Sciences,* 2**,** 351-5.

AMUNDSON, L. A., HERNANDEZ, L. L. & CRENSHAW, T. D. 2017. Serum and tissue 25-OH vitamin D3 concentrations do not predict bone abnormalities and molecular markers of vitamin D metabolism in the hypovitaminosis D kyphotic pig model. *British Journal of Nutrition,* 118**,** 30-40.

AMUNDSON, L. A., HERNANDEZ, L. L., LAPORTA, J. & CRENSHAW, T. D. 2016. Maternal dietary vitamin D carry-over alters offspring growth, skeletal mineralisation and tissue mRNA expressions of genes related to vitamin D, calcium and phosphorus homoeostasis in swine. *British Journal of Nutrition,* 116**,** 774-87.

ANDERSON, M. D., SPEER, V. C., MCCALL, J. T. & HAYS, V. W. 1966. Hypervitaminosis A in the young pig. *Journal of Animal Science,* 25**,** 1123-7.

APPUNNI, S., ANAND, V., KHANDELWAL, M., SETH, A., MATHUR, S. & SHARMA, A. 2017. Altered expression of small leucine-rich proteoglycans (Decorin, Biglycan and Lumican): Plausible diagnostic marker in urothelial carcinoma of bladder. *Tumour Biology,* 39.

ARNOLD, J., MADSON, D. M., ENSLEY, S. M., GOFF, J. P., SPARKS, C., STEVENSON, G. W., CRENSHAW, T., WANG, C. & HORST, R. L. 2015. Survey of serum vitamin D status across stages of swine production and evaluation of supplemental bulk vitamin D premixes used in swine diets. *Journal of Swine Health and Production,* 23**,** 28-34.

BALKAN, W., RODRÍGUEZ-GONZALEZ, M., PANG M, F., I. & TROEN, B. R. 2011. Retinoic acid inhibits NFATc1 expression and osteoclast differentiation. *Journal of Bone and Mineral Metabolism,* 29**,** 652-61.

BALMER, J. E. & BLOMHOFF, R. 2002. Gene expression regulation by retinoic acid. *Journal of Lipid Research,* 43**,** 1773-808.

BELSUE, J. B. Kyphosis and Lordosis: Possible link to nutrition International Pig Veterinary Society 2010 Vancouver, Canada. IPVS.

BERENDSEN, A. D. & OLSEN, B. R. 2015. Bone development. *Bone,* 80**,** 14-8.

BIKKER, P., JONGBLOED, A. W. & THISSEN, J. T. N. M. 2013. Meta-analysis of effects of microbial phytase on digestibility and bioavailability of copper and zinc in growing pigs *Journal of Animal Science,* 90**,** 134-6.

BOCK, H. C., MICHAELI, P., BODE, C., SCHULTZ, W., KRESSE, H., HERKEN, R. & MIOSGE, N. 2001. The small proteoglycans decorin and biglycan in human articular cartilage of late-stage osteoarthritis. *Osteoarthritis Cartilage,* 9**,** 654-63.

BOREL, P., CAILLAUD, D. & CANO, N. J. 2015. Vitamin D bioavailability: state of the art. *Critical Reviews in Food Science and Nutrition,* 55**,** 1193-205.

BOWLER, W. B., GALLAGHER, J. A. & BILBE, G. 1998. G-protein coupled receptors in bone *Frontiers in Bioscience,* 3**,** 769-80.

BOYCE, B. F. & XING, L. 2007. Biology of RANK, RANKL, and osteoprotegerin. *Arthritis Research & Therapy,* 9.

BOYLE, W. J., SIMONET, W. S. & LACEY, D. L. 2003. Osteoclast differentiation and activation. *Nature* 423**,** 337-42.

BROULIK, P. D., RASKA, I. & BROULIKOVA, K. 2013. Prolonged overdose of all-trans retinoic acid enhances bone sensitivity in castrated mice. *Nutrition,* 29**,** 1166-9.

BURR, D. B. & ALLEN, M. R. 2014. *Basic and Applied Bone Biology*, Elsevier

BURTON-WURSTER, N., LIU, W., MATTHEWS, G. L., LUST, G., ROUGHLEY, P. J., GLANT, T. T. & CS-SZABÓ, G. 2003. TGF beta 1 and biglycan, decorin, and fibromodulin metabolism in canine cartilage. *Osteoarthritis and Cartilage,* 11**,** 167-76.

CAPIN-GUTIERREZ, N., TALAMAS-ROHANA, P., GONZALEZ-ROBLES, A., LAVALLE-MONTALVO, C. & KOURI, J. B. 2004. Cytoskeleton disruption in chondrocytes from a rat osteoarthrosic (OA) - induced model: its potential role in OA pathogenesis. *Histology and Histopathology,* 19**,** 1125-32.

CHEN, D., JI, X., HARRIS, M. A., FENG, J. Q., KARSENTY, G., CELESTE, A. J., ROSEN, V., MUNDY, G. R. & HARRIS, S. E. 1998. Differential Roles for Bone Morphogenetic Protein (BMP) Receptor Type IB and IA *Journal of Cell Biology,* 142**,** 295-305.

CHEN, G., DENG, C. & LI, Y. P. 2012. TGF-beta and BMP signaling in osteoblast differentiation and bone formation. *International Journal of Biological Sciences,* 8**,** 272-88.

CHEN, T. C., LU, Z. & HOLICK, M. F. 2010. *Nutrition and Health: Vitamin D*, Springer Science+Business Media

CLARK, I. & BASSETT, C. A. L. 1961. The amelioration of hypervitaminosis D in rats with vitamin A *Journal of Experimental Medicine,* 115**,** 147-56.

COFFEY, J. D., HINES, E. A., STARKEY, J. D., STARKEY, C. W. & CHUNG, T. K. 2012. Feeding 25-hydroxycholecalciferol improves gilt reproductive performance and fetal vitamin D status. *Journal of Animal Science,* 90**,** 3783-8.

CONAWAY, H. H., PIRHAYATI, A., PERSSON, E., PETTERSSON, U., SVENSSON, O., LINDHOLM, C., HENNING, P., TUCKERMANN, J. & LERNER, U. H. 2011. Retinoids stimulate periosteal bone resorption by enhancing the protein RANKL, a response inhibited by monomeric glucocorticoid receptor. *Journal of Biological Chemistry,* 286**,** 31425-36.

CRADDOCK, R. J., HODSON, N. W., OZOLS, M., SHEARER, T., HOYLAND, J. A. & SHERRATT, M. J. 2018. Extracellular matrix fragmentation in young, healthy cartilaginous tissues. *European Cells and Materials* 35**,** 34-53.

CRENSHAW, T. D., RORTVEDT, L. A. & HASSEN, Z. 2011. Triennial Growth Symposium: a novel pathway for vitamin D-mediated phosphate homeostasis: implications for skeleton growth and mineralization. *Journal of Animal Science,* 89**,** 1957-64.

DAVID, L., FEIGE, J. J. & BAILLY, S. 2009. Emerging role of bone morphogenetic proteins in angiogenesis. *Cytokine and Growth Factor Reviews,* 20**,** 203-12.

DAYDREAMANATOMY. 2017. *Anatomy Human* [Online]. Available: https://daydreamanatomy.com [Accessed].

DE LERA, A. R., BOURGUET, W., ALTUCCI, L. & GRONEMEYER, H. 2007. Design of selective nuclear receptor modulators: RAR and RXR as a case study. *Nature Reviews Drug Discovery,* 6**,** 811-20.

DELANY, A. M., AMLING, M., PRIEMEL, M., HOWE, C., BARON, R. & CANALIS, E. 2000. Osteopenia and decreased bone formation in osteonectin-deficient mice. *Journal of Clinical Investigation,* 105**,** 915-23.

DELANY, A. M. & HANKENSON, K. D. 2009. Thrombospondin-2 and SPARC/osteonectin are critical regulators of bone remodeling. *Journal of Cell Communication and Signaling,* 3**,** 227-38.

DELANY, A. M., KALAJZIC, I., BRADSHAW, A. D., SAGE, E. H. & CANALIS, E. 2003. Osteonectin-null mutation compromises osteoblast formation, maturation, and survival. *Endocrinology,* 144**,** 2588-96.

DEMAIS, V., AUDRAIN, C., MABILLEAU, G., CHAPPARD, D. & BASLE, M. F. 2014. Diversity of bone matrix adhesion proteins modulates osteoblast attachment and organization of actin cytoskeleton. *Morphologie,* 98**,** 53-64.

DEWEY, C. E., FRIENDSHIP, R. M. & WILSON, M. R. 1993. Clinical and postmortem examination of sows culled for lameness. *Canadian Veterinary Journal* 34**,** 555-6.

DONE, S. H. & GRESHAM, A. C. J. 1988. Lordosis and Kyphosis (-humpy-back-) in pigs. *Pig Journal,* 41**,** 134-41.

DONE, S. H. & PEARSON, R. 2004. Porcine lordosis and kyphosis (a third variant of 'humpy-back') associated with increased muscle masses and subsequent disc protrusion. *The Pig Journal,* 53**,** 207-20.

DONE, S. H., POTTER, R. A., COURTENAY, A. & PEISSEL, K. 1999. Lordosis and Kyphosis (-humpy-back) in pigs a second type of the condition associated with hemivertebrae. *Pig Journal* 43**,** 148-53.

DROLET, R., DENICOURT, M. & D'ALLAIRE, S. 2012. Alopecia areata and humpy-back syndrome in suckling piglets. *Canadian Veterinary Journal,* 53**,** 865-9.

DSM. 2016. *DSM Vitamin Supplementation Guidelines 2016 for animal nutrition* [Online]. [Accessed].

EKLOU-KALONJI, E., ZERATH, E., COLIN, C., LACROIX, C., HOLY, X., DENIS, I. & POINTILLART, A. 1999. Calcium-Regulating Hormones, Bone Mineral Content, Breaking Load and Trabecular Remodeling Are Altered in Growing Pigs Fed Calcium-Deficient Diets. *Journal of Nutrition,* 129**,** 188-93.

ETTERLIN, P. E., MORRISON, D. A., OSTERBERG, J., YTREHUS, B., HELDMER, E. & EKMAN, S. 2015. Osteochondrosis, but not lameness, is more frequent among free-range pigs than confined herd-mates. *Acta Veterinaria Scandinavica,* 57.

EUROPEAN FOOD SAFETY AUTHORITY, E. 2008. Consequences for the consumer of the use of vitamin A in animal nutrition. *EFSA Journal,* 873**,** 1-81.

FLOHR, J. R., TOKACH, M. D., WOODWORTH, J. C., DEROUCHEY, J. M., GOODBAND, R. D. & DRITZ, S. S. A survey of added vitamin concentrations used in the U.S. swine industry. American Society of Animal Science, Annual Meeting 2015 Des Moines, Iowa ASAS

FRANKEL, T. L., SESHADRI, M. S., MCDOWALL, D. B. & CORNISH, C. J. 1986. Hypervitaminosis A and Calcium-Regulating Hormones in the Rat. *The Journal of Nutrition,* 116**,** 578-87.

GAO, L., GORSKI, J. L. & CHEN, C. S. 2011. The Cdc42 Guanine Nucleotide Exchange Factor FGD1 Regulates Osteogenesis in Human Mesenchymal Stem Cells. *American Journal of Pathology,* 178**,** 969-74.

GIMBLE, J. M., ZVONIC, S., FLOYD, Z. E., KASSEM, M. & NUTTALL, M. E. 2006. Playing with bone and fat. *Journal of Cellular Biochemistry,* 98**,** 251-66.

GOEL, S. A., GUO, L. W., SHI, X. D., KUNDI, R., SOVINSKI, G., SEEDIAL, S., LIU, B. & KENT, K. C. 2013. Preferential secretion of collagen type 3 versus type 1 from adventitial fibroblasts stimulated by TGF-beta/Smad3-treated medial smooth muscle cells. *Cell Signal,* 25**,** 955-60.

GOLDBERG, S., GLOGAUER, J., GRYNPAS, M. D. & GLOGAUER, M. 2015. Deletion of filamin A in monocytes protects cortical and trabecular bone from post-menopausal changes in bone microarchitecture. *Calcified Tissue International,* 97**,** 113-24.

GONCHARENKO, A. V., MALYUCHENKO, N. V., MOISENOVICH, A. M., KOTLYAROVA, M. S., ARKHIPOVA, A. Y., KON'KOV, A. S., AGAPOV, I. I., MOLOCHKOV, A. V., MOISENOVICH, M. M. & KIRPICHNIKOV, M. P. 2016. Changes in morphology of actin filaments and expression of alkaline phosphatase at 3D cultivation of MG-63 osteoblast-like cells on mineralized fibroin scaffolds. *Doklady Biochemistry and Biophysics,* 470**,** 368-70.

GOUMANS, M. J., LIU, Z. & TEN DIJKE, P. 2009. TGF-beta signaling in vascular biology and dysfunction. *Cell Research,* 19**,** 116-27.

GREEN, A. C., KOCOVSKI, P., JOVIC, T., WALIA, M. K., CHANDRARATNA, R. A. S., MARTIN, T. J., BAKER, E. K. & PURTON, L. E. 2017. Retinoic acid receptor signalling directly regulates osteoblast and

adipocyte differentiation from mesenchymal progenitor cells. *Experimental Cell Research,* 350**,** 284-97.
GREEN, A. C., POULTON, I. J., VRAHNAS, C., HAUSLER, K. D., WALKLEY, C. R., WU, J. Y., MARTIN, T. J., GILLESPIE, M. T., CHANDRARATNA, R. A., QUINN, J. M., SIMS, N. A. & PURTON, L. E. 2015. RARgamma is a negative regulator of osteoclastogenesis. *Journal of Steroid Biochemistry and Molecular Biology,* 150**,** 46-53.
GUBBIOTTI, M. A., VALLET, S. D., RICARD-BLUM, S. & IOZZO, R. V. 2016. Decorin interacting network: A comprehensive analysis of decorin-binding partners and their versatile functions. *Matrix Biology* 55**,** 7-21.
HALANSKI, M. A., HILDAHL, B., AMUNDSON, L. A., LEIFERMAN, E., GENDRON-FITZPATRICK, A., CHAUDHARY, R., HARTWIG-STOKES, H. M., MCCABE, R., LENHART, R., CHIN, M., BIRSTLER, J. & CRENSHAW, T. D. 2018. Maternal Diets Deficient in Vitamin D Increase the Risk of Kyphosis in Offspring: A Novel Kyphotic Porcine Model. *The Journal of Bone and Joint Surgery,* 100**,** 406-15.
HAMIDOUCHE, Z., FROMIGUE, O., RINGE, J., HAUPL, T., VAUDIN, P., PAGES, J. C., SROUJI, S., LIVNE, E. & MARIE, P. J. 2009. Priming integrin alpha5 promotes human mesenchymal stromal cell osteoblast differentiation and osteogenesis. *Proceedings of the National Academy of Sciences of the United States of America,* 106**,** 18587-91.
HARRISON, E. H. 2005. Mechanisms of digestion and absorption of dietary vitamin A. *Annual Review of Nutrition,* 25**,** 87-103.
HAUSSLER, M. R., HAUSSLER, C. A., JURUTKA, P. W., THOMPSON, P. D., HSIEH, J. C., REMUS, L. S., SELZNICK, S. H. & WHITFIELD, G. K. 1997. The vitamin D hormone and its nuclear receptor molecular actions and disease states. *Journal of Endocrinology,* 154**,** 57-73.
HENDESI, H., BARBE, M. F., SAFADI, F. F., MONROY, M. A. & POPOFF, S. N. 2015. Integrin mediated adhesion of osteoblasts to connective tissue growth factor (CTGF/CCN2) induces cytoskeleton reorganization and cell differentiation. *PLoS One,* 10.
HENNING, P., CONAWAY, H. H. & LERNER, U. H. 2015. Retinoid Receptors in Bone and Their Role in Bone Remodeling. *Frontiers in Endocrinology (Lausanne),* 6.
HILDEBRAND, A., ROMARÍS, M., RASMUSSEN, L. M., HEINEGÅRD, D., TWARDZIK, D. R., BORDER, W. A. & RUOSLAHTI, E. 1994. Interaction of the small interstitial proteoglycans biglycan, decorin and fibromodulin with transforming growth factor beta. *Biochemical Journal,* 302**,** 527-34.
HOEBERTZ, A., ARNETT, T. R. & BURNSTOCK, G. 2003. Regulation of bone resorption and formation by purines and pyrimidines. *Trends in Pharmacological Sciences,* 24**,** 290-7.
HOEFEN, R. J. & BERK, B. C. 2006. The multifunctional GIT family of proteins. *Journal of Cell Science,* 119**,** 1469-75.
HOLICK, M. F. 2005. The Vitamin D Epidemic and its Health Consequences. *Journal of Nutrition,* 135**,** 2739–48.
HOLL, J. W., ROHRER, G. A., SHACKELFORD, S. D., WHEELER, T. L. & KOOHMARAIE, M. 2008. Estimates of genetic parameters for kyphosis in two crossbred swine populations. *Journal of Animal Science* 86**,** 1765-9.
HONG, D., CHEN, H. X., YU, H. Q., LIANG, Y., WANG, C., LIAN, Q. Q., DENG, H. T. & GE, R. S. 2010. Morphological and proteomic analysis of early stage of osteoblast differentiation in osteoblastic progenitor cells. *Experimental Cell Research,* 316**,** 2291-3000.
HU, J., LU, J., GOYAL, A., WONG, T., LIAN, G., ZHANG, J., HECHT, J. L., FENG, Y. & SHEEN, V. L. 2017. Opposing FlnA and FlnB interactions regulate RhoA activation in guiding dynamic actin stress fiber formation and cell spreading. *Human Molecular Genetics* 26**,** 1294-1304.
HU, L., LIND, T., SUNDQVIST, A., JACOBSON, A. & MELHUS, H. 2010. Retinoic acid increases proliferation of human osteoclast progenitors and inhibits RANKL-stimulated osteoclast differentiation by suppressing RANK. *PLoS One,* 5.

ITO, Y., TEITELBAUM, S. L., ZOU, W., ZHENG, Y., JOHNSON, J. F., CHAPPEL, J., ROSS, F. P. & ZHAO, H. 2010. Cdc42 regulates bone modeling and remodeling in mice by modulating RANKL/M-CSF signaling and osteoclast polarization. *The Journal of Clinical Investigation,* 120**,** 1981-93.

JACKSON, H. A. & SHEEHAN, A. H. 2005. Effect of vitamin A on fracture risk. *Annals of Pharmacotherapy,* 39**,** 2086-90.

JACOBSON, A., JOHANSSON, S., BRANTING, M. & MELHUS, H. 2004. Vitamin A differentially regulates RANKL and OPG expression in human osteoblasts. *Biochemical and Biophysical Research Communications,* 322**,** 162-7.

JAVANMARD, A. & MONTANARI, A. 2017. Online Rules for Control of False Discovery Rate and False Discovery Exceedance. *Annals of Statistics* 46**,** 526-54.

JENSEN, O. N. 2004. Modification-specific proteomics: characterization of post-translational modifications by mass spectrometry. *Current Opinion in Chemical Biology,* 8**,** 33-41.

JENSEN, T. B., KRISTENSEN, H. H. & TOFT, N. 2012. Quantifying the impact of lameness on welfare and profitability of finisher pigs using expert opinions. *Livestock Science,* 149**,** 209-14.

JIN, W. J., KIM, B., KIM, J. W., KIM, H. H., HA, H. & LEE, Z. H. 2016. Notch2 signaling promotes osteoclast resorption via activation of PYK2. *Cellular Signalling,* 28**,** 357-65.

JOHANSSON, S. & MELHUS, H. 2001. Vitamin A Antagonizes Calcium Response to Vitamin D in man. *Journal of Bone and Mineral Research,* 16**,** 1899-1905.

JOHNSTONE, B., HERING, T. M., CAPLAN, A. I., GOLDBERG, V. M. & YOO, J. U. 1998. In Vitro Chondrogenesis of Bone Marrow-Derived Mesenchymal Progenitor Cells. *Experimental Cell Research,* 238**,** 265-72.

JURUTKA, P. W., BARTIK, L., WHITFIELD, G. K., MATHERN, D. R., BARTHEL, T. K., GUREVICH, M., HSIEH, J. C., KACZMARSKA, M., HAUSSLER, C. A. & HAUSSLER, M. R. 2007. Vitamin D receptor: key roles in bone mineral pathophysiology, molecular mechanism of action, and novel nutritional ligands. *Journal of Bone Mineral Research,* 22 2-10.

JUSTESEN, J., STENDERUP, K., EBBESEN, E. N., MOSEKILDE, L., STEINICHE, T. & KASSEMM. 2001. Adipocyte tissue volume in bone marrow is increased with aging and in patients with osteoporosis. *Biogerontology* 2**,** 165-71.

KALAMAJSKI, S., ASPBERG, A., LINDBLOM, K., HEINEGÅ RD, D. & OLDBERG, Å. K. 2009. Asporin competes with decorin for collagen binding, binds calcium and promotes osteoblast collagen mineralization. *Biochemical Journal* 423**,** 53-9.

KAMIYA, N., SHUXIAN, L., YAMAGUCHI, R., PHIPPS, M., ARUWAJOYE, O., ADAPALA, N. S., YUAN, H., KIM, H. & FENG, J. Q. 2016. Targeted disruption of BMP signaling through type IA receptor (BMPR1A) in osteocyte suppresses SOST and RANKL, leading to dramatic increase in bone mass, bone mineral density and mechanical strength. *Bone,* 91**,** 53-63.

KARSENTY, G., KRONENBERG, H. M. & SETTEMBRE, C. 2009. Genetic control of bone formation. *Annual Review of Cell and Developmental Biology,* 25**,** 629-48.

KEDISHVILI, N. Y. 2013. Enzymology of retinoic acid biosynthesis and degradation. *Journal of Lipid Research,* 54**,** 1744-60.

KELM, R. J., JR. & MANN, K. G. 1991. The collagen binding specificity of bone and platelet osteonectin is related to differences in glycosylation. *Journal of Biological Chemistry,* 266**,** 9632-9.

KENKRE, J. S. & BASSETT, J. 2018. The bone remodelling cycle. *Annals of Clinical Biochemistry,* 55**,** 308-27.

KIM, J., PARK, S., JEONG, D., NAM, J. & KANG, Y. 2012. Osteogenic activity of silymarin through enhancement of alkaline phosphatase and osteocalcin in osteoblasts and tibia-fractured mice. *Experimental Biology and Medicine,* 237**,** 417-28.

KINDBLOM, J. M., GEVERS, E. F., SKRTIC, S. M., LINDBERG, M. K., GOTHE, S., TORNELL, J., VENNSTROM, B. & OHLSSON, C. 2005. Increased adipogenesis in bone marrow but decreased bone mineral density in mice devoid of thyroid hormone receptors. *Bone,* 36**,** 607-16.

KNEISSEL, M., STUDER, A., CORTESI, R. & SUSA, M. 2005. Retinoid-induced bone thinning is caused by subperiosteal osteoclast activity in adult rodents. *Bone,* 36**,** 202-14.
KOHL, M., WIESE, S. & WARSCHEID, B. 2011. Cytoscape: software for visualization and analysis of biological networks. *Methods in Molecular Biology,* 696**,** 291-303.
KOSZEWSKI, N. J., HERBERTH, J. & MALLUCHE, H. H. 2010. Retinoic acid receptor gamma 2 interactions with vitamin D response elements. *Journal of Steroid Biochemistry and Molecular Biology,* 120**,** 200-7.
KOU, I., NAKAJIMA, M. & IKEGAWA, S. 2007. Expression and regulation of the osteoarthritis-associated protein asporin. *Journal of Biological Chemistry,* 282**,** 32193-9.
KOUADJO, K. E., NISHIDA, Y., CADRIN-GIRARD, J. F., YOSHIOKA, M. & ST-AMAND, J. 2007. Housekeeping and tissue-specific genes in mouse tissues. *BMC Genomics,* 8.
KRONENBERG, H. M. 2003. Developmental regulation of the growth plate. *Nature* 423**,** 332-6.
KUMAR, A., CRAWFORD, K., CLOSE, L., MADISON, M., LORENZ, J., DOETSCHMAN, T., PAWLOWSKI, S., DUFFY, J., NEUMANN, J., ROBBINS, J., BOIVIN, G. P., O'TOOLE, B. A. & LESSARD, J. L. 1997. Rescue of cardiac α-actin-deficient mice by enteric smooth muscle γ-actin. *Proceedings of the National Academy of Sciences USA,* 94**,** 4406-11.
LADUNGA, I. 2009. Finding similar nucleotide sequences using network BLAST searches. *Current Protocols in Bioinformatics,* 58**,** 3.3.1-3.3.26.
LANGELIER, E., SUETTERLIN, R., HOEMANN, C. D., AEBI, U. & BUSCHMANN, M. D. 2000. The Chondrocyte Cytoskeleton in Mature Articular Cartilage Structure and Distribution of Actin, Tubulin, and Vimentin Filaments. *The Journal of Histochemistry & Cytochemistry,* 48**,** 1307-20.
LAURIDSEN, C., HALEKOH, U., LARSEN, T. & JENSEN, S. K. 2010. Reproductive performance and bone status markers of gilts and lactating sows supplemented with two different forms of vitamin D. *Journal of Animal Science,* 88**,** 202-13.
LEE, S. Y., SOLOW-CORDERO, D. E., KESSLER, E., AKAHARA, K. & GREENSPAN, D. S. 1997. Transforming Growth Factor-β Regulation of Bone Morphogenetic Protein-1Procollagen C-proteinase and Related Proteins in Fibrogenic Cells and Keratinocytes. *The Journal of Biological Chemistry,* 272**,** 19059-66.
LEUNG, R., WANG, Y., CUDDY, K., SUN, C., MAGALHAES, J., GRYNPAS, M. & GLOGAUER, M. 2010. Filamin A regulates monocyte migration through Rho small GTPases during osteoclastogenesis. *Journal of Bone Mineral Research,* 25**,** 1077-91.
LEVIN, A. A., STURZENBECKER, L. J., KAZMER, S., BOSAKOWSKI, T., HUSELTON, C., ALLENBY, G., SPECK, J., KRATZEISEN, C., ROSENBERGER, M., LOVEY, A. & ET AL. 1992. 9-cis retinoic acid stereoisomer binds and activates the nuclear receptor RXR alpha. *Nature,* 355**,** 359-61.
LI, B., LING CHAU, J. F., WANG, X. & LEONG, W. F. 2011. Bisphosphonates, specific inhibitors of osteoclast function and a class of drugs for osteoporosis therapy. *Journal of Cellular Biochemistry,* 112**,** 1229-42.
LI, X., JIE, Q., ZHANG, H., ZHAO, Y., LIN, Y., DU, J., SHI, J., WANG, L., GUO, K., LI, Y., WANG, C., GAO, B., HUANG, Q., LIU, J., YANG, L. & LUO, Z. 2016. Disturbed MEK/ERK signaling increases osteoclast activity via the Hedgehog-Gli pathway in postmenopausal osteoporosis. *Progress in Biophysics & Molecular Biology* 122**,** 101-11.
LI, Y., LI, A., STRAIT, K., ZHANG, H., NANES, M. S. & WEITZMANN, M. N. 2007. Endogenous TNFalpha lowers maximum peak bone mass and inhibits osteoblastic Smad activation through NF-kappaB. *Journal of Bone and Mineral Research,* 22**,** 646-55.
LI, Z., SHEN, J., WU, W. K., WANG, X., LIANG, J., QIU, G. & LIU, J. 2012. Vitamin A deficiency induces congenital spinal deformities in rats. *PLoS One,* 7.
LIAN, G., KANAUJIA, S., WONG, T. & SHEEN, V. 2017. FilaminA and Formin2 regulate skeletal, muscular, and intestinal formation through mesenchymal progenitor proliferation. *PLoS One,* 12.

LIBAL, G. W., PEO, J. E. R., ANDREWS, R. P. & VIPPERMAN, J. P. E. 1969. Levels of Calcium and Phosphorus for Growing-Finishing Swine. *Journal of Animal Science,* 28**,** 331-5.

LIEBEN, L., MASUYAMA, R., TORREKENS, S., VAN LOOVEREN, R., SCHROOTEN, J., BAATSEN, P., LAFAGE-PROUST, M. H., DRESSELAERS, T., FENG, J. Q., BONEWALD, L. F., MEYER, M. B., PIKE, J. W., BOUILLON, R. & CARMELIET, G. 2012. Normocalcemia is maintained in mice under conditions of calcium malabsorption by vitamin D-induced inhibition of bone mineralization. *Journal of Clinical Investigation,* 122**,** 1803-15.

LIESEGANG, A., URSPRUNG, R., GASSER, J., SASSI, M. L., RISTELI, J., RIOND, J. L. & WANNER, M. 2002. Influence of dietary phosphorus deficiency with or without addition of fumaric acid to a diet in pigs on bone parameters. *Journal of Animal Physiology and Animal Nutrition (Berlin),* 86**,** 1-16.

LIM, J., TU, X., CHOI, K., AKIYAMA, H., MISHINA, Y. & LONG, F. 2015. BMP-Smad4 signaling is required for precartilaginous mesenchymal condensation independent of Sox9 in the mouse *Developmental Biology,* 400**,** 132-8.

LIND, T., HU L, LIND PM, SUGARS R, ANDERSSON G, JACOBSON A & H., M. 2012. Microarray Profiling of Diaphyseal Bone of Rats Suffering from Hypervitaminosis A. *Calcified Tissue International,* 90**,** 219-29.

LIND, T., LIND, P. M., JACOBSON, A., HU, L., SUNDQVIST, A., RISTELI, J., YEBRA-RODRIGUEZ, A., LARSSON, S., RODRIGUEZ-NAVARRO, A., ANDERSSON, G. & MELHUS, H. 2011. High dietary intake of retinol leads to bone marrow hypoxia and diaphyseal endosteal mineralization in rats. *Bone,* 48**,** 496-506.

LIND, T., OHMAN, C., CALOUNOVA, G., RASMUSSON, A., ANDERSSON, G., PEJLER, G. & MELHUS, H. 2017. Excessive dietary intake of vitamin A reduces skull bone thickness in mice. *PLoS One,* 12.

LINDHOLM-PERRY, A. K., ROHRER, G. A., KUEHN, L. A., KEELE, J. W., HOLL, J. W., SHACKELFORD, S. D., WHEELER, T. L. & NONNEMAN, D. J. 2010. Genomic regions associated with kyphosis in swine. *BMC Genetics,* 11.

LIU, Z., CHANG, A. N., GRINNELL, F., TRYBUS, K. M., MILEWICZ, D. M., STULL, J. T. & KAMM, K. E. 2017. Vascular disease-causing mutation, smooth muscle alpha-actin R258C, dominantly suppresses functions of alpha-actin in human patient fibroblasts. *Proceedings of the National Academy of Sciences USA,* 114**,** 5569-78.

LIZARDO, R., TORRALLARDONA, D. & BRUFAU, J. 2004. Zinc oxide in phytase-low phosphorus diets impairs performance of weanling pigs. *55nd annual meeting of EAAP* Bled, Slovenia EAAP

LOMRI, A. & MARIE, P. J. 1996. The Cytoskeleton in the Biology of Bone Cells. *The Cytoskeleton,* 3**,** 229-63.

LOOK, J., LANDWEHR, J., BAUER, F., HOFFMANN, A. S., BLUETHMANN, H. & LEMOTTE, P. 1995. Marked resistance of RAR gamma-deficient mice to the toxic effects of retinoic acid. *American Journal of Physiology,* 269**,** 91-8.

LOTY, S., FOREST, N., BOULEKBACHE, H. & SAUTIERA, J. M. 1995. Cytochalasin D induces changes in cell shape and promotes in vitro chondrogenesis A morphological study *Biology of the Cell,* 83**,** 149-61.

MACFARLANE, E. G., HAUPT, J., DIETZ, H. C. & SHORE, E. M. 2017. TGF-beta Family Signaling in Connective Tissue and Skeletal Diseases. *Cold Spring Harbor Perspectives in Biology,* 9.

MADSON, D. M., ENSLEY, S. M., GAUGER, P. C., SCHWARTZ, K. J., STEVENSON, G. W., COOPER, V. L., JANKE, B. H., BURROUGH, E. R., GOFF, J. P. & HORST, R. L. 2012. Rickets: case series and diagnostic review of hypovitaminosis D in swine. *The Journal of Veterinary Diagnostic Investigation* 24**,** 1137-44.

MAES, C., KOBAYASHI, T., SELIG, M. K., TORREKENS, S., ROTH, S. I., MACKEM, S., CARMELIET, G. & KRONENBERG, H. M. 2010. Osteoblast precursors, but not mature osteoblasts, move into developing and fractured bones along with invading blood vessels. *Developmental Cell,* 19**,** 329-44.

MAHAJAN, A., ALEXANDER, L. S., SEABOLT, B. S., CATRAMBONE, D. E., MCCLUNG, J. P., ODLE, J., PFEILER, T. W., LOBOA, E. G. & STAHL, C. H. 2011. Dietary Calcium Restriction Affects Mesenchymal Stem Cell Activity and Bone Development in Neonatal Pigs. *The Journal of Nutrition,* 141**,** 373-9.

MAJCHRZAK, D., FABIAN, E. & ELMADFA, I. 2006. Vitamin A content (retinol and retinyl esters) in livers of different animals. *Food Chemistry,* 98**,** 704-10.

MANOLAGAS, S. C. 2000. Birth and Death of Bone Cells Basic Regulatory Mechanisms and Implications for the Pathogenesis and Treatment of Osteoporosis. *Endocrine Reviews,* 21**,** 115-37.

MARILL, J., IDRES, N., CAPRON, C. C., NGUYEN, E. & CHABOT, G. G. 2003. Retinoic Acid Metabolism and Mechanism of Action A Review. *Current Drug Metabolism,* 4**,** 1-10.

MEDEIROS, D. M. 2016. Copper, iron, and selenium dietary deficiencies negatively impact skeletal integrity: A review. *Experimental Biology and Medicine (Maywood),* 241**,** 1316-22.

MELROSE, J., GHOSH, P. & TAYLOR, T. K. F. 2001. A comparative analysis of the differential spatial and temporal distributions of the large (aggrecan, versican) and small (decorin, biglycan, fibromodulin) proteoglycans of the intervertebral disc. *Journal of Anatomy,* 198**,** 3-15.

MELROSE, J., GHOSH, P., TAYLOR, T. K. F., VERNON-ROBERTS, B., LATHAM, J. & MOORE, R. 1997. Elevated synthesis of biglycan and decorin in an ovine annular lesion model of experimental disc degeneration. *European Spine Journal,* 6**,** 376-84.

METZ, A. L., WALSER, M. M. & OLSON, W. G. 1985. The Interaction of Dietary Vitamin A and Vitamin D Related to Skeletal Development in the Turkey Poult. *Journal of Nutrition,* 115**,** 929-35.

MLECNIK, B., BINDEA, G. & GALON, J. 2013 ClueGo

MONROE, D. G., HAWSE, J. R., SUBRAMANIAM, M. & SPELSBERG, T. C. 2010. Retinoblastoma binding protein-1 (RBP1) is a Runx2 coactivator and promotes osteoblastic differentiation. *BMC Musculoskeletal Disorders,* 11.

MORI, M., NAKAJIMA, M., MIKAMI, Y., SEKI, S., TAKIGAWA, M., KUBO, T. & IKEGAWA, S. 2006. Transcriptional regulation of the cartilage intermediate layer protein (CILP) gene. *Biochemical and Biophysical Research Communications,* 341**,** 121-7.

MOUSSA, F. M., HISIJARA, I. A., SONDAG, G. R., SCOTT, E. M., FRARA, N., ABDELMAGID, S. M. & SAFADI, F. F. 2014. Osteoactivin promotes osteoblast adhesion through HSPG and alphavbeta1 integrin. *Journal of Cellular Biochemistry,* 115**,** 1243-53.

MÜLLER-GERBL, M., WEIßER, S. & LINSENMEIER, U. 2008. The distribution of mineral density in the cervical vertebral endplates. *European Spine Journal,* 17**,** 432-8.

MUNSHI, H. G., WU, Y. I., MUKHOPADHYAY, S., OTTAVIANO, A. J., SASSANO, A., KOBLINSKI, J. E., PLATANIAS, L. C. & STACK, M. S. 2004. Differential regulation of membrane type 1-matrix metalloproteinase activity by ERK 1/2- and p38 MAPK-modulated tissue inhibitor of metalloproteinases 2 expression controls transforming growth factor-beta1-induced pericellular collagenolysis. *Journal of Biological Chemistry,* 279**,** 39042-50.

MUSZYŃSKI, S., TOMASZEWSKA, E., KWIECIEŃ, M., DOBROWOLSKI, P. & TOMCZYK, A. 2018. Effect of Dietary Phytase Supplementation on Bone and Hyaline Cartilage Development of Broilers Fed with Organically Complexed Copper in a Cu-Deficient Diet. *Biological Trace Element Research,* 182**,** 339-53.

NAKAJIMA, H., KIZAKI, M., SONODA, A., MORI, S., HARIGAYA, K. & IKEDA, Y. 1994. Retinoids (all-trans and 9-cis retinoic acid) stimulate production of macrophage colony-stimulating factor and granulocyte-macrophage colony-stimulating factor by human bone marrow stromal cells. *Blood,* 84**,** 4107-15.

NAKAJIMA, M., KIZAWA, H., SAITOH, M., KOU, I., MIYAZONO, K. & IKEGAWA, S. 2007. Mechanisms for asporin function and regulation in articular cartilage. *Journal of Biological Chemistry,* 282**,** 32185-92.

NATIONAL RESEARCH COUNCIL, N. 2012. *Nutrient Requirements of Swine* National Academies Press.

NAVARRO-VALVERDE, C., CABALLERO-VILLARRASO, J., MATA-GRANADOS, J. M., CASADO-DIAZ, A., SOSA-HENRIQUEZ, M., MALOUF-SIERRA, J., NOGUES-SOLAN, X., RODRIGUEZ-MANAS, L., CORTES-GIL, X., DELGADILLO-DUARTE, J. & QUESADA-GOMEZ, J. M. 2018. High Serum Retinol as a Relevant Contributor to Low Bone Mineral Density in Postmenopausal Osteoporotic Women. *Calcified Tissue International,* 102**,** 651-56.

NG, K. W., MANJI, S. S., YOUNG, M. F. & FINDLAY, D. M. 1989. Opposing Influences of Glucocorticoid and Retinoic Acid on Transcriptional Control in Preosteoblasts. *Molecular Endocrinology,* 3**,** 20179-85.

NICODEMO, M. L., SCOTT, D., BUCHAN, W., DUNCAN, A. & ROBINS, S. P. 1998. Effects of variations in dietary calcium and phosphorus supply on plasma and bone osteocalcin concentrations and bone mineralisation in growing pigs. *Experimental Physiology,* 83**,** 659-65.

NIELSEN, L. W. D., HØGEDAL, P., ARNBJERG, J. & JENSEN, H. E. 2005. Juvenile kyphosis in pigs. A spontaneous model of Scheuermann's kyphosis. *APMIS : acta pathologica, microbiologica, et immunologica Scandinavica,* 113**,** 702-7.

NIKITOVIC, D., AGGELIDAKIS, J., YOUNG, M. F., IOZZO, R. V., KARAMANOS, N. K. & TZANAKAKIS, G. N. 2012. The biology of small leucine-rich proteoglycans in bone pathophysiology. *Journal of Biological Chemistry,* 287**,** 33926-33.

NOBES, C. D. & HALL, A. 1995. Rho, Rac, and Cdc42 GTPases Regulate the Assembly of Multimolecular Focal Complexes Associated with Actin Stress Fibers, Lamellipodia, and Filopodia. *Cell,* 81**,** 53-62.

OH, S. H., KIM, J. W., KIM, Y., LEE, M. N., KOOK, M. S., CHOI, E. Y., IM, S. Y. & KOH, J. T. 2017. The extracellular matrix protein Edil3 stimulates osteoblast differentiation through the integrin alpha5beta1/ERK/Runx2 pathway. *PLoS One,* 12.

OLSEN, J. J., POHL, S. O., DESHMUKH, A., VISWESWARAN, M., WARD, N. C., ARFUSO, F., AGOSTINO, M. & DHARMARAJAN, A. 2017. The Role of Wnt Signalling in Angiogenesis. *Clinical Biochemist Reviews,* 38**,** 131-42.

ORNSRUD, R., LOCK, E. J., GLOVER, C. N. & FLIK, G. 2009. Retinoic acid cross-talk with calcitriol activity in Atlantic salmon (Salmo salar). *Journal of Endocrinology,* 202**,** 473-82.

PALLARÉS, F. J., GÓMEZ, S., PÉREZ, M. C., STRICKLAND, T., GARCÍA-NICOLÁS, O., SEVA, J. I. & SALGUERO, F. J. 2013. Humpy backed pigs syndrome in Spain *Anales de Veterinaria de Murcia,* 29**,** 87-91.

PARK, C. K., ISHIMI, Y., OHMURA, M., YAMAGUCHI, M. & IKEGAMI, S. 1997. Vitamin A and Carotenoids Stimulate Differentiation of mouse osteoblastic cells *Journal of Nutritional Science and Vitaminology (Tokyo),* 43**,** 281-96.

PENNY, R. H. C. & WALTERS, J. R. 1986. A humpy backed syndrome of pigs *The Veterinary Annual* 128-35.

POULSEN, H. D., BLAABJERG, K. & SØRENSEN, K. U. 2016. High dietary zinc supply reduces the digestibility of phosphorus in pig diets. *Journal of Animal Science,* 94**,** 332-4.

PREMONT, R. T., CLAING, A., VITALE, N., FREEMAN, J. L. R., PITCHER, J. A., PATTON, W. A., MOSS, J., VAUGHAN, M. & LEFKOWIT, R. J. 1998. β2-Adrenergic receptor regulation by GIT1, a G protein-coupled receptor kinase-associated ADP ribosylation factor GTPase-activating protein. *Proceedings of the National Academy of Sciences USA,* 95**,** 14082-87.

PREMONT, R. T., CLAING, A., VITALE§, N., PERRY, S. J. & LEFKOWITZ, R. J. 2000. The GIT Family of ADP-ribosylation Factor GTPase-activating Proteins *Journal of Biological Chemistry,* 275**,** 22373-80.

PROMISLOW, J. H., GOODMAN-GRUEN, D., SLYMEN, D. J. & BARRETT-CONNOR, E. 2002. Retinol Intake and Bone Mineral Density in the Elderly: the Rancho Bernardo Study. *Journal of Bone and Mineral Research,* 17**,** 1349-58.

PRYOR, W. J., SEAWRIGHT, A. A. & MCCOSKER, P. J. 1969. Hypervitaminosis A in the pig. *Australian Veterinary Journal,* 45**,** 563-9.

QIAN, Q., SHI, X., LEI, Z., ZHAN, L., LIU, R. Y., ZHAO, J., YANG, B., LIU, Z. & ZHANG, H. T. 2014. Methylated +58CpG site decreases DCN mRNA expression and enhances TGF-beta/Smad signaling in NSCLC cells with high metastatic potential. *International Journal of Oncology* 44**,** 874-82.

QU, X., HE, Z., QIAO, H., ZHAI, Z., MAO, Z., YU, Z. & DAI, K. 2018. Serum copper levels are associated with bone mineral density and total fracture. *Journal of Orthopaedic Translatation,* 14**,** 34-44.

RANE, C. K. & MINDEN, A. 2014. P21 activated kinases: structure, regulation, and functions. *Small GTPases,* 5.

REBOUL, E. 2015. Intestinal absorption of vitamin D: from the meal to the enterocyte. *Food and Function,* 6**,** 356-62.

RODAN, G. A. & MARTIN, T. J. 2000. Therapeutic Approaches to Bone Diseases. *Science,* 289**,** 1508-14.

ROHDE, C. M. & DELUCA, H. F. 2005. All-trans Retinoic Acid Antagonizes the Action of Calciferol and Its Active Metabolite, 1,25-Dihydroxycholecalciferol, in Rats *Journal of Nutrition,* 135**,** 1647–52.

RORTVEDT, L. A. & CRENSHAW, T. D. 2012. Expression of kyphosis in young pigs is induced by a reduction of supplemental vitamin D in maternal diets and vitamin D, Ca, and P concentrations in nursery diets. *Journal of Animal Science,* 90**,** 4905-15.

ROSS, F. P. 2006. M-CSF, c-Fms, and signaling in osteoclasts and their precursors. *Annals of the New York Academy of Sciences,* 1068**,** 110-6.

ROSS, S. A., MCCAFFERY, P. J., DRAGER, U. C. & DE LUCA, L. M. 2000. Retinoids in embryonal development. *Physiological Reviews,* 80**,** 1021-54.

ROSSET, E. M. & BRADSHAW, A. D. 2016. SPARC/osteonectin in mineralized tissue. *Matrix Biology,* 52-54**,** 78-87.

RUIZ-GASPA, S., BLANCH-RUBIO, J., CIRIA-RECASENS, M., MONFORT, J., TIO, L., GARCIA-GIRALT, N., NOGUES, X., MONLLAU, J. C., CARBONELL-ABELLO, J. & PEREZ-EDO, L. 2010. Reduced proliferation and osteocalcin expression in osteoblasts of male idiopathic osteoporosis. *Calcified Tissue International,* 86**,** 220-6.

SALINAS, C. N. & ANSETH, K. S. 2009. Decorin moieties tethered into PEG networks induce chondrogenesis of human mesenchymal stem cells. *Journal of Biomedical Materials Research Part A,* 90**,** 456-64.

SCHRADER, M., BENDIK, I., BECKER-ANDRE, M. & CARLBERG, C. 1993. Interaction between retinoic acid and vitamin D signaling pathways. *Journal of Biological Chemistry,* 268**,** 17830-6.

SCOTTER, M. J., THORPE, S. A., REYNOLDS, S. L., WILSON, L. A. & LEWIS, D. J. 1992. Survey of animal livers for vitamin A content. *Food Additives and Contaminants* 9**,** 237-42.

SEDMAN, A. B., ALFREY, A. C., MILLER, N. L. & GOODMAN, W. G. 1987. Tissue and Cellular Basis for Impaired Bone Formation in Aluminum-related Osteomalacia in the Pig. *Journal of Clinical Investigation,* 79**,** 86-92.

SHUI, C., SPELSBERG, T. C., RIGGS, B. L. & KHOSLA, S. 2003. Changes in Runx2/Cbfa1 expression and activity during osteoblastic differentiation of human bone marrow stromal cells. *Journal of Bone Mineral Research,* 18**,** 213-21.

SILVA, M. C. & FURLANETTO, T. W. 2018. Intestinal absorption of vitamin D: a systematic review. *Nutrition Reviews,* 76**,** 60-76.

SIMONS, P. C. M., VERSTEEGH, H. A. J., JONGBLOED, A. W., KEMME, P. A., SLUMP, P., BOS, K. D., WOLTERS, M. G. E., BEUDEKER, R. F. & VERSCHOOR, G. J. 1990. Improvement of phosphorus availability by microbial phytase in broilers and pigs. *British Journal of Nutrition,* 64**,** 525-40.

SKILLINGTON, J., CHOY, L. & DERYNCK, R. 2002. Bone morphogenetic protein and retinoic acid signaling cooperate to induce osteoblast differentiation of preadipocytes. *Journal of Cell Biology,* 159**,** 135-46.

SOETA, S., MORI, R., KODAKA, T., NAITO, Y. & TANIGUCHI, K. 2000. Histological disorders related to the focal disappearance of the epiphyseal growth plate in rats induced by high dose of vitamin A. *The Journal of Veterinary Medical Science,* 62**,** 293-9.

STOLTZFUS, R. J. & UNDERWOOD, B. A. 1995. Breast-milk vitamin A as an indicator of the vitamin A status of women and infants. *Bulletin of the World Health Organization,* 73**,** 703-11.

STRAW, B., BATES, R. & MAY, G. 2009. Anatomical abnormalities in a group of finishing pigs: prevalence and pig performance. *Journal of Swine and Health production,* 17**,** 28-31.

TAKEUCHI, Y., KODAMA, Y. & MATSUMOTO, T. 1994. Bone Matrix Decorin Binds Transforming Growth Factor and Enhances Its Bioactivity. *The Journal of Biological Chemistry,* 269**,** 32634-638.

TEITELBAUM, S. L. 2011. The osteoclast and its unique cytoskeleton. *Annals of New York Academy of Sciences,* 1240**,** 14-7.

THEPIGSITE. 2014. *Garth Pig Stockmanship Standards* [Online]. Available: http://www.thepigsite.com/stockstds/18/daily-feed-intake/ [Accessed].

THIBODEAU, G. A. & PATTON, K. T. 2010. *The human body in health and disease* Elsevier

THOMAS, C. J., CLELAND, T. P., ZHANG, S., GUNDBERG, C. M. & VASHISHTH, D. 2017. Identification and characterization of glycation adducts on osteocalcin. *Analytical Biochemistry,* 525**,** 46-53.

TOMOEDA, M., YAMADA, S., SHIRAI, H., OZAWA, Y., YANAGITA, M. & MURAKAMI, S. 2008. PLAP-1/asporin inhibits activation of BMP receptor via its leucine-rich repeat motif. *Biochemical and Biophysical Research Communications,* 371**,** 191-6.

TOURKOVA, I. L., LIU, L., SUTJARIT, N., LARROUTURE, Q. C., LUO, J., ROBINSON, L. J. & BLAIR, H. C. 2017. Adrenocorticotropic hormone and 1,25-dihydroxyvitamin D3 enhance human osteogenesis in vitro by synergistically accelerating the expression of bone-specific genes. *Laboratory Investigation,* 97**,** 1072-83.

TOUSIGNANT, S. J. P., HENRY, S. C., ROVIRA, A. & MORRISON, R. B. 2013. Effect of oral vitamin D3 supplementation on growth and serum 25-hydroxy vitamin D levels of pigs up to 7 weeks of age *Journal of Swine Health and Production,* 21**,** 94-8.

TRAN, T. M., AGHILI, A., LI, S., ONGOIBA, A., KAYENTAO, K., DOUMBO, S., TRAORE, B. & CROMPTON, P. D. 2014. A nested real-time PCR assay for the quantification of Plasmodium falciparum DNA extracted from dried blood spots. *Malaria Journal,* 13.

TRUMBO, P., A., Y. A., SCHLICKER, S. & POOS, M. 2001. Dietary reference intakes Vitamin A, vitamin K, arsenic, boron, chromium, copper, iodine, iron, manganese, molybdenum, nickel, silicon, vanadium, and zinc. *Journal of the American Dietetic Assocation* 101**,** 294-301.

TSAO, Y. T., HUANG, Y. J., WU, H. H., LIU, Y. A., LIU, Y. S. & LEE, O. K. 2017. Osteocalcin Mediates Biomineralization during Osteogenic Maturation in Human Mesenchymal Stromal Cells. *International Journal of Molecular Sciences,* 18.

TSENG, K. Y., CHEN, Y. H. & LIN, S. 2017. Zinc finger protein ZFP36L1 promotes osteoblastic differentiation but represses adipogenic differentiation of mouse multipotent cells. *Oncotarget,* 8**,** 20588-601.

UNTERGASSER, A., CUTCUTACHE, I., KORESSAAR, T., YE, J., FAIRCLOTH, B. C., REMM, M. & ROZEN, S. G. 2012. Primer3—new capabilities and interfaces. *Nucleic Acids Res,* 40**,** e115.

VAN GASTEL, J., BODDAERT, J., JUSHAJ, A., PREMONT, R. T., LUTTRELL, L. M., JANSSENS, J., MARTIN, B. & MAUDSLEY, S. 2018. GIT2-A keystone in ageing and age-related disease. *Ageing Research Reviews,* 43**,** 46-63.

VAN RIET, M. M. J., MILLET, S., ALUWÉ, M. & JANSSENS, G. P. J. 2013. Impact of nutrition on lameness and claw health in sows. *Livestock Science,* 156**,** 24-35.

WAN, M. & CAO, X. 2005. BMP signaling in skeletal development. *Biochemical and Biophysical Research Communications,* 328**,** 651-7.

WANG, X., LIAO, S., NELSON, E. R., SCHMALZIGAUG, R., SPURNEY, R. F., GUILAK, F., PREMONT, R. T. & GESTY-PALMER, D. 2012. The cytoskeletal regulatory scaffold protein GIT2 modulates

mesenchymal stem cell differentiation and osteoblastogenesis. *Biochemical and Biophysical Research Communications,* 425**,** 407-12.
WANG, Z., GERSTEIN, M. & SNYDER, M. 2009. RNA-Seq: a revolutionary tool for transcriptomics. *Nature Reviews Genetics,* 10**,** 57-63.
WANGPING, D., LEI, W., XIAOMING, C., HENG, G., LEI, W., YONGZHUANG, H. & XIAOCHUN, W. 2014. Effect of the disruption of three cytoskeleton components on chondrocyte metabolism in rabbit knee cartilage. *Chinese Medical Journal* 127**,** 3764-70.
WEIS, S. M., LIM, S. T., LUTU-FUGA, K. M., BARNES, L. A., CHEN, X. L., GOTHERT, J. R., SHEN, T. L., GUAN, J. L., SCHLAEPFER, D. D. & CHERESH, D. A. 2008. Compensatory role for Pyk2 during angiogenesis in adult mice lacking endothelial cell FAK. *Journal of Cell Biology,* 181**,** 43-50.
WESTENDORF, J. J., KAHLER, R. A. & SCHROEDER, T. M. 2004. Wnt signaling in osteoblasts and bone diseases. *Gene,* 341**,** 19-39.
WHITTEMORE, C. T. & KYRIAZAKIS, I. 2006. *Whittemore's Science and Practice of Pig Production* Blackwell Publishing Ltd.
WITSCHI, A. K. M., LIESEGANG, A., GEBERT, S., WEBER, G. M. & WENK, C. 2011. Effect of source and quantity of dietary vitamin D in maternal and creep diets on bone metabolism and growth in piglets. *Journal of Animal Science,* 89**,** 1844-52.
WOLKE, R. E., NIELSEN, S. W. & ROUSSEAU, J. E. 1968. Bone lesions of hypervitaminosis A in the pig. *American Journal of Veterinary Research,* 29**,** 1009-24.
WOODS, A., WANG, G. & BEIER, F. 2007. Regulation of chondrocyte differentiation by the actin cytoskeleton and adhesive interactions. *Journal of Cellular Physiology,* 213**,** 1-8.
WRAY, A. E., OKITA, N. & ROSS, A. C. 2011. Cortical and Trabecular Bone, Bone Mineral Density, and Resistance to ex Vivo Fracture Are Not Altered in Response to Life-Long Vitamin A Supplementation in Aging Rats. *Journal of Nutrition* 141**,** 660-6.
WU, A. M., HUANG, C. Q., LIN, Z. K., TIAN, N. F., NI, W. F., WANG, X. Y., XU, H. Z. & CHI, Y. L. 2014. The relationship between vitamin A and risk of fracture: meta-analysis of prospective studies. *Journal of Bone Mineral Research,* 29**,** 2032-9.
WU, B., XU, B., HUANG, T. & WANG, J. 1996. A model of osteoporosis induced by retinoic acid in male Wistar rats. *Yao Xue Xue Bao.,* 31**,** 241-5.
XIAO, F., QIU, H., CUI, H., NI, X., LI, J., LIAO, W., LU, L. & DING, K. 2015. MicroRNA-885-3p inhibits the growth of HT-29 colon cancer cell xenografts by disrupting angiogenesis via targeting BMPR1A and blocking BMP/Smad/Id1 signaling. *Oncogene,* 34**,** 1968-78.
XIAO, G., JIANG, D., THOMAS, P., BENSON, M. D., GUAN, K., KARSENTY, G. & FRANCESCHI, R. T. 2000. MAPK pathways activate and phosphorylate the osteoblast-specific transcription factor, Cbfa1. *Journal of Biological Chemistry,* 275**,** 4453-9.
XU, G., BOCHATON-PIALLAT, M. L., ANDREUTTI, D., LOW, R. B., GABBIANI, G. & NEUVILLE, P. 2001. Regulation of alpha-smooth muscle actin and CRBP-1 expression by retinoic acid and TGF-beta in cultured fibroblasts. *Journal of Cellular Physiology,* 187**,** 315-25.
YANG, L., TSANG, K. Y., TANG, H. C., CHAN, D. & CHEAH, K. S. 2014. Hypertrophic chondrocytes can become osteoblasts and osteocytes in endochondral bone formation. *Proceedings of the National Academy of Sciences of the United States of America,* 111**,** 12097-102.
YAO, T., ZHANG, C. G., GONG, M. T., ZHANG, M., WANG, L. & DING, W. 2016. Decorin-mediated inhibition of the migration of U87MG glioma cells involves activation of autophagy and suppression of TGF-beta signaling. *FEBS Open Bio,* 6**,** 707-19.
YING, J., WANG, P., ZHANG, S., XU, T., ZHANG, L., DONG, R., XU, S., TONG, P., WU, C. & JIN, H. 2018. Transforming growth factor-beta1 promotes articular cartilage repair through canonical Smad and Hippo pathways in bone mesenchymal stem cells. *Life Science,* 192**,** 84-90.
ZHANG, Y., WRAY, A. E. & ROSS, A. C. 2012. Perinatal exposure to vitamin A differentially regulates chondrocyte growth and the expression of aggrecan and matrix metalloprotein genes in the femur of neonatal rats. *Journal of Nutrition,* 142**,** 649-54.

ZHANG, Z., MESSANA, J., HWANG, N. S. & ELISSEEFF, J. H. 2006. Reorganization of actin filaments enhances chondrogenic differentiation of cells derived from murine embryonic stem cells. *Biochemical and Biophysical Research Communications,* 348**,** 421-7.

ZHAO, X. L., CHEN, J. J., ZHANG, G. N., WANG, Y. C., SI, S. Y., CHEN, L. F. & WANG, Z. 2017. Small molecule T63 suppresses osteoporosis by modulating osteoblast differentiation via BMP and WNT signaling pathways. *Scientific Reports,* 7.

ZIEROLD, C. & DELUCA, H. F. 1998. Additional Protein Factors Play a Role in the Formation of VDR/RXR Complexes on Vitamin D Response Elements. *Journal of Cellular Biochemistry,* 71**,** 512-53.

ZOUANI, O. F., RAMI, L., LEI, Y. & DURRIEU, M. C. 2013. Insights into the osteoblast precursor differentiation towards mature osteoblasts induced by continuous BMP-2 signaling. *Biology Open,* 2**,** 872-81.

Appendix

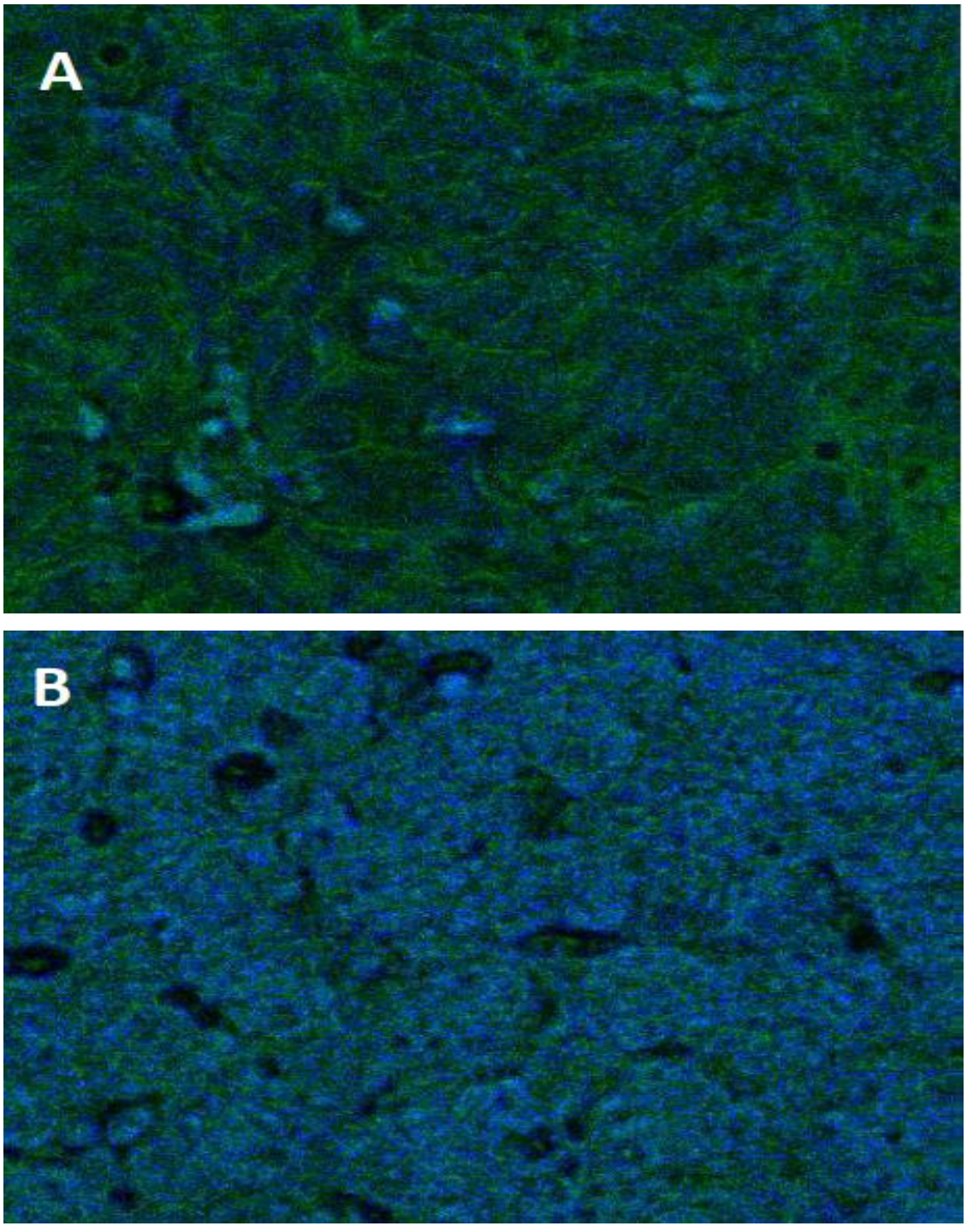

Appendix A: *Confocal microscopy images of retinyl esters (REs), stained blue, in stellate cells in livers from* ***A.*** *Controls and* ***B****. pigs receiving 3000µg RP/kg BW: blue staining, and therefore RE abundance, is clearly more concentrated in the treated group.*

0305166888190c701V7.0

ALP2

cobas®

Alkaline Phosphatase acc. to IFCC Gen.2

Order information

REF	CONTENT		Analyzer(s) on which **cobas c** pack(s) can be used
05166888 190	Alkaline Phosphatase acc. to IFCC Gen.2 (1050 tests)	System-ID 05 6760 3	Roche/Hitachi **cobas c** 701/702
10759350 190	Calibrator f.a.s. (12 x 3 mL)	Code 401	
10759350 360	Calibrator f.a.s. (12 x 3 mL, for USA)	Code 401	
12149435 122	Precinorm U plus (10 x 3 mL)	Code 300	
12149435 160	Precinorm U plus (10 x 3 mL, for USA)	Code 300	
12149443 122	Precipath U plus (10 x 3 mL)	Code 301	
12149443 160	Precipath U plus (10 x 3 mL, for USA)	Code 301	
10171743 122	Precinorm U (20 x 5 mL)	Code 300	
10171735 122	Precinorm U (4 x 5 mL)	Code 300	
10171778 122	Precipath U (20 x 5 mL)	Code 301	
10171760 122	Precipath U (4 x 5 mL)	Code 301	
05117003 190	PreciControl ClinChem Multi 1 (20 x 5 mL)	Code 391	
05947626 190	PreciControl ClinChem Multi 1 (4 x 5 mL)	Code 391	
05947626 160	PreciControl ClinChem Multi 1 (4 x 5 mL, for USA)	Code 391	
05117216 190	PreciControl ClinChem Multi 2 (20 x 5 mL)	Code 392	
05947774 190	PreciControl ClinChem Multi 2 (4 x 5 mL)	Code 392	
05947774 160	PreciControl ClinChem Multi 2 (4 x 5 mL, for USA)	Code 392	
05172152 190	Diluent NaCl 9 % (119 mL)	System-ID 08 6869 3	

English

System information

ALP2L: ACN 8683

Intended use

In vitro test for the quantitative determination of alkaline phosphatase in human serum and plasma on Roche/Hitachi **cobas c** systems.

Summary[1,2,3,4,5,6]

Alkaline phosphatase in serum consists of four structural genotypes: the liver-bone-kidney type, the intestinal type, the placental type and the variant from the germ cells. It occurs in osteoblasts, hepatocytes, leukocytes, the kidneys, spleen, placenta, prostate and the small intestine. The liver-bone-kidney type is particularly important.

A rise in the alkaline phosphatase occurs with all forms of cholestasis, particularly with obstructive jaundice. It is also elevated in diseases of the skeletal system, such as Paget's disease, hyperparathyroidism, rickets and osteomalacia, as well as with fractures and malignant tumors. A considerable rise in the alkaline phosphatase activity is sometimes seen in children and juveniles. It is caused by increased osteoblast activity following accelerated bone growth.

The assay method was first described by King and Armstrong, modified by Ohmori, Bessey, Lowry and Brock and later improved by Hausamen et al. In 2011 the International Federation of Clinical Chemistry and Laboratory Medicine (IFCC) Scientific Division, Committee on Reference Systems of Enzymes (C-RSE) recommended a reference procedure for the determination of alkaline phosphatase using an optimized substrate concentration and 2-amino-2-methyl-1-propanol as buffer plus the cations magnesium and zinc at 37 °C. This assay follows the recommendations of the IFCC, but was optimized for performance and stability.

Test principle[5]

Colorimetric assay in accordance with a standardized method.

In the presence of magnesium and zinc ions, p-nitrophenyl phosphate is cleaved by phosphatases into phosphate and p-nitrophenol.

$$\text{p-nitrophenyl phosphate} + H_2O \xrightarrow{ALP} \text{phosphate} + \text{p-nitrophenol}$$

The p-nitrophenol released is directly proportional to the catalytic ALP activity. It is determined by measuring the increase in absorbance.

Reagents - working solutions

R1 2-amino-2-methyl-1-propanol: 1.724 mol/L, pH 10.44 (30 °C); magnesium acetate: 3.83 mmol/L; zinc sulfate: 0.766 mmol/L; N-(2-hydroxyethyl)-ethylenediamine triacetic acid: 3.83 mmol/L

R3 p-nitrophenyl phosphate: 132.8 mmol/L, pH 8.50 (25 °C); preservatives

R1 is in position B and R3 is in position C.

Precautions and warnings

For in vitro diagnostic use.
Exercise the normal precautions required for handling all laboratory reagents.
Disposal of all waste material should be in accordance with local guidelines.
Safety data sheet available for professional user on request.

For USA: Caution: Federal law restricts this device to sale by or on the order of a physician.

This kit contains components classified as follows in accordance with the Regulation (EC) No. 1272/2008:

Warning

H315	Causes skin irritation.
H319	Causes serious eye irritation.
H412	Harmful to aquatic life with long lasting effects.

Prevention:

P264	Wash skin thoroughly after handling.
P273	Avoid release to the environment.
P280	Wear protective gloves/ eye protection/ face protection.

Response:

P332 + P313	If skin irritation occurs: Get medical advice/attention.

Appendix B: *Standard operating procedure (SOP) for analysis of alkaline phosphatase in serum on a Roche Cobas 8000 system.*

ALP2

Alkaline Phosphatase acc. to IFCC Gen.2

cobas®

P337 + P313 If eye irritation persists: Get medical advice/attention.

Disposal:

P501 Dispose of contents/container to an approved waste disposal plant.

Product safety labeling follows EU GHS guidance.

Contact phone: all countries: +49-621-7590, USA: 1-800-428-2336

Reagent handling

Ready for use

Storage and stability

ALP2

Shelf life at 2-8 °C:	See expiration date on **cobas c** pack label.
On-board in use and refrigerated on the analyzer:	4 days
On-board on the Reagent Manager:	24 hours

Diluent NaCl 9 %

Shelf life at 2-8 °C:	See expiration date on **cobas c** pack label.
On-board in use and refrigerated on the analyzer:	4 weeks
On-board on the Reagent Manager:	24 hours

Specimen collection and preparation

For specimen collection and preparation only use suitable tubes or collection containers.

Only the specimens listed below were tested and found acceptable.

Serum

Plasma: Li-heparin plasma.

The sample types listed were tested with a selection of sample collection tubes that were commercially available at the time of testing, i.e. not all available tubes of all manufacturers were tested. Sample collection systems from various manufacturers may contain differing materials which could affect the test results in some cases. When processing samples in primary tubes (sample collection systems), follow the instructions of the tube manufacturer.

Centrifuge samples containing precipitates before performing the assay.

Stability:[7]	7 days at 20-25 °C 7 days at 4-8 °C 2 months at -20 °C

Materials provided

See "Reagents – working solutions" section for reagents.

Materials required (but not provided)

See "Order information" section

General laboratory equipment

Assay

For optimum performance of the assay follow the directions given in this document for the analyzer concerned. Refer to the appropriate operator's manual for analyzer-specific assay instructions.

The performance of applications not validated by Roche is not warranted and must be defined by the user.

Application for serum and plasma

cobas c 701/702 test definition

Assay type	Rate A
Reaction time / Assay points	10 / 24-38
Wavelength (sub/main)	480/450 nm
Reaction direction	Increase
Units	U/L (µkat/L)
Reagent pipetting	Diluent (H_2O)
R1	75 µL 25 µL
R3	17 µL 21 µL

Sample volumes	*Sample*	*Sample dilution*	
		Sample	*Diluent (NaCl)*
Normal	2.8 µL	–	–
Decreased	2.8 µL	20 µL	80 µL
Increased	5.6 µL	–	–

Calibration

Calibrators	S1: H_2O S2: C.f.a.s.
Calibration mode	Linear
Calibration frequency	2-point calibration - after reagent lot change - as required following quality control procedures

Calibration interval may be extended based on acceptable verification of calibration by the laboratory.

Traceability: This method has been standardized against the IFCC procedure (2011).[6]

Quality control

For quality control, use control materials as listed in the "Order information" section. In addition, other suitable control material can be used.

The control intervals and limits should be adapted to each laboratory's individual requirements. Values obtained should fall within the defined limits. Each laboratory should establish corrective measures to be taken if values fall outside the defined limits.

Follow the applicable government regulations and local guidelines for quality control.

Calculation

Roche/Hitachi **cobas c** systems automatically calculate the analyte activity of each sample.

Conversion factor: U/L x 0.0167 = µkat/L

Limitations - interference

Criterion: Recovery within ± 10 % of initial value at an alkaline phosphatase activity of 100 U/L (1.67 µkat/L).

Icterus:[8] No significant interference up to an I index of 60 for conjugated and unconjugated bilirubin (approximate conjugated and unconjugated bilirubin concentration: 1026 µmol/L or 60 mg/dL).

Hemolysis:[8] No significant interference up to an H index of 200 (approximate hemoglobin concentration: 124 µmol/L or 200 mg/dL).

Lipemia (Intralipid):[8] No significant interference up to an L index of 2000. There is poor correlation between the L index (corresponds to turbidity) and triglycerides concentration.

Drugs: No interference was found at therapeutic concentrations using common drug panels.[9,10]

In very rare cases, gammopathy, in particular type IgM (Waldenström's macroglobulinemia), may cause unreliable results.[11]

For diagnostic purposes, the results should always be assessed in conjunction with the patient's medical history, clinical examination and other findings.

ACTION REQUIRED

Special Wash Programming: The use of special wash steps is mandatory when certain test combinations are run together on Roche/Hitachi **cobas c** systems. All special wash programming necessary for avoiding carry-over is available via the **cobas** link, manual input is not required. The latest version of the carry-over evasion list can also be found with the NaOHD/SMS/SmpCln1+2/SCCS Method Sheet and for further instructions refer to the operator's manual.

ALP2

Alkaline Phosphatase acc. to IFCC Gen.2

cobas®

Where required, special wash/carry-over evasion programming must be implemented prior to reporting results with this test.

Limits and ranges

Measuring range

5-1200 U/L (0.084-20.0 µkat/L)

Determine samples having higher activities via the rerun function. Dilution of samples via the rerun function is a 1:5 dilution. Results from samples diluted using the rerun function are automatically multiplied by a factor of 5.

Lower limits of measurement

Lower detection limit of the test:

5 U/L (0.084 µkat/L)

The lower detection limit represents the lowest measurable analyte level that can be distinguished from zero. It is calculated as the value lying 3 standard deviations above that of the lowest standard (standard 1 + 3 SD, repeatability, n = 21).

Values below the lower detection limit (< 5 U/L) will not be flagged by the instrument.

Expected values

(measured at 37 °C)

Adults[12]		
Males (n = 221)	40-129 U/L	(0.67-2.15 µkat/L)
Females (n = 229)	35-104 U/L	(0.58-1.74 µkat/L)
Children[13]		
Males		
Age		
0 – 14 days	83-248 U/L	(1.39-4.14 µkat/L)
15 days – < 1 year	122-469 U/L	(2.04-7.83 µkat/L)
1 – < 10 years	142-335 U/L	(2.37-5.59 µkat/L)
10 – < 13 years	129-417 U/L	(2.15-6.96 µkat/L)
13 – < 15 years	116-468 U/L	(1.94-7.82 µkat/L)
15 – < 17 years	82-331 U/L	(1.37-5.53 µkat/L)
17 – < 19 years	55-149 U/L	(0.92-2.49 µkat/L)
Females		
Age		
0 – 14 days	83-248 U/L	(1.39-4.14 µkat/L)
15 days – < 1 year	122-469 U/L	(2.04-7.83 µkat/L)
1 – < 10 years	142-335 U/L	(2.37-5.59 µkat/L)
10 – < 13 years	129-417 U/L	(2.15-6.96 µkat/L)
13 – < 15 years	57-254 U/L	(0.95-4.24 µkat/L)
15 – < 17 years	50-117 U/L	(0.84-1.95 µkat/L)
17 – < 19 years	45-87 U/L	(0.75-1.45 µkat/L)

Roche has not evaluated reference ranges in a pediatric population.

Each laboratory should investigate the transferability of the expected values to its own patient population and if necessary determine its own reference ranges.

Specific performance data

Representative performance data on the analyzers are given below. Results obtained in individual laboratories may differ.

Precision

Precision was determined using human samples and controls in an internal protocol with repeatability (n = 21) and intermediate precision (3 aliquots per run, 1 run per day, 21 days). The following results were obtained:

Repeatability	*Mean U/L (µkat/L)*	*SD U/L (µkat/L)*	*CV %*
Precinorm U	84.3 (1.41)	0.6 (0.01)	0.7
Precipath U	222 (3.70)	1 (0.02)	0.5
Human serum A	52.6 (0.88)	0.5 (0.01)	1.0
Human serum B	160 (2.66)	1 (0.02)	0.6
Human serum C	966 (16.1)	3 (0.1)	0.3
Intermediate precision	*Mean U/L (µkat/L)*	*SD U/L (µkat/L)*	*CV %*
Precinorm U	92.8 (1.56)	2.2 (0.04)	2.4
Precipath U	224 (3.74)	4 (0.06)	1.7
Human serum 3	82.2 (1.37)	1.8 (0.03)	2.1
Human serum 4	1025 (17.1)	9 (0.2)	0.9

Results for intermediate precision were obtained on the master system **cobas c** 501 analyzer.

Method comparison

Alkaline phosphatase values for human serum and plasma samples obtained on a Roche/Hitachi **cobas c** 701 analyzer (y) were compared with those determined using the corresponding reagent on a Roche/Hitachi **cobas c** 501 analyzer (x).

Sample size (n) = 73

Passing/Bablok[14]	Linear regression
y = 1.0x - 1.0 U/L	y = 0.999x - 1.6 U/L
τ = 0.991	r = 1.0

The sample activities were between 52 and 1089 U/L (0.87 and 18.2 µkat/L).

References

1 Greiling H, Gressner AM, eds. Lehrbuch der Klinischen Chemie und Pathobiochemie, 3rd ed. Stuttgart/New York: Schattauer Verlag 1995.

2 King EJ, Armstrong AR. A convenient method for determining serum and bile phosphatase activity. Can Med Assoc J 1934;31(4):376-381.

3 Ohmori Y. Enzymologica 1937;4:217.

4 Bessey OA, Lowry OH, Brock MJ. A method for the rapid determination of alkaline phosphatase with five cubic millimeters of serum. J Biol Chem 1946;164:321-329.

5 Hausamen TU, Helger R, Rick W, et al. Optimal conditions for the determination of serum alkaline phosphatase by a new kinetic method. Clin Chim Acta 1967;15:241-245.

6 Schumann G, Klauke R, Canalias F, et al. IFCC primary reference procedures for the measurement of catalytic activity concentrations of enzymes at 37° C. - Part 9. Reference procedure for the measurement of catalytic concentration of alkaline phosphatase. Clin Chem Lab Med 2011 Sep;49 (9):1439-46.

7 Guder WG, Narayanan S, Wisser H, et al. List of Analytes; Preanalytical Variables. Brochure in: Samples: From the Patient to the Laboratory. Darmstadt: GIT-Verlag 1996.

8 Glick MR, Ryder KW, Jackson SA. Graphical Comparisons of Interferences in Clinical Chemistry Instrumentation. Clin Chem 1986;32:470-475.

9 Breuer J. Report on the Symposium "Drug effects in Clinical Chemistry Methods". Eur J Clin Chem Clin Biochem 1996;34:385-386.

10 Sonntag O, Scholer A. Drug interference in clinical chemistry: recommendation of drugs and their concentrations to be used in drug interference studies. Ann Clin Biochem 2001;38:376-385.

11 Bakker AJ, Mücke M. Gammopathy interference in clinical chemistry assays: mechanisms, detection and prevention. Clin Chem Lab Med 2007;45(9):1240-1243.

12 Abicht K, El-Samalouti V, Junge W, et al. Multicenter evaluation of new GGT and ALP reagents with new reference standardization and determination of 37 °C reference intervals. Clin Chem Lab Med 2001;39:Special Supplement pp S 346.

ALP2

Alkaline Phosphatase acc. to IFCC Gen.2

cobas®

13 Estey MP, Cohen AH, Colantonio DA, et al. CLSI-based transference of the CALIPER database of pediatric reference intervals from Abbott to Beckman, Ortho, Roche and Siemens Clinical Chemistry Assays: Direct validation using reference samples from the CALIPER cohort. Clin Biochem 2013;46:1197–1219.

14 Bablok W, Passing H, Bender R, et al. A general regression procedure for method transformation. Application of linear regression procedures for method comparison studies in clinical chemistry, Part III. J Clin Chem Clin Biochem 1988 Nov;26(11):783-790.

A point (period/stop) is always used in this Method Sheet as the decimal separator to mark the border between the integral and the fractional parts of a decimal numeral. Separators for thousands are not used.

Symbols

Roche Diagnostics uses the following symbols and signs in addition to those listed in the ISO 15223-1 standard (for USA: see https://usdiagnostics.roche.com for definition of symbols used):

CONTENT	Contents of kit
→	Volume after reconstitution or mixing
GTIN	Global Trade Item Number

FOR US CUSTOMERS ONLY: LIMITED WARRANTY

Roche Diagnostics warrants that this product will meet the specifications stated in the labeling when used in accordance with such labeling and will be free from defects in material and workmanship until the expiration date printed on the label. THIS LIMITED WARRANTY IS IN LIEU OF ANY OTHER WARRANTY, EXPRESS OR IMPLIED, INCLUDING ANY IMPLIED WARRANTY OF MERCHANTABILITY OR FITNESS FOR PARTICULAR PURPOSE. IN NO EVENT SHALL ROCHE DIAGNOSTICS BE LIABLE FOR INCIDENTAL, INDIRECT, SPECIAL OR CONSEQUENTIAL DAMAGES.

Additions, deletions or changes are indicated by a change bar in the margin.

CE

Roche Diagnostics GmbH, Sandhofer Strasse 116, D-68305 Mannheim
www.roche.com

Distribution in USA by:
Roche Diagnostics, Indianapolis, IN
US Customer Technical Support 1-800-428-2336

Roche

0005168449190c701V3.0

CA2

cobas®

Calcium Gen.2

Order information

REF	CONTENT		Analyzer(s) on which **cobas c** pack(s) can be used
05168449 190	Calcium Gen.2 2250 tests	System-ID 05 7476 6	Roche/Hitachi **cobas c** 701/702
10759350 190	Calibrator f.a.s. (12 x 3 mL)	Code 401	
10759350 360	Calibrator f.a.s. (12 x 3 mL, for USA)	Code 401	
12149435 122	Precinorm U plus (10 x 3 mL)	Code 300	
12149435 160	Precinorm U plus (10 x 3 mL, for USA)	Code 300	
12149443 122	Precipath U plus (10 x 3 mL)	Code 301	
12149443 160	Precipath U plus (10 x 3 mL, for USA)	Code 301	
10171743 122	Precinorm U (20 x 5 mL)	Code 300	
10171735 122	Precinorm U (4 x 5 mL)	Code 300	
10171778 122	Precipath U (20 x 5 mL)	Code 301	
10171760 122	Precipath U (4 x 5 mL)	Code 301	
05117003 190	PreciControl ClinChem Multi 1 (20 x 5 mL)	Code 391	
05947626 190	PreciControl ClinChem Multi 1 (4 x 5 mL)	Code 391	
05947626 160	PreciControl ClinChem Multi 1 (4 x 5 mL, for USA)	Code 391	
05117216 190	PreciControl ClinChem Multi 2 (20 x 5 mL)	Code 392	
05947774 190	PreciControl ClinChem Multi 2 (4 x 5 mL)	Code 392	
05947774 160	PreciControl ClinChem Multi 2 (4 x 5 mL, for USA)	Code 392	
05172152 190	Diluent NaCl 9 % (119 mL)	System-ID 08 6869 3	

English

System information

CA2: ACN 8698
S-CA2: ACN 8699 (STAT, reaction time: 3)

Intended use

In vitro test for the quantitative determination of calcium in human serum, plasma and urine on Roche/Hitachi **cobas c** systems.

Summary[1]

Calcium is the most abundant mineral element in the body with about 99 % in the bones primarily as hydroxyapatite. The remaining calcium is distributed between the various tissues and the extracellular fluids where it performs a vital role for many life sustaining processes. Among the extra skeletal functions of calcium are involvement in blood coagulation, neuromuscular conduction, excitability of skeletal and cardiac muscle, enzyme activation, and the preservation of cell membrane integrity and permeability.

Serum calcium levels and hence the body content are controlled by parathyroid hormone (PTH), calcitonin, and vitamin D. An imbalance in any of these modulators leads to alterations of the body and serum calcium levels. Increases in serum PTH or vitamin D are usually associated with hypercalcemia. Increased serum calcium levels may also be observed in multiple myeloma and other neoplastic diseases. Hypocalcemia may be observed e.g. in hypoparathyroidism, nephrosis, and pancreatitis.

Test principle

Calcium ions react with 5-nitro-5'-methyl-BAPTA (NM-BAPTA) under alkaline conditions to form a complex. This complex reacts in the second step with EDTA.

$$Ca^{2+} + \text{NM-BAPTA} \xrightarrow{\text{alkaline pH}} \text{calcium-NM-BAPTA complex}$$

$$\text{calcium-NM-BAPTA complex} + \text{EDTA} \longrightarrow \text{NM-BAPTA} + \text{calcium EDTA complex}$$

The change in absorbance is directly proportional to the calcium concentration and is measured photometrically.

Reagents - working solutions

R1	CAPSO[a)] 557 mmol/L; NM-BAPTA: 2 mmol/L; pH 10.0; non-reactive surfactant; preservative
R3 (STAT R2)	EDTA: 7.5 mmol/L; pH 7.3; non-reactive surfactant; preservative

a) 3-[cyclohexylamino]-2-hydroxy-1-propanesulfonic acid

R1 is in position B and R3 (STAT R2) is in position C.

Precautions and warnings

For in vitro diagnostic use.
Exercise the normal precautions required for handling all laboratory reagents.
Disposal of all waste material should be in accordance with local guidelines.
Safety data sheet available for professional user on request.

Reagent handling

Ready for use

Storage and stability

CA2

Shelf life at 2-8 °C:	See expiration date on **cobas c** pack label.
On-board in use and refrigerated on the analyzer:	6 weeks
On-board on the Reagent Manager:	24 hours

Diluent NaCl 9 %

Shelf life at 2-8 °C:	See expiration date on **cobas c** pack label.
On-board in use and refrigerated on the analyzer:	4 weeks
On-board on the Reagent Manager:	24 hours

Specimen collection and preparation

For specimen collection and preparation only use suitable tubes or collection containers.

Only the specimens listed below were tested and found acceptable.
Serum: Fresh serum collected in the fasting state is the preferred specimen.
Plasma: Li-heparin plasma.

Serum or plasma should be separated from blood cells as soon as possible, because prolonged contact with the clot may cause lower calcium values.[2] Sera from patients receiving EDTA (treatment of hypercalcemia) are unsuitable for analysis, since EDTA will chelate the calcium and render it unavailable for reaction with NM-BAPTA. Co-precipitation of calcium with fibrin (i.e. heparin plasma), lipids, or denatured protein has been reported with storage or freezing.[1,3]

Appendix C: *Standard operating procedure (SOP) for analysis of serum Calcium in a Roche Cobas 8000 system.*

00051684491904701V3.0

CA2

Calcium Gen.2

cobas®

The sample types listed were tested with a selection of sample collection tubes that were commercially available at the time of testing, i.e. not all available tubes of all manufacturers were tested. Sample collection systems from various manufacturers may contain differing materials which could affect the test results in some cases. When processing samples in primary tubes (sample collection systems), follow the instructions of the tube manufacturer.

Urine: Urine specimens should be collected in acid-washed bottles. 24-hour specimens should be collected in containers containing 20-30 mL of 6 mol/L HCl to prevent calcium salt precipitation. Precipitated calcium salts may not be completely dissolved by the addition of HCl following urine collection.[4]

Stability in *serum/plasma*:[5]	7 days at 15-25 °C 3 weeks at 2-8 °C 8 months at (-15)-(-25) °C
Stability in *urine*:[5]	2 days at 15-25 °C 4 days at 2-8 °C 3 weeks at (-15)-(-25) °C

Stored serum or urine specimens must be mixed well prior to analysis.

Centrifuge samples containing precipitates before performing the assay.

Materials provided

See "Reagents – working solutions" section for reagents.

Materials required (but not provided)

See "Order information" section

General laboratory equipment

Assay

For optimum performance of the assay follow the directions given in this document for the analyzer concerned. Refer to the appropriate operator's manual for analyzer-specific assay instructions.

The performance of applications not validated by Roche is not warranted and must be defined by the user.

Application for serum and plasma

cobas c 701/702 **test definition**

Assay type	2-Point End	
Reaction time / Assay points	10 / 18-22 (STAT 3 / 6-10)	
Wavelength (sub/main)	376/340 nm	
Reaction direction	Decrease	
Units	mmol/L (mg/dL)	
Reagent pipetting		Diluent (H_2O)
R1	20 µL	160 µL
R3 (STAT R2)	20 µL	–

Sample volumes	*Sample*	*Sample dilution*	
		Sample	*Diluent (NaCl)*
Normal	3 µL	–	–
Decreased	3 µL	–	–
Increased	3 µL	–	–

Application for urine

cobas c 701/702 **test definition**

Assay type	2-Point End	
Reaction time / Assay points	10 / 18-22 (STAT 3 / 6-10)	
Wavelength (sub/main)	376/340 nm	
Reaction direction	Decrease	
Units	mmol/L (mg/dL)	
Reagent pipetting		Diluent (H_2O)
R1	20 µL	160 µL
R3 (STAT R2)	20 µL	–

Sample volumes	*Sample*	*Sample dilution*	
		Sample	*Diluent (NaCl)*
Normal	2 µL	–	–
Decreased	4 µL	15 µL	135 µL
Increased	2 µL	–	–

Calibration

Calibrators	S1: H_2O S2: C.f.a.s.
Calibration mode	Linear
Calibration frequency	2-point calibration - after reagent lot change - as required following quality control procedures

Traceability: This method has been standardized against the SRM 956 c level 2 reference material.

Quality control

Serum/plasma

For quality control, use control materials as listed in the "Order information" section.

In addition, other suitable control material can be used.

Urine

Quantitative urine controls are recommended for routine quality control.

The control intervals and limits should be adapted to each laboratory's individual requirements. Values obtained should fall within the defined limits. Each laboratory should establish corrective measures to be taken if values fall outside the defined limits.

Follow the applicable government regulations and local guidelines for quality control.

Calculation

Roche/Hitachi **cobas c** systems automatically calculate the analyte concentration of each sample.

Conversion factors: mmol/L × 4.01 = mg/dL

In studies with 24-hour urine, multiply the value obtained by the 24-hour volume in order to obtain a measurement in mg/24 h or mmol/24 h.

Limitations - interference

Criterion: Recovery within ± 0.22 mmol/L (0.9 mg/dL) of initial value of samples ≤ 2.2 mmol/L (8.8 mg/dL) and within ± 10 % for samples > 2.2 mmol/L.

Serum/plasma

Icterus:[6] No significant interference up to an I index of 60 for conjugated and unconjugated bilirubin (approximate conjugated and unconjugated bilirubin concentration: 1026 µmol/L or 60 mg/dL).

Hemolysis:[6] No significant interference up to an H index of 1000 (approximate hemoglobin concentration: 621 µmol/L or 1000 mg/dL).

Lipemia (Intralipid):[6] No significant interference up to an L index of 1000. There is a poor correlation between the L index (corresponds to turbidity) and triglycerides concentration.

Magnesium: No significant interference up to a concentration of 15 mmol/L.

Drugs: No interference was found at therapeutic concentrations using common drug panels.[7,8]

The interference of intravenously administered gadolinium containing MRI (magnetic resonance imaging) contrast media was tested (Omniscan®, Optimark®) but no interference was found at the therapeutic concentration. Interferences at higher concentrations were observed.

In very rare cases, gammopathy, in particular type IgM (Waldenström's macroglobulinemia), may cause unreliable results.[9]

Urine

Icterus: No significant interference up to a conjugated bilirubin concentration of 1026 µmol/L or 60 mg/dL.

CA2

Calcium Gen.2

cobas®

Hemolysis: No significant interference up to a hemoglobin concentration of 621 µmol/L or 1000 mg/dL.

Magnesium: No significant interference up to a concentration of 60 mmol/L.

Drugs: No interference was found at therapeutic concentrations using common drug panels.[8]

The interference of intravenously administered gadolinium containing MRI (magnetic resonance imaging) contrast media was tested (Omniscan®, Optimark®). For Omniscan® no interference was observed at the therapeutic concentration, but there was interference at higher concentrations. For Optimark® interference was observed at therapeutic and higher concentrations.

For diagnostic purposes, the results should always be assessed in conjunction with the patient's medical history, clinical examination and other findings.

ACTION REQUIRED

Special Wash Programming: The use of special wash steps is mandatory when certain test combinations are run together on Roche/Hitachi **cobas c** systems. All special wash programming necessary for avoiding carry-over is available via the **cobas** link, manual input is not required. The latest version of the carry-over evasion list can also be found with the NaOHD/SMS/SmpCln1+2/SCCS Method Sheet and for further instructions refer to the operator's manual.

Where required, special wash/carry-over evasion programming must be implemented prior to reporting results with this test.

Limits and ranges

Measuring range

Serum/plasma

0.20-5.0 mmol/L (0.8-20.1 mg/dL)

Urine

0.20-7.5 mmol/L (0.8-30.1 mg/dL)

Determine urine samples having higher concentrations via the rerun function. Dilution of samples via the rerun function is a 1:5 dilution. Results from samples diluted using the rerun function are automatically multiplied by a factor of 5.

Lower limits of measurement

Limit of Blank (LoB), Limit of Detection (LoD) and Limit of Quantitation (LoQ)

Serum/plasma and urine

Limit of Blank:	= 0.10 mmol/L (0.4 mg/dL)
Limit of Detection:	= 0.20 mmol/L (0.8 mg/dL)
Limit of Quantitation	= 0.20 mmol/L (0.8 mg/dL)

The Limit of Blank, Limit of Detection and Limit of Quantitation were determined in accordance with the CLSI (Clinical and Laboratory Standards Institute) EP17-A2 requirements.

The Limit of Blank is the 95th percentile value from n ≥ 60 measurements of analyte-free samples over several independent series. The Limit of Blank corresponds to the concentration below which analyte-free samples are found with a probability of 95 %.

The Limit of Detection is determined based on the Limit of Blank and the standard deviation of low concentration samples.

The Limit of Detection corresponds to the lowest analyte concentration which can be detected (value above the Limit of Blank with a probability of 95 %).

The Limit of Quantitation is the lowest analyte concentration that can be reproducibly measured with a total error of 30 %. It has been determined using low concentration calcium samples.

Expected values[10]

Serum/plasma

Children (0-10 days):	1.90-2.60 mmol/L (7.6-10.4 mg/dL)
Children (10 days-2 years):	2.25-2.75 mmol/L (9.0-11.0 mg/dL)
Children (2-12 years):	2.20-2.70 mmol/L (8.8-10.8 mg/dL)
Children (12-18 years):	2.10-2.55 mmol/L (8.4-10.2 mg/dL)
Adults (18-60 years):	2.15-2.50 mmol/L (8.6-10.0 mg/dL)
Adults (60-90 years):	2.20-2.55 mmol/L (8.8-10.2 mg/dL)
Adults (> 90 years):	2.05-2.40 mmol/L (8.2-9.6 mg/dL)

Urine

2.5-7.5 mmol/24 h (100-300 mg/24 h) with normal food intake.

Roche has not evaluated reference ranges in a pediatric population.

Each laboratory should investigate the transferability of the expected values to its own patient population and if necessary determine its own reference ranges.

Specific performance data

Representative performance data on the analyzers are given below. Results obtained in individual laboratories may differ.

Precision

Repeatability was determined using human samples and controls in an internal protocol (n = 21, 1 run). Intermediate precision was determined using human samples and controls in accordance with the CLSI (Clinical and Laboratory Standards Institute) EP5 requirements (2 aliquots per run, 2 runs per day, 21 days). The following results were obtained:

Serum/plasma

Repeatability	*Mean mmol/L (mg/dL)*	*SD mmol/L (mg/dL)*	*CV %*
Human serum 1	0.59 (2.4)	0.01 (0.0)	2.0
Human serum 2	2.57 (10.3)	0.02 (0.1)	0.7
Human serum 3	4.54 (18.2)	0.02 (0.1)	0.4
Precinorm U	2.31 (9.3)	0.02 (0.1)	0.7
Precipath U	3.63 (14.6)	0.02 (0.1)	0.5
Intermediate precision	*Mean mmol/L (mg/dL)*	*SD mmol/L (mg/dL)*	*CV %*
Human serum 1	0.60 (2.4)	0.02 (0.1)	2.5
Human serum 2	2.55 (10.2)	0.02 (0.1)	0.9
Human serum 3	4.46 (17.9)	0.04 (0.2)	0.9
Precinorm U	2.25 (9.0)	0.02 (0.1)	0.8
Precipath U	3.51 (14.1)	0.03 (0.1)	0.9

Urine

Repeatability	*Mean mmol/L (mg/dL)*	*SD mmol/L (mg/dL)*	*CV %*
Human urine 1	0.56 (2.2)	0.03 (0.1)	5.9
Human urine 2	3.96 (15.9)	0.03 (0.1)	0.7
Human urine 3	5.29 (21.2)	0.04 (0.2)	0.8
Human urine 4	6.21 (24.9)	0.04 (0.2)	0.6
Control Level 1	1.91 (7.7)	0.02 (0.1)	1.2
Control Level 2	2.77 (11.1)	0.03 (0.1)	0.9
Intermediate precision	*Mean mmol/L (mg/dL)*	*SD mmol/L (mg/dL)*	*CV %*
Human urine 1	0.58 (2.3)	0.02 (0.1)	3.1
Human urine 2	3.92 (15.7)	0.05 (0.2)	1.2
Human urine 3	5.18 (20.8)	0.06 (0.2)	1.1
Human urine 4	6.09 (24.4)	0.08 (0.3)	1.3
Control Level 1	1.85 (7.4)	0.03 (0.1)	1.5
Control Level 2	2.72 (10.9)	0.04 (0.2)	1.3

Results for intermediate precision were obtained on the master system **cobas c** 501 analyzer.

Method comparison

Calcium values for human serum, plasma and urine samples obtained on a Roche/Hitachi **cobas c** 701 analyzer (y) using the Roche Calcium Gen.2

reagent were compared with those determined using the corresponding reagent on a Roche/Hitachi **cobas c** 501 analyzer (x).

Serum/plasma

Sample size (n) = 69

Passing/Bablok[11]	Linear regression
y = 0.995x + 0.023 mmol/L	y = 0.991x + 0.031 mmol/L
τ = 0.978	r = 1.00

The sample concentrations were between 0.27 and 4.72 mmol/L (1.1 and 18.9 mg/dL).

Urine

Sample size (n) = 61

Passing/Bablok[11]	Linear regression
y = 1.028x + 0.003 mmol/L	y = 1.027x + 0.012 mmol/L
τ = 0.990	r = 1.00

The sample concentrations were between 0.29 and 7.32 mmol/L (1.2 and 29.4 mg/dL).

References

1 Endres DB, Rude RK. Mineral and Bone Metabolism. In: Burtis CA, Ashwood ER, Bruns ED, eds. Tietz Textbook of Clinical Chemistry and Molecular Diagnostics, 4th ed. St. Louis (MO): Saunders Elsevier 2006:1891-1965.

2 Heins M, Heil W, Withold W. Storage of Serum or Whole Blood Samples? Effect of Time and Temperature on 22 Serum Analytes. Eur J Clin Chem Clin Biochem 1995;33:231-238.

3 Wilding P, Zilva JF, Wilde CE. Transport of specimens for clinical chemistry analysis. Ann Clin Biochem 1977;14:301-306.

4 Burtis CA, Ashwood ER, Bruns DE, eds. Tietz Fundamentals of Clinical Chemistry, 6th ed.St. Louis (MO): Saunders Elsevier 2008:715.

5 WHO Publication: Use of anticoagulants in diagnostic laboratory investigations, WHO/DIL/LAB/99.1 Rev.2:Jan 2002

6 Glick MR, Ryder KW, Jackson SA. Graphical Comparisons of Interferences in Clinical Chemistry Instrumentation. Clin Chem 1986;32:470-475.

7 Breuer J. Report on the Symposium "Drug effects in Clinical Chemistry Methods". Eur J Clin Chem Clin Biochem 1996;34:385-386.

8 Sonntag O, Scholer A. Drug interference in clinical chemistry: recommendation of drugs and their concentrations to be used in drug interference studies. Ann Clin Biochem 2001;38:376-385.

9 Bakker AJ, Mücke M. Gammopathy interference in clinical chemistry assays: mechanisms, detection and prevention. Clin Chem Lab Med 2007;45(9):1240-1243.

10 Wu AHB, ed. Tietz Clinical Guide to Laboratory Tests, 4th ed. St. Louis (MO): Saunders Elsevier 2006:202-207.

11 Bablok W, Passing H, Bender R, et al. A general regression procedure for method transformation. Application of linear regression procedures for method comparison studies in clinical chemistry, Part III. J Clin Chem Clin Biochem 1988 Nov;26(11):783-790.

A point (period/stop) is always used in this Method Sheet as the decimal separator to mark the border between the integral and the fractional parts of a decimal numeral. Separators for thousands are not used.

Symbols

Roche Diagnostics uses the following symbols and signs in addition to those listed in the ISO 15223-1 standard.

CONTENT	Contents of kit
→	Volume after reconstitution or mixing

FOR US CUSTOMERS ONLY: LIMITED WARRANTY

Roche Diagnostics warrants that this product will meet the specifications stated in the labeling when used in accordance with such labeling and will be free from defects in material and workmanship until the expiration date printed on the label. THIS LIMITED WARRANTY IS IN LIEU OF ANY OTHER WARRANTY, EXPRESS OR IMPLIED, INCLUDING ANY IMPLIED WARRANTY OF MERCHANTABILITY OR FITNESS FOR PARTICULAR PURPOSE. IN NO EVENT SHALL ROCHE DIAGNOSTICS BE LIABLE FOR INCIDENTAL, INDIRECT, SPECIAL OR CONSEQUENTIAL DAMAGES.

CE

Roche Diagnostics GmbH, Sandhofer Strasse 116, D-68305 Mannheim
www.roche.com

Distribution in USA by:
Roche Diagnostics, Indianapolis, IN
US Customer Technical Support 1-800-428-2336

00051713771900v701V8.0

PHOS2

cobas®

Phosphate (Inorganic) ver.2

Order information

REF	CONTENT		Analyzer(s) on which **cobas c** pack(s) can be used
05171377 190	Phosphate (Inorganic) ver.2 (600 tests)	System-ID 05 6614 3	Roche/Hitachi **cobas c** 701/702
10759350 190	Calibrator f.a.s. (12 x 3 mL)	Code 401	
10759350 360	Calibrator f.a.s. (12 x 3 mL, for USA)	Code 401	
12149435 122	Precinorm U plus (10 x 3 mL)	Code 300	
12149435 160	Precinorm U plus (10 x 3 mL, for USA)	Code 300	
12149443 122	Precipath U plus (10 x 3 mL)	Code 301	
12149443 160	Precipath U plus (10 x 3 mL, for USA)	Code 301	
10171743 122	Precinorm U (20 x 5 mL)	Code 300	
10171735 122	Precinorm U (4 x 5 mL)	Code 300	
10171778 122	Precipath U (20 x 5 mL)	Code 301	
10171760 122	Precipath U (4 x 5 mL)	Code 301	
05117003 190	PreciControl ClinChem Multi 1 (20 x 5 mL)	Code 391	
05947626 190	PreciControl ClinChem Multi 1 (4 x 5 mL)	Code 391	
05947626 160	PreciControl ClinChem Multi 1 (4 x 5 mL, for USA)	Code 391	
05117216 190	PreciControl ClinChem Multi 2 (20 x 5 mL)	Code 392	
05947774 190	PreciControl ClinChem Multi 2 (4 x 5 mL)	Code 392	
05947774 160	PreciControl ClinChem Multi 2 (4 x 5 mL, for USA)	Code 392	
05172152 190	Diluent NaCl 9 % (119 mL)	System-ID 08 6869 3	

English

System information

PHOS2: ACN 8714 (serum, plasma)
SPHO2: ACN 8675 (serum, plasma, STAT, reaction time: 7)
PHO2U: ACN 8716 (urine)
SPH2U: ACN 8656 (urine, STAT, reaction time: 7)

Intended use

In vitro test for the quantitative determination of phosphorus in human serum, plasma and urine on Roche/Hitachi **cobas c** systems.

Summary[1,2,3,4,5]

88 % of the phosphorus contained in the body is localized in bone in the form of calcium phosphate as the apatite $Ca^{2+}[Ca_3(PO_4)_2]_3^{2-}$. The remainder is involved in intermediary carbohydrate metabolism and in physiologically important substances such as phospholipids, nucleic acids and ATP. Phosphorus occurs in blood in the form of inorganic phosphate and in organically bound phosphoric acid. The small amount of extracellular organic phosphorus is found almost exclusively in the form of phospholipids.

The ratio of phosphate to calcium in the blood is approximately 6:10. An increase in the level of phosphorus causes a decrease in the calcium level. The mechanism is influenced by interactions between parathormone and vitamin D. Hypoparathyroidism, vitamin D intoxication and renal failure with decreased glomerular phosphate filtration give rise to hyperphosphatemia. Hypophosphatemia occurs in rickets, hyperparathyroidism and Fanconi's syndrome.

The preferred method for the determination of inorganic phosphorus is based on the formation of ammonium phosphomolybdate with subsequent reduction to molybdenum blue. Reagent stability problems often occur with this method. The method presented here is based on the reaction of phosphate with ammonium molybdate to form ammonium phosphomolybdate without reduction. The addition of an accelerator gives rise to a more rapid rate of reaction and the application of sample blanking yields more precise results.

Test principle[5]

Molybdate UV.

Inorganic phosphate forms an ammonium phosphomolybdate complex having the formula $(NH_4)_3[PO_4(MoO_3)_{12}]$ with ammonium molybdate in the presence of sulfuric acid.

$$\text{Phosphate + ammonium molybdate} \xrightarrow{H_2SO_4} \text{ammonium phosphomolybdate}$$

The concentration of phosphomolybdate formed is directly proportional to the inorganic phosphate concentration and is measured photometrically.

Reagents - working solutions

R1	Sulfuric acid: 0.36 mol/L; detergent
R3 (STAT R2)	Ammonium molybdate: 3.5 mmol/L; sulfuric acid: 0.36 mol/L; sodium chloride: 150 mmol/L

R1 is in position B and R3 (STAT R2) is in position C.

Precautions and warnings

For in vitro diagnostic use.
Exercise the normal precautions required for handling all laboratory reagents.
Disposal of all waste material should be in accordance with local guidelines.
Safety data sheet available for professional user on request.

For USA: For prescription use only.

This kit contains components classified as follows in accordance with the Regulation (EC) No. 1272/2008:

Warning

H290 May be corrosive to metals.

Prevention:

P234 Keep only in original container.

Response:

P390 Absorb spillage to prevent material damage.

Product safety labeling primarily follows EU GHS guidance.
Contact phone: all countries: +49-621-7590, USA: 1-800-428-2336

Reagent handling

Ready for use

Appendix D: *Standard operating procedure (SOP) for analysis of serum Phosphorus in a Roche Cobas 8000 system.*

00051763771/90c701V8.0

PHOS2

Phosphate (Inorganic) ver.2

cobas®

Storage and stability

PHOS2

Shelf life at 2-8 °C:	See expiration date on **cobas c** pack label.
On-board in use and refrigerated on the analyzer:	4 weeks
On-board on the Reagent Manager:	24 hours

Diluent NaCl 9 %

Shelf life at 2-8 °C:	See expiration date on **cobas c** pack label.
On-board in use and refrigerated on the analyzer:	4 weeks
On-board on the Reagent Manager:	24 hours

Specimen collection and preparation

For specimen collection and preparation only use suitable tubes or collection containers.

Only the specimens listed below were tested and found acceptable.

Serum

Plasma: Li-heparin and K_2-EDTA plasma

The sample types listed were tested with a selection of sample collection tubes that were commercially available at the time of testing, i.e. not all available tubes of all manufacturers were tested. Sample collection systems from various manufacturers may contain differing materials which could affect the test results in some cases. When processing samples in primary tubes (sample collection systems), follow the instructions of the tube manufacturer.

Urine

Collect in detergent-free containers. Acidify with hydrochloric acid after collection (pH < 3).[6,7]

Stability in serum/plasma:[8]	24 hours at 15-25 °C 4 days at 2-8 °C 1 year at (-15)-(-25) °C
Stability in urine: [6,7]	6 months at 2-8 °C (when acidified)
24-hour urine:	Store cooled during collection.

Centrifuge samples containing precipitates before performing the assay.

Materials provided

See "Reagents – working solutions" section for reagents.

Materials required (but not provided)

See "Order information" section

General laboratory equipment

Assay

For optimum performance of the assay follow the directions given in this document for the analyzer concerned. Refer to the appropriate operator's manual for analyzer-specific assay instructions.

The performance of applications not validated by Roche is not warranted and must be defined by the user.

Application for serum and plasma

cobas c 701/702 **test definition**

Assay type	2-Point End	
Reaction time / Assay points	10 / 18-38 (STAT 7 / 6-26)	
Wavelength (sub/main)	700/340 nm	
Reaction direction	Increase	
Units	mmol/L (mg/dL, mg/L)	
Reagent pipetting		Diluent (H_2O)
R1	90 µL	28 µL
R3 (STAT R2)	38 µL	–

Sample volumes	*Sample*	*Sample dilution*	
		Sample	*Diluent (NaCl)*
Normal	2.5 µL	–	–
Decreased	12.5 µL	15 µL	135 µL
Increased	5 µL	–	–

Application for urine

cobas c 701/702 **test definition**

Assay type	2-Point End	
Reaction time / Assay points	10 / 18-38 (STAT 7 / 6-26)	
Wavelength (sub/main)	700/340 nm	
Reaction direction	Increase	
Units	mmol/L (mg/dL, mg/L)	
Reagent pipetting		Diluent (H_2O)
R1	90 µL	28 µL
R3 (STAT R2)	38 µL	–

Sample volumes	*Sample*	*Sample dilution*	
		Sample	*Diluent (NaCl)*
Normal	2.5 µL	15 µL	150 µL
Decreased	2.5 µL	8 µL	168 µL
Increased	5 µL	15 µL	150 µL

Calibration

Calibrators	S1: H_2O S2: C.f.a.s.
Calibration mode	Linear
Calibration frequency	2-point calibration - after reagent lot change - as required following quality control procedures

Traceability: This method has been standardized against NERL primary reference material.

For USA: This method has been standardized against NIST traceable primary reference material.

Quality control

Serum/plasma

For quality control, use control materials as listed in the "Order Information" section. In addition, other suitable control material can be used.

Urine

Quantitative urine controls are recommended for routine quality control.

The control intervals and limits should be adapted to each laboratory's individual requirements. Values obtained should fall within the defined limits. Each laboratory should establish corrective measures to be taken if values fall outside the defined limits.

Follow the applicable government regulations and local guidelines for quality control.

Calculation

Roche/Hitachi **cobas c** systems automatically calculate the analyte concentration of each sample.

Conversion factors:	mmol/L x 3.10 = mg/dL mmol/L x 31 = mg/L mg/L x 0.0323 = mmol/L

Limitations - interference[6]

Criterion: Recovery within ± 10 % of initial value at a phosphate concentration of 0.87 mmol/L (2.7 mg/dL).

PHOS2

Phosphate (Inorganic) ver.2

cobas®

Serum/plasma

Icterus:[9] No significant interference up to an I index of 40 for conjugated bilirubin and 60 for unconjugated bilirubin (approximate conjugated bilirubin concentration: 684 µmol/L or 40 mg/dL; approximate unconjugated bilirubin concentration: 1026 µmol/L or 60 mg/dL).

Hemolysis:[9] Significant positive interference up to an H index of > 300 (approximate hemoglobin concentration: 186 µmol/L or 300 mg/dL).

Note: This interference results from inorganic phosphates produced by the action of phosphatases on organic phosphates, both of which are released from the red cells upon hemolysis.

Lipemia (Intralipid):[9] No significant interference up to an L index of 800. There is poor correlation between the L index (corresponds to turbidity) and triglycerides concentration.

Drugs: No interference was found at therapeutic concentrations using common drug panels.[10,11] Exception: Phospholipids contained in liposomal drug formulations (eg AmBisome) may be hydrolyzed in the test due to the acidic reaction pH and thus lead to elevated phosphate results.[12]

In very rare cases, gammopathy, in particular type IgM (Waldenström's macroglobulinemia), may cause unreliable results.[13]

Urine

Drugs: No interference was found at therapeutic concentrations using common drug panels.[11]

For diagnostic purposes, the results should always be assessed in conjunction with the patient's medical history, clinical examination and other findings.

ACTION REQUIRED

Special Wash Programming: The use of special wash steps is mandatory when certain test combinations are run together on Roche/Hitachi **cobas c** systems. All special wash programming necessary for avoiding carry-over is available via the **cobas** link, manual input is not required. The latest version of the carry-over evasion list can also be found with the NaOH/SMS/SmpClnl+2/SCCS Method Sheet and for further instructions refer to the operator's manual.

Where required, special wash/carry-over evasion programming must be implemented prior to reporting results with this test.

Limits and ranges

Measuring range

Serum/plasma

0.10-6.46 mmol/L (0.31-20.0 mg/dL)

Determine samples having higher concentrations via the rerun function. Dilution of samples via the rerun function is a 1:2 dilution. Results from samples diluted using the rerun function are automatically multiplied by a factor of 2.

Urine

1.1-92 mmol/L (3.4-285 mg/dL)

Determine samples having higher concentrations via the rerun function. Dilution of samples via the rerun function is a 1:2 dilution. Results from samples diluted using the rerun function are automatically multiplied by a factor of 2.

Lower limits of measurement

Lower detection limit of the test:

Serum/plasma

0.10 mmol/L (0.31 mg/dL)

The lower detection limit represents the lowest measurable analyte level that can be distinguished from zero. It is calculated as the value lying 3 standard deviations above that of the lowest standard (standard 1 + 3 SD, repeatability, n = 21).

Values below the lower detection limit (< 0.10 mmol/L) will not be flagged by the instrument.

Urine

1.1 mmol/L (3.4 mg/dL)

The lower detection limit represents the lowest measurable analyte level that can be distinguished from zero. It is calculated as the value lying 3 standard deviations above that of the lowest standard (standard 1 + 3 SD, repeatability, n = 21).

Values below the lower detection limit (< 1.1 mmol/L) will not be flagged by the instrument.

Expected values

Adults:[14]

0.81-1.45 mmol/L (2.5-4.5 mg/dL)

Children:[15]

Age	*Male mmol/L (mg/dL)*	*Female mmol/L (mg/dL)*
1-30 days	1.25-2.25 (3.9-6.9)	1.40-2.50 (4.3-7.7)
1-12 months	1.15-2.15 (3.5-6.6)	1.20-2.10 (3.7-6.5)
1-3 years	1.00-1.95 (3.1-6.0)	1.10-1.95 (3.4-6.0)
4-6 years	1.05-1.80 (3.3-5.6)	1.05-1.80 (3.2-5.5)
7-9 years	0.95-1.75 (3.0-5.4)	1.00-1.80 (3.1-5.5)
10-12 years	1.05-1.85 (3.2-5.7)	1.05-1.70 (3.3-5.3)
13-15 years	0.95-1.65 (2.9-5.1)	0.90-1.55 (2.8-4.8)
16-18 years	0.85-1.60 (2.7-4.9)	0.80-1.55 (2.5-4.8)

Roche has not evaluated reference ranges in a pediatric population.

Urine

1st morning urine[16]	13-44 mmol/L (40-136 mg/dL)
24-hour urine[6]	13-42 mmol/d (0.4-1.3 g/d)

Each laboratory should investigate the transferability of the expected values to its own patient population and if necessary determine its own reference ranges.

Specific performance data

Representative performance data on the analyzers are given below. Results obtained in individual laboratories may differ.

Precision

Precision was determined using human samples and controls in an internal protocol. *Serum/plasma:* Repeatability (n = 21), intermediate precision (3 aliquots per run, 1 run per day, 21 days); *urine:* Repeatability (n = 21), intermediate precision (3 aliquots per run, 1 run per day, 10 days). The following results were obtained:

Serum/plasma

PHOS2:

Repeatability	*Mean mmol/L (mg/dL)*	*SD mmol/L (mg/dL)*	*CV %*
Precinorm U	1.24 (3.84)	0.01 (0.03)	0.8
Precipath U	1.97 (6.11)	0.01 (0.03)	0.7
Human serum A	0.743 (2.29)	0.007 (0.02)	0.9
Human serum B	3.11 (9.64)	0.02 (0.06)	0.8
Human serum C	6.16 (19.1)	0.03 (0.1)	0.5

SPHO2:

Repeatability	*Mean mmol/L (mg/dL)*	*SD mmol/L (mg/dL)*	*CV %*
Precinorm U	1.24 (3.84)	0.01 (0.03)	0.9
Precipath U	1.97 (6.11)	0.01 (0.03)	0.7
Human serum A	0.733 (2.27)	0.007 (0.02)	0.9
Human serum B	3.15 (9.77)	0.02 (0.06)	0.7
Human serum C	6.24 (19.3)	0.02 (0.1)	0.4

PHOS2 / SPHO2:

Intermediate precision	*Mean mmol/L (mg/dL)*	*SD mmol/L (mg/dL)*	*CV %*
Precinorm U	1.23 (3.81)	0.02 (0.06)	1.4

PHOS2

Phosphate (Inorganic) ver.2

cobas®

Precipath U	2.04 (6.32)	0.02 (0.06)	1.2
Human serum 3	2.67 (8.28)	0.04 (0.12)	1.4
Human serum 4	1.55 (4.81)	0.02 (0.06)	1.4

Urine

PHO2U:

Repeatability	*Mean mmol/L (mg/dL)*	*SD mmol/L (mg/dL)*	*CV %*
Control Level 1	7.90 (24.5)	0.09 (0.3)	1.1
Control Level 2	17.1 (53.0)	0.2 (0.6)	0.9
Human urine A	5.95 (18.4)	0.08 (0.2)	1.3
Human urine B	40.1 (124)	0.3 (1)	0.9
Human urine C	89.2 (277)	0.7 (2)	0.8

SPH2U:

Repeatability	*Mean mmol/L (mg/dL)*	*SD mmol/L (mg/dL)*	*CV %*
Control Level 1	7.87 (24.4)	0.11 (0.3)	1.3
Control Level 2	16.9 (52.4)	0.2 (0.6)	1.0
Human urine A	5.79 (17.9)	0.10 (0.3)	1.7
Human urine B	40.3 (125)	0.3 (1)	0.6
Human urine C	90.0 (279)	0.5 (2)	0.6

PHO2U / SPH2U:

Intermediate precision	*Mean mmol/L (mg/dL)*	*SD mmol/L (mg/dL)*	*CV %*
Control Level 1	10.0 (31.0)	0.2 (0.6)	1.6
Control Level 2	19.6 (60.8)	0.3 (0.9)	1.7
Human urine 3	40.4 (125)	0.5 (2)	1.3
Human urine 4	6.23 (19.3)	0.12 (0.4)	2.0

Results for intermediate precision were obtained on the master system **cobas c** 501 analyzer.

Method comparison

Inorganic phosphate values for human serum, plasma and urine samples obtained on a Roche/Hitachi **cobas c** 701 analyzer (y) were compared with those determined using the corresponding reagent on a Roche/Hitachi **cobas c** 501 analyzer (x).

Serum/plasma

Sample size (n) = 131

PHOS2:

Passing/Bablok[17]	Linear regression
y = 1.001x - 0.005 mmol/L	y = 1.011x - 0.011 mmol/L
τ = 0.968	r = 0.999

The sample concentrations were between 0.421 and 6.15 mmol/L (1.31 and 19.1 mg/dL).

SPHO2:

Passing/Bablok[17]	Linear regression
y = 1.010x + 0.00 mmol/L	y = 1.011x + 0.00 mmol/L
τ = 0.980	r = 1.000

The sample concentrations were between 0.415 and 6.05 mmol/L (1.29 and 18.8 mg/dL).

Urine

PHO2U:

Sample size (n) = 101

Passing/Bablok[17]	Linear regression
y = 1.022x - 0.061 mmol/L	y = 1.031x - 0.052 mmol/L
τ = 0.985	r = 0.999

The sample concentrations were between 1.28 and 87.8 mmol/L (3.97 and 272 mg/dL).

SPH2U:

Sample size (n) = 102

Passing/Bablok[17]	Linear regression
y = 1.014x + 0.054 mmol/L	y = 1.022x + 0.067 mmol/L
τ = 0.981	r = 0.999

The sample concentrations were between 1.19 and 90.2 mmol/L (3.69 and 280 mg/dL).

References

1 Külpmann WR, Stummvoll HK, Lehmann P. Elektrolyte, Klinik und Labor. Heidelberg: Verlag Klinisches Labor 1993.

2 Tietz NW, ed. Fundamentals of Clinical Chemistry Philadelphia, PA: WB Saunders Company 1976;901.

3 Fiske CH, Subbarow Y. The colorimetric determination of phosphorus. J Biol Chem 1925;66:375-400.

4 Taussky HH, Shorr E. A microcolorimetric method for the determination of inorganic phosphorus. J Biol Chem 1953;202:675-685.

5 Henry R ed. Clinical Chemistry: Principles and Technics, 2nd ed. New York, NY: Harper & Row 1974;723.

6 Tietz NW, ed. Clinical Guide to Laboratory Tests, 4th ed. Philadelphia.WB Saunders Co 2006;852-855.

7 NCCLS GP-16A2, Urineanalysis and Collection, Transportation and Preservation of Urine specimens, 2nd edition 2001.

8 WHO Publication: Use of anticoagulants in diagnostic laboratory investigations, WHO/DIL/LAB/99.1 Rev.2:Jan 2002.

9 Glick MR, Ryder KW, Jackson SA. Graphical Comparisons of Interferences in Clinical Chemistry Instrumentation. Clin Chem 1986;32:470-475.

10 Breuer J. Report on the Symposium "Drug effects in Clinical Chemistry Methods". Eur J Clin Chem Clin Biochem 1996;34:385-386.

11 Sonntag O, Scholer A. Drug interference in clinical chemistry: recommendation of drugs and their concentrations to be used in drug interference studies. Ann Clin Biochem 2001;38:376-385.

12 Lane JW, Rehak NN, Hortin GL, et al. Pseudohyperphosphatemia associated with high-dose liposomal amphotericin B therapy. Clin Chim Acta 2008;387:145-149.

13 Bakker AJ, Mücke M. Gammopathy interference in clinical chemistry assays: mechanisms, detection and prevention. Clin Chem Lab Med 2007;45(9):1240-1243.

14 Burtis CA, Ashwood ER, Bruns DE (eds.). Tietz Textbook of Clinical Chemistry and Molecular Diagnostics, 4th ed. St Louis, Missouri; Elsevier Saunders 2006;2290.

15 Soldin JS, Brugnara C, Wong EC. Pediatric Reference Intervals. AACC Press. 2005, 5th ed., p. 153.

16 Krieg M, Gunsser KJ, Steinhagen-Thiessen E, et al. Comparative quantitative clinico-chemical analysis of the characteristics of 24-hour urine and morning urine. J Clin Chem Clin Biochem 1986 Nov;24(11):863-869.

17 Bablok W, Passing H, Bender R, et al. A general regression procedure for method transformation. Application of linear regression procedures for method comparison studies in clinical chemistry, Part III. J Clin Chem Clin Biochem 1988 Nov;26(11):783-790.

A point (period/stop) is always used in this Method Sheet as the decimal separator to mark the border between the integral and the fractional parts of a decimal numeral. Separators for thousands are not used.